INSTITUTO POTOSINO DE INVESTIGACIÓN CIENTÍFICA Y TECNOLÓGICA, A.C.

POSGRADO EN CIENCIAS APLICADAS

Adaptive control of robot manipulators with bounded inputs

Tesis que presenta

Daniela Juanita López Araujo

Para obtener el grado de

Doctora en Ciencias Aplicadas

En la opción de

Control y Sistemas Dinámicos

Director de la Tesis:

Dr. Arturo Zavala Río

San Luis Potosí, S.L.P., Agosto de 2013

IPICYT

Constancia de aprobación de la tesis

La tesis **"Adaptive control of robot manipulators with bounded inputs"** presentada para obtener el Grado de Doctora en Ciencias Aplicadas en la opción de Control y Sistemas Dinámicos fue elaborada por **Daniela Juanita López Araujo** y aprobada el **dieciséis de agosto del dos mil trece** por los suscritos, designados por el Colegio de Profesores de la División de Matemáticas Aplicadas del Instituto Potosino de Investigación Científica y Tecnológica, A.C.

Dr. Arturo Zavala Río
Director de la tesis

Dr. Víctor Adrián Santibáñez Dávila
Jurado en el Examen

Dr. Daniel Ulises Campos Delgado
Jurado en el Examen

Dr. David Antonio Lizárraga Navarro
Jurado en el Examen

Dr. Eric Campos Cantón
Jurado en el Examen

Dr. José Fernando Reyes Cortés
Jurado en el Examen

Créditos Institucionales

Esta tesis fue elaborada en la División de Matemáticas Aplicadas del Instituto Potosino de Investigación Científica y Tecnológica, A.C., bajo la dirección del Dr. Arturo Zavala Río.

Durante la realización del trabajo el autor recibió una beca académica del Consejo Nacional de Ciencia y Tecnología CONACYT-209539 y del Instituto Potosino de Investigación Científica y Tecnológica, A. C.

Instituto Potosino de Investigación Científica y Tecnológica, A.C.

Acta de Examen de Grado

El Secretario Académico del Instituto Potosino de Investigación Científica y Tecnológica, A.C., certifica que en el Acta 014 del Libro Primero de Actas de Exámenes de Grado del Programa de Doctorado en Ciencias Aplicadas en la opción de Control y Sistemas Dinámicos está asentado lo siguiente:

En la ciudad de San Luis Potosí a los 16 días del mes de agosto del año 2013, se reunió a las 10:00 horas en las instalaciones del Instituto Potosino de Investigación Científica y Tecnológica, A.C., el Jurado integrado por:

Dr. Víctor Adrián Santibáñez Dávila	**Presidente**	**ITL**
Dr. Arturo Zavala Río	**Secretario**	**IPICYT**
Dr. Daniel Ulises Campos Delgado	**Sinodal externo**	**UASLP**
Dr. David Antonio Lizárraga Navarro	**Sinodal**	**IPICYT**
Dr. Eric Campos Cantón	**Sinodal**	**IPICYT**
Dr. José Fernando Reyes Cortés	**Sinodal externo**	**BUAP**

a fin de efectuar el examen, que para obtener el Grado de:

DOCTORA EN CIENCIAS APLICADAS
EN LA OPCIÓN DE CONTROL Y SISTEMAS DINÁMICOS

sustentó la C.

Daniela Juanita López Araujo

sobre la Tesis intitulada:

Adaptive control of robot manipulators with bounded inputs

que se desarrolló bajo la dirección de

Dr. Arturo Zavala Río

El Jurado, después de deliberar, determinó

APROBARLA

Dándose por terminado el acto a las 12:00 horas, procediendo a la firma del Acta los integrantes del Jurado. Dando fe el Secretario Académico del Instituto.

A petición de la interesada y para los fines que a la misma convengan, se extiende el presente documento en la ciudad de San Luis Potosí, S.L.P., México, a los 16 días del mes de agosto de 2013.

Dr. Marcial Bonilla Marín
Secretario Académico

Mtra. Ivonne Lizette Cuevas Vélez
Jefa del Departamento del Posgrado

INSTITUTO POTOSINO DE INVESTIGACIÓN CIENTÍFICA Y TECNOLÓGICA, A.C.
IPICYT
SECRETARIA ACADEMICA

To my family

Acknowledgements

I take this opportunity to express my gratitude to the people who have helped in the successful completion of this dissertation. First, I would like to express my gratitude to Dr. Arturo Zavala Río. I cannot thank enough his tremendous support, motivation, and help. I deeply appreciate your friendship and trust.

I would also like to thank Dr. Víctor Santibáñez and Dr. Fernando Reyes for their support and valuable contributions throughout the development of the dissertation, as well as for the disposition of their robot manipulators to carry out the experimental part of this research.

I also acknowledge the IPICYT for the financial support provided. It made possible to carry out the experimental part of this work in addition to allowing me to attend a congress to present some results of the research. Special thanks to CONACyT for the student grant given.

Resumen

La tesis se enfoca en el diseño de leyes de control adaptables para robots manipuladores que consideran la naturaleza acotada de los actuadores. Se proponen esquemas generalizados para regulación y seguimiento globales por retroalimentación de estados, cuyas estructuras permiten obtener versiones adaptables acotadas de algoritmos tipo PD previamente propuestos para el caso de conocimiento paramétrico exacto. También se diseñó una ley de control tipo SP-SD por retroalimentación de salida para la estabilización global de posición. Con respecto a trabajos previos, los esquemas adaptables propuestos son los primeros que resuelven los problemas de control formulados: globalmente, sin involucrar discontinuidades, evitando saturación de entrada y liberando las ganancias de control de restricciones para evitar el fenómeno de saturación. Más aún, ninguno de los esquemas propuestos está restringido a usar una función de saturación específica para lograr el acotamiento deseado sino que es posible escoger cualquiera dentro de un conjunto de funciones pasivas acotadas que incluye la tangente hiperbólica como caso particular. La eficacia de los controladores propuestos es probada tanto en simulación como experimentalmente.

Palabras clave: Robots manipuladores, entradas acotadas, regulación global, seguimiento global, control adaptable.

Abstract

This thesis focuses on the design of adaptive control schemes for robot manipulators under the consideration of the bounded nature of actuators. Generalized state-feedback controllers are proposed for global regulation and trajectory tracking, whose structures allow to obtain adaptive versions of bounded PD-type algorithms previously developed under the consideration of the exact knowledge of the system parameters. A globally stabilizing SP-SD-type output-feedback adaptive regulation scheme is also developed. With respect to previous works, the proposed adaptive controllers are the first to solve the formulated control problems: globally, free of discontinuities throughout the scheme, avoiding input saturation, and liberating the control gains from the satisfaction of *saturation-avoidance* inequalities. Moreover, the developed controllers are not restricted to use a specific saturation function to achieve the required boundedness, but may involve any one within a set of bounded passive functions that include the hyperbolic tangent as a particular case. The efficiency of the proposed methodology was proven both through simulation and experimental implementations

Key words: Robot manipulators, bounded inputs, global regulation, global tracking, adaptive control.

Contents

1 Introduction

1.1 Notation

We denote $\mathbb{R}$ the set of real numbers and $\mathbb{R}^n$ the set of n-dimensional vectors whose entries are real numbers. Let $X \in \mathbb{R}^{m\times n}$ and $y \in \mathbb{R}^n$. Throughout this work, X_{ij} denotes the component of X at its i^{th} row and j^{th} column, X_i represents the i^{th} row of X, and y_i stands for the i^{th} element of y. 0_n represents the origin of $\mathbb{R}^n$, I_n the $n \times n$ identity matrix, $0_{n\times n}$ is the $n \times n$ matrix whose elements are all zero, and $\mathbb{R}_+$ the set of nonnegative real numbers, *i.e.* $\mathbb{R}_+ = [0, \infty)$. $\|\cdot\|$ denotes the standard Euclidean norm for vectors, *i.e.* $\|y\| = \sqrt{\sum_{i=0}^{n} y_i^2}$, and induced norm for matrices, *i.e.* $\|X\| = \sqrt{\lambda_{\max}(X^T X)}$, where $\lambda_{\max}(X^T X)$ represents the maximum eigenvalue of $X^T X$. The kernel of X is denoted $\ker(X)$ while, for $m = n$, $\det(X)$ denotes the determinant of X. We denote $\mathcal{B}_r \subset \mathbb{R}^n$ an origin-centered ball of radius $r > 0$, *i.e.* $\mathcal{B}_r = \{x \in \mathbb{R}^n : \|x\| \leq r\}$. Let $\mathcal{D}$ and $\mathcal{E}$ be subsets (with non-empty interior) of some vector spaces $\mathbb{D}$ and $\mathbb{E}$ respectively. We denote $\mathcal{C}^m(\mathcal{D}; \mathcal{E})$ the set of m-times continuously differentiable functions from $\mathcal{D}$ to $\mathcal{E}$ (with differentiability at any point on the boundary of $\mathcal{D}$, when included in the set, meant as the limit from the interior of $\mathcal{D}$). For a dynamic/time variable υ, $\dot{\upsilon}$ and $\ddot{\upsilon}$ respectively denote its first- and second-order evolution/change rate. Consider a continuously differentiable scalar function $\zeta : \mathbb{R} \to \mathbb{R}$ and a locally Lipschitz-continuous scalar function $\phi : \mathbb{R} \to \mathbb{R}$, both vanishing at zero, *i.e.* $\zeta(0) = \phi(0) = 0$. Let ζ' denote the derivative of ζ, *i.e.* $\zeta'(\varsigma) = \frac{d\zeta}{d\varsigma}(\varsigma)$, and $D^+\phi$ stand for the upper-right (Dini) derivative of ϕ, *i.e.* $D^+\phi(\varsigma) = \limsup_{h\to 0^+} \frac{\phi(\varsigma+h)-\phi(\varsigma)}{h}$, with $D^+\phi = \phi'$ at points of differentiability [22, App. C.2] [38, App. I]. Thus, $\phi(\varsigma) = \int_0^\varsigma D^+\phi(r)dr$; moreover, $(\zeta \circ \phi)(\varsigma) = \zeta(\phi(\varsigma)) = \int_0^\varsigma \zeta'(\phi(r))D^+\phi(r)dr$. Furthermore, as conventionally, ϕ^{-1} represents the inverse function of ϕ (whenever invertible), and $\text{sat}(\cdot)$ denotes de standard (unitary) saturation function, *i.e.* $\text{sat}(\varsigma) = \text{sign}(\varsigma)\min\{|\varsigma|, 1\}$.

The following acronyms are used to name and distinguish the control schemes de-

scribed throughout this work.

PD	Proportional plus derivative control actions.
PDgc	Proportional plus derivative with gravity compensation term.
SP-SD	Scheme with saturated proportional term plus saturated derivative term.
SPD	Scheme with both proportional and derivative actions within a single saturation.
SPDgc-like	Saturated proportional plus saturated derivative plus gravity compensation, all terms embedded in a single saturation function.
SP-SD$_c$-g$_a$	Saturated proportional plus saturated derivative with calculated velocity and adaptable gravity compensation.
SP-SD+	Saturated proportional plus saturated derivative plus system dynamics compensation.
SPD+	Proportional and derivative actions within a single saturation plus system dynamics compensation.
SPDhc+-like	Saturated proportional plus saturated derivative plus hybrid system dynamics compensation, all terms in a single saturation.
Z$_e$00	Represents the control scheme proposed in [50].
L00	Algorithm presented in [25].
D$_e$99	Control scheme appearing in [12].

1.2 Robot manipulators

Mechanical manipulators are articulated systems created from links connected by joints forming a *kinematic chain*. Links are the rigid part of the manipulator while joints are the movable components that produce relative motion between adjoining links. Joints are usually revolute —allowing a relative rotation between consecutive links— or prismatic —allowing a linear displacement between two consecutive links—. The relative displacement between adjacent links is represented by *joint variables*. The configuration of the manipulator can be specified by knowing the value of all the joint variables; the set of all posible configurations a manipulator can adopt is called *configuration space*. If the configuration of a system can be described uniquely by n independent coordinates —generally corresponding to the joint variables— and is said to have n *degrees of freedom* (DOF). These n independent coordinates are referred to as *generalized coordinates*. As an example, the configuration of a rigid object in a three dimensional space can be fully described by six parameters, three for position and three for orientation, and hence it has six degrees of freedom.

The *kinematic model* represents the motion of the robot without regard to the forces that created motion, while the *dynamic model* relates the motion to the forces involved in its generation. The dynamic model can be obtained using Newtonian mechanics. The disadvantage of this method is that the analysis becomes more difficult when the number of degrees of freedom increases. Alternatively, the dynamic model can be easily

derived from the Lagrange's equations of motion. This method is discussed in greater detail in the following section.

1.2.1 Lagrange's equations of motion

The equations obtained through this procedure are derived from a single function, namely, the *Lagrangian*. The Lagrangian is defined as the difference between the kinetic and potential energy functions, *i.e.*

$$\mathcal{L}(q, \dot{q}) = \mathcal{K}(q, \dot{q}) - U(q)$$

where $q = [q_1, \ldots, q_n]^T$ are the generalized coordinates, $\mathcal{K}(q, \dot{q}) = \frac{1}{2}\dot{q}^T H(q)\dot{q}$ is the kinetic energy with $H(q)$ being the inertia matrix, and $U(q)$ is the potential energy. The Lagrange's equation of motion can be derived from Hamilton's principle and is given by (for further details see [15], [31]):

$$\frac{d}{dt}\frac{\partial \mathcal{L}}{\partial \dot{q}_i} - \frac{\partial \mathcal{L}}{\partial q_i} = \tau_i$$

for $i = 1, \ldots, n$. The resulting equation can be written as

$$\sum_{j=1}^{n} H_{ij}(q)\ddot{q}_j + \sum_{j=1}^{n}\sum_{k=1}^{n} c_{ijk}(q)\dot{q}_j\dot{q}_k + g_i(q) = \tau_i$$

where $g_i(q) = \frac{\partial U}{\partial q_i}(q)$ (the gravity terms), c_{ijk} are known as Christoffel symbols of the first kind, and are defined by

$$c_{ijk} = \frac{1}{2}\left[\frac{\partial H_{kj}}{\partial q_i} + \frac{\partial H_{ki}}{\partial q_j} + \frac{\partial H_{ij}}{\partial q_k}\right]$$

The $\mathbb{R}^{n\times n}$ arrangement whose elements are computed as

$$C_{kj}(q, \dot{q}) = \begin{pmatrix} c_{1jk}(q) \\ \vdots \\ c_{njk}(q) \end{pmatrix}^T \dot{q}$$

is called the Coriolis matrix, denoted $C(q, \dot{q})$, which has important properties summarized in the next section.

1.2.2 The manipulator dynamics and its properties

The general n-DOF serial rigid robot manipulator dynamics with viscous friction can be expressed as [4, §2.1], [42, §6.2], [26, §7.2]:

$$H(q)\ddot{q} + C(q, \dot{q})\dot{q} + F\dot{q} + g(q) = \tau \tag{1.1}$$

where q, $\dot{q}$, $\ddot{q} \in \mathbb{R}^n$ are, respectively, the position (generalized coordinates), velocity, and acceleration vectors, $H(q) \in \mathbb{R}^{n\times n}$ is the inertia matrix, and $C(q, \dot{q})\dot{q}$, $F\dot{q}$, $g(q)$,

$\tau \in \mathbb{R}^n$ are, respectively, the vectors of Coriolis and centrifugal, viscous friction, gravity, and external input generalized forces, with with $F = \mathrm{diag}[f_1, \ldots, f_n]$ where $f_i > 0$, $i = 1, \ldots, n$, are the viscous friction coefficients[1]. The terms of such model posses widely known properties, (see for instance [20, Chap. 4 & 14] and [14] concerning Property 1.5 and 1.7). Some of them are recalled here. Subsequently we denote $\dot{H} : \mathbb{R}^n \times \mathbb{R}^n \to \mathbb{R}^{n \times n} : (q, \dot{q}) \mapsto \left[\frac{\partial H_{ij}}{\partial q}(q)\dot{q}\right]$ for every $i, j = 1, \ldots, n$.

Property 1.1 *The inertia matrix $H(q)$ is positive definite, symmetric, and bounded, i.e. there exist positive constants $\mu_m \leq \mu_M$ such that*

$$\mu_m I_n \leq H(q) \leq \mu_M I_n$$

$\forall q \in \mathbb{R}^n$. ◁

Property 1.2 *The Coriolis matrix satisfies:*

1.2.1 $\dot{q}^T \left[\frac{1}{2}\dot{H}(q, \dot{q}) - C(q, \dot{q})\right] \dot{q} = 0$, $\forall (q, \dot{q}) \in \mathbb{R}^n \times \mathbb{R}^n$;

1.2.2 $\dot{H}(q, \dot{q}) = C(q, \dot{q}) + C^T(q, \dot{q})$, $\forall (q, \dot{q}) \in \mathbb{R}^n \times \mathbb{R}^n$;

1.2.3 $C(w, x + y)z = C(w, x)z + C(w, y)z$, $\forall w, x, y, z \in \mathbb{R}^n$;

1.2.4 $C(x, y)z = C(x, z)y$, $\forall x, y, z \in \mathbb{R}^n$;

1.2.5 $\|C(x, y)z\| = k_C \|y\| \|z\|$, $\forall (x, y, z) \in \mathbb{R}^n \times \mathbb{R}^n \times \mathbb{R}^n$, *for some constant* $k_C \geq 0$.

◁

Property 1.3 *The viscous friction coefficient matrix satisfies*

$$f_m \|x\|^2 \leq x^T F x \leq f_M \|x\|^2$$

$\forall x \in \mathbb{R}^n$, *where* $0 < f_m \triangleq \min_i\{f_i\} \leq \max_i\{f_i\} \triangleq f_M$. ◁

Property 1.4 *The gravity vector is bounded, or equivalently, every element of the gravity vector, $g_i(q)$, $i = 1, \ldots, n$, satisfies $|g_i(q)| \leq B_{gi}$, $\forall q \in \mathbb{R}^n$, for some positive constants B_{gi}, $i = 1, \ldots, n$.*[2] ◁

[1] The terms in the left-hand side of the manipulator dynamics in Eq. (1.1) involve a set of parameters $\theta \in \mathbb{R}^p$. Subsequently, whenever convenient, such a parametric dependence of $H(q)$, $C(q, \dot{q})$, F, and $g(q)$ will be explicitly denoted as $H(q, \theta)$, $C(q, \dot{q}, \theta)$, $F(\theta)$, and $g(q, \theta)$.

[2] Property 1.4 is not satisfied by all types of robot manipulators but it is for instance by those having only revolute joints [20, §4.3]. This work is addressed to manipulators satisfying Property 1.4.

Property 1.5 *The gravity vector can be rewritten as $g(q,\theta) = G(q)\theta$, where $\theta \in \mathbb{R}^p$ is a constant vector whose elements depend exclusively on the system parameters, and $G(q) \in \mathbb{R}^{n\times p}$ —the regression matrix— is a continuous matrix function whose elements depend exclusively on the configuration variables and do not involve any of the system parameters. Equivalently, the potential energy function of the robot can be rewritten as $U(q,\theta) = \Upsilon(q)\theta$, where $\Upsilon(q) \in \mathbb{R}^{1\times p}$ —the regression vector— is a continuous row vector function whose elements depend exclusively on the configuration variables and do not involve any of the system parameters. Actually, $G^T(q) = \frac{\partial}{\partial q}\Upsilon^T(q)$, or equivalently, $\Upsilon_j(q) = \sum_{i=1}^{n}\int_{q_i^*}^{q_i} G_{ij}(q_1,\ldots,q_{i-1},r_i,q_{i+1}^*,\ldots,q_n^*)dr_i$, $\forall j \in \{1,\ldots,p\}$, with $q^* = (q_1^*,\ldots,q_n^*)^T$ being the reference configuration where $U(q^*,\theta) = 0$.*[3] ◁

Property 1.6 *Consider the gravity vector $g(q,\theta)$. Let θ_{Mj} represent an upper bound of $|\theta_j|$, such that $|\theta_j| \leq \theta_{Mj}$, $\forall \in \{1,\ldots,p\}$, and let $\theta_M \triangleq \left(\theta_{M1},\ldots,\theta_{M_P}\right)^T$ and $\Theta \triangleq [-\theta_{M1},\theta_{M1}]\times\cdots\times[-\theta_{M_P},\theta_{M_P}]$. By Properties 1.4 and 1.5, there exist positive constants $B_{gi}^{\theta_M}$, $i = 1,\ldots,n$, such that $|g_i(x,y)| = |G_i(x)y| \leq B_{gi}^{\theta_M}$, $i = 1,\ldots,n$, $\forall x \in \mathbb{R}^n$, $\forall y \in \Theta$. Furthermore, there exist positive constants $B_{G_{ij}}$, B_{G_i}, and B_G such that $|G_{ij}(x)| \leq B_{G_{ij}}$, $\|G_i(x)\| \leq B_{G_i}$, and $\|G(x)\| \leq B_G$, $\forall x \in \mathbb{R}^n$, $i = 1,\ldots,n$, $j = 1,\ldots,p$.* ◁

Property 1.7 *The left-hand side of the robot dynamic model in Eq. (1.1) can be rewritten as*

$$H(q,\psi)\ddot{q} + C(q,\dot{q},\psi)\dot{q} + F(\psi)\dot{q} + g(q,\psi) = Y(q,\dot{q},\ddot{q})\psi$$

where $\psi \in \mathbb{R}^\rho$ is a constant vector whose elements depend exclusively on the system parameters, and $Y(q,\dot{q},\ddot{q}) \in \mathbb{R}^{n\times\rho}$ —the regression matrix —is a continuous matrix function whose elements depend exclusively on configuration, velocity and acceleration variables and do not involve any of the system parameters. Even more, each term of the left-hand side of (1.1) can be analogously rewritten as $H(q,\psi)\ddot{q} = Y_H(q,\ddot{q})\psi$, $C(q,\dot{q},\psi)\dot{q} = Y_C(q,\dot{q})\psi$, $F(\psi)\dot{q} = Y_F(\dot{q})\psi$, and $g(q,\psi) = Y_g(q)\psi$, and actually $Y(q,\dot{q},\ddot{q}) = Y_H(q,\ddot{q}) + Y_C(q,\dot{q}) + Y_F(\dot{q}) + Y_g(q)$. ◁

Property 1.8 *Consider the manipulator dynamics $Y(q,\dot{q},\ddot{q})\psi = H(q,\psi)\ddot{q}+C(q,\dot{q},\psi)\dot{q}+F(\psi)\dot{q}+g(q,\psi) = \tau$. Let ψ_{Mj} represent an upper bound of ψ_j, such that $\psi_j \leq \psi_{Mj}$, $\forall j \in \{1,\ldots,\rho\}$, and let $\psi_M \triangleq \left(\psi_{M1},\ldots,\psi_{M\rho}\right)^T$ and $\Psi \triangleq [-\psi_{M1},\psi_{M1}]\times\cdots\times[-\psi_{M\rho},\psi_{M\rho}]$.*

a. By Properties 1.4 and 1.7, there exist positive constants $B_{gi}^{\psi_M} \geq B_{gi}$, $i = 1,\ldots,n$, such that $|g_i(x,y)| = |Y_{gi}(x)y| \leq B_{gi}^{\psi_M}$, $i = 1,\ldots,n$, $\forall x \in \mathbb{R}^n$, $\forall y \in \Psi$. Furthermore, there exist positive constants $B_{G_{ij}}$, B_{G_i}, and B_G such that $|Y_{gij}(x)| \leq B_{G_{ij}}$, $\|Y_{gi}(x)\| \leq B_{G_i}$, and $\|Y_g(x)\| \leq B_G$, $\forall x \in \mathbb{R}^n$, $i = 1,\ldots,n$, $j = 1,\ldots,\rho$.

[3]The reference configuration q^* is the generalized position with respect to which $U(q,\theta)$ is quantified. In other words, $U(q,\theta)$ represents the amount of work needed to relocate the system configuration at q departing from q^*.

b. Let $\mathcal{X}$ and $\mathcal{Y}$ be any compact subsets of $\mathbb{R}^n$. By Properties 1.1, 1.2.5, 1.7, and 1.8a., there exist positive constants $B_{Di}^{\psi_M}$, $i = 1, \ldots, n$ such that

$$|Y_i(w, x, y)z| \leq B_{Di}^{\psi_M}, \quad i = 1, \ldots, n, \quad \forall (w, x, y, z) \in \mathbb{R}^n \times \mathcal{X} \times \mathcal{Y} \times \Psi$$

Further, there exist positive constants $B_{Y_{ij}}$, B_{Y_i}, and B_Y such that $|Y_{ij}(w, x, y)| \leq B_{Y_{ij}}$, $\|Y_i(w, x, y)\| \leq B_{Y_i}$, and $\|Y(w, x, y)\| \leq B_Y$, for all $(w, x, y) \in \mathbb{R}^n \times \mathcal{X} \times \mathcal{Y}$, $i = 1, \ldots n$, $j = 1, \ldots, \rho$.

◁

Remark 1.1 Let us note that under the consideration of Property 1.8, by Properties 1.1, 1.2.5, 1.3, 1.7, and 1.8a., there exist positive constants $\mu_M^{\psi_M}$, $k_C^{\psi_M}$, and $f_M^{\psi_M}$, such that $|Y_i(w, x, y)z| \leq \mu_M^{\psi_M}\|y\| + k_C^{\psi_M}\|x\|^2 + f_M^{\psi_M}\|x\| + B_{gi}^{\psi_M}$, $i = 1, \ldots, n$, for all $(w, x, y, z) \in \mathbb{R}^n \times \mathcal{X} \times \mathcal{Y} \times \Psi$. Observe from this expression that for any $T_i > B_{gi}^{\psi_M}$, there always exist sufficiently small positive values a and b (for instance, such that $\mu_M^{\psi_M} b + k_C^{\psi_M} a^2 + f_M^{\psi_M} a < T_i - B_{gi}^{\psi_M}$) that guarantee $|Y_i(w, x, y)z| < T_i$, $i = 1, \ldots, n$, on $\mathbb{R}^n \times \mathcal{B}_a \times \mathcal{B}_b \times \Psi$. ◁

In Appendix A, the dynamic models of a 2-DOF robotic arm and a 3-DOF anthropomorphic manipulator are thoroughly obtained.

1.3 Bounded inputs

Real-life actuators have a limited range of operation which is a natural consequence of their power supply limitations. When a controller does not account for this natural limitation input *saturation* may occur. This unavoidable nonlinear phenomenon generally characterizes the signal transfer from the controller outputs to the plant inputs. Ignoring such a physical constraint may lead to unexpected or undesirable consequences, as pointed out for instance in [10], [18], [23], and [24]. Control synthesis under the consideration of such inevitable nonlinearity has consequently become important and considerably attracted the attention of the feedback control community [7].

1.4 Control of robot manipulators

If we use the control objective as a way to classify controllers, it can be said that there exist two kinds of control schemes: those who aim for *position control* or *regulation* and those whose objective is *motion control* or *tracking*. The problem of *position control* for robot manipulators consists in designing a control law $u(q, \dot{q}, \theta)$, with $\theta \in \mathbb{R}^p$ a system parameter vector, such that, given a desired or target (constant) configuration $q_d \in \mathbb{R}^n$, when $\tau = u(q, \dot{q}, \theta)$ in (1.1), $q(t) \equiv q_d$ becomes an asymptotically stable solution of the closed loop. This becomes a global regulation problem if, in addition to the asymptotic stability, $q(t) \equiv q_d$ is aimed at being rendered globally attractive, *i.e.* $q(t) \to q_d$ as $t \to \infty$, $\forall (q, \dot{q})(0) \in \mathbb{R}^n \times \mathbb{R}^n$.

When the parameter vector θ is unknown *adaptive control* may be useful to achieve the desired objective. In this context, position control becomes an adaptive regulation problem, which may be formulated in the following terms. Given $q_d \in \mathbb{R}^n$, one should be able to propose a dynamic control law $u(q, \dot{q}, \hat{\theta})$, $\dot{\hat{\theta}} = h(q, \dot{q})$, independent of the exact values of the system parameters, such that, for the closed-loop system

$$\begin{cases} H(q)\ddot{q} + C(q, \dot{q})\dot{q} + F\dot{q} + g(q) = u(q, \dot{q}, \hat{\theta}) \\ \dot{\hat{\theta}} = h(q, \dot{q}) \end{cases}$$

$(q, \hat{\theta})(t) \equiv (q_d, \theta)$ becomes a stable solution of the closed loop, simultaneously guaranteeing the existence of a subset $D \subset \mathbb{R}^n \times \mathbb{R}^n \times \mathbb{R}^p$, containing $(q_d, 0_n, \theta)$, such that $q(t) \to q_d$ as $t \to \infty$, $\forall (q, \dot{q}, \hat{\theta})(0) \in D$. This becomes a global adaptive regulation problem if the convergence of $q(t)$ towards q_d is aimed at being achieved for any initial condition, *i.e.* if $D = \mathbb{R}^n \times \mathbb{R}^n \times \mathbb{R}^p$.

Under the consideration of the input saturation phenomenon, the bounded adaptive regulation objective can be stated as designing a dynamic control law $u = u(q, \dot{q}, \hat{\theta})$, $\dot{\hat{\theta}} = h(q, \dot{q})$, independent of the exact values of the system parameters, such that, for the closed loop system

$$\begin{cases} H(q)\ddot{q} + C(q, \dot{q})\dot{q} + F\dot{q} + g(q) = \tau \\ \tau_i = T_i \text{sat}\left(u(q, \dot{q}, \hat{\theta})/T_i\right) \quad i = 1, ..., n \\ \dot{\hat{\theta}} = h(q, \dot{q}) \end{cases}$$

the (global) adaptive regulation objective is guaranteed with (along the system trajectories)

$$|\tau_i(t)| = |u_i(t)| < T_i, \quad \forall t \geq 0, \quad i = 1, ..., n.$$

Analogously, the problem of *motion* or *tracking control* consists in finding a control input $u = u(t, q, \dot{q}, \theta)$, such that, given a desired trajectory $q_d(t) \in \mathbb{R}^n$, when $\tau = u(t, q, \dot{q}, \theta)$ in (1.1), $q(t) \equiv q_d(t)$ becomes a uniformly asymptotically stable solution of the closed loop. This becomes a global tracking control problem if, in addition to the uniformly asymptotic stability, $q(t) \equiv q_d(t)$ is aimed at being uniformly globally attractive, *i.e.* $q(t) \to q_d(t)$ as $t \to \infty$, $\forall (q, \dot{q})(0) \in \mathbb{R}^n \times \mathbb{R}^n$.

Adaptive tracking control may be useful to overcome system parameter uncertainties. It can be defined as follows. Given $q_d(t) \in \mathbb{R}^n$, propose a dynamic control law $u(t, q, \dot{q}, \hat{\theta})$, $\dot{\hat{\theta}} = h(t, q, \dot{q})$, independent of the exact values of the system parameters, such that, for the closed-loop system

$$\begin{cases} H(q)\ddot{q} + C(q, \dot{q})\dot{q} + F\dot{q} + g(q) = u(t, q, \dot{q}, \hat{\theta}) \\ \dot{\hat{\theta}} = h(t, q, \dot{q}) \end{cases}$$

$\left(q(t), \hat{\theta}(t)\right) \equiv \left(q_d(t), \theta\right)$ is a uniformly stable solution of the closed loop, while guaranteeing $q(t) \to q_d(t)$ as $t \to \infty$, for initial conditions sufficiently close to the desired trajectory. If this objective is achieved for any initial condition this becomes a global adaptive tracking problem.

Considering in the control design input saturation, the bounded adaptive tracking objective can be stated as proposing a dynamic control law $u = u(t, q, \dot{q}, \hat{\theta})$, $\dot{\hat{\theta}} = h(t, q, \dot{q})$, independent of the exact values of the system parameters, such that, for the closed loop system

$$\begin{cases} H(q)\ddot{q} + C(q,\dot{q})\dot{q} + F\dot{q} + g(q) = \tau \\ \tau_i = T_i \text{sat}\left(u(t, q, \dot{q}, \hat{\theta})/T_i\right) \quad i = 1, ..., n \\ \dot{\hat{\theta}} = h(t, q, \dot{q}) \end{cases}$$

the (global) adaptive tracking objective is achieved with

$$|\tau_i(t)| = |u_i(t)| < T_i, \quad \forall t \geq 0, \quad i = 1, ..., n.$$

1.5 Previous works

Disregarding input saturation, one of the simplest control techniques for the global regulation of robot manipulators is the so-called *PD with gravity compensation* [20, Chap. 7] (**PDgc**). In its original form, it achieves the global stabilization objective under ideal conditions, for instance: unconstrained input, availability of all the link positions and velocities, and exact knowledge of the system parameters. Inspired by this control method, and in view of the undesirable effects of saturation, researchers have developed alternative (nonlinear or dynamic) PDgc-based approaches that deal with the limitations on the actuator capabilities and/or on the available system data, while keeping the natural energy properties of the original PDgc controller: definition of a unique arbitrarily-located closed-loop equilibrium configuration and motion dissipation. For instance, assuming that the exact value of the system parameters and accurate measurements of all the system states (positions and velocities) are available, a basic approach was proposed in [19] and [41]. In these works the P and D parts (at every joint) are, each of them, explicitly bounded through specific *saturation functions*: a continuously differentiable one —more precisely, the hyperbolic tangent function— is used in [19] and the conventional non-smooth one in [41]. Because of their structure, this type of algorithms have been denoted *SP-SD* controllers in [39] (where a previous version of the work in [41] was presented). Further, two alternative schemes, that prove to be simpler and/or give rise to improved closed-loop performances, were recently proposed in [47]. The first approach includes both the P and D parts (at every joint) within a single saturation function, while in the second one all the terms of the controller (P, D, and gravity compensation) are covered by one of such functions, with the P terms internally embedded within an additional saturation.

Moreover, free-of-velocity-measurement versions of the SP-SD controllers in [19] and [41] —still depending on the exact values of the system parameters— are obtained through the design methodologies developed in [29] and [40]. In [40], global regulation is proved to be achieved when each velocity measurement is replaced by the *dirty derivative* [33] of the respective position in the SP-SD controller of [41]. A similar replacement in a more general form of the SP-SD controller is proved to achieve global

regulation through the design procedure proposed in [29] (where an alternative type of dirty derivative, that involves a saturation function in the auxiliary dynamics giving rise to the estimated velocity, results from the application of the proposed methodology). Furthermore, an output feedback dynamic controller with a structure similar to that resulting from the methodology in [29], but which considers a single saturation function (at every joint) where both the position errors and velocity estimation states are involved, was proposed in [8] (where a *dissipative* linear term on the auxiliary state is added to the saturating velocity error dynamics involved for the dirty derivative calculation); extensions of this approach to the elastic-joint case were further developed in [9].

In view of the gravity compensation terms, the implementation of the above mentioned saturating schemes becomes specially problematic when the system parameters are uncertain. Because of the potential undesirable effects that this constraint can induce, bounded adaptive SP-SD-type algorithms have been developed in [11, 12, 25, 50].

- In [11] global regulation is aimed through a discontinuous scheme that switches among two different control laws, under the consideration of state and output feedback. Both proposed control laws keep an SP-SD structure similar to that of [41]. These algorithms were designed under the consideration of the manipulator dynamics without friction, *i.e.*

$$H(q)\ddot{q} + C(q,\dot{q})\dot{q} + G(q,\theta) = \tau \tag{1.2}$$

For the state feedback case the authors first propose a non-adaptive scheme without gravity compensation of the form

$$\tau = k_D\gamma \mathrm{sat}(\dot{e}) + k_P\gamma^2 \mathrm{sat}(e) \tag{1.3}$$

where $e = q_d - q$ represents the position error vector, $k_P, k_D, \gamma \in \mathbb{R}$ are positive constants, and $\mathrm{sat}(\cdot)$ is the standard saturation function. The authors prove that the closed-loop system, Eqs. (1.2) and (1.3), possesses a unique equilibrium vector that can be approached to q_d by increasing γ, and this equilibrium position is globally asymptotically stable. To achieve the convergence the authors propose to switch the algorithm in Eq. (1.3) to the unbounded adaptive control law

$$\tau = f(t) + k_D\gamma\dot{e} + k_P\gamma^2 e \tag{1.4a}$$

$$\dot{f} = \beta\left(1 - b\frac{ff^T}{\|f\|}\right)\left(\dot{e} - \frac{k_P}{k_D\gamma}e\right) \tag{1.4b}$$

with

$$b = \begin{cases} 0 & \text{if} \quad (\|f\| \le f_{\max}) \wedge \left[f^T\left(\dot{e} - \frac{k_P}{k_D\gamma}e\right) \le 0\right] \\ 1 & \text{if} \quad \text{Otherwise} \end{cases}$$

where $f_{\max} \triangleq G_{\max} + \delta_2$, and $\beta, \delta_2 \in \mathbb{R}$ are positive constants. For this algorithm, proposed to achieve the desired convergence, the author shows that all signals are bounded and that the error vectors e, $\dot{e}$ converge asymptotically to the origin,

provided that e and $\dot{e}$ are within the region of attraction of the closed-loop system (1.2)–(1.4). It was also concluded that the region of attraction can be made arbitrarily large by increasing γ in the control law (1.4).

In the output feedback case each velocity measurement is replaced by the dirty derivative of the corresponding position. The followed methodology and stability properties are the same as in the state feedback case. Unfortunately, a precise criterion to determine the switching moment (from the first control law to the second one) is not furnished for either of the proposed schemes.

- In [50], semiglobal regulation is proved to be achieved through a state feedback scheme that keeps the same structure of the SP-SD controller of [19] but additionally considers adaptive gravity compensation. The proposed controller was designed under the consideration of the manipulator dynamics with viscous and Coulomb friction, *i.e.*

$$H(q)\ddot{q} + C(q,\dot{q})\dot{q} + F_d\dot{q} + F_s\text{sign}(\dot{q}) + g(q,\theta) = \tau \tag{1.5}$$

where $\text{sign}(\dot{q})$ denotes a vector whose elements are given by $\big(\text{sign}(\dot{q}_1),\ldots,\text{sign}(\dot{q}_n)\big)^T$ The adaptation algorithm is defined as

$$\tau = G^T(q)\hat{\theta} - K_P T_h(\bar{q}) - K_D T_h(\dot{q}) \tag{1.6a}$$

$$\dot{\hat{\theta}} = P\big(Q(\bar{q},\dot{q}),\hat{\theta}\big) \tag{1.6b}$$

where $\bar{q} = q - q_d$, for any desired configuration vector $q_d \in \mathbb{R}^n$, $T_h(x) = \big(\tanh(x_1),\ldots,\tanh(x_n)\big)^T$, $Q(\bar{q},\dot{q}) = -\Gamma G^T(q)[\dot{q} + \varepsilon T_h(\bar{q})]$, P is defined in terms of a discontinuous expression —by means of which the parameter estimators are prevented to take values beyond some pre-specified limits, which consequently keeps the adaptive gravity term bounded—, whose elements are given as

$$P_j(Q,\hat{\theta}) = \begin{cases} Q_j & \text{if } \theta_{jm} < \hat{\theta}_j < \theta_{jM} \text{ or } \big(\hat{\theta}_j \le \theta_{jm} \text{ and } Q_j \ge 0\big) \text{ or } \big(\hat{\theta}_j \ge \theta_{jM} \text{ and } Q_j \le 0\big) \\ 0 & \text{if } \big(\hat{\theta}_j \le \theta_{jm} \text{ and } Q_j < 0\big) \text{ or } \big(\hat{\theta}_j \ge \theta_{jM} \text{ and } Q_j > 0\big) \end{cases}$$

$j = 1,\ldots,p$, where θ_{jm} and θ_{jM} are known lower and upper bounds of θ_i respectively. The author prove that given the system dynamics Eq. (1.5), the control law in Eqs. (1.6) ensures asymptotic stability, provided that K_P, K_D, and ε satisfy some inequalities, with a region of attraction that may be enlarged by increasing the control gains. Once the gains are defined, the author provides an explicit bound on the torque input, namely

$$\|\tau\| \le \|G(q)\|_{i\infty}\|\bar{\theta}\| + \lambda_M K_P + \lambda_M K_D$$

where $\bar{\theta} = \theta - \hat{\theta}$ and $\|\cdot\|_{i\infty}$ denotes the induced infinity norm of a matrix. This approach was further extended in [13] to the case when the control objective is defined in *task coordinates* and the kinematic parameters —additionally to the dynamic ones— are considered to be uncertain too.

- In [25], an adaptive output feedback regulation scheme was proposed. The considered system dynamics is shown in Eq. (1.2). The author replaces each velocity measurement by the dirty derivative of the corresponding position, and considers an unbounded adaptive gravity compensation term. The proposed control law is of the form

$$\tau = -K_P T_h(\lambda \bar{q}) - K_D T_h(\delta \vartheta) + G_d \hat{\theta} \tag{1.7a}$$

where $G_d = G(q_d)$, $T_h(x) = \big(\tanh(x_1), \ldots, \tanh(x_n)\big)^T$, $K_P \in \mathbb{R}^{n\times n}$ and $K_D \in \mathbb{R}^{n\times n}$ are positive definite diagonal matrices, λ and δ are positive constants, and $\vartheta \in \mathbb{R}^n$ and $\hat{\theta} \in \mathbb{R}^p$ are the output variables of (interconnected) auxiliary dynamic subsystems that take the form:

$$\dot{q}_c = -\alpha K(q_c + K\bar{q}) \tag{1.7b}$$
$$\vartheta = q_c + K\bar{q} \tag{1.7c}$$

and

$$\dot{\phi}_c = \beta G_d^T \big[\eta T_h(\delta\vartheta) - \mu T_h(\lambda\bar{q})\big] \tag{1.7d}$$
$$\hat{\theta} = \phi_c - \beta G_d^T \bar{q} \tag{1.7e}$$

where $K \in \mathbb{R}^{n\times n}$ is a positive definite diagonal matrix, and α, β, η, and μ are positive constants. Arguing simplicity of development, the gain matrices involved in this control algorithm are taken in [25] as $K_P = k_P I_n$, $K_D = k_D I_n$, and $K = kI_n$, with k_P, k_D, and k being positive constants.

Through the proof of the main result, asymptotic stabilization is concluded to be achieved through the proposed scheme with a region of attraction that may be enlarged by increasing the control gains, while the input is guaranteed to remain within bounds that depend on initial conditions.

- An adaptive state feedback scheme aiming for tracking control was developed in [12]. The dynamic model used considers the viscous friction F, as follows

$$H(q)\dot{q} + C(q,\dot{q})\dot{q} + F\dot{q} + g(q,\theta) = \tau$$

The proposed controller is

$$\tau = Y_d(t)\hat{\theta} - K_P T_h(\bar{q}) - K_D T_h(r) \tag{1.8a}$$
$$\dot{\hat{\theta}} = P\left(Q(t,r), \hat{\theta}\right) \tag{1.8b}$$

where $Y_d(t) = Y(q_d(t), \dot{q}_d(t), \ddot{q}_d(t))$; $T_h(x) = (tanh(x_1), \ldots, tanh(x_n))^T$;

$$r = \dot{\bar{q}} + \varepsilon T_h(\bar{q}) \tag{1.8c}$$

with ε being a positive constant;

$$Q(t,r) = -\Gamma Y_d^T(t) r \tag{1.8d}$$

where K_P, $K_D \in \mathbb{R}^{n\times n}$ and $\Gamma \in \mathbb{R}^{p\times p}$ are positive definite diagonal matrices; the elements of P are defined in terms of the following discontinuous expression

$$P_j(Q,\hat{\theta}) = \begin{cases} Q_j & \text{if } \theta_{jm} < \hat{\theta}_j < \theta_{jM} \text{ or } \left(\hat{\theta}_j \leq \theta_{jm} \text{ and } Q_j \geq 0\right) \text{ or } \left(\hat{\theta}_j \geq \theta_{jM} \text{ and } Q_j \leq 0\right) \\ 0 & \text{if } \left(\hat{\theta}_j \leq \theta_{jm} \text{ and } Q_j < 0\right) \text{ or } \left(\hat{\theta}_j \geq \theta_{jM} \text{ and } Q_j > 0\right) \end{cases}$$

$j = 1, \ldots, p$ with θ_{jm} and θ_{jM} being known lower and upper bounds of θ_j respectively. The authors conclude asymptotic tracking provided that the minimum eigenvalue of K_D is high enough, with a region of attraction that may be enlarged by increasing the control gains. They also provide an explicit bound of the control expression in Eq. (1.8a).

1.6 Motivation

The previously described works are generally local results with a region of attraction that may be enlarged through the control gain values. Only the work in [11] aims at contributing a global result through a variable structure scheme that involves two different control output expressions implying a discontinuous change among them. Unfortunately, such an approach in [11] fails to furnish an analytical criterion to determine the exact condition at which the mentioned a discontinuous change (among the involved output control expressions) should be done. Global results on adaptive control in a bounded input context though continuous (fix structure) algorithms miss in the literature and constitutes one of the main motivations of this dissertation.

On the other hand, all previously described adaptive schemes define the SP and SD terms using only hyperbolic tangent functions to bound the position and velocity error vectors, and with the control gains multiplying the saturation functions. This gives rise to controllers whose saturation bound is defined in terms of the sum of the P and D control gains (and the bound of the parameter estimator), which limits the choice of such gains. This in turn restrains the closed-loop region of attraction in the cases where it can be enlarged by increasing the control gains.

Even more, adaptive control schemes where the parameter estimates are aimed to remain bounded within pre-specified values generally appeal to an adaptation dynamics with discontinuous right hand side, like those appearing in [11] and [50]. The discontinuous character of such type of adaptation dynamics is not necessarily a drawback, but a bounded adaptive scheme avoiding discontinuities constitutes a better alternative developed within a simpler analytical context and making use of more natural ways to cope with the need to bound the parameter estimates.

On the other hand, the control laws appearing in [1, 47] which assume the knowledge of all system parameters, release the gains from satisfying a saturation-avoidance inequality while achieving globally stabilizing results, and also allow the user to choose any saturation function within a set. Adaptive versions of the alternative saturating schemes in [1, 47] have not yet been proposed. Moreover, as far as the authors are aware, a continuous adaptive scheme, with continuous auxiliary dynamics, that achieve the global regulation objective is still missing in the literature.

1.7 Structure of the dissertation

The rest of the work is organized as follows: Chapter 2 presents presents definitions and results that were used in the analyzes developed in this dissertation.

Chapter 3 deals with the development and stability proof of the proposed adaptive control laws. First, the results corresponding to position control are shown in the case of availability of all system states. Then a control scheme that does not involve system velocities is presented. Finally, a trajectory tracking controller is presented assuming availability of states.

Simulation results of all developed schemes are presented in Chapter 4 using the nominal dynamic model of a 2-DOF robot manipulator. Each proposed scheme is compared against one of the controllers of previous works.

Chapter 5 shows experimental results obtained using two different manipulators: the 2-DOF mechanical arm in [36] and the 3-revolute-joint anthropomorphic robot appearing in [37]. The goal is to experimentally compare and corroborate the efficiency of the proposed control laws.

Conclusions and future work perspectives are finally presented in Chapter 6.

2

Mathematical Background

Theorems and definitions used throughout this dissertation are detailed in this chapter. These results were taken from [4, 22, 32, 38, 45].

2.1 Lipschitz continuity

A function $f : D \to \mathbb{R}^n$, with D being a domain (open connected set) contained in $\mathbb{R}^n$, that satisfies

$$\|f(x) - f(y)\| \leq L\|x - y\| \tag{2.1}$$

for all x and y in D and some non-negative constant L, is said to be Lipschitz-continuous in x and the positive constant L is called a *Lipschitz constant*. It is said to be locally Lipschitz-continuous if, for every $x \in D$, there exists a neighborhood D_0 of x such that f restricted to D_0 is Lipschitz-continuous. With $D = \mathbb{R}^n$, it is said to be globally Lipschitz-continuous if (2.1) is satisfied for all x and y in $\mathbb{R}^n$. Similarly, a function $f : \mathbb{R}^n \to \mathbb{R}^n$ is said to be Lipschitz/locally Lipschitz on $D \subset \mathbb{R}^n$ if f restricted to D is Lipschitz-continuous/locally Lipschitz-continuous. An analog terminology is employed for a function $f(t, x)$, provided that the Lipschitz condition holds uniformly in t for all t in a given interval of time. Thus, a function $f(t, x)$ mapping $I \times D \subset \mathbb{R}_+ \times \mathbb{R}^n$ to $\mathbb{R}^n$, with D being a domain contained in $\mathbb{R}^n$, that satisfies

$$\|f(t, y) - f(t, z)\| \leq L\|y - z\| \tag{2.2}$$

for all (t, y) and (t, z) in $I \times D$ and some non-negative constant L, is said to be Lipschitz-continuous in x. It is said to be locally Lipschitz-continuous in x if, for every $y \in D$, there exists a neighborhood D_0 of y such that f restricted to $I \times D_0$ is Lipschitz-continuous. With $D = \mathbb{R}^n$, it is said to be globally Lipschitz-continuous in x if (2.2) is satisfied for all (t, y) and (t, z) in $I \times \mathbb{R}^n$. Similarly, a function $f(t, x)$ mapping $\mathbb{R}_+ \times \mathbb{R}^n$

to $\mathbb{R}^n$ is said to be Lipschitz/locally Lipschitz in x on $I \times D \subset \mathbb{R}_+ \times \mathbb{R}^n$ if f restricted to $I \times D$ is Lipschitz-continuous/locally Lipschitz-continuous.

Lemma 2.1 [22, Lemma 3.1] *Let $f : [a, b] \times D \to \mathbb{R}^n$ be continuous for some domain $D \in \mathbb{R}^n$. Suppose that $[\partial f/\partial x]$ exists and is continuous on $[a, b] \times D$. If, for a convex subset $W \subset D$, there is a constant $L \geq 0$ such that*

$$\left\| \frac{\partial f}{\partial x}(t, x) \right\| \leq L$$

on $[a, b] \times W$, then

$$\|f(t, x) - f(t, y)\| \leq L \|x - y\|$$

for all $t \in [a, b]$, $x \in W$, and $y \in W$. ◁

Lemma 2.1 shows how using the knowledge of $[\partial f/\partial x]$ a Lipschitz constant can be calculated.

The Lipschitz property is stronger than continuity but is weaker than continuous differentiability as stated in the following lemmas.

Lemma 2.2 [22, Lemma 3.2] *If $f(t, x)$ and $[\partial f/\partial x](t, x)$ are continuous on $[a, b] \times D$, for some domain $D \subset \mathbb{R}^n$, then f is locally Lipschitz in x on $[a, b] \times D$.* ◁

Lemma 2.3 [22, Lemma 3.3] *If $f(t, x)$ and $[\partial f/\partial x](t, x)$ are continuous on $[a, b] \times \mathbb{R}^n$, then f is globally Lipschitz in x on $[a, b] \times \mathbb{R}^n$ if and only if $[\partial f/\partial x]$ is uniformly bounded on $[a, b] \times \mathbb{R}^n$.* ◁

2.2 Lyapunov stability

Throughout this section we consider a system of the form

$$\dot{x} = f(t, x) \tag{2.3}$$

where $f : I \times \Omega \to \mathbb{R}^n$, is piecewise continuous in t and locally Lipschitz in x on $I \times \Omega$, with $I \triangleq (\tau, \infty)$, for some $\tau \in \mathbb{R}$, Ω being a domain of $\mathbb{R}^n$ containing de origin, and such that $f(t, 0_n) = 0_n$, $\forall t \geq 0$.

Definition 2.1 [22, Definition 4.4] *The origin of* (2.3) *is*

- ***stable*** *if, for every $\epsilon > 0$ there exists δ such that*

$$\|x(t_0)\| < \delta \quad \Rightarrow \quad \|x(t)\| < \epsilon \qquad \forall t \geq t_0 \geq 0 \tag{2.4}$$

- ***uniformly stable*** *if, for each $\epsilon > 0$, there is $\delta = \delta(\epsilon) > 0$ independent of t_0 such that Eq.* (2.4) *is satisfied.*

- ***unstable*** *if it is not stable;*

- ***asymptotically stable*** *if it is stable and there is a positive constant* $c = c(t_0)$ *such that* $x(t) \to 0$ *as* $t \to \infty, \forall \|x(t_0)\| < c$.

- ***uniformly asymptotically stable*** *if its uniformly stable and there is a positive constant* c*, independent of* t_0*, such that for all* $\|x(t_0)\| < c$*,* $x(t) \to t$ *as* $t \to \infty$*, uniformly in* t_0*, that is, for each* $\eta > 0$*, there is* $T = T(\eta) > 0$ *such that*

$$\|x(t)\| < \eta, \ \forall t \geq t_0 + T(\eta), \ \forall \|x(t_0)\| < c$$

- ***globally uniformly asymptotically stable*** *if its uniformly stable,* $\delta(\epsilon)$ *can be chosen to satisfy* $\lim_{\epsilon \to \infty} \delta(\epsilon) = \infty$*, and, for each pair of positive numbers* η *and* c*, there is* $T = T(\eta, c) > 0$ *such that*

$$\|x(t)\| < \eta, \ \forall t \geq t_0 + T(\eta, c), \ \forall \|x(t_0)\| < c$$

◁

The following result allows the use of continuous Lyapunov functions being locally Lipschitz-continuous in x.

Theorem 2.1 [38, Theorem 6.2] *If there exist a continuous function* $V(t, x) : I \times \Omega \to \mathbb{R}$*, locally Lipschitz in* x *and such that*

- $V(t, x) \geq a(\|x\|)$*;* $V(t, 0) = 0$*;*
- $D^+ V(t, x) \leq 0$*;*

for some $a \in \mathcal{K}$ *and for all* $(t, x) \in I \times \Omega$*, then the origin is stable* ◁

A scalar mapping $a : \mathbb{R}_+ \to \mathbb{R}_+$ is said to be a class $\mathcal{K}$ function, denoted $a \in \mathcal{K}$, if it is strictly increasing and $a(0) = 0$. Let us further note that, in view of the time-independence of their dynamics (and consequently of the initial-time-independence of their solutions), for autonomous systems, stability is always uniform.

2.3 Invariance theory

The result presented in this section may be seen as a version/extension of LaSalle's invariance principle that may be applied to autonomous systems with continuous dynamics (in contrast for instance to the statement of LaSalle's theorem presented in [22, Theorem 4.4] which considers autonomous state equations with Lipschitz-continuous vector fields). Before we state such an important theorem, some definitions are given.

We consider autonomous systems of the form

$$\dot{x} = f(x) \tag{2.5}$$

where $f \in \mathcal{C}[\Omega, \mathbb{R}^n]$, $\Omega \subset \mathbb{R}^n$ is an open connected set.

Definition 2.2 *A set M is said to be*

- *an **invariant set** with respect to* (2.5) *if*

$$x(0) \in M \Rightarrow x(t) \in M, \qquad \forall t \in \mathbb{R}.$$

- *a **positively invariant set** with respect to* (2.5) *if*

$$x(0) \in M \Rightarrow x(t) \in M, \qquad \forall t \geq 0.$$

◁

We say that $x(t)$ approaches a set M as t approaches infinity, if for each $\varepsilon > 0$ there is a $T > 0$ such that

$$\operatorname{dist}\big(x(t), M\big) < \varepsilon, \quad \forall t > T$$

where $\operatorname{dist}(p, M)$ denotes the distance from a point p to a set M, that is the smallest distance from p to any point in M. More precisely,

$$\operatorname{dist}(p, M) = \inf_{x \in M} \|p - x\|$$

Theorem 2.2 [32, Theorem 7.2.1] *Assume that there exists a function $V \in \mathcal{C}[\Omega, \mathbb{R}]$, with $\Omega \subset \mathbb{R}$ being an open connected set, such that $D^+V(x) \leq 0$ for x in Ω and such that, for some constant $c \in \mathbb{R}$, the set H_c is a closed and bounded component of the set $\{x \in \Omega : V(x) \leq c\}$. Let M be the largest invariant set in*

$$Z = \{x \in \Omega : D^+V(x) = 0\}$$

with respect to (2.5)*. Then, every solution $x(t)$ of* (2.5) *starting in H_c approaches to M as $t \to \infty$.* ◁

If we want to show that $x(t) \to 0_n$ as $t \to \infty$, we need to establish that the largest invariant set in Z is the origin.

Invariance-like theorem

The following result proves to be helpful to determine convergence in the context of non-autonomous systems.

Theorem 2.3 [22, Theorem 8.4] *Let $D \in \mathbb{R}^n$ be a domain containing $x = 0$ and suppose $f(t, x)$ is piecewise continuous in t and locally Lipschitz in x, uniformly in t, on $[0, \infty) \times D$. Furthermore, suppose $f(t, 0)$ is uniformly bounded for all $t \geq 0$. Let $V : [0, \infty) \times D \to \mathbb{R}$ be a continuously differentiable function such that*

$$W_1(x) \leq V(t, x) \leq W_2(x)$$
$$\dot{V}(t, x) = \frac{\partial V}{\partial t} + \frac{\partial V}{\partial x} f(t, x) \leq -W(x)$$

$\forall t \geq 0$, $\forall x \in D$, *where* $W_1(x)$ *and* $W_2(x)$ *are continuous positive definite functions and* $W(x)$ *is a continuous positive semidefinite function on* D. *Choose* $r > 0$ *such that* $B_r \in D$ *and let* $\rho < \min_{\|x\|=r} W_1(x)$. *Then, all solutions of* $\dot{x} = f(t,x)$ *with* $x(t_0) \in \{x \in B_r | W_2(x) \leq \rho\}$ *are bounded and satisfy*

$$W(x(t)) \to 0 \quad as \quad t \to \infty$$

Moreover, if all the assumptions hold globally and W_1 *is radially unbounded, the statement is true for all* $x(t_0) \in \mathbb{R}^n$ ◁

2.4 Passivity

Consider a dynamical system defined by the state model

$$\dot{x} = f(x,u) \tag{2.6a}$$

$$y = h(x,u) \tag{2.6b}$$

where $f : \mathbb{R}^n \times \mathbb{R}^p \to \mathbb{R}^n$ is locally Lipschitz, $h : \mathbb{R}^n \times \mathbb{R}^p \to \mathbb{R}^p$ is continuous, $f(0_n, 0_p) = 0_n$, and $h(0_n, 0_p) = 0_p$. The following definition shows the various notions of passivity for the state model (2.6)

Definition 2.3 [22, Definition 6.3] *The system* (2.6) *is said to be passive if there exist a continuously differentiable positive semi definite function* $V(x)$ *(called storage function) such that*

$$u^T y \geq \dot{V} = \frac{\partial V}{\partial x} f(x,u), \quad \forall (x,u) \in \mathbb{R}^n \times \mathbb{R}^p \tag{2.7}$$

Moreover, it is said to be

- ***lossless*** *if* $u^T y = \dot{V}$
- ***input-feedforward passive*** *if* $u^T y \geq \dot{V} + u^T \varphi(u)$, *for some function* φ.
- ***input strictly passive*** *if* $u^T y \geq \dot{V} + u^T \varphi(u)$, *and* $u^T \varphi(u) > 0$, *for all* $u \neq 0$.
- ***output-feedforward passive*** *if* $u^T y \geq \dot{V} + y^T \rho(y)$, *for some function* ρ.
- ***output strictly passive*** *if* $u^T y \geq \dot{V} + y^T \rho(y)$, *and* $y^T \rho(y) > 0$, *for all* $y \neq 0$.
- ***strictly passive*** *if* $u^T y \geq \dot{V} + \phi(x)$, *for some positive definite function* ϕ.

In all cases the inequality should hold for all (x,u). ◁

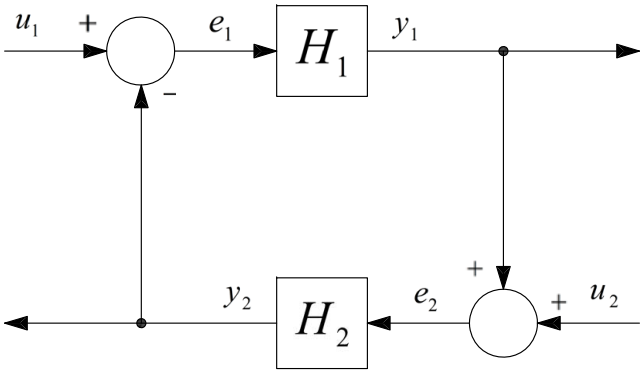

Figure 2.1: Feedback connection

Feedback systems

Consider the feedback connection presented in figure 2.1 where each of the feedback components H_1 and H_2 can be a time-invariant dynamical system represented in Eqs. (2.8)

$$\dot{x}_i = f_i(x_i, e_i) \tag{2.8a}$$

$$y_i = h_i(t, e_i) \tag{2.8b}$$

$i = 1, 2$, or a possibly (time-varying) memoryless functions represented by

$$y_i = h_i(t, e_i) \qquad i = 1, 2 \tag{2.9}$$

Theorem 2.4 [22, Theorem 6.1] *The feedback connection of two passive systems is passive.* ◁

2.5 Generalized saturation functions

The control schemes proposed in this work involve special functions fitting the following definition.

Definition 2.4 *Given a positive constant M, a nondecreasing Lipschitz-continuous function $\sigma : \mathbb{R} \to \mathbb{R}$ is said to be a* ***generalized saturation*** *with bound M if*

(a) $\varsigma\sigma(\varsigma) > 0$ *for all* $\varsigma \neq 0$*;*

(b) $|\sigma(\varsigma)| \leq M$ *for all* $\varsigma \in \mathbb{R}$*.*

If in addition

(c) $\sigma(\varsigma) = \varsigma$ *when* $|\varsigma| \leq L$*,*

for some positive constant $L \leq M$, σ is said to be a ***linear saturation*** *for (L, M) [45].* ◁

Any function satisfying Definition 2.4 has the following properties.

Lemma 2.4 *Let $\sigma : \mathbb{R} \to \mathbb{R}$ be a generalized saturation function with bound M, and let k be a positive constant. Then*

1. $\lim_{|\varsigma|\to\infty} D^+\sigma(\varsigma) = 0$;
2. $\exists \sigma'_M \in (0, \infty)$ *such that* $0 \leq D^+\sigma(\varsigma) \leq \sigma'_M$, $\forall \varsigma \in \mathbb{R}$;
3. $|\sigma(k\varsigma + \eta) - \sigma(\eta)| < k|\varsigma|$, $\forall \varsigma, \eta \in \mathbb{R}$;
4. $|\sigma(k\varsigma)| < k|\varsigma|$, $\forall \varsigma \in \mathbb{R}$;
5. $\frac{\sigma^2(k\varsigma)}{2k\sigma'_M} \leq \int_0^\varsigma \sigma(kr)dr \leq \frac{k\sigma'_M\varsigma^2}{2}$, $\forall \varsigma \in \mathbb{R}$;
6. $\int_0^\varsigma \sigma(kr)dr > 0$, $\forall \varsigma \neq 0$;
7. $\int_0^\varsigma \sigma(kr)dr \to \infty$ *as* $|\varsigma| \to \infty$;
8. *if σ is strictly increasing, then*
   (a) $\varsigma[\sigma(\varsigma + \eta) - \sigma(\eta)] > 0$, $\forall \varsigma \neq 0$, $\forall \eta \in \mathbb{R}$;
   (b) *for any constant $a \in \mathbb{R}$, $\bar{\sigma}(\varsigma) = \sigma(\varsigma + a) - \sigma(a)$ is a strictly increasing generalized saturation function with bound $\bar{M} = M + |\sigma(a)|$;*
9. *if σ is a linear saturation for (L, M) then, for any continuous function $\nu : \mathbb{R} \to \mathbb{R}$ such that $|\nu(\eta)| < L$, $\forall \eta \in \mathbb{R}$, we have that $\varsigma\big[\sigma\big(\varsigma + \nu(\eta)\big) - \sigma\big(\nu(\eta)\big)\big] > 0$, $\forall \varsigma \neq 0$, $\forall \eta \in \mathbb{R}$.*

◁

Proof.

1. Since σ is a Lipschitz-continuous function that keeps the sign of its argument (according to item (a) of Definition 2.4), and is nondecreasing and bounded by M, there exist positive constants $c^- \leq M$ and $c^+ \leq M$ such that

$$\lim_{|\varsigma|\to\infty} \sigma(\varsigma) = \frac{(\text{sign}(\varsigma) - 1)c^- + (\text{sign}(\varsigma) + 1)c^+}{2} \triangleq \sigma_\infty$$

   Hence, we have that:

$$\begin{aligned}
\lim_{|\varsigma|\to\infty} D^+\sigma(\varsigma) &= \lim_{|\varsigma|\to\infty} \limsup_{h\to 0^+} \frac{\sigma(\varsigma + h) - \varsigma(\varsigma)}{h} \\
&= \limsup_{h\to 0^+} \lim_{|\varsigma|\to\infty} \frac{\sigma(\varsigma + h) - \varsigma(\varsigma)}{h} \\
&= \limsup_{h\to 0^+} \frac{\sigma_\infty - \sigma_\infty}{h} = 0
\end{aligned}$$

2. Since σ is a Lipschitz-continuous nondecreasing function, we have that $D^+\sigma(\varsigma)$ exists and is piecewise-continuous on $\mathbb{R}$, and that $D^+\sigma(\varsigma) \geq 0$, $\forall \varsigma \in \mathbb{R}$. On the other hand, because of its piecewise-continuity, $D^+\sigma(\varsigma)$ is bounded on any compact interval on $\mathbb{R}$. Thus, its boundedness holds on $\mathbb{R}$ if $\lim_{|\varsigma|\to\infty} D^+\sigma(\varsigma) < \infty$. Since $\lim_{|\varsigma|\to\infty} D^+\sigma(\varsigma) = 0$ (according to item 1 of the statement), we conclude boundedness of $D^+\sigma(\varsigma)$ (on $\mathbb{R}$), *i.e.* there exists a non-negative finite scalar σ'_M such that $D^+\sigma(\varsigma) \leq \sigma'_M$, $\forall \varsigma \in \mathbb{R}$. Finally, observe that by virtue of item (a) of Definition 2.4, there exists $a \in (0, \infty]$ such that $D^+\sigma(\varsigma) > 0$, $\forall \varsigma \in (-a, a) \setminus \{0\}$, whence we conclude that $\sigma'_M > 0$.

3. This item is a direct consequence of the Lipschitz-continuity of σ and item 2 of the statement (as analogously stated for instance in Lemma 2.3).

4. This point follows from item 3 of the statement with $\eta = 0$.

5. From Lipschitz-continuity of σ, its satisfaction of item (a) of Definition 2.4, and the boundedness of $D^+\sigma$ by a positive constant σ'_M (according to item 2 of the statement), it follows that

$$\frac{D^+\sigma(k\varsigma)}{\sigma'_M}|\sigma(k\varsigma)| \leq |\sigma(k\varsigma)| \leq \sigma'_M|k\varsigma|$$

$\forall \varsigma \in \mathbb{R}$, whence —considering that σ has the sign of its argument (according to item (a) of Definition 2.4)— we have that

$$\int_0^\varsigma \frac{\sigma(kr)}{\sigma'_M} D^+\sigma(kr)dr \leq \int_0^\varsigma \sigma(kr)dr \leq \int_0^\varsigma k\sigma'_M r dr$$

wherefrom we get

$$\frac{\sigma^2(k\varsigma)}{2k\sigma'_M} \leq \int_0^\varsigma \sigma(kr)dr \leq \frac{k\sigma'_M\varsigma^2}{2}$$

$\forall \varsigma \in \mathbb{R}$.

6. Strict positivity of $\int_0^\varsigma \sigma(kr)dr$ on $\mathbb{R} \setminus \{0\}$ follows from items 5 of the statement and (a) of Definition 2.4, by noting that $\sigma^2(k\varsigma) > 0$, $\forall \varsigma \neq 0$.

7. From the Lipschitz-continuous and nondecreasing characters of σ, and its satisfaction of item (a) of Definition 2.4, we have that there exist constants $a > 0$, $k_a > 0$, and $c \geq 1$ such that $|\sigma(\varsigma)| \geq k_a \left|a \operatorname{sat}(\varsigma/a)\right|^c$, whence we get

$$S_a(\varsigma) \triangleq \int_0^\varsigma \operatorname{sign}(r) k_a \left|a \operatorname{sat}(r/a)\right|^c dr \leq \int_0^\varsigma \sigma(k\varsigma)dr$$

$\forall \varsigma \in \mathbb{R}$, with

$$S_a(\varsigma) = \begin{cases} \frac{k_a}{c+1}|\varsigma|^{c+1} & \forall |\varsigma| \leq a \\ k_a a^c\left(|\varsigma| - \frac{ac}{c+1}\right) & \forall |\varsigma| > a \end{cases}$$

Thus, from these expressions we observe, on the one hand, that

$$\lim_{|\varsigma|\to\infty} S_a(\varsigma) \leq \lim_{|\varsigma|\to\infty} \int_0^{\varsigma} \sigma(kr)dr$$

and, on the other, that $S_a(\varsigma) \to \infty$ as $|\varsigma| \to \infty$, wherefrom we conclude that $\int_0^{\varsigma} \sigma(kr)dr \to \infty$ as $|\varsigma| \to \infty$.

8. Suppose σ is strictly increasing. Let $\psi, \eta, \varsigma \in \mathbb{R}$.

   (a) Since σ is strictly increasing, we have that

   $$\sigma(\psi) > \sigma(\eta) \iff \psi > \eta$$

   and

   $$\sigma(\psi) < \sigma(\eta) \iff \psi < \eta$$

   Let $\psi = \varsigma + \eta$. Then

   $$\sigma(\varsigma + \eta) - \sigma(\eta) > 0 \iff \varsigma > 0 \quad \forall \eta \in \mathbb{R}$$

   and

   $$\sigma(\varsigma + \eta) - \sigma(\eta) < 0 \iff \varsigma < 0 \quad \forall \eta \in \mathbb{R}$$

   whence it follows that $\varsigma[\sigma(\varsigma + \eta) - \sigma(\eta)] > 0$, $\forall \varsigma \neq 0$, $\forall \eta \in \mathbb{R}$.

   (b) For any constant $a \in \mathbb{R}$, let $\bar{\sigma}(\varsigma) = \sigma(\varsigma + a) - \sigma(a)$.

   - *Lipschitz-continuity.* From the Lipschitz-continuity of σ and item 2 of the statement, we have that $|\sigma(\varsigma) - \sigma(\eta)| \leq \sigma'_M|\varsigma - \eta|$, $\forall \varsigma, \eta \in \mathbb{R}$. Then

   $$\begin{aligned} \big|\bar{\sigma}(\varsigma) - \bar{\sigma}(\eta)\big| &= \big|\big(\sigma(\varsigma + a) - \sigma(a)\big) - \big(\sigma(\eta + a) - \sigma(a)\big)\big| \\ &= \big|\sigma(\varsigma + a) - \sigma(\eta + a)\big| \\ &\leq \sigma'_M\big|(\varsigma + a) - (\eta + a)\big| \\ &\leq \sigma'_M\big|\varsigma - \eta\big| \end{aligned}$$

   $\forall \varsigma, \eta \in \mathbb{R}$, which shows that $\bar{\sigma}$ is Lipschitz-continuous.

   - *Strictly increasing monotonicity.* From the strictly increasing monotonicity of σ, we have that

   $$\begin{aligned} \bar{\sigma}(\varsigma) > \bar{\sigma}(\eta) &\iff \sigma(\varsigma + a) - \sigma(a) > \sigma(\eta + a) - \sigma(a) \\ &\iff \sigma(\varsigma + a) > \sigma(\eta + a) \\ &\iff \varsigma + a > \eta + a \\ &\iff \varsigma > \eta \end{aligned}$$

   which shows that $\bar{\sigma}$ is strictly increasing.

   - $\varsigma\bar{\sigma}(\varsigma) > 0$, $\forall \varsigma \neq 0$. From item 8a of the Lemma, we have that $\varsigma\bar{\sigma}(\varsigma) = \varsigma[\sigma(\varsigma + a) - \sigma(a)] > 0$, for all $\varsigma \neq 0$ and any $a \in \mathbb{R}$.

- $|\bar{\sigma}(\varsigma)| \leq \bar{M} = M + |\sigma(a)|$, $\forall \varsigma \in \mathbb{R}$. Since $|\sigma(\varsigma)| \leq M$, $\forall \varsigma \in \mathbb{R}$, we have that

$$|\bar{\sigma}(\varsigma)| = |\sigma(\varsigma + a) - \sigma(a)| \leq |\sigma(\varsigma + a)| + |\sigma(a)| \leq M + |\sigma(a)| = \bar{M}$$

  Thus, according to Definition 2.4, $\bar{\sigma}$ is concluded to be a strictly increasing generalized saturation with bound $\bar{M} = M + |\sigma(a)|$.

9. Let us begin by noting, from item (c) of Definition 2.4, that $|\nu(\eta)| < L \implies \sigma\big(\nu(\eta)\big) \equiv \nu(\eta)$, $\forall \eta \in \mathbb{R}$. Furthermore, $|\varsigma + \nu(\eta)| < L \implies \sigma\big(\varsigma + \nu(\eta)\big) = \varsigma + \nu(\eta)$, $\forall \eta \in \mathbb{R}$. Hence,

$$\varsigma\big[\sigma\big(\varsigma + \nu(\eta)\big) - \sigma\big(\nu(\eta)\big)\big] = \varsigma^2 > 0$$
$$\text{for all } \varsigma \neq 0 \text{ such that } |\varsigma + \nu(\eta)| < L, \text{ and all } \eta \in \mathbb{R}. \quad (2.10)$$

On the other hand, if $\varsigma + \nu(\eta) \geq L$, which implies that

$$\varsigma \geq L - \nu(\eta) \geq L - |\nu(\eta)| > 0$$

$\forall \eta \in \mathbb{R}$, then (from item (c) of Definition 2.4 and the nondecreasing character of σ)

$$\sigma\big(\varsigma + \nu(\eta)\big) - \sigma\big(\nu(\eta)\big) \geq L - \nu(\eta) \geq L - |\nu(\eta)| > 0$$

$\forall \eta \in \mathbb{R}$, while if $\varsigma + \nu(\eta) \leq -L$, which implies that

$$\varsigma \leq -L - \nu(\eta) \leq -L + |\nu(\eta)| < 0$$

$\forall \eta \in \mathbb{R}$, then

$$\sigma\big(\varsigma + \nu(\eta)\big) - \sigma\big(\nu(\eta)\big) \leq -L - \nu(\eta) \leq -L + |\nu(\eta)| < 0$$

$\forall \eta \in \mathbb{R}$, and consequently

$$\varsigma\big[\sigma\big(\varsigma + \nu(\eta)\big) - \sigma\big(\nu(\eta)\big)\big] > 0$$
$$\text{for all } \varsigma \in \mathbb{R} \text{ such that } |\varsigma + \nu(\eta)| \geq L, \text{ and all } \eta \in \mathbb{R}. \quad (2.11)$$

Thus, from (2.10) and (2.11), it follows that $\varsigma\big[\sigma\big(\varsigma + \nu(\eta)\big) - \sigma\big(\nu(\eta)\big)\big] > 0$, $\forall \varsigma \neq 0$, $\forall \eta \in \mathbb{R}$.

$\triangleleft$

3
Proposed approaches

We begin by recalling the manipulator dynamics as exposed in Section 1.2, *i.e.*

$$H(q)\ddot{q} + C(q,\dot{q})\dot{q} + F\dot{q} + g(q) = \tau \tag{3.1}$$

whose various terms and properties had been described in subsection 1.2.2. Let us suppose that the absolute value of each input τ_i (i^{th} element of the input vector τ) is constrained to be smaller than a given saturation bound $T_i > 0$, *i.e.* $|\tau_i| \leq T_i$, $i = 1, \ldots, n$. In other words, letting u_i represent the control variable (controller output) relative to the i^{th} degree of freedom, we have that

$$\tau_i = T_i \text{sat}\left(\frac{u_i}{T_i}\right) \tag{3.2}$$

$i = 1, \ldots, n$.

Let us note from (3.1)-(3.2) that $T_i \geq B_{gi}$ (see Property 1.4), $\forall i \in \{1, \ldots, n\}$, is a necessary condition for the manipulator to be stabilizable at any desired equilibrium configuration $q_d \in \mathbb{R}^n$. Thus, the following assumption turns out to be crucial within the analytical setting considered in this work:

Assumption 3.1 $T_i > B_{gi}$, $\forall i \in \{1, \ldots, n\}$. ◁

3.1 State-feedback regulation approach

A generalized non adaptive approach is first presented. Developments and results from this section will be used to present the proposed adaptive schemes.

3.1.1 Global regulation involving exact gravity compensation: a generalized approach

Let us consider the following *generalized* expression defining saturating controllers for the global regulation of system (3.1)-(3.2):

$$u(q,\dot{q},\theta) = -s_d(\bar{q},\dot{q},\theta) - s_P(K_P\bar{q}) + G(q)\theta \tag{3.3}$$

where $\bar{q} = q - q_d$, for any constant (desired equilibrium position) vector $q_d \in \mathbb{R}^n$. The third term in the right-hand side of (3.3) is the gravity compensation term where $G(q)$ is the regression matrix related to the gravity vector, *i.e.* such that $g(q,\theta) = G(q)\theta$. The second term in the right-hand side of (3.3) is a (bounded non-linear) position error correction term where $K_P \in \mathbb{R}^{n\times n}$ is a positive definite diagonal matrix, *i.e.* $K_P = \mathrm{diag}[k_{P1},\ldots,k_{Pn}]$ with $k_{Pi} > 0$ for all $i = 1,\ldots,n$, and

$$\begin{aligned} s_P : \mathbb{R}^n &\to \mathbb{R}^n \\ x &\mapsto \big(\sigma_{P1}(x_1)\ ,\ \ldots\ ,\ \sigma_{Pn}(x_n)\big)^T \end{aligned}$$

with $\sigma_{Pi}(\cdot)$, $i = 1,\ldots,n$ being (suitable) **generalized saturation functions** with bounds M_{Pi}. The first term in the right-hand side of (3.3) corresponds to a motion dissipation term where $s_d : \mathbb{R}^n\times\mathbb{R}^n\times\mathbb{R}^p \to \mathbb{R}^n$ is a bounded continuous vector function satisfying $s_d : \mathbb{R}^n \times \mathbb{R}^n \times \mathbb{R}^p \to \mathbb{R}^n$ is a bounded continuous vector function satisfying

$$s_d(x, 0_n, z) = 0_n \tag{3.4}$$

$\forall x \in \mathbb{R}^n$, $\forall z \in \mathbb{R}^p$,

$$\|s_d(x,y,z)\| \leq \kappa\|y\| \tag{3.5}$$

$\forall (x,y,z) \in \mathbb{R}^n \times \mathbb{R}^n \times \mathbb{R}^p$, for some positive constant κ, and given $z \in \mathbb{R}^p$ such that $|G_i(q)z| < T_i$, $i = 1,\ldots,n$, $\forall q \in \mathbb{R}^n$:

$$y^T s_d(x,y,z) > 0 \tag{3.6}$$

$\forall y \neq 0_n$, $\forall x \in \mathbb{R}^n$, and

$$|u_i(x,y,z)| < T_i \tag{3.7}$$

$i = 1,\ldots,n$, $\forall x \in \mathbb{R}^n$, $\forall y \in \mathbb{R}^n$, for suitable bounds M_{Pi} of $\sigma_{Pi}(\cdot)$.

Proposition 3.1 *Consider system* (3.1)–(3.2) *taking* $u = u(q,\dot{q},\theta)$ *as defined in Eq.* (3.3)*, under Assumption 3.1 and the conditions on the vector function* s_d *stated through Eq.* (3.4) *and inequalities* (3.5)–(3.7)*. Thus, for any positive definite diagonal matrix* K_P*, global asymptotic stability of the closed-loop trivial solution* $\bar{q}(t) \equiv 0_n$ *is guaranteed with* $|\tau_i(t)| = |u_i(t)| < T_i$*,* $i = 1,\ldots,n$*,* $\forall t \geq 0$*.* ◁

Proof. Observe that the satisfaction of (3.7), under the consideration of (3.2), shows that

$$T_i > |u_i(q,\dot{q},\theta)| = |u_i| = |\tau_i|$$

$i = 1, \ldots, n$, $\forall (q, \dot{q}) \in \mathbb{R}^n \times \mathbb{R}^n$. Hence it can be seen that, along the system trajectories

$$|\tau_i(t)| = |u_i(t)| < T_i$$

$i = 1, \ldots, n$, $\forall t \geq 0$. This proves that with the proposed scheme, the input saturation values, T_i, are never reached. Thus, under the consideration of Property 1.5, the closed-loop dynamics takes the form[1]

$$H(q)\ddot{q} + C(q, \dot{q})\dot{q} + F\dot{q} = -s_d(\bar{q}, \dot{q}, \theta) - s_P(K_P\bar{q}) \tag{3.8}$$

Let us define the scalar function

$$V_0(\bar{q}, \dot{q}) = \frac{1}{2}\dot{q}^T H(q)\dot{q} + \varepsilon \dot{q}^T H(q) s_P(K_P\bar{q}) + \int_{0_n}^{\bar{q}} s_P^T(K_P r)dr \tag{3.9}$$

with $\int_{0_n}^{\bar{q}} s_P^T(K_P r)dr = \sum_{i=1}^{n} \int_0^{\bar{q}_i} \sigma_{Pi}(k_{Pi} r_i)dr_i$ and ε being a positive constant satisfying

$$\varepsilon < \varepsilon_M \triangleq \min\{\varepsilon_1, \varepsilon_2\} \tag{3.10}$$

where

$$\varepsilon_1 \triangleq \sqrt{\frac{\mu_m}{\mu_M^2 \beta_P}} \qquad \text{and} \qquad \varepsilon_2 \triangleq \frac{f_m}{\beta_M + \frac{(f_M + \kappa)^2}{4}}$$

with

$$\beta_P \triangleq \max_i\{\sigma'_{PiM} k_{Pi}\} \quad , \quad \beta_M \triangleq k_C B_P + \mu_M \beta_P \quad , \quad B_P \triangleq \sqrt{\sum_{i=0}^{n} M_{Pi}^2}$$

σ'_{PiM} being the positive bound of $D^+\sigma_{Pi}(\cdot)$ in accordance to item 2 of Lemma 2.4, κ as defined through (3.5), and μ_m, μ_M, k_C, f_m, and f_M as defined in Properties 1.1, 1.2.5, and 1.3. Observe that from Property 1.1 and item 5 of Lemma 2.4, we have that

$$V_0(\bar{q}, \dot{q}) \geq W_0(\bar{q}, \dot{q}) + (1 - \alpha) \int_{0_n}^{\bar{q}} s_P^T(K_P r)dr \tag{3.11}$$

where

$$\begin{aligned} W_0(\bar{q}, \dot{q}) &= \frac{\mu_m}{2}\|\dot{q}\|^2 - \varepsilon\mu_M \|s_P(K_P\bar{q})\|\|\dot{q}\| + \frac{\alpha}{2\beta_P}\|s_P(K_P\bar{q})\|^2 \\ &= \frac{1}{2}\begin{pmatrix} \|s_P(K_P\bar{q})\| \\ \|\dot{q}\| \end{pmatrix}^T \begin{pmatrix} \frac{\alpha}{\beta_P} & -\varepsilon\mu_M \\ -\varepsilon\mu_M & \mu_m \end{pmatrix} \begin{pmatrix} \|s_P(K_P\bar{q})\| \\ \|\dot{q}\| \end{pmatrix} \end{aligned} \tag{3.12}$$

and α is a positive constant satisfying

$$\frac{\varepsilon^2}{\varepsilon_1^2} < \alpha < 1 \tag{3.13}$$

[1] In the error variable space $q = \bar{q} + q_d$, and hence $H(q) = H(\bar{q} + q_d)$, $C(q, \dot{q}) = C(\bar{q} + q_d, \dot{q})$, and $G(q) = G(\bar{q} + q_d)$. However, for the sake of simplicity, $H(q)$, $C(q, \dot{q})$, and $G(q)$ are used throughout this work.

(see (3.10)). Note further that, by (3.13), $W_0(\bar{q},\dot{q})$ is positive definite (since with $\varepsilon < \varepsilon_M \leq \varepsilon_1$, in accordance to (3.10), any α satisfying (3.13) renders positive definite the matrix at the right-hand side of (3.12)), and observe that $W_0(0_n,\dot{q}) \to \infty$ as $\|\dot{q}\| \to \infty$. From this, inequality (3.13), and items 6 and 7 of Lemma 2.4 (through which one sees that the integral term in the right-hand side of inequality (3.11) is a radially unbounded positive definite function of $\bar{q}$), $V_0(\bar{q},\dot{q})$ is concluded to be positive definite and radially unbounded. Its upper-right derivative along the system trajectories, $\dot{V}_0 = D^+V_0$ [38, App. I] [32, §6.1A], is given by

$$\begin{aligned}
\dot{V}_0(\bar{q},\dot{q}) = {} & \dot{q}^T H(q)\ddot{q} + \frac{1}{2}\dot{q}^T\dot{H}(q,\dot{q})\dot{q} + \varepsilon s_P^T(K_P\bar{q})H(q)\ddot{q} + \varepsilon\dot{q}^T\dot{H}(q,\dot{q})s_P(K_P\bar{q}) \\
& + \varepsilon\dot{q}^T H(q)s_P'(K_P\bar{q})K_P\dot{q} + s_P^T(K_P\bar{q})\dot{q} \\
= {} & \dot{q}^T\big[-C(q,\dot{q})\dot{q} - F\dot{q} - s_d(\bar{q},\dot{q},\theta) - s_P(K_P\bar{q})\big] + \frac{1}{2}\dot{q}^T\dot{H}(q,\dot{q})\dot{q} \\
& + \varepsilon s_P^T(K_P\bar{q})\big[-C(q,\dot{q})\dot{q} - F\dot{q} - s_d(\bar{q},\dot{q},\theta) - s_P(K_P\bar{q})\big] \\
& + \varepsilon\dot{q}^T\dot{H}(q,\dot{q})s_P(K_P\bar{q}) + \varepsilon\dot{q}^T H(q)s_P'(K_P\bar{q})K_P\dot{q} + s_P^T(K_P\bar{q})\dot{q} \\
= {} & -\dot{q}^T F\dot{q} - \dot{q}^T s_d(\bar{q},\dot{q},\theta) - \varepsilon s_P^T(K_P\bar{q})F\dot{q} - \varepsilon s_P^T(K_P\bar{q})s_d(\bar{q},\dot{q},\theta) \\
& - \varepsilon s_P^T(K_P\bar{q})s_P(K_P\bar{q}) + \varepsilon\dot{q}^T C(q,\dot{q})s_P(K_P\bar{q}) + \varepsilon\dot{q}^T H(q)s_P'(K_P\bar{q})K_P\dot{q}
\end{aligned}$$

where $H(q)\ddot{q}$ has been replaced by its equivalent expression from the closed-loop dynamics in (3.8), Property 1.2.1 has been used, and

$$s_P'(K_P\bar{q}) \triangleq \mathrm{diag}[D^+\sigma_{P1}(k_{P1}\bar{q}_1),\ldots,D^+\sigma_{Pn}(k_{Pn}\bar{q}_n)] \tag{3.14}$$

Observe that from Properties 1.1, 1.2.5, and 1.3, the satisfaction of (3.5), items (b) of Definition 2.4 and 2 of Lemma 2.4, and the positive definite character of K_P, we have that

$$\dot{V}_0(\bar{q},\dot{q}) \leq -\dot{q}^T s_d(\bar{q},\dot{q},\theta) - W_1(\bar{q},\dot{q})$$

with

$$\begin{aligned}
W_1(\bar{q},\dot{q}) = {} & f_m\|\dot{q}\|^2 - \varepsilon f_M\|s_P(K_P\bar{q})\|\|\dot{q}\| - \varepsilon\kappa\|s_P(K_P\bar{q})\|\|\dot{q}\| + \varepsilon\|s_P(K_P\bar{q})\|^2 \\
& - \varepsilon k_C B_P\|\dot{q}\|^2 - \varepsilon\mu_M\beta_P\|\dot{q}\|^2 \\
= {} & \begin{pmatrix}\|s_P(K_P\bar{q})\| \\ \|\dot{q}\|\end{pmatrix}^T \begin{pmatrix}\varepsilon & -\frac{\varepsilon}{2}(f_M+\kappa) \\ -\frac{\varepsilon}{2}(f_M+\kappa) & f_m - \varepsilon\beta_M\end{pmatrix}\begin{pmatrix}\|s_P(K_P\bar{q})\| \\ \|\dot{q}\|\end{pmatrix}
\end{aligned} \tag{3.15}$$

Note further that, from the satisfaction of (3.10), $W_1(\bar{q},\dot{q})$ is positive definite (since any $\varepsilon < \varepsilon_M \leq \varepsilon_2$ renders positive definite the matrix at the right-hand side of (3.15)). From this and (3.6), by Lyapunov's second method,[2] the trivial solution $\bar{q}(t) \equiv 0_n$ is concluded to be globally asymptotically stable, which completes the proof. ◁

[2]See for instance [38, Chap. II, §6], where (generalized) statements of Lyapunov's second method are presented under the consideration of locally Lipschitz-continuous Lyapunov functions and their upper-right derivative along the system trajectories.

Remark 3.1 Let $K_D \in \mathbb{R}^{n\times n}$ be a positive definite diagonal matrix, *i.e.* $K_D = \text{diag}[k_{D1}, \ldots, k_{Dn}]$ with $k_{Di} > 0$ for all $i = 1, \ldots, n$. A generalized version of the SP-SD controller is retrieved from (3.3) by defining

$$s_d(\bar{q}, \dot{q}, \theta) = s_D(K_D\dot{q}) \tag{3.16}$$

where $s_D : \mathbb{R}^n \to \mathbb{R}^n : x \mapsto \big(\sigma_{D1}(x_1)\ ,\ \ldots\ ,\ \sigma_{Dn}(x_n)\big)^T$, with $\sigma_{Di}(\cdot)$, $i = 1, \ldots, n$, being **generalized saturation functions** with bounds M_{Di}; and the involved bound values, M_{Pi} and M_{Di}, satisfy

$$M_{Pi} + M_{Di} < T_i - B_{gi} \tag{3.17}$$

$i = 1, \ldots, n$. Special cases of the generalized SP-SD controller in Eqs. (3.3) and (3.16) were defined in [19] and [41], taking $\sigma_{Pi}(x_i) = k_{Pi}\tanh\left(\frac{\lambda_{Pi}x_i}{k_{Pi}}\right)$ and $\sigma_{Pi}(x_i) = k_{Di}\tanh\left(\frac{\lambda_{Di}x_i}{k_{Di}}\right)$, with $k_{Pi} + k_{Di} < T_i - B_{gi}$, in [19], and $\sigma_{Pi}(x_i) = \delta_{Pi}\text{sat}\left(\frac{x_i}{\delta_{Pi}}\right)$ and $\sigma_{Di}(x_i) = \delta_{Di}\text{sat}\left(\frac{x_i}{\delta_{Di}}\right)$, with $\delta_{Pi} + \delta_{Di} < T_i - B_{gi}$, in [41]. Further, generalized versions of the SPD and SPDgc-like schemes proposed in [47] are retrieved from (3.3) as well, by respectively defining

$$s_d(\bar{q}, \dot{q}, \theta) = s_P(K_P\bar{q} + K_D\dot{q}) - s_P(K_P\bar{q}) \tag{3.18}$$

with the generalized saturations $\sigma_{Pi}(\cdot)$, $i = 1, \ldots, n$, being **strictly increasing**, and bound values satisfying

$$M_{Pi} \leq T_i - B_{gi} \tag{3.19}$$

$i = 1, \ldots, n$ (for the SPD case),[3] and

$$s_d(\bar{q}, \dot{q}, \theta) = s_0\big(G(q)\theta - s_P(K_P\bar{q})\big) - s_0\big(G(q)\theta - s_P(K_P\bar{q}) - K_D\dot{q}\big) \tag{3.20}$$

where $s_0 : \mathbb{R}^n \to \mathbb{R}^n : x \mapsto \big(\sigma_{01}(x_1)\ ,\ \ldots\ ,\ \sigma_{0n}(x_n)\big)^T$, with $\sigma_{0i}(\cdot)$, $i = 1, \ldots, n$, being **linear saturation functions** for (L_{0i}, M_{0i}), and the involved linear/generalized saturation function parameters satisfying

$$B_{gi} + M_{Pi} < L_{0i} \leq M_{0i} < T_i \tag{3.21}$$

$i = 1, \ldots, n$ (for the SPDgc-like case).[4] Observe from (3.21) that, by virtue of item (c) of Definition 2.4 (under the consideration of Properties 1.4 and 1.5), we have that $s_0\big(G(q)\theta - s_P(K_P\bar{q})\big) \equiv G(q)\theta - s_P(K_P\bar{q})$ (see (3.20) and (3.3)). Furthermore, note that, from items (a) of Definition 2.4 and 8a and 9 of Lemma 2.4 (under the fulfilment of inequalities (3.21) in the SPDgc-like case), $s_d(\bar{q}, \dot{q}, \theta)$ in every one of the above cases in (3.16), (3.18), and (3.20) satisfies the expressions in (3.4) and (3.6). Further, notice that, through the fulfilment of (3.17), (3.19) (under the consideration of the

[3]Note that the generalized saturations, $\sigma_{Pi}(\cdot)$, in (3.18) are not restricted to be continuously differentiable as originally formulated in [47].

[4]Notice that the *internal* saturations, $\sigma_{Pi}(\cdot)$, in (3.20) are permitted to be any function satisfying Definition 2.4 and are consequently not tied to be linear saturations as originally formulated in [47].

strictly increasing character of the generalized saturation functions σ_{Pi} involved in the SPD case), and (3.21), every $s_d(\bar{q}, \dot{q}, \theta)$ in expressions (3.16), (3.18), and (3.20) satisfies inequalities (3.7) too. Moreover, from the Lipschitz-continuous character of generalized saturation functions, one sees that $s_d(\bar{q}, \dot{q}, \theta)$ in every one of the above cases in (3.16), (3.18), and (3.20) satisfies inequality (3.5) with

$$\kappa = \max_i \{\sigma'_{iM} k_{Di}\} \tag{3.22a}$$

where

$$\sigma'_{iM} = \begin{cases} \sigma'_{DiM} & \text{in the SP-SD case} \\ \sigma'_{PiM} & \text{in the SPD case} \\ \sigma'_{0iM} & \text{in the SPDgc-like case} \end{cases} \tag{3.22b}$$

σ'_{DiM}, σ'_{PiM}, and σ'_{0iM} respectively being the positive bounds of $D^+\sigma_{Di}(\cdot)$, $D^+\sigma_{Pi}(\cdot)$, and $D^+\sigma_{0i}(\cdot)$, in accordance to item 2 of Lemma 2.4. ◁

3.1.2 Global adaptive set-point control

If the accurate values of the elements of θ in $g(q, \theta)$ are unknown, exact gravity compensation is no longer possible. However, in such a situation, global position stabilization avoiding input saturation can still be accomplished through adaptive gravity compensation. This is achieved by means of suitable strict bounds on the elements of θ, as described next.

Let $M_a \triangleq \big(M_{a1}, \ldots, M_{ap}\big)^T$ and $\Theta_a \triangleq [-M_{a1}, M_{a1}] \times \cdots \times [-M_{ap}, M_{ap}]$, with M_{aj}, $j = 1, \ldots, p$, being positive constants such that

$$\theta_j < M_{aj} \tag{3.23a}$$

$\forall j \in \{1, \ldots, p\}$, and

$$B_{gi}^{M_a} < T_i \tag{3.23b}$$

$\forall i \in \{1, \ldots, n\}$, where, in accordance to Property 1.6, $B_{gi}^{M_a}$ are positive constants such that $|g_i(x, y)| = |G_i(x)y| \leq B_{gi}^{M_a}$, $i = 1, \ldots, n$, $\forall x \in \mathbb{R}^n$, $\forall y \in \Theta_a$. Let us note that Assumption 3.1 ensures the existence of such positive values M_{aj}, $j = 1, \ldots, p$, satisfying inequalities (3.23). Notice further that inequalities (3.23b) are satisfied if $\sum_{j=1}^{p} B_{G_{ij}} M_{aj} < T_i$, $B_{G_i}\|M_a\| < T_i$, or $B_G\|M_a\| < T_i$, $i = 1, \ldots, n$; actually, $\sum_{j=1}^{p} B_{G_{ij}} M_{aj}$, $B_{G_i}\|M_a\|$, or $B_G\|M_a\|$, may be taken as the value of $B_{gi}^{M_a}$ as long as inequality (3.23b) is satisfied.

Based on the generalized algorithm in Eq. (3.3), the proposed adaptive control scheme is defined as

$$u(q, \dot{q}, \hat{\theta}) = -s_d(\bar{q}, \dot{q}, \hat{\theta}) - s_P(K_P \bar{q}) + G(q)\hat{\theta} \tag{3.24}$$

with $s_P(\cdot)$, K_p, and $s_d(\cdot)$ being as defined in Section 3.1.1, and $\hat{\theta}$ (vector of estimated parameters) being the output variable of an auxiliary dynamic subsystem defined as

$$\dot{\phi} = -\Gamma G^T(q)\big[\dot{q} + \varepsilon s_P(K_P \bar{q})\big] \tag{3.25a}$$

$$\hat{\theta} = s_a(\phi) \tag{3.25b}$$

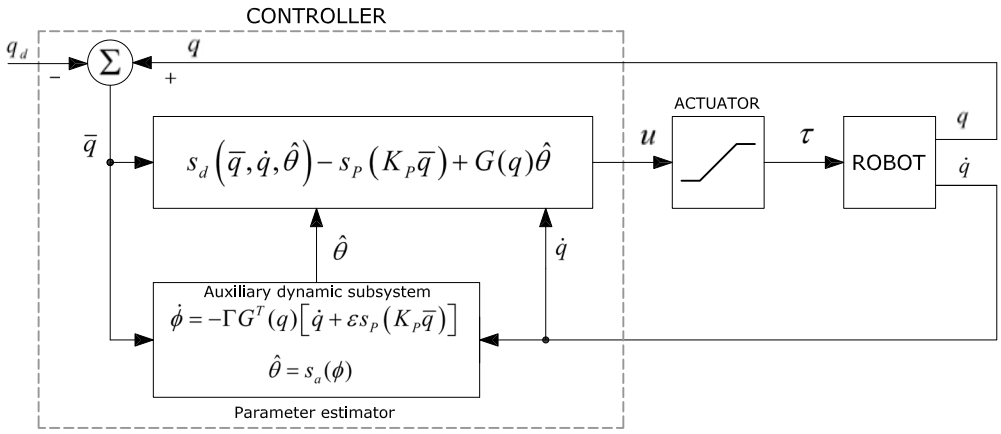

Figure 3.1: Block diagram of the proposed state feedback adaptive control scheme

where ϕ is the (internal) state of the auxiliary dynamics in Eq. (3.25a);

$$\begin{aligned} s_a : \mathbb{R}^p &\to \mathbb{R}^p \\ x &\mapsto \left(\sigma_{a1}(x_1)\ ,\ \ldots\ ,\ \sigma_{an}(x_p)\right)^T \end{aligned}$$

$\sigma_{aj}(\cdot)$, $j = 1, \ldots, p$, being **strictly increasing generalized saturation functions** with bounds M_{aj} as defined above, *i.e.* satisfying inequalities (3.23); $\Gamma \in \mathbb{R}^{p\times p}$ is a positive definite diagonal constant matrix, *i.e.* $\Gamma = \mathrm{diag}[\gamma_1 \ldots, \gamma_p]$ with $\gamma_j > 0$ for all $j = 1, \ldots, p$; and ε is a positive constant satisfying inequality (3.10). A block diagram of the proposed adaptive control scheme is shown in Fig. 3.1.

Remark 3.2 Observe that the control scheme in (3.24)-(3.25) does not involve the exact values of the elements of θ. It only requires the satisfaction of inequalities (3.23). In other words, only strict bounds M_{aj} of θ_j, $j = 1, \ldots, p$, —*i.e.* any set of them satisfying inequalities (3.23b)— are involved. Notice further that a suitable choice of ε does not require the exact knowledge of the system parameters either. Indeed, observe, on the one hand, that an estimation of the right-hand side of inequality (3.10) may be obtained by means of upper and lower bounds of the system parameters and viscous friction coefficients (more precisely, nonzero lower bounds of μ_m and f_m, and upper bounds of μ_M, k_C, and f_M; see Properties 1.1, 1.2.5, and 1.3). On the other hand, the fulfilment of inequality (3.10) is not necessary but only sufficient for the closed-loop analysis to hold, as shown next, which permits the consideration of values of ε higher than ε_M (up to certain limit) without destabilizing the closed loop. ◁

Remark 3.3 The auxiliary subsystem in Eqs. (3.25) is the adaptation algorithm. Its particular form gives rise to parameter estimates evolving within pre-specified limits, avoiding discontinuities throughout its dynamical structure. Let us note that the ε-term in the adaptation subsystem forces q_d to be the unique equilibrium configuration of the closed-loop system. This eliminates the steady-state position error generated by conventional approaches that include *exact* gravity compensation through generally-inexact (or biassed) parameter estimates. Further, inequality (3.10) states a (sufficient)

condition that guarantees the required stability/convergence properties. It is obtained from the closed-loop analysis, by looking for the conditions through which the involved Lyapunov function adopts the required analytical properties. This is corroborated next. ◁

Closed-loop analysis

Consider system (3.1)-(3.2) taking $u = u(q, \dot{q}, \hat{\theta})$ as defined through Eqs. (3.24)-(3.25). Observe that —under Assumption 3.1, the satisfaction of inequalities (3.23), and the consideration of (3.2)— the fulfilment of (3.7) shows that

$$T_i > \big|u_i\big(q, \dot{q}, s_a(\phi)\big)\big| = |u_i| = |\tau_i| \quad i = 1, \ldots, n \quad \forall (q, \dot{q}, \phi) \in \mathbb{R}^n \times \mathbb{R}^n \times \mathbb{R}^p \tag{3.26}$$

Thus, under the consideration of Property 1.5, the closed-loop system takes the form

$$H(q)\ddot{q} + C(q, \dot{q})\dot{q} + F\dot{q} = -s_d\big(\bar{q}, \dot{q}, s_a(\phi)\big) - s_P(K_P\bar{q}) + G(q)\bar{s}_a(\bar{\phi}) \tag{3.27a}$$

$$\dot{\bar{\phi}} = -\Gamma G^T(q)\big[\dot{q} + \varepsilon s_P(K_P\bar{q})\big] \tag{3.27b}$$

where $\bar{\phi} = \phi - \phi^*$ and

$$\bar{s}_a(\bar{\phi}) = s_a(\bar{\phi} + \phi^*) - s_a(\phi^*) \tag{3.28}$$

with $\phi^* = \big(\phi_1^*, \ldots, \phi_p^*\big)^T$ such that $s_a(\phi^*) = \theta$, or equivalently, $\phi_j^* = \sigma_{aj}^{-1}(\theta_j)$, $j = 1, \ldots, p$.[5] Observe that, by item 8b of Lemma 2.4, the elements of $\bar{s}_a(\bar{\phi})$ in (3.28), *i.e.*

$$\bar{\sigma}_{aj}(\bar{\phi}_j) = \sigma_{aj}(\bar{\phi}_j + \phi_j^*) - \sigma_{aj}(\phi_j^*)$$

$j = 1, \ldots, p$, turn out to be strictly increasing generalized saturation functions.

Remark 3.4 Let us note that, from Eqs. (3.27) under stationary conditions, *i.e.* by considering $\ddot{q} = \dot{q} = 0_n$ and $\dot{\bar{\phi}} = 0_p$, q_d proves to be the unique equilibrium position of the closed-loop system —or equivalently, 0_n proves to be the unique equilibrium position error of the closed loop—, while the parameter estimation error equilibrium vector $\bar{\phi}_e$ turns out to be defined by the solutions of the equation $G(q_d)\bar{s}_a(\bar{\phi}_e) = 0_n$, and consequently $\bar{s}_a(\bar{\phi}_e) \in \ker(G(q_d))$.[6] ◁

[5] Notice that their strictly increasing character renders the generalized saturation functions σ_{aj}, $j = 1, \ldots, p$, (involved in the definition of s_a) invertible.

[6] From the closed-loop system Eq. 3.27, under stationary conditions, one gets

$$-s_P(K_P\bar{q}) + G(q)\bar{s}_a(\bar{\phi}) = 0_n \tag{3.29}$$

$$G^T(q)s_P(K_P\bar{q}) = 0_p \tag{3.30}$$

Hence premultiplying Eq. (3.29) by $-s_P^T(K_P\bar{q})$ and using Eq. (3.30), we obtain

$$s_P^T(K_P\bar{q})s_P(K_P\bar{q}) - \underbrace{s_P^T(K_P\bar{q})G(q)}_{0_p^T}\bar{s}_a(\bar{\phi}) = s_P^T(K_P\bar{q})s_P(K_P\bar{q}) = 0 \Longleftrightarrow \bar{q} = 0_n \tag{3.31}$$

Finally, using the result from Eq. (3.31) in Eq. (3.29), one gets $G(q_d)\bar{s}_a(\bar{\phi}) = 0_n$.

Proposition 3.2 *For the closed-loop system in Eqs.* (3.27)*, under the consideration of Assumption 3.1, the trivial solution* $(\bar{q},\bar{\phi})(t) \equiv (0_n, 0_p)$ *is stable and, for any initial condition* $(\bar{q},\dot{q},\bar{\phi})(0) \in \mathbb{R}^n \times \mathbb{R}^n \times \mathbb{R}^p$*,* $\bar{q}(t) \to 0_n$ *as* $t \to \infty$*, and* $\bar{s}_a(\bar{\phi}(t)) \to \ker(G(q_d))$ *as* $t \to \infty$*, with* $|\tau_i(t)| = |u_i(t)| < T_i$*,* $i = 1, \ldots, n$*,* $\forall t \geq 0$*.* $\triangleleft$

Proof. By (3.26), we see that, along the system trajectories, $|\tau_i(t)| = |u_i(t)| < T_i$, $\forall t \geq 0$. This proves that, under the proposed adaptive scheme, input saturation is avoided. Now, in order to develop the stability/convergence analysis, let us define the scalar function

$$V_1(\bar{q},\dot{q},\bar{\phi}) = V_0(\bar{q},\dot{q}) + \int_{0_p}^{\bar{\phi}} \bar{s}_a^T(r)\Gamma^{-1}dr \tag{3.32}$$

where $\int_{0_p}^{\bar{\phi}} \bar{s}_a^T(r)\Gamma^{-1}dr = \sum_{j=1}^{p} \int_0^{\bar{\phi}_j} \bar{s}_{aj}(r_j)\gamma_j^{-1}dr_j$, and $V_0(\bar{q},\dot{q})$ is as defined in Eq. (3.9).[7] Note that, from the positive definite and radially unbounded characters of $V_0(\bar{q},\dot{q})$ (shown in the proof of Proposition 3.1) and items 8b, 6, and 7 of Lemma 2.4 (through which the integral term in the right-hand side of Eq. (3.32) is concluded to be a radially unbounded positive definite function of $\bar{\phi}$), $V_1(\bar{q},\dot{q},\bar{\phi})$ proves to be positive definite and radially unbounded. Its upper-right derivative along the system trajectories, $\dot{V}_1 = D^+V_1$ [38, App. I] [32, §6.1A], is given by

$$\begin{aligned}
&\dot{V}_1(\bar{q},\dot{q},\bar{\phi}) \\
&\quad= \dot{q}^T H(q)\ddot{q} + \frac{1}{2}\dot{q}^T\dot{H}(q,\dot{q})\dot{q} + \varepsilon s_P^T(K_P\bar{q})H(q)\ddot{q} + \varepsilon\dot{q}^T\dot{H}(q,\dot{q})s_P(K_P\bar{q}) \\
&\qquad+ \varepsilon\dot{q}^T H(q)s_P'(K_P\bar{q})K_P\dot{q} + s_P^T(K_P\bar{q})\dot{q} + \bar{s}_a^T(\bar{\phi})\Gamma^{-1}\dot{\bar{\phi}} \\
&\quad= \dot{q}^T\big[-C(q,\dot{q})\dot{q} - F\dot{q} - s_d\big(\bar{q},\dot{q},s_a(\phi)\big) - s_P(K_P\bar{q}) + G(q)\bar{s}_a(\bar{\phi})\big] + \frac{1}{2}\dot{q}^T\dot{H}(q,\dot{q})\dot{q} \\
&\qquad+ \varepsilon s_P^T(K_P\bar{q})\big[-C(q,\dot{q})\dot{q} - F\dot{q} - s_d\big(\bar{q},\dot{q},s_a(\phi)\big) - s_P(K_P\bar{q}) + G(q)\bar{s}_a(\bar{\phi})\big] \\
&\qquad+ \varepsilon\dot{q}^T\dot{H}(q,\dot{q})s_P(K_P\bar{q}) + \varepsilon\dot{q}^T H(q)s_P'(K_P\bar{q})K_P\dot{q} + s_P^T(K_P\bar{q})\dot{q} \\
&\qquad- \bar{s}_a^T(\bar{\phi})G^T(q)\big[\dot{q} + \varepsilon s_P(K_P\bar{q})\big] \\
&\quad= -\dot{q}^T F\dot{q} - \dot{q}^T s_d\big(\bar{q},\dot{q},s_a(\phi)\big) - \varepsilon s_P^T(K_P\bar{q})F\dot{q} - \varepsilon s_P^T(K_P\bar{q})s_d\big(\bar{q},\dot{q},s_a(\phi)\big) \\
&\qquad- \varepsilon s_P^T(K_P\bar{q})s_P(K_P\bar{q}) + \varepsilon\dot{q}^T C(q,\dot{q})s_P(K_P\bar{q}) + \varepsilon\dot{q}^T H(q)s_P'(K_P\bar{q})K_P\dot{q}
\end{aligned}$$

where $H(q)\ddot{q}$ and $\dot{\bar{\phi}}$ have been replaced by their equivalent expressions from the closed-loop manipulator dynamics in Eq. (3.27), Property 1.2.1 has been used, and $s_P'(K_P\bar{q})$ was defined in (3.14). Observe that from Properties 1.1, 1.2.5, and 1.3, the satisfaction of (3.5), items (b) of Definition 2.4 and 2 of Lemma 2.4, and the positive definite character of K_P, we have that

$$\dot{V}_1(\bar{q},\dot{q},\bar{\phi}) \leq -\dot{q}^T s_d\big(\bar{q},\dot{q},s_a(\phi)\big) - W_1(\bar{q},\dot{q})$$

[7] The complete expression is given as

$$V_1(\bar{q},\dot{q},\bar{\phi}) = \frac{1}{2}\dot{q}^T H(q)\dot{q} + \varepsilon s_P^T(K_P\bar{q})H(q)\dot{q} + \int_{0_n}^{\bar{q}} s_P^T(K_P r)dr + \int_{0_p}^{\bar{\phi}} \bar{\sigma}_a^T(r)\Gamma^{-1}dr$$

where $W_1(\bar{q},\dot{q})$ was defined in (3.15) and shown to be a positive definite function in the proof of Proposition 3.1. From this and (3.6), we have that $\dot{V}_1(\bar{q},\dot{q},\bar{\phi}) \leq 0$, $\forall(\bar{q},\dot{q},\bar{\phi}) \in \mathbb{R}^n \times \mathbb{R}^n \times \mathbb{R}^p$, with $\dot{V}_1(\bar{q},\dot{q},\bar{\phi}) = 0 \iff (\bar{q},\dot{q}) = (0_n, 0_n)$. Therefore, by Lyapunov's second method (see Footnote 2), the trivial solution $(\bar{q},\bar{\phi})(t) \equiv (0_n, 0_p)$ is concluded to be stable. Now, in view of the radially unbounded character of $V_1(\bar{q},\dot{q},\bar{\phi})$, the set

$$\Omega \triangleq \{(\bar{q},\dot{q},\bar{\phi}) \in \mathbb{R}^n \times \mathbb{R}^n \times \mathbb{R}^p : V_1(\bar{q},\dot{q},\bar{\phi}) \leq c\} \tag{3.33}$$

is compact for any positive constant c [22, p. 128]. Moreover, in view of the seminegative definite character of $\dot{V}_1(\bar{q},\dot{q},\bar{\phi})$, Ω is positively invariant with respect to the closed-loop system. Furthermore, from previous arguments, we have that $E \triangleq \{(\bar{q},\dot{q},\bar{\phi}) \in \Omega : \dot{V}_1(\bar{q},\dot{q},\bar{\phi}) = 0\} = \{(\bar{q},\dot{q},\bar{\phi}) \in \Omega : \bar{q} = \dot{q} = 0_n\}$. Further, from Remark 3.4, the largest invariant set in E, denoted $\mathcal{M}$, is given as $\mathcal{M} = \{(\bar{q},\dot{q},\bar{\phi}) \in E : \bar{s}_a(\bar{\phi}) \in \ker(G(q_d))\}$. Thus, by the invariance theory [32, §7.2] —more specifically, by [32, Theorem 7.2.1][8]—, we have that $(\bar{q},\dot{q},\bar{\phi})(0) \in \Omega \implies (\bar{q},\dot{q},\bar{\phi})(t) \to \mathcal{M}$ as $t \to \infty$. Since this holds for any $c > 0$ and $V_1(\bar{q},\dot{q},\bar{\phi})$ is radially unbounded (in view of which Ω may be rendered arbitrarily large), we conclude that, for any $(\bar{q},\dot{q},\bar{\phi})(0) \in \mathbb{R}^n \times \mathbb{R}^n \times \mathbb{R}^p$, $\bar{q}(t) \to 0_n$ as $t \to \infty$ and $\bar{s}_a(\bar{\phi}(t)) \to \ker(G(q_d))$ as $t \to \infty$, which completes the proof. ◁

Corollary 3.1 *If $G^T(q_d)G(q_d)$ is nonsingular, then the trivial solution $(\bar{q},\bar{\phi})(t) \equiv (0_n, 0_p)$ is globally asymptotically stable.* ◁

Proof. This is concluded by noting on the one hand that non-singularity of $G^T(q_d)G(q_d)$ implies that $\ker(G(q_d)) = \{0_p\}$, and on the other hand that $\bar{s}_a(\bar{\phi}) = 0_p \iff \bar{\phi} = 0_p$. Then, from Proposition (3.2), we have that, for any $(\bar{q},\dot{q},\bar{\phi})(0) \in \mathbb{R}^n \times \mathbb{R}^n \times \mathbb{R}^p$, $(\bar{q},\bar{\phi})(t) \to (0_n, 0_p)$ as $t \to \infty$, whence the stability of the trivial solution $(\bar{q},\bar{\phi})(t) \equiv (0_n, 0_p)$ is concluded to be globally asymptotical [22, §4.1], [16, §26], [38, Chap. I, §2.10–2.11], [43, §2.3.1]. ◁

If $G^T(q_d)G(q_d)$ is non-singular, $G(q_d)$ is said to be pseudo-invertible. Pseudo-invertibility of $G(q_d)$ is fulfilled if $G(q_d)$ has full-column rank. The fulfillment of this property will depend on the specific (geometrical) structure of each manipulator and the particular value of q_d.

Remark 3.5 Let $e_1 = -y_2 = -\left(I_n \;\; I_n\right)^T G(q)\bar{s}_a(\bar{\phi})$, $e_2 = y_1 = -\left(\varepsilon s_P^T(K_P\bar{q}) \;\; \dot{q}^T\right)^T$, $V_2(\bar{\phi}) = \int_{0_P}^{\bar{\phi}} \bar{s}_a^T(r)\Gamma^{-1}dr$ and consider $V_0(\bar{q},\dot{q})$ as defined in Eq. (3.9). By previous arguments and developments, V_0 and V_2 are radially unbounded positive definite functions in their respective arguments. Following an analysis analog to that of the proofs of Propositions 3.1 and (3.2), one obtains

$$\dot{V}_0 \leq -W_1(\bar{q},\dot{q}) + e_1^T y_1$$

[8]Theorem 7.2.1 in [32] may be seen as a version of La Salle's invariance principle that considers autonomous systems with continuous dynamics and makes use of continuous scalar functions and their upper-right derivative along the system trajectories [32, §6.1A] (in contrast, for instance, with the statement presented in [22, Theorem 4.4], which is addressed to autonomous state equations with locally Lipschitz-continuous vector fields and makes use of continuously differentiable scalar functions).

and

$$\dot{V}_2 \leq e_2^T y_2$$

with $W_1(\bar{q}, \dot{q})$ as defined in the proof of Proposition 3.1 where it was proven to be positive definite in its arguments. Hence, the closed-loop system, in Eqs. (3.27), may be seen as a (negative) feedback connection among a strictly passive subsystems Σ_1 with dynamical model

$$\Sigma_1 : \begin{cases} H(q)\ddot{q} + C(q,\dot{q})\dot{q} + F\dot{q} = -s_d(\bar{q}, \dot{q}, \theta - e_1) - s_P(K_P\bar{q}) - (I_n \;\; 0_{n\times n})\, e_1 \\ y_1 = -\left(\varepsilon s_P^T(K_P\bar{q}) \;\; \dot{q}^T\right)^T \end{cases}$$

and a storage function $V_1(\bar{q}, \dot{q})$, and a (lossless) passive subsystem Σ_2 with state model

$$\Sigma_2 : \begin{cases} \dot{\bar{q}} = -\left(0_{n\times n} \;\; I_n\right) e_2 \\ \dot{\bar{\phi}} = \Gamma G^T(q) \left(I_n \;\; I_n\right) e_2 \\ y_2 = \left(I_n \;\; I_n\right)^T G(q) \bar{s}_a(\bar{\phi}) \end{cases}$$

and storage function $V_2(\bar{\phi})$. This representation shows that, at non-equilibrium conditions, the system energy flows from Σ_1 to Σ_2, through y_1, and back from Σ_2 to Σ_1, through y_2, generating a mutual excitation among Σ_1 and Σ_2. The energy dissipation carried out in Σ_1 —which involves the velocity and position errors and does not stop until they are all vanished— instantaneously decreases the closed loop stored energy and its flow entailing a continuous reduction on the mutual excitation intensity. This process holds as long as $(e_1, e_2) \neq (0_{2n}, 0_{2n})$, or equivalently $(y_1, y_2) \neq (0_{2n}, 0_{2n})$, and consequently $\|y_i(t)\| \to 0$ as $t \to \infty$, $i = 1, 2$. Note that the vanishing of y_1 implies that $(\bar{q}, \dot{q})(t) \to (0_n, 0_n)$ as $t \to \infty$ in view of which the global regulation objective is guaranteed. On the other hand, the vanishing of y_2 implies that

$$\lim_{t\to\infty} G\left(q(t)\right) \bar{s}_a\left(\bar{\phi}(t)\right) = G(q_d) \lim_{t\to\infty} \bar{s}_a\left(\bar{\phi}(t)\right) = 0_n$$

and consequently

$$\bar{s}_a\left(\bar{\phi}(t)\right) \to \ker\left(G(q_d)\right) \quad \text{as} \quad t \to \infty$$

which permits a steady state-error on the parameter estimations, unless $\ker\left(G(q_d)\right) = \{0_p\}$ which is implied by the conditions stated in Corollary 3.1 ◁

Remark 3.6 Adaptive versions of the SP-SD controller and of the SPD and SPDgc-like algorithms of [47] are obtained by considering in the proposed design method the expressions in (3.16), (3.18), and (3.20), respectively, with suitable adjustments on the saturation function parameter conditions. Thus, the SP-SD controller with adaptive gravity compensation is obtained from (3.24) taking

$$s_d(\bar{q}, \dot{q}, \hat{\theta}) = s_D(K_D\dot{q}) \tag{3.34}$$

with $s_D(\cdot)$ and K_D as defined in Remark 3.1, and the involved bound values, M_{Pi} and M_{Di}, satisfying

$$M_{Pi} + M_{Di} < T_i - B_{gi}^{Ma} \tag{3.35}$$

$i = 1, \ldots, n$, the adaptive SPD scheme is gotten taking

$$s_d(\bar{q}, \dot{q}, \hat{\theta}) = s_P(K_P\bar{q} + K_D\dot{q}) - s_P(K_P\bar{q}) \tag{3.36}$$

with $s_P(\cdot)$ as defined for this case in Remark 3.1, and bound values satisfying

$$M_{Pi} \leq T_i - B_{gi}^{Ma} \tag{3.37}$$

$i = 1, \ldots, n$, and the adaptive SPDgc-like algorithm is obtained taking

$$s_d(\bar{q}, \dot{q}, \hat{\theta}) = s_0\big(G(q)\hat{\theta} - s_P(K_P\bar{q})\big) - s_0\big(G(q)\hat{\theta} - s_P(K_P\bar{q}) - K_D\dot{q}\big) \tag{3.38}$$

with $s_0(\cdot)$ as defined in Remark 3.1, and the involved saturation function parameters satisfying

$$B_{gi}^{M_a} + M_{Pi} < L_{0i} \leq M_{0i} < T_i \tag{3.39}$$

$i = 1, \ldots, n$. For these cases, κ in (3.10) remains as specified in Remark 3.1 (see Eqs. (3.22)). ◁

3.2 Output-feedback regulation approach

In the case when velocity measurements are not available either, output-feedback adaptive control is still possible as presented next.

3.2.1 Output-feedback global adaptive regulation

We propose an output-feedback adaptive control scheme defined as

$$u(q, \vartheta, \hat{\theta}) = -s_P(K_P\bar{q}) - s_D(K_D\vartheta) + G(q)\hat{\theta} \tag{3.40}$$

with $\bar{q}$ and $G(q)$ as previously described in Section 3.1; $K_P \in \mathbb{R}^{n\times n}$ and $K_D \in \mathbb{R}^{n\times n}$ are positive definite diagonal matrices; $s_P(x) = \Big(\sigma_{P1}(x_1), \ldots, \sigma_{Pn}(x_n)\Big)^T$ and $s_D(x) = \Big(\sigma_{D1}(x_1), \ldots, \sigma_{Dn}(x_n)\Big)^T$, with $\sigma_{Pi}(\cdot)$ and $\sigma_{Di}(\cdot)$, $i = 1, \ldots, n$, being **generalized saturation functions** with bounds M_{Pi} and M_{Di} such that

$$M_{Pi} + M_{Di} < T_i - B_{gi}^{M_a} \tag{3.41}$$

$i = 1, \ldots, n$;[9] $\vartheta \in \mathbb{R}^n$ (the velocity estimator) and $\hat{\theta} \in \Theta_a \subset \mathbb{R}^p$ (the vector of estimated parameters) are the output vector variables of auxiliary dynamic subsystems defined as

$$\dot{q}_c = -AK_D^{-1}s_D\big(K_D(q_c + B\bar{q})\big) \tag{3.42a}$$

$$\vartheta = q_c + B\bar{q} \tag{3.42b}$$

[9]Note that the satisfaction of inequalities (3.23) guarantees positivity of the right-hand side of inequalities (3.41).

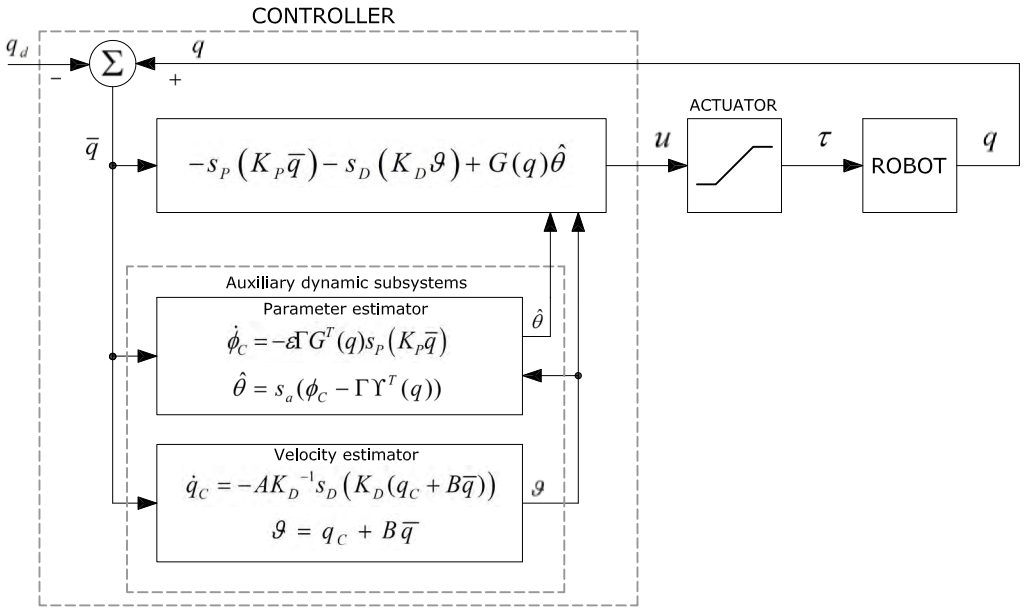

Figure 3.2: Block diagram of the output-feedback adaptive scheme

and

$$\dot{\phi}_c = -\varepsilon\Gamma G^T(q)s_P(K_P\bar{q}) \tag{3.43a}$$

$$\hat{\theta} = s_a\big(\phi_c - \Gamma\Upsilon^T(q)\big) \tag{3.43b}$$

where $A \in \mathbb{R}^{n\times n}$, $B \in \mathbb{R}^{n\times n}$, and $\Gamma \in \mathbb{R}^{p\times p}$ are positive definite diagonal matrices; q_c and ϕ_c are the state vectors of the auxiliary dynamics in Eqs. (3.42a) and (3.43a) respectively; $\Upsilon(q)$ is the regression vector related to the potential energy function, according to Property 1.5, *i.e.* such that $U(q,\theta) = \Upsilon(q)\theta$; for all $x \in \mathbb{R}^n$: $s_a(x) = \Big(\sigma_{a1}(x_1),\ldots,\sigma_{ap}(x_p)\Big)^T$, with $\sigma_{aj}(\cdot)$, $j = 1,\ldots,p$, being **strictly increasing generalized saturation functions** with bounds M_{aj} satisfying inequalities (3.23); and ε is a positive constant satisfying

$$\varepsilon < \varepsilon_M \triangleq \min\{\varepsilon_0, \varepsilon_1, \varepsilon_2\} \tag{3.44}$$

where

$$\varepsilon_0 \triangleq \sqrt{\frac{\mu_m}{\mu_M^2\beta_P}} \qquad \varepsilon_1 \triangleq \frac{f_m}{\beta_M + f_M^2/2} \qquad \varepsilon_2 \triangleq 2\beta_m$$

with $\beta_P \triangleq \max_i\{\sigma'_{PiM}k_{Pi}\}$, $\beta_m \triangleq \min_i\left\{\frac{a_i}{b_i k_{Di}}\right\}$, $\beta_M \triangleq k_C B_P + \mu_M\beta_P$, $B_P \triangleq \sqrt{\sum_{i=0}^{n} M_{Pi}^2}$, σ'_{PiM} being the positive bound of $D^+\sigma_{Pi}(\cdot)$ in accordance to point 2 of Lemma 2.4, and μ_m, μ_M, k_C, f_m, and f_M as defined in Properties 1.1, 1.2.5, and 1.3. A block diagram of the output-feedback adaptive control scheme is shown in Fig. 3.2.

Remark 3.7 Analogously to the state-feedback case of Section 3.1, one can see from expressions (3.40),(3.42)-(3.43), and (3.44) that the developed control scheme does not

involve the exact values of the elements of θ. Note further that the velocity vector $\dot{q}$ is not involved in any of the expressions in Eqs. (3.40),(3.42)-(3.43) either. $\triangleleft$

Remark 3.8 The auxiliary subsystem in Eqs. (3.42) is an alternative version of the dirty derivative (applied to $\bar{q}$) involving the saturation vector function $s_D(\cdot)$ in its dynamics. In its conventional form, where the function $s_D(\cdot)$ is not included (or equivalently, which is obtained by replacing $s_D(\cdot)$ in (3.42a) by the identity function), it leads (through its output variable ϑ) to the derivative of $\bar{q}$ (or equivalently, to the velocity vector $\dot{q}$) with every of its components going through a first-order low-pass filter. This is commonly done in practice to bound the gain of the high frequency components, giving rise to a causal (approximated) derivative operator. The consideration of $s_D(\cdot)$ in (3.42a) proves to be helpful to show the expected stability/convergence closed-loop properties, as will be seen in Section 3.2.2. $\triangleleft$

Closed-loop analysis

Consider system (3.1)-(3.2) taking $u = u(q, \vartheta, \hat{\theta})$ as defined through (3.40),(3.42)-(3.43). Define the variable transformation

$$\begin{pmatrix} \bar{q} \\ \vartheta \\ \bar{\phi} \end{pmatrix} = \begin{pmatrix} q - q_d \\ q_c + B(q - q_d) \\ \phi_c - \Gamma \Upsilon^T(q) - \phi^* \end{pmatrix} \tag{3.45}$$

with $\phi^* = \big(\phi_1^*, \ldots, \phi_p^*\big)^T$ such that $s_a(\phi^*) = \theta$, or equivalently, $\phi_j^* = \sigma_{aj}^{-1}(\theta_j)$, $j = 1, \ldots, p$. Observe that, from the fulfilment of inequalities (3.23) and (3.41), we have that $\big|u_i\big(\bar{q} + q_d, \vartheta, s_a(\bar{\phi} + \phi^*)\big)\big| \leq M_{Pi} + M_{Di} + B_{gi}^{M_a} < T_i$, $i = 1, \ldots, n$, $\forall (\bar{q}, \vartheta, \bar{\phi}) \in \mathbb{R}^n \times \mathbb{R}^n \times \mathbb{R}^n$, whence, in view of (3.2), one sees that

$$T_i > \big|u_i\big(\bar{q} + q_d, \vartheta, s_a(\bar{\phi} + \phi^*)\big)\big| = |u_i| = |\tau_i| \ , \\ i = 1, \ldots, n \ , \ \forall (\bar{q}, \vartheta, \bar{\phi}) \in \mathbb{R}^n \times \mathbb{R}^n \times \mathbb{R}^n \tag{3.46}$$

Thus, under the consideration of Property 1.5 and the variable transformation (3.45), the closed-loop dynamics adopts the form

$$H(q)\ddot{q} + C(q, \dot{q})\dot{q} + F\dot{q} = -s_P(K_P\bar{q}) - s_D\big(K_D\vartheta\big) + G(q)\bar{s}_a(\bar{\phi}) \tag{3.47a}$$

$$\dot{\vartheta} = -AK_D^{-1}s_D(K_D\vartheta) + B\dot{q} \tag{3.47b}$$

$$\dot{\bar{\phi}} = -\Gamma G^T(q)\big[\varepsilon s_P(K_P\bar{q}) + \dot{q}\big] \tag{3.47c}$$

where $\bar{s}_a(\bar{\phi}) = s_a(\bar{\phi} + \phi^*) - s_a(\phi^*)$. Observe that, by point 8b of Lemma 2.4, the elements of $\bar{s}_a(\bar{\phi})$, *i.e.* $\bar{\sigma}_{aj}(\bar{\phi}_j) = \sigma_{aj}(\bar{\phi}_j + \phi_j^*) - \sigma_{aj}(\phi_j^*)$, $j = 1, \ldots, p$, turn out to be strictly increasing generalized saturation functions.

Remark 3.9 Analogously to the adaptive approach of Section 3.1, let us note, from Eqs. (3.47), that under stationary conditions: $\ddot{q} = \dot{q} = \dot{\vartheta} = 0_n$ and $\dot{\bar{\phi}} = 0_p$, the desired position vector q_d is the unique equilibrium position of the closed-loop system —or equivalently, 0_n is the unique equilibrium position error of the closed loop— while the parameter estimation error equilibrium vector $\bar{\phi}_e$ turns out to be defined by the solutions of the equation $G(q_d)\bar{s}_a(\bar{\phi}_e) = 0_n$, and consequently $\bar{s}_a(\bar{\phi}_e) \in \ker(G(q_d))$. $\triangleleft$

Proposition 3.3 *Consider the closed-loop system in Eqs.* (3.47) *under the satisfaction of Assumption 3.1 and inequalities* (3.23) *and* (3.41)*. Then, for any positive definite diagonal matrices K_P, K_D, A, B, and Γ, and any ε satisfying inequality* (3.44)*, the trivial solution $(\bar{q}, \vartheta, \bar{\phi})(t) \equiv (0_n, 0_n, 0_p)$ is stable and, for any initial condition $(\bar{q}, \dot{q}, \vartheta, \bar{\phi})(0) \in \mathbb{R}^n \times \mathbb{R}^n \times \mathbb{R}^n \times \mathbb{R}^p$, $(\bar{q}, \vartheta)(t) \to (0_n, 0_n)$ as $t \to \infty$, and $\bar{s}_a(\bar{\phi}(t)) \to \ker(G(q_d))$ as $t \to \infty$, with $|\tau_i(t)| = |u_i(t)| < T_i$, $i = 1, \ldots, n$, $\forall t \geq 0$.* $\triangleleft$

Proof. By (3.46), one sees that, along the system trajectories, $|\tau_i(t)| = |u_i(t)| < T_i$, $\forall t \geq 0$. This proves that under the proposed output-feedback adaptive scheme, the input saturation values, T_i, are never reached. Now, in order to develop the stability/convergence analysis, let us define the scalar function

$$V(\bar{q}, \dot{q}, \vartheta, \bar{\phi}) = \frac{1}{2}\dot{q}^T H(q)\dot{q} + \varepsilon s_P^T(K_P\bar{q})H(q)\dot{q} + \int_{0_n}^{\bar{q}} s_P^T(K_P r)dr + \int_{0_p}^{\bar{\phi}} \bar{s}_a^T(r)\Gamma^{-1}dr + \int_{0_n}^{\vartheta} s_D^T(K_D r)B^{-1}dr \tag{3.48}$$

where

$$\int_{0_n}^{\bar{q}} s_P^T(K_P r)dr = \sum_{i=1}^{n} \int_0^{\bar{q}_i} \sigma_{Pi}(k_{Pi} r_i)dr_i,$$

$$\int_{0_n}^{\vartheta} s_D^T(K_D r)B^{-1}dr = \sum_{i=1}^{n} \int_0^{\vartheta_i} \sigma_{Di}(k_{Di} r_i)b_i^{-1}dr_i,$$

$$\text{and} \quad \int_{0_p}^{\bar{\phi}} \bar{s}_a^T(r)\Gamma^{-1}dr = \sum_{j=1}^{p} \int_0^{\bar{\phi}_j} \bar{\sigma}_{aj}(r_j)\gamma_j^{-1}dr_j$$

Observe that, under the consideration of Property 1.1, we have that

$$V(\bar{q}, \dot{q}, \vartheta, \bar{\phi}) \geq \frac{\mu_m}{2}\|\dot{q}\|^2 - \varepsilon\mu_M\|s_P(K_P\bar{q})\|\|\dot{q}\| + \alpha_0 \int_{0_n}^{\bar{q}} s_P^T(K_P r)dr + W_{01}(\bar{q}, \vartheta, \bar{\phi})$$

with

$$W_{01}(\bar{q}, \vartheta, \bar{\phi}) = \int_{0_n}^{\vartheta} s_D^T(K_D r)B^{-1}dr + \int_{0_p}^{\bar{\phi}} \bar{s}_a^T(r)\Gamma^{-1}dr + (1 - \alpha_0)\int_{0_n}^{\bar{q}} s_P^T(K_P r)dr$$

for any constant $\alpha_0 \in (0, 1)$. Moreover, from point 5 of Lemma 2.4, we have:

$$\int_0^{\bar{q}_i} \sigma_{Pi}(k_{Pi} r_i)dr_i \geq \frac{\sigma_{Pi}^2(k_{Pi}\bar{q}_i)}{2k_{Pi}\sigma'_{PiM}} \quad \forall \bar{q}_i \in \mathbb{R}$$

$\forall \bar{q}_i \in \mathbb{R}$, whence we get:

$$\alpha_0 \int_{0_n}^{\bar{q}} s_P^T(K_P r)dr = \alpha_0 \sum_{i=1}^{n} \int_0^{\bar{q}_i} \sigma_{Pi}(k_{Pi} r_i)dr_i \geq \alpha_0 \sum_{i=1}^{n} \frac{\sigma_{Pi}^2(k_{Pi}\bar{q}_i)}{2k_{Pi}\sigma'_{PiM}}$$

$$\geq \frac{\alpha_0}{2\max_i\{k_{Pi}\sigma'_{PiM}\}} \sum_{i=1}^{n} \sigma_{Pi}^2(k_{Pi}\bar{q}_i) = \frac{\alpha_0}{2\beta_P}\|s_P(K_P\bar{q})\|^2$$

and consequently

$$V(\bar{q},\dot{q},\vartheta,\bar{\phi}) \geq \frac{\mu_m}{2}\|\dot{q}\|^2 - \varepsilon\mu_M\|s_P(K_P\bar{q})\|\|\dot{q}\| + \frac{\alpha_0}{2\beta_P}\|s_P(K_P\bar{q})\|^2 + W_{01}(\bar{q},\vartheta,\bar{\phi})$$

which may be rewritten as

$$V(\bar{q},\dot{q},\vartheta,\bar{\phi}) \geq W_{00}(\bar{q},\dot{q}) + W_{01}(\bar{q},\vartheta,\bar{\phi}) \triangleq W_0(\bar{q},\dot{q},\vartheta,\bar{\phi})$$

with

$$W_{00}(\bar{q},\dot{q}) = \frac{1}{2}\begin{pmatrix}\|s_P(K_P\bar{q})\| \\ \|\dot{q}\|\end{pmatrix}^T\begin{pmatrix}\frac{\alpha_0}{\beta_P} & -\varepsilon\mu_M \\ -\varepsilon\mu_M & \mu_m\end{pmatrix}\begin{pmatrix}\|s_P(K_P\bar{q})\| \\ \|\dot{q}\|\end{pmatrix}$$

where α_0 is chosen such that

$$\frac{\varepsilon^2}{\varepsilon_0^2} < \alpha_0 < 1 \tag{3.49}$$

Note that (3.44) guarantees the existence of positive values α_0 satisfying (3.49) (since $\varepsilon < \varepsilon_M \leq \varepsilon_0 \implies \frac{\varepsilon^2}{\varepsilon_0^2} < 1$). Moreover, by (3.49), W_{00} is a positive definite function of $(\bar{q},\dot{q})$,[10] while from point 6 of Lemma 2.4, one sees that $W_{01}(\bar{q},\vartheta,\bar{\phi}) \geq 0$, $\forall(\bar{q},\vartheta,\bar{\phi}) \in \mathbb{R}^n\times\mathbb{R}^n\times\mathbb{R}^p$, with $W_{01}(\bar{q},\vartheta,\bar{\phi}) = 0 \iff (\bar{q},\vartheta,\bar{\phi}) = (0_n,0_n,0_p)$. Hence, $W_0(\bar{q},\dot{q},\vartheta,\bar{\phi})$ is concluded to be positive definite. Taking this into account, by noting that $W_{00}(0_n,\dot{q}) \to \infty$ as $\|\dot{q}\| \to \infty$, and from point 7 of Lemma 2.4 that $W_{01}(\bar{q},0_n,0_p) \to \infty$ as $|\bar{q}_i| \to \infty$ for every $i \in \{1,\ldots,n\}$, $W_{01}(0_n,\vartheta,0_p) \to \infty$ as $|\vartheta_i| \to \infty$ for every $i \in \{1,\ldots,n\}$, and $W_{01}(0_n,0_n,\bar{\phi}) \to \infty$ as $|\bar{\phi}_j| \to \infty$ for every $j \in \{1,\ldots,p\}$, $W_0(\bar{q},\dot{q},\vartheta,\bar{\phi})$ additionally proves to be radially unbounded [21, p. 115]. Therefore, $V(\bar{q},\dot{q},\vartheta,\bar{\phi})$ is concluded to be positive definite and radially unbounded. Its upper-right derivative along the system trajectories, $\dot{V} = D^+V$ [38, App. I] [32, §6.1A], is given by

$$\begin{aligned}\dot{V}(\bar{q},\dot{q},\vartheta,\bar{\phi}) = {} & \dot{q}^TH(q)\ddot{q} + \frac{1}{2}\dot{q}^T\dot{H}(q,\dot{q})\dot{q} + \varepsilon s_P^T(K_P\bar{q})H(q)\ddot{q} + \varepsilon s_P^T(K_P\bar{q})\dot{H}(q,\dot{q})\dot{q} \\ & + \varepsilon\dot{q}^TH(q)s_P'(K_P\bar{q})K_P\dot{q} + s_P^T(K_P\bar{q})\dot{q} + s_D^T(K_D\vartheta)B^{-1}\dot{\vartheta} + \bar{s}_a^T(\bar{\phi})\Gamma^{-1}\dot{\bar{\phi}} \\ = {} & -\dot{q}^TF\dot{q} - \varepsilon s_P^T(K_P\bar{q})F\dot{q} - \varepsilon s_P^T(K_P\bar{q})s_P(K_P\bar{q}) - \varepsilon s_P^T(K_P\bar{q})s_D(K_D\vartheta) \\ & + \varepsilon\dot{q}^TC(q,\dot{q})s_P(K_P\bar{q}) + \varepsilon\dot{q}^TH(q)s_P'(K_P\bar{q})K_P\dot{q} \\ & - s_D^T(K_D\vartheta)B^{-1}AK_D^{-1}s_D(K_D\vartheta)\end{aligned}$$

where $H(q)\ddot{q}$, $\dot{\vartheta}$, and $\dot{\bar{\phi}}$ have been replaced by their equivalent expression from the closed-loop manipulator dynamics in Eqs. (3.47), Property 1.2.1 has been used, and $s_P'(K_P\bar{q}) \triangleq \mathrm{diag}[D^+\sigma_{P1}(k_{P1}\bar{q}_1),\ldots,D^+\sigma_{Pn}(k_{Pn}\bar{q}_n)]$. Observe that from Properties 1.1, 1.2.5, 1.3, and points (b) of Definition 2.4 and 2 of Lemma 2.4, we have that

$$\begin{aligned}\dot{V}(\bar{q},\dot{q},\vartheta,\bar{\phi}) \leq {} & -f_m\|\dot{q}\|^2 + \varepsilon f_M\|s_P(K_P\bar{q})\|\|\dot{q}\| - \varepsilon\|s_P(K_P\bar{q})\|^2 \\ & + \varepsilon\|s_P(K_P\bar{q})\|\|s_D(K_D\vartheta)\| + \varepsilon\big(k_CB_P + \mu_M\beta_P\big)\|\dot{q}\|^2 - \beta_m\|s_D(K_D\vartheta)\|^2\end{aligned}$$

[10] By (3.49), it follows that $\varepsilon^2\left(\frac{\mu_M^2\beta_P}{\mu_m}\right) = \frac{\varepsilon^2}{\varepsilon_0^2} < \alpha_0 \implies \varepsilon^2\mu_M^2 < \frac{\alpha_0\mu_m}{\beta_P} \implies 0 < \frac{\alpha_0\mu_m}{\beta_P} - \varepsilon^2\mu_M^2 = \det(Q_0)$ whence (taking into account that $\frac{\alpha_0}{\beta_P} > 0$, by the leading principal minor criterion) Q_0 is concluded to be a positive definite symmetric matrix.

which may be rewritten as

$$\dot{V}(\bar{q},\dot{q},\vartheta,\bar{\phi}) \leq -W_1(\bar{q},\dot{q}) - W_2(\bar{q},\vartheta)$$

where

$$W_1(\bar{q},\dot{q}) = \begin{pmatrix} \|s_P(K_P\bar{q})\| \\ \|\dot{q}\| \end{pmatrix}^T \begin{pmatrix} \frac{\varepsilon}{2} & -\frac{\varepsilon f_M}{2} \\ -\frac{\varepsilon f_M}{2} & f_m - \varepsilon\beta_M \end{pmatrix} \begin{pmatrix} \|s_P(K_P\bar{q})\| \\ \|\dot{q}\| \end{pmatrix}$$

$$W_2(\bar{q},\vartheta) = \begin{pmatrix} \|s_P(K_P\bar{q})\| \\ \|s_D(K_D\vartheta)\| \end{pmatrix}^T \begin{pmatrix} \frac{\varepsilon}{2} & -\frac{\varepsilon}{2} \\ -\frac{\varepsilon}{2} & \beta_m \end{pmatrix} \begin{pmatrix} \|s_P(K_P\bar{q})\| \\ \|s_D(K_D\vartheta)\| \end{pmatrix}$$

Let us note that the fulfillment of (3.44) renders W_1 and W_2 positive definite functions of $(\bar{q},\dot{q})$ and $(\bar{q},\vartheta)$ respectively.[11] Hence, $\dot{V}(\bar{q},\dot{q},\vartheta,\bar{\phi}) \leq 0$, $\forall(\bar{q},\dot{q},\vartheta,\bar{\phi}) \in \mathbb{R}^n \times \mathbb{R}^n \times \mathbb{R}^n \times \mathbb{R}^p$, with $\dot{V}(\bar{q},\dot{q},\vartheta,\bar{\phi}) = 0 \iff (\bar{q},\dot{q},\vartheta) = (0_n, 0_n, 0_n)$. Thus, by Lyapunov's 2nd method (see footnote 2), the trivial solution $(\bar{q},\vartheta,\bar{\phi})(t) \equiv (0_n, 0_n, 0_p)$ is concluded to be stable. Now, in view of the radially unbounded character of $V(\bar{q},\dot{q},\vartheta,\bar{\phi})$, the set $\Omega \triangleq \{(\bar{q},\dot{q},\vartheta,\bar{\phi}) \in \mathbb{R}^n \times \mathbb{R}^n \times \mathbb{R}^n \times \mathbb{R}^p : V(\bar{q},\dot{q},\vartheta,\bar{\phi}) \leq c\}$ is compact for any positive constant c [21, p. 115]. Moreover, in view of the negative semidefinite character of $\dot{V}(\bar{q},\dot{q},\vartheta,\bar{\phi})$, Ω is positively invariant with respect to the closed-loop dynamics [21, p. 101]. Furthermore, from previous arguments, we have that $E \triangleq \{(\bar{q},\dot{q},\vartheta,\bar{\phi}) \in \Omega : \dot{V}(\bar{q},\dot{q},\vartheta,\bar{\phi}) = 0\} = \{(\bar{q},\dot{q},\vartheta,\bar{\phi}) \in \Omega : \bar{q} = \dot{q} = \vartheta = 0_n\}$. Further, from Remark 3.9, the largest invariant set in E, denoted $\mathcal{M}$, is given as $\mathcal{M} = \{(\bar{q},\dot{q},\vartheta,\bar{\phi}) \in E : \bar{s}_a(\bar{\phi}) \in \ker(G(q_d))\}$. Thus, by the invariance theory [32, §7.2] —more specifically, by [32, Theorem 7.2.1] (see footnote 8)—, we have that $(\bar{q},\dot{q},\vartheta,\bar{\phi})(0) \in \Omega \implies (\bar{q},\dot{q},\vartheta,\bar{\phi})(t) \to \mathcal{M}$ as $t \to \infty$. Since this holds for any $c > 0$ and $V(\bar{q},\dot{q},\vartheta,\bar{\phi})$ is radially unbounded (in view of which Ω may be rendered arbitrarily large), we conclude that, for any $(\bar{q},\dot{q},\vartheta,\bar{\phi})(0) \in \mathbb{R}^n \times \mathbb{R}^n \times \mathbb{R}^n \times \mathbb{R}^p$, $(\bar{q},\vartheta)(t) \to (0_n, 0_n)$ as $t \to \infty$ and $\bar{s}_a(\bar{\phi}(t)) \to \ker(G(q_d))$ as $t \to \infty$, which completes the proof. ◁

Corollary 3.2 *If $G^T(q_d)G(q_d)$ is nonsingular, then the trivial solution $(\bar{q},\vartheta,\bar{\phi})(t) \equiv (0_n, 0_n, 0_p)$ is globally asymptotically stable.* ◁

Proof. Note, on the other hand, that non-singularity of $G^T(q_d)G(q_d)$ implies that $\ker(G(q_d)) = \{0_p\}$, and on the other hand that $\bar{s}_a(\bar{\phi}) = 0_p \iff \bar{\phi} = 0_p$. Then, from Proposition 3.4, we have that, for any $(\bar{q},\dot{q},\vartheta,\bar{\phi})(0) \in \mathbb{R}^n \times \mathbb{R}^n \times \mathbb{R}^n \times \mathbb{R}^p$, $(\bar{q},\vartheta,\bar{\phi})(t) \to (0_n, 0_n, 0_p)$ as $t \to \infty$, whence the stability of the trivial solution $(\bar{q},\vartheta,\bar{\phi})(t) \equiv (0_n, 0_n, 0_p)$ is concluded to be globally asymptotical [22, §4.1], [16, §26], [38, Chap. I, §2.10–2.11], [43, §2.3.1]. ◁

[11] By (3.44), it follows that $\varepsilon < \varepsilon_M \leq \varepsilon_1 = \frac{f_m}{\beta_M + f_M^2/2} \implies \frac{\varepsilon^2}{2}\left(\beta_M + \frac{f_M^2}{2}\right) < \frac{\varepsilon f_m}{2} \implies 0 < \frac{\varepsilon}{2}(f_m - \varepsilon\beta_M) - \left(\frac{\varepsilon f_M}{2}\right)^2 = \det(Q_1)$, and $\varepsilon < \varepsilon_M \leq \varepsilon_2 = 2\beta_m \implies 0 < \frac{\varepsilon\beta_m}{2} - \frac{\varepsilon^2}{4} = \det(Q_2)$ whence (taking into account that $\frac{\varepsilon}{2} > 0$, by the leading principal minor criterion) Q_1 and Q_2 are concluded to be positive definite symmetric matrices.

Remark 3.10 Let

$$\begin{aligned}
e_1 &= -y_2 = -\left(I_n \;\; I_n\right)^T G(q)\bar{s}_a(\bar{\phi}) \\
e_2 &= y_1 = -\left(\varepsilon s_P^T(K_P\bar{q}) \;\; \dot{q}^T\right)^T \\
V_1(\bar{q},\vartheta) &= \frac{1}{2}\dot{q}^T H(q)\dot{q} + \varepsilon s_P^T(K_P\bar{q})H(q)\dot{q} + \int_{0_n}^{\bar{q}} s_P^T(K_P r)dr + \int_{0_n}^{\vartheta} s_D^T(K_D r)B^{-1}dr \\
V_2(\bar{\phi}) &= \int_{0_P}^{\bar{\phi}} \bar{s}_a^T(r)\Gamma^{-1}dr
\end{aligned}$$

By previous arguments and developments, V_1 and V_2 are radially unbounded positive definite functions in their respective arguments. Following an analysis similar to that of the proof of Proposition 3.4, one obtains

$$\dot{V}_1 \leq -W_1(\bar{q},\dot{q}) - W_2(\dot{q},\vartheta) - W_3(\bar{q},\vartheta) + e_1^T y_1$$

and

$$\dot{V}_2 \leq e_2^T y_2$$

with $W_1(\bar{q},\dot{q})$, $W_2(\dot{q},\vartheta)$, and $W_3(\bar{q},\vartheta)$ being positive definite in their arguments. Hence, the closed-loop system, in Eqs. (3.47), may be seen as a (negative) feedback connection among a strictly passive subsystems Σ_1 with dynamical model

$$\Sigma_1 : \begin{cases} H(q)\ddot{q} + C(q,\dot{q})\dot{q} + F\dot{q} = -s_P(K_P\bar{q}) - s_D(K_D\vartheta) - \left(I_n \;\; 0_{n\times n}\right)e_1 \\ \dot{\vartheta} = -AK_D^{-1}s_D\left(K_D\vartheta\right) + B\dot{q} \\ y_1 = -\left(\varepsilon s_P^T(K_P\bar{q}) \;\; \dot{q}^T\right)^T \end{cases}$$

and a storage function $V_1(\bar{q},\dot{q})$, and a (lossless) passive subsystem Σ_2 with state model

$$\Sigma_2 : \begin{cases} \dot{q} = -\left(0_{n\times n} \;\; I_n\right)e_2 \\ \dot{\bar{\phi}} = \Gamma G^T(q)\left(I_n \;\; I_n\right)e_2 \\ y_2 = \left(I_n \;\; I_n\right)^T G(q)\bar{s}_a(\bar{\phi}) \end{cases}$$

and storage function $V_2(\bar{\phi})$. Analogously to the state-feedback case described in Remark 3.5, this representation shows that, at non-equilibrium conditions, the system energy flows from Σ_1 to Σ_2, through y_1, and back from Σ_2 to Σ_1, through y_2, generating a mutual excitation among Σ_1 and Σ_2. The energy dissipation carried out in Σ_1 —which involves the velocity and position errors and does not stop until they are all vanished— instantaneously decreases the closed loop stored energy and its flow entailing a continuous reduction on the mutual excitation intensity. This process holds as long as $(e_1,e_2) \neq (0_{2n},0_{2n})$, or equivalently $(y_1,y_2) \neq (0_{2n},0_{2n})$, and consequently $\|y_i(t)\| \to 0$ as $t \to \infty$, $i = 1,2$. Note that the vanishing of y_1 implies that $(\bar{q},\dot{q})(t) \to (0_n,0_n)$ as $t \to \infty$ in view of which the global regulation objective is guaranteed. On the other hand, the vanishing of y_2 implies that

$$\lim_{t\to\infty} G\left(q(t)\right)\bar{s}_a\left(\bar{\phi}(t)\right) = G(q_d)\lim_{t\to\infty}\bar{s}_a\left(\bar{\phi}(t)\right) = 0_n$$

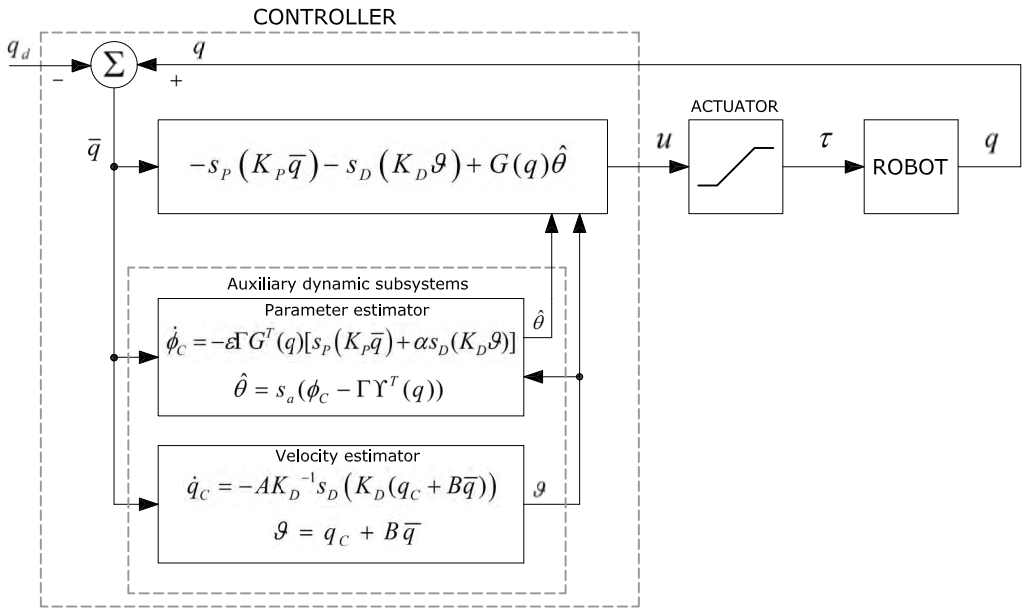

Figure 3.3: Block diagram of the extended output-feedback adaptive scheme

and consequently

$$\bar{s}_a\left(\bar{\phi}(t)\right) \to \ker\left(G(q_d)\right) \quad \text{as} \quad t \to \infty$$

which permits a steady state-error on the parameter estimations, unless $\ker\left(G(q_d)\right) = \{0_p\}$ which is implied by the conditions stated in Corollary 3.1 ◁

3.2.2 Output-feedback global adaptive regulation with extended adaptation algorithm

An alternative version of the output-feedback adaptive scheme is proposed under the consideration of Eqs. (3.40), (3.42), and the extended adaptation dynamics given by

$$\dot{\phi}_c = -\varepsilon\Gamma G^T(q)\left[s_P(K_P\bar{q}) + \alpha s_D(K_D\vartheta)\right] \tag{3.50a}$$

$$\hat{\theta} = s_a\left(\phi_c - \Gamma\Upsilon^T(q)\right) \tag{3.50b}$$

where α is a constant that may arbitrarily take any real value. A block diagram of the extended output-feedback adaptive control scheme is shown in Fig. 3.3.

The α-term extending the adaptation dynamics in (3.50a) has been included for the sake of generality, since an analogue term was considered in a previous approach [25]. Furthermore, the α-term in (3.50a) has a natural influence in the closed-loop responses which could be used for performance adjustment purposes. This aspect will not be explored in this dissertation.

Closed-loop analysis

Consider system (3.1)-(3.2) taking $u = u(q, \vartheta, \hat{\theta})$ as defined in Eqs. (3.40),(3.42), in Eqs. (3.50). By Property 1.5 and the variable transformation (3.45), the closed-loop

dynamics adopts the form

$$H(q)\ddot{q} + C(q,\dot{q})\dot{q} + F\dot{q} = -s_P(K_P\bar{q}) - s_D\big(K_D\vartheta\big) + G(q)\bar{s}_a(\bar{\phi}) \tag{3.51a}$$

$$\dot{\vartheta} = -AK_D^{-1}s_D(K_D\vartheta) + B\dot{q} \tag{3.51b}$$

$$\dot{\bar{\phi}} = -\Gamma G^T(q)\big[\varepsilon s_P(K_P\bar{q}) + \alpha\varepsilon s_D(K_D\vartheta) + \dot{q}\big] \tag{3.51c}$$

where $\bar{s}_a(\bar{\phi}) = s_a(\bar{\phi} + \phi^*) - s_a(\phi^*)$.

Let

$$\varepsilon_0 \triangleq \sqrt{\frac{\mu_m}{\mu_M^2\left(\beta_P + \alpha^2\beta_{D0}\right)}} \tag{3.52a}$$

$$\varepsilon_1 \triangleq \frac{f_m}{\beta_{MP} + \dfrac{f_M^2}{2} + |\alpha|\left(\beta_{MD} + \dfrac{f_m}{\bar{\varepsilon}_3}\right)} \tag{3.52b}$$

$$\varepsilon_2 \triangleq \frac{2\beta_m}{1 + \alpha^2 + \dfrac{2\beta_m}{\bar{\varepsilon}_3}|\alpha|} \tag{3.52c}$$

where

$$\beta_P \triangleq \max_i\{\sigma'_{PiM}k_{Pi}\} \quad , \quad \beta_{D0} \triangleq \max_i\left\{\frac{\sigma'_{DiM}k_{Di}}{b_i}\right\}$$

$$\beta_{MP} \triangleq k_C B_P + \mu_M\beta_P \quad , \quad \beta_{MD} \triangleq k_C B_D + \mu_M\beta_{D1}$$

$$\beta_m \triangleq \min_i\left\{\frac{a_i}{b_i k_{Di}}\right\} \quad , \quad \bar{\varepsilon}_3 \triangleq \frac{2\sqrt{f_m\beta_m}}{\beta_{Ma}}$$

$$B_P \triangleq \sqrt{\sum_{i=0}^{n} M_{Pi}^2} \quad , \quad B_D \triangleq \sqrt{\sum_{i=0}^{n} M_{Di}^2}$$

$$\beta_{D1} \triangleq \max_i\left\{\sigma'_{DiM}k_{Di}b_i\right\} \quad , \quad \beta_{Ma} \triangleq f_M + \mu_M\beta_{Da}$$

$$\beta_{Da} \triangleq \max_i\left\{\sigma'_{DiM}a_i\right\}$$

with σ'_{PiM} and σ'_{DiM} being the positive bounds of $D^+\sigma_{Pi}(\cdot)$ and $D^+\sigma_{Di}(\cdot)$, respectively, in accordance to point 2 of Lemma 2.4, and μ_m, μ_M, k_C, f_m, and f_M as defined in Properties 1.1, 1.2.5, and 1.3. We are ready to state the main analytical result.

Proposition 3.4 *Consider the closed-loop system in Eqs.* (3.51)*, under the satisfaction of Assumption 3.1 and inequalities* (3.23) *and* (3.41)*, and the positive constants* ε_k*,* $k = 0, 1, 2$*, defined in Eqs.* (3.52)*. Then, given any positive definite diagonal matrices* K_P*,* K_D*,* A*,* B*, and* Γ*, and any* $\alpha \in \mathbb{R}$*, there exists* $\varepsilon^* \geq \min\{\varepsilon_0, \varepsilon_1, \varepsilon_2\}$ *such that, for any* $\varepsilon \in (0, \varepsilon^*)$*, the trivial solution* $(\bar{q}, \varphi, \bar{\phi})(t) \equiv (0_n, 0_n, 0_p)$ *is stable and, for any initial condition* $(\bar{q}, \dot{q}, \varphi, \bar{\phi})(0) \in \mathbb{R}^n \times \mathbb{R}^n \times \mathbb{R}^n \times \mathbb{R}^p$*,* $(\bar{q}, \vartheta)(t) \to (0_n, 0_n)$ *as* $t \to \infty$*, and* $\bar{s}_a(\bar{\phi}(t)) \to \ker(G(q_d))$ *as* $t \to \infty$*, with* $|\tau_i(t)| = |u_i(t)| < T_i$*,* $i = 1, \ldots, n$*,* $\forall t \geq 0$*.* $\triangleleft$

Proof. By (3.46), it can be seen that, along the system trajectories, $|\tau_i(t)| = |u_i(t)| < T_i$, $\forall t \geq 0$. This proves that, under the proposed output-feedback adaptive scheme, the input saturation values T_i are never reached. Now, in order to develop the stability/convergence analysis, let us define the scalar function[12]

$$V_E(\bar{q}, \dot{q}, \vartheta, \bar{\phi}) = V(\bar{q}, \dot{q}, \vartheta, \bar{\phi}) + \alpha\varepsilon s_D^T(K_D\vartheta)H(q)\dot{q}$$

where $\int_{0_n}^{\vartheta} s_D^T(K_D r)B^{-1}dr = \sum_{i=1}^{n}\int_0^{\vartheta_i}\sigma_{Di}(k_{Di}r_i)b_i^{-1}dr_i$ and V as defined in Eq. (3.48), with ε satisfying

$$\varepsilon < \varepsilon_M \triangleq \min\{\varepsilon_0, \varepsilon_1, \varepsilon_2\} \tag{3.53}$$

Observe that, from Property 1.1 and point 5 of Lemma 2.4, we have that

$$\begin{aligned} V_E(\bar{q}, \dot{q}, \vartheta, \bar{\phi}) \geq W_0(\bar{q}, \dot{q}, \vartheta) + (1-\delta_0)\int_{0_n}^{\bar{q}} s_P^T(K_P r)dr \\ + (1-\delta_0)\int_{0_n}^{\vartheta} s_D^T(K_D r)B^{-1}dr + \int_{0_p}^{\bar{\phi}} \bar{s}_a^T(r)\Gamma^{-1}dr \end{aligned} \tag{3.54}$$

where

$$W_0(\bar{q}, \dot{q}, \vartheta) = \frac{1}{2}\begin{pmatrix} \|s_P(K_P\bar{q})\| \\ \|\dot{q}\| \\ \|s_D(K_D\vartheta)\| \end{pmatrix}^T Q_0 \begin{pmatrix} \|s_P(K_P\bar{q})\| \\ \|\dot{q}\| \\ \|s_D(K_D\vartheta)\| \end{pmatrix}$$

$$Q_0 = \begin{pmatrix} \frac{\delta_0}{\beta_P} & -\varepsilon\mu_M & 0 \\ -\varepsilon\mu_M & \mu_m & -|\alpha|\varepsilon\mu_M \\ 0 & -|\alpha|\varepsilon\mu_M & \frac{\delta_0}{\beta_{D0}} \end{pmatrix}$$

and δ_0 is a positive constant satisfying

$$\frac{\varepsilon^2}{\varepsilon_0^2} < \delta_0 < 1 \tag{3.55}$$

(see (3.53)). Note further that, by (3.55), $W_0(\bar{q}, \dot{q}, \vartheta)$ is positive definite (since with $\varepsilon < \varepsilon_M \leq \varepsilon_0$, in accordance to (3.53), any δ_0 satisfying (3.55) renders positive definite Q_0), and observe that $W_0(0_n, \dot{q}, 0_n) \to \infty$ as $\|\dot{q}\| \to \infty$. From this, inequality (3.55), and points 6 and 7 of Lemma 2.4 (through which one sees that the integral terms in the right-hand side of (3.54) are radially unbounded positive definite functions), $V_E(\bar{q}, \dot{q}, \vartheta, \bar{\phi})$ is concluded to be positive definite and radially unbounded. Its upper-right derivative along the system trajectories, $\dot{V}_E = D^+V_E$ [38, App. I] [32, §6.1A], is

[12]The whole expression is given by $V_E(\bar{q}, \dot{q}, \vartheta, \bar{\phi}) = \frac{1}{2}\dot{q}^T H(q)\dot{q} + \varepsilon s_P^T(K_P\bar{q})H(q)\dot{q} + \alpha\varepsilon s_D^T(K_D\vartheta)H(q)\dot{q} + \int_{0_n}^{\bar{q}} s_P^T(K_P r)dr + \int_{0_n}^{\vartheta} s_D^T(K_D r)B^{-1}dr + \int_{0_p}^{\bar{\phi}} \bar{s}_a^T(r)\Gamma^{-1}dr$

given by

$$\begin{aligned}
\dot{V}_E(\bar{q},\dot{q},\vartheta,\bar{\phi}) = \; & \dot{q}^T H(q)\ddot{q} + \frac{1}{2}\dot{q}^T\dot{H}(q,\dot{q})\dot{q} + \varepsilon s_P^T(K_P\bar{q})H(q)\ddot{q} + \varepsilon\dot{q}^T\dot{H}(q,\dot{q})s_P(K_P\bar{q}) \\
& + \varepsilon\dot{q}^T H(q)s_P'(K_P\bar{q})K_P\dot{q} + \alpha s_D^T(K_D\vartheta)H(q)\ddot{q} + \alpha\dot{q}^T\dot{H}(q,\dot{q})s_D(K_D\vartheta) \\
& + \alpha\dot{q}^T H(q)s_D'(K_D\vartheta)K_D\dot{q} + s_P^T(K_P\bar{q})\dot{q} + s_D^T(K_D\vartheta)B^{-1}\dot{\vartheta} + \bar{s}_a^T(\bar{\phi})\Gamma^{-1}\dot{\bar{\phi}} \\
= \; & -\dot{q}^T F\dot{q} - \varepsilon s_P^T(K_P\bar{q})F\dot{q} - \varepsilon s_P^T(K_P\bar{q})s_P(K_P\bar{q}) \\
& - (1+\alpha)\varepsilon s_P^T(K_P\bar{q})s_D(K_D\vartheta) + \varepsilon\dot{q}^T C(q,\dot{q})s_P(K_P\bar{q}) \\
& + \varepsilon\dot{q}^T H(q)s_P'(K_P\bar{q})K_P\dot{q} - \alpha\varepsilon s_D^T(K_P\vartheta)F\dot{q} - \alpha\varepsilon s_D^T(K_P\vartheta)s_D(K_D\vartheta) \\
& + \alpha\varepsilon\dot{q}^T C(q,\dot{q})s_D(K_D\vartheta) - \alpha\varepsilon\dot{q}^T H(q)s_D'(K_D\vartheta)As_D(K_D\vartheta) \\
& + \alpha\varepsilon\dot{q}^T H(q)s_D'(K_D\vartheta)K_D B\dot{q} - s_D^T(K_D\vartheta)B^{-1}AK_D^{-1}s_D(K_D\vartheta)
\end{aligned}$$

where $H(q)\ddot{q}$, $\dot{\vartheta}$, and $\dot{\bar{\phi}}$ have been replaced by their equivalent expression from the closed-loop manipulator dynamics in Eqs. (3.51), Property 1.2.1 has been used, and

$$s_D'(K_D\bar{q}) \triangleq \mathrm{diag}[D^+\sigma_{D1}(k_{D1}\bar{q}_1),\ldots,D^+\sigma_{Dn}(k_{Dn}\bar{q}_n)]$$

Observe that from Properties 1.1, 1.2.5, and 1.3, and points (b) of Definition 2.4 and 2 of Lemma 2.4, we have that

$$\begin{aligned}
\dot{V}_E(\bar{q},\dot{q},\vartheta,\bar{\phi}) \leq & -f_m\|\dot{q}\|^2 + \varepsilon f_M\|s_P(K_P\bar{q})\|\|\dot{q}\| - \varepsilon\|s_P(K_P\bar{q})\|^2 \\
& + |1+\alpha|\varepsilon\|s_P(K_P\bar{q})\|\|s_D(K_D\vartheta)\| + \varepsilon k_C B_P\|\dot{q}\|^2 + \varepsilon\mu_M\beta_P\|\dot{q}\|^2 \\
& + |\alpha|\varepsilon f_M\|\dot{q}\|\|s_D(K_D\vartheta)\| - \varepsilon\alpha\|s_D(K_D\vartheta)\|^2 + |\alpha|\varepsilon k_C B_D\|\dot{q}\|^2 \\
& + |\alpha|\varepsilon\mu_M\beta_{Da}\|\dot{q}\|\|s_D(K_D\vartheta)\| + |\alpha|\varepsilon\mu_M\beta_{D1}\|\dot{q}\|^2 - \beta_m\|s_D(K_D\vartheta)\|^2 \\
\leq & -W_1(\bar{q},\dot{q}) - W_2(\dot{q},\vartheta) - W_3(\bar{q},\vartheta)
\end{aligned}$$

where

$$W_1(\bar{q},\dot{q}) = \begin{pmatrix}\|s_P(K_P\bar{q})\| \\ \|\dot{q}\|\end{pmatrix}^T Q_1 \begin{pmatrix}\|s_P(K_P\bar{q})\| \\ \|\dot{q}\|\end{pmatrix}$$

$$W_2(\dot{q},\vartheta) = \begin{pmatrix}\|\dot{q}\| \\ \|s_D(K_D\vartheta)\|\end{pmatrix}^T Q_2 \begin{pmatrix}\|\dot{q}\| \\ \|s_D(K_D\vartheta)\|\end{pmatrix}$$

$$W_3(\bar{q},\vartheta) = \begin{pmatrix}\|s_P(K_P\bar{q})\| \\ \|s_D(K_D\vartheta)\|\end{pmatrix}^T Q_3 \begin{pmatrix}\|s_P(K_P\bar{q})\| \\ \|s_D(K_D\vartheta)\|\end{pmatrix}$$

with

$$Q_1 = \begin{pmatrix}\frac{\varepsilon}{2} & -\frac{\varepsilon f_M}{2} \\ -\frac{\varepsilon f_M}{2} & \delta_1 f_m - \varepsilon\left(\beta_{MP} + |\alpha|\beta_{MD}\right)\end{pmatrix}$$

$$Q_2 = \begin{pmatrix}(1-\delta_1)f_m & -\frac{|\alpha|\varepsilon\beta_{Ma}}{2} \\ -\frac{|\alpha|\varepsilon\beta_{Ma}}{2} & (1-\delta_1)\beta_m\end{pmatrix}$$

$$Q_3 = \begin{pmatrix}\frac{\varepsilon}{2} & -\frac{|1+\alpha|\varepsilon}{2} \\ -\frac{|1+\alpha|\varepsilon}{2} & \alpha\varepsilon + \delta_1\beta_m\end{pmatrix}$$

where δ_1 is a positive constant satisfying

$$0 < \delta_{1m} \triangleq \varepsilon \left[\max\left\{ \frac{1}{\varepsilon_1}, \frac{1}{\varepsilon_2} \right\} - \frac{|\alpha|}{\bar{\varepsilon}_3} \right] < \delta_1 < 1 - \frac{|\alpha|\varepsilon}{\bar{\varepsilon}_3} \triangleq \delta_{1M} < 1 \tag{3.56}$$

Let us note that the fulfillment of (3.53) guarantees the existence of values $\delta_1 \in (0,1)$ satisfying (3.56) (since $\varepsilon < \varepsilon_M \leq \min\{\varepsilon_1, \varepsilon_2\}$, in accordance to (3.53), implies that $\delta_{1m} < \delta_{1M}$), while the satisfaction of (3.56) renders $W_1(\bar{q}, \dot{q})$, $W_2(\dot{q}, \vartheta)$, and $W_3(\bar{q}, \vartheta)$ positive definite (with respect to their arguments, since, under such a condition, Q_1, Q_2, and Q_3 turn out to be positive definite). Hence, $\dot{V}_E(\bar{q}, \dot{q}, \vartheta, \bar{\phi}) \leq 0$, $\forall (\bar{q}, \dot{q}, \vartheta, \bar{\phi}) \in \mathbb{R}^n \times \mathbb{R}^n \times \mathbb{R}^n \times \mathbb{R}^p$, with $\dot{V}_E(\bar{q}, \dot{q}, \vartheta, \bar{\phi}) = 0 \iff (\bar{q}, \dot{q}, \vartheta) = (0_n, 0_n, 0_n)$. Therefore, by Lyapunov's second method, the trivial solution $(\bar{q}, \vartheta, \bar{\phi})(t) \equiv (0_n, 0_n, 0_p)$ is concluded to be stable. Now, in view of the radially unbounded character of $V_E(\bar{q}, \dot{q}, \vartheta, \bar{\phi})$, the set $\Omega \triangleq \{(\bar{q}, \dot{q}, \vartheta, \bar{\phi}) \in \mathbb{R}^n \times \mathbb{R}^n \times \mathbb{R}^n \times \mathbb{R}^p : V_E(\bar{q}, \dot{q}, \vartheta, \bar{\phi}) \leq c\}$ is compact for any positive constant c [22, p. 128]. Moreover, in view of the seminegative definite character of $\dot{V}(\bar{q}, \dot{q}, \vartheta, \bar{\phi})$, Ω is positively invariant with respect to the closed-loop dynamics [22, p. 115]. Furthermore, from previous arguments: $E \triangleq \{(\bar{q}, \dot{q}, \vartheta, \bar{\phi}) \in \Omega : \dot{V}(\bar{q}, \dot{q}, \vartheta, \bar{\phi}) = 0\} = \{(\bar{q}, \dot{q}, \vartheta, \bar{\phi}) \in \Omega : \bar{q} = \dot{q} = \vartheta = 0_n\}$. Further, from Remark 3.9, the largest invariant set in E, denoted $\mathcal{M}$, is given as $\mathcal{M} = \{(\bar{q}, \dot{q}, \vartheta, \bar{\phi}) \in E : \bar{s}_a(\bar{\phi}) \in \ker(G(q_d))\}$. Thus, by the invariance theory [32, §7.2] —more specifically, by [32, Theorem 7.2.1]—, we have that $(\bar{q}, \dot{q}, \vartheta, \bar{\phi})(0) \in \Omega \implies (\bar{q}, \dot{q}, \vartheta, \bar{\phi})(t) \to \mathcal{M}$ as $t \to \infty$. Since this holds for any $c > 0$ and $V(\bar{q}, \dot{q}, \vartheta, \bar{\phi})$ is radially unbounded (in view of which Ω may be rendered arbitrarily large), we conclude that, for any $(\bar{q}, \dot{q}, \vartheta, \bar{\phi})(0) \in \mathbb{R}^n \times \mathbb{R}^n \times \mathbb{R}^n \times \mathbb{R}^p$, $(\bar{q}, \vartheta)(t) \to (0_n, 0_n)$ as $t \to \infty$ and $\bar{s}_a(\bar{\phi}(t)) \to \ker(G(q_d))$ as $t \to \infty$. Finally, from (3.53) and its sufficient character, as a condition supporting the proof, the stated stability/convergence result is concluded to hold with $\varepsilon \in (0, \varepsilon^*)$ for some $\varepsilon^* \geq \varepsilon_M$. $\triangleleft$

The result presented in Corollary 3.2 is also concluded for the presented extended version.

Remark 3.11 Let

$$\begin{aligned}
e_1 &= -y_2 = -\left(I_n \;\; I_n \;\; I_n\right)^T G(q) \bar{s}_a(\bar{\phi}) \\
e_2 &= y_1 = -\left(\varepsilon s_P^T(K_P \bar{q}) \quad \varepsilon\alpha s_D^T(K_D \vartheta) \quad \dot{q}^T\right)^T \\
V_1(\bar{q}, \vartheta) &= \frac{1}{2}\dot{q}^T H(q)\dot{q} + \varepsilon\left[s_P^T(K_P\bar{q}) + \alpha s_D^T(K_D\varphi)\right] H(q)\dot{q} + \int_{0_n}^{\bar{q}} s_P^T(K_P r)dr \\
&\quad + \int_{0_n}^{\vartheta} s_D^T(K_D r) B^{-1} dr \\
V_2(\bar{\phi}) &= \int_{0_P}^{\phi_c} \bar{s}_a^T(r)\Gamma^{-1}dr
\end{aligned}$$

Analogously to the output-feedback adaptive approach of the precedent subsection, through the extended scheme, the closed-loop system, in Eqs. (3.47), may be seen as a (negative) feedback connection among a strictly passive subsystems Σ_1 with dynamical

model

$$\Sigma_1 : \begin{cases} H(q)\ddot{q} + C(q,\dot{q})\dot{q} + F\dot{q} = -s_P(K_P\bar{q}) - s_D(K_D\vartheta) - (I_n \;\; 0_{n\times n})\, e_1 \\ \dot{\vartheta} = -AK_D^{-1} s_D\left(K_D\vartheta\right) + B\dot{\bar{q}} \\ y_1 = -\left(\varepsilon s_P^T(K_P\bar{q}) + \varepsilon\alpha s_D^T(K_D\vartheta) \;\; \dot{q}^T\right)^T \end{cases}$$

and a storage function $V_1(\bar{q},\dot{q})$, and a (lossless) passive subsystem Σ_2 with state model

$$\Sigma_2 : \begin{cases} \dot{q} = -\left(0_{n\times n} \;\; 0_{n\times n} \;\; I_n\right) e_2 \\ \dot{\bar{\phi}} = \Gamma G^T(q)\left(I_n \;\; I_n \;\; I_n\right) e_2 \\ y_2 = \left(I_n \;\; I_n \;\; I_n\right)^T G(q)\bar{s}_a(\bar{\phi}) \end{cases}$$

and storage function $V_2(\bar{\phi})$. An interpretation in the context of passive feedback interconnected systems analog to the one described in Remark 3.9 for the precedent output-feedback adaptive algorithm, applies in this case as well. ◁

3.3 State-feedback trajectory tracking approach

In this section a general adaptive scheme for the motion control through state feedback is presented. The developed analytical framework will be used to formulate the generalized adaptive controller. It is important to note that the bounded nature of the inputs restricts the tractable trajectories. In this direction, the following assumption turns out to be crucial within the analytical setting considered in this section.

Assumption 3.2 *The desired trajectory vector function $q_d(t)$ belongs to*

$$\mathcal{Q}_d \triangleq \left\{q_d \in \mathcal{C}^2(\mathbb{R}_+;\mathbb{R}^n) : \|\dot{q}_d(t)\| \leq B_{dv}, \|\ddot{q}_d(t)\| \leq B_{da}\right\}$$

for some positive constants B_{da} and $B_{dv} < \frac{f_m}{k_C}$ (see Properties 1.2.5 and 1.3) ◁

3.3.1 Global trajectory tracking with exact gravity compensation: a generalized approach

Let us consider the following *generalized* expression defining global-tracking controllers for system (3.1)-(3.2):

$$u(t,q,\dot{q},\psi) = -s_d(t,\bar{q},\dot{\bar{q}},\psi) - s_P(K_P\bar{q}) + Y(q,\dot{q}_d(t),\ddot{q}_d(t))\psi \tag{3.57}$$

where $\bar{q} = q - q_d$, for any suitable (desired trajectory) vector function $q_d(t) \in \mathbb{R}^n$. The third term in the right-hand side of (3.57) is a *hybrid* compensation term (since it involves online position measurements but desired velocities and accelerations), where θ is the system parameter vector and $Y(\cdot,\cdot,\cdot)$ is the regression matrix characterizing the system open-loop structure, according to Property 1.7, *i.e.* such that

$$Y\left(q,\dot{q}_d(t),\ddot{q}_d(t)\right)\psi = H(q,\psi)\ddot{q}_d(t) + C\left(q,\dot{q}_d(t),\psi\right)\dot{q}_d(t) + F(\psi)\dot{q}_d(t) + g(q,\psi) \tag{3.58}$$

The second term in the right-hand side of (3.57) is a (bounded non-linear) position error correction term where $K_P \in \mathbb{R}^{n\times n}$ is a positive definite diagonal matrix, *i.e.* $K_P = \text{diag}[k_{P1}, \ldots, k_{Pn}]$ with $k_{Pi} > 0$ for all $i = 1, \ldots, n$, and

$$\begin{aligned} s_P : \mathbb{R}^n &\to \mathbb{R}^n \\ x &\mapsto \Big(\sigma_{P1}(x_1) \ , \ \ldots \ , \ \sigma_{Pn}(x_n)\Big)^T \end{aligned}$$

with $\sigma_{Pi}(\cdot)$, $i = 1, \ldots, n$ being (suitable) **generalized saturation functions** with bounds M_{Pi}. The first term in the right-hand side of (3.57) corresponds to a motion dissipation term where $s_d : \mathbb{R}_+ \times \mathbb{R}^n \times \mathbb{R}^n \times \mathbb{R}^p \to \mathbb{R}^n$ is a bounded continuous vector function satisfying

$$s_d(t, x, 0_n, z) = 0_n \tag{3.59}$$

$\forall x \in \mathbb{R}^n$, $\forall z \in \mathbb{R}^\rho$, $\forall t \geq 0$,

$$\|s_d(t, x, y, z)\| \leq \kappa \|y\| \tag{3.60}$$

$\forall (t, x, y, z) \in \mathbb{R}_+ \times \mathbb{R}^n \times \mathbb{R}^n \times \mathbb{R}^\rho$, for some positive constant κ, and given $q_d \in \mathcal{Q}_d$ (see Assumption 3.2) and $z \in \mathbb{R}^\rho$ such that $|Y_i(q, \dot{q}_d(t), \ddot{q}_d(t))z| < T_i$, $i = 1, \ldots, n$, $\forall q \in \mathbb{R}^n$, $\forall t \geq 0$:

$$y^T s_d(t, x, y, z) > 0 \tag{3.61}$$

$\forall y \neq 0_n$, $\forall x \in \mathbb{R}^n$, $\forall t \geq 0$, and

$$|u_i(t, x, y, z)| < T_i \tag{3.62}$$

$i = 1, \ldots, n$, $\forall x \in \mathbb{R}^n$, $\forall y \in \mathbb{R}^n$, $\forall t \geq 0$, for suitable bounds M_{Pi} of $\sigma_{Pi}(\cdot)$.

Proposition 3.5 *Consider system* (3.1)-(3.2) *taking* $u = u(t, q, \dot{q}, \psi)$*, with* u *as defined in Eq.* (3.57)*, under the satisfaction of Assumptions 3.1 and 3.2, and the conditions on the vector function* s_d *stated through expressions* (3.59)–(3.62)*. Thus, for any positive definite diagonal matrix* K_P*, global uniform asymptotic stability of the closed loop trivial solution* $\bar{q}(t) \equiv 0_n$ *is guaranteed with* $|\tau_i(t)| = |u_i(t)| < T_i$*,* $i = 1, \ldots, n$*,* $\forall t \geq 0$*.* ◁

Proof. Observe that the satisfaction of (3.62), under the consideration of (3.2), shows that $T_i > |u(q, \dot{q}, \psi)| = |u_i| = |\tau_i|$, $i = 1, \ldots, n$, $\forall (q, \dot{\tilde{q}}) \in \mathbb{R}^n \times \mathbb{R}^n$. From this expression we see that, along the system trajectories, $|\tau_i(t)| = |u_i(t)| < T_i$, $i = 1, \ldots, n$, $\forall t \geq 0$. This proves that under the proposed scheme, the input saturation values, T_i, are never reached. Thus, under the consideration of Property 1.5, the closed-loop dynamics takes the form

$$H(q)\ddot{\bar{q}} + \big[C(q, \dot{q}) + C\big(q, q_d(t)\big)\big]\,\dot{\bar{q}} + F\dot{\bar{q}} = -s_d(\bar{q}, \dot{\bar{q}}, \psi) - s_P(K_P\bar{q}) \tag{3.63}$$

where Property 1.2.4 has been used and $q = \bar{q} + q_d(t)$ in the error variable space. Let us define the scalar function

$$V_0(t, \bar{q}, \dot{\bar{q}}) = \frac{1}{2}\dot{\bar{q}}^T H\big(\bar{q} + q_d(t)\big)\dot{\bar{q}} + \varepsilon \dot{\bar{q}}^T H\big(\bar{q} + q_d(t)\big) s_P(K_P\bar{q}) + \int_{0_n}^{\bar{q}} s_P^T(K_P r)dr \tag{3.64}$$

with $\int_{0_n}^{\bar{q}} s_P^T(K_P r)dr = \sum_{i=1}^{n}\int_0^{\bar{q}_i} \sigma_{Pi}(k_{Pi}r_i)dr_i$ and ε being a positive constant satisfying

$$\varepsilon < \varepsilon_M \triangleq \min\{\varepsilon_1, \varepsilon_2\} \tag{3.65}$$

where

$$\varepsilon_1 \triangleq \sqrt{\frac{\mu_m}{\mu_M^2 \beta_P}} \qquad \text{and} \qquad \varepsilon_2 \triangleq \frac{f_m - k_C B_{dv}}{\beta_M + \left(k_C B_{dv} + \frac{f_M + \kappa}{2}\right)^2}$$

(note that the satisfaction of Assumption 2 ensures positivity of ε_2) with

$$\beta_P \triangleq \max_i\{\sigma'_{PiM} k_{Pi}\} \quad , \quad \beta_M \triangleq k_C B_P + \mu_M \beta_P \quad , \quad B_P \triangleq \sqrt{\sum_{i=0}^{n} M_{Pi}^2}$$

σ'_{PiM} being the positive bound of $\sigma_{Pi}(\cdot)$ in accordance to item 2 of Lemma 2.4, κ as defined through (3.60), and μ_m, μ_M, k_C, f_m, and f_M as defined in Properties 1.1–1.3. Observe that from Property 1.1, items 4 and 5 of Lemma 2.4, and Lipschitz continuity of σ, $V_0(\bar{q}, \dot{\bar{q}})$ can be bounded above and below by

$$W_{01}(\bar{q}, \dot{\bar{q}}) + (1-\alpha)\int_{0_n}^{\bar{q}} s_P^T(K_P r)dr \leq V_0(\bar{q}, \dot{\bar{q}}) \leq W_{02}(\bar{q}, \dot{\bar{q}})$$

where

$$\begin{aligned} W_{01}(\bar{q}, \dot{\bar{q}}) &= \frac{\mu_m}{2}\|\dot{\bar{q}}\|^2 - \varepsilon\mu_M \|s_P(K_P\bar{q})\|\|\dot{\bar{q}}\| + \frac{\alpha}{2\beta_P}\|s_P(K_P\bar{q})\|^2 \\ &= \frac{1}{2}\begin{pmatrix} \|s_P(K_P\bar{q})\| \\ \|\dot{\bar{q}}\| \end{pmatrix}^T \begin{pmatrix} \frac{\alpha}{\beta_P} & -\varepsilon\mu_M \\ -\varepsilon\mu_M & \mu_m \end{pmatrix} \begin{pmatrix} \|s_P(K_P\bar{q})\| \\ \|\dot{\bar{q}}\| \end{pmatrix} \end{aligned} \tag{3.66}$$

with α being a positive constant satisfying

$$\frac{\varepsilon^2}{\varepsilon_1^2} < \alpha < 1 \tag{3.67}$$

(see (3.65)), and

$$\begin{aligned} W_{02}(\bar{q}, \dot{\bar{q}}) &= \frac{\mu_M}{2}\|\dot{\bar{q}}\|^2 + \varepsilon\mu_M\beta_P\|\bar{q}\|\|\dot{\bar{q}}\| + \frac{\beta_P}{2}\|\bar{q}\|^2 \\ &= \frac{1}{2}\begin{pmatrix} \|\bar{q}\| \\ \|\dot{\bar{q}}\| \end{pmatrix}^T \begin{pmatrix} \beta_P & \varepsilon\mu_M\beta_P \\ \varepsilon\mu_M\beta_P & \mu_M \end{pmatrix} \begin{pmatrix} \|\bar{q}\| \\ \|\dot{\bar{q}}\| \end{pmatrix} \end{aligned} \tag{3.68}$$

Notice that, by (3.67), $W_{01}(\bar{q}, \dot{\bar{q}})$ and $W_{02}(\bar{q}, \dot{\bar{q}})$ are positive definite (since with $\varepsilon < \varepsilon_M \leq \varepsilon_1$, in accordance to (3.65), the matrix at the right-hand side of (3.68) is positive definite; and, in conjunction with any α satisfying (3.67), the matrix at the right-hand side of (3.66) is also positive definite). Further observe that $W_{01}(0_n, \dot{\bar{q}}) \to \infty$ as $\|\dot{\bar{q}}\| \to \infty$. From this, inequality (3.67) (whence $1-\alpha > 0$), and items 6 and 7 of Lemma 2.4 (through which one sees that the integral term in the right-hand side of (3.64) is a radially unbounded positive definite function of $\bar{q}$), $V_0(t, \bar{q}, \dot{\bar{q}})$ is concluded

to be positive definite and radially unbounded. Its upper-right derivative along the system trajectories, is given by

$$\begin{aligned}
\dot{V}_0(t,\bar{q},\dot{\bar{q}}) = {} & \dot{\bar{q}}^T H\big(\bar{q}+q_d(t)\big)\ddot{\bar{q}} + \frac{1}{2}\dot{\bar{q}}^T \dot{H}\big(\bar{q}+q_d(t),\dot{\bar{q}}+\dot{q}_d(t)\big)\dot{\bar{q}} + \varepsilon s_P^T(K_P\bar{q})H(q)\ddot{\bar{q}} \\
& + \varepsilon\dot{\bar{q}}^T \dot{H}\big(\bar{q}+q_d(t),\dot{\bar{q}}+\dot{q}_d(t)\big)s_P(K_P\bar{q}) + \varepsilon\dot{\bar{q}}^T H\big(\bar{q}+q_d(t)\big)s_P'(K_P\bar{q})K_P\dot{\bar{q}} \\
& + s_P^T(K_P\bar{q})\dot{\bar{q}} \\
= {} & \dot{\bar{q}}^T\Big[-C\big(\bar{q}+q_d(t),\dot{\bar{q}}+\dot{q}_d(t)\big)\dot{\bar{q}} - C\big(\bar{q}+q_d(t),\dot{q}_d(t)\big)\dot{\bar{q}} - F\dot{\bar{q}} - s_d(t,\bar{q},\dot{\bar{q}},\psi) \\
& \quad - s_P(K_P\bar{q})\Big] + \frac{1}{2}\dot{\bar{q}}^T \dot{H}\big(\bar{q}+q_d(t),\dot{\bar{q}}+\dot{q}_d(t)\big)\dot{\bar{q}} \\
& + \varepsilon s_P^T(K_P\bar{q})\Big[-C\big(\bar{q}+q_d(t),\dot{\bar{q}}+\dot{q}_d(t)\big)\dot{\bar{q}} - C\big(\bar{q}+q_d(t),\dot{q}_d(t)\big)\dot{\bar{q}} - F\dot{\bar{q}} \\
& \quad - s_d(\bar{q},\dot{\bar{q}},\theta) - s_P(K_P\bar{q})\Big] \\
& + \varepsilon\dot{\bar{q}}^T \dot{H}\big(\bar{q}+q_d(t),\dot{\bar{q}}+\dot{q}_d(t)\big)s_P(K_P\bar{q}) + \varepsilon\dot{\bar{q}}^T H\big(\bar{q}+q_d(t)\big)s_P'(K_P\bar{q})K_P\dot{\bar{q}} \\
& + s_P^T(K_P\bar{q})\dot{\bar{q}} \\
= {} & -\dot{\bar{q}}^T C\big(\bar{q}+q_d(t),\dot{q}_d(t)\big)\dot{\bar{q}} - \dot{\bar{q}}^T F\dot{\bar{q}} - \dot{\bar{q}}^T s_d(t,\bar{q},\dot{\bar{q}},\psi) \\
& - \varepsilon s_P^T(K_P\bar{q})C\big(\bar{q}+q_d(t),\dot{q}_d(t)\big)\dot{\bar{q}} - \varepsilon s_P^T(K_P\bar{q})F\dot{\bar{q}} - \varepsilon s_P^T(K_P\bar{q})s_d(t,\bar{q},\dot{\bar{q}},\psi) \\
& - \varepsilon s_P^T(K_P\bar{q})s_P(K_P\bar{q}) + \varepsilon\dot{\bar{q}}^T\Big[C\big(\bar{q}+q_d(t),\dot{\bar{q}}\big) + C\big(\bar{q}+q_d(t),\dot{q}_d(t)\big)\Big]s_P(K_P\bar{q}) \\
& + \varepsilon\dot{\bar{q}}^T H\big(\bar{q}+q_d(t)\big)s_P'(K_P\bar{q})K_P\dot{\bar{q}}
\end{aligned}$$

where $H(q)\ddot{\bar{q}}$ has been replaced by its equivalent expression from the closed-loop dynamics in (3.63), Properties 1.2.1 and 1.2.3 had been used, and

$$s_P'(K_P\bar{q}) \triangleq \mathrm{diag}[\sigma_{P1}(k_{P1}\bar{q}_1),\ldots,\sigma_{Pn}(k_{Pn}\bar{q}_n)] \tag{3.69}$$

Observe that from Assumption 3.2, Properties 1.1–1.3, the satisfaction of (3.60) and (3.61), items (b) of Definition 2.4 and 2 of Lemma 2.4 (recall that for continuously differentiable functions σ_{Pi}, $D^+\sigma_{Pi} = \sigma'_{Pi}$), and the positive definite character of K_P, we have that

$$\dot{V}_0(t,\bar{q},\dot{\bar{q}}) \leq -W_1(\bar{q},\dot{\bar{q}})$$

with

$$\begin{aligned}
W_1(\bar{q},\dot{\bar{q}}) = {} & f_m\|\dot{\bar{q}}\|^2 - \varepsilon f_M\|s_P(K_P\bar{q})\|\|\dot{\bar{q}}\| - \varepsilon\kappa\|s_P(K_P\bar{q})\|\|\dot{\bar{q}}\| - 2\varepsilon k_C B_{dv}\|s_P(K_P\bar{q})\|\|\dot{\bar{q}}\| \\
& + \varepsilon\|s_P(K_P\bar{q})\|^2 - \varepsilon k_C B_P\|\dot{\bar{q}}\|^2 - \varepsilon\mu_M\beta_P\|\dot{\bar{q}}\|^2 - k_C B_{dv}\|\dot{\bar{q}}\|^2 \\
= {} & \begin{pmatrix}\|s_P(K_P\bar{q})\| \\ \|\dot{\bar{q}}\|\end{pmatrix}^T \begin{pmatrix}\varepsilon & -\varepsilon\left(\frac{f_M+\kappa}{2}+k_C B_{dv}\right) \\ -\varepsilon\left(\frac{f_M+\kappa}{2}+k_C B_{dv}\right) & f_m - k_C B_{dv} - \varepsilon\beta_M\end{pmatrix}\begin{pmatrix}\|s_P(K_P\bar{q})\| \\ \|\dot{\bar{q}}\|\end{pmatrix}
\end{aligned} \tag{3.70}$$

Note further that, from the satisfaction of (3.65), $W_1(\bar{q},\dot{q})$ is positive definite (since any $\varepsilon < \varepsilon_M \leq \varepsilon_2$ renders positive definite the matrix at the right-hand side of (3.70)). Thus, by Lyapunov's stability theory (applied to non-autonomous systems, see for instance [22, Theorem 4.9]), the trivial solution $\bar{q}(t) \equiv 0$ is concluded to be globally uniformly asymptotically stable, which completes the proof. ◁

Remark 3.12 Let $K_D \in \mathbb{R}^{n\times n}$ be a positive definite diagonal matrix, *i.e.* $K_D = \mathrm{diag}[k_{D1},\ldots,k_{Dn}]$ with $k_{Di} > 0$ for all $i = 1,\ldots,n$. A generalized version of the SP-SD+ and SPD+ controllers of [1] are retrieved from (3.57) by respectively defining

$$s_d(t,\bar{q},\dot{\bar{q}},\psi) = s_D(K_D\dot{\bar{q}}) \tag{3.71}$$

where $s_D : \mathbb{R}^n \to \mathbb{R}^n : x \mapsto \Big(\sigma_{D1}(x_1)\ ,\ \ldots\ ,\ \sigma_{Dn}(x_n)\Big)^T$, with $\sigma_{Di}(\cdot)$, $i = 1,\ldots,n$, being **generalized saturation functions** with bounds M_{Di}; and the involved bound values, M_{Pi} and M_{Di}, satisfy

$$M_{Pi} + M_{Di} < T_i - B_{Di} \tag{3.72}$$

$i = 1,\ldots,n$, with

$$B_{Di} = \mu_M B_{da} + k_C B_{dv}^2 + f_M B_{dv} + B_{gi}$$

and

$$s_d(t,\bar{q},\dot{\bar{q}},\psi) = s_P(K_P\bar{q} + K_D\dot{\bar{q}}) - s_P(K_P\bar{q}) \tag{3.73}$$

with the generalized saturations $\sigma_{Pi}(\cdot)$, $i = 1,\ldots,n$, being **strictly increasing**, and bound values satisfying

$$M_{Pi} \leq T_i - B_{Di} \tag{3.74}$$

$i = 1,\ldots,n$, both SP-SD+ and SPD+ cases under the consideration of sufficiently small desired-trajectory-related bound values B_{dv} and B_{da} (see Assumption 3.2) as stated in [1]. Furthermore a tracking version of the SPDgc-like controller proposed in [47], that (in addition to the SP and D actions) includes the hybrid compensation terms within a single saturation function (at each link) is obtained from (3.57) by defining

$$\begin{aligned} s_d(t,\bar{q},\dot{\bar{q}},\psi) = {} & s_0\big(Y(q,\dot{q}_d(t),\ddot{q}_d(t))\psi - s_P(K_P\bar{q})\big) \\ & - s_0\big(Y(q,\dot{q}_d(t),\ddot{q}_d(t))\psi - s_P(K_P\bar{q}) - K_D\dot{\bar{q}}\big) \end{aligned} \tag{3.75}$$

where $s_0 : \mathbb{R}^n \to \mathbb{R}^n : x \mapsto \Big(\sigma_{01}(x_1)\ ,\ \ldots\ ,\ \sigma_{0n}(x_n)\Big)^T$, with $\sigma_{0i}(\cdot)$, $i = 1,\ldots,n$, being **linear saturation functions** for (L_{0i}, M_{0i}), and the involved linear/generalized saturation function parameters satisfying

$$B_{Di} + M_{Pi} < L_{0i} \leq M_{0i} < T_i \tag{3.76}$$

$i = 1,\ldots,n$, with sufficiently small desired-trajectory-related bounds B_{dv} and B_{da} as stated in [1][13]. Observe from (3.76) that, by virtue of item (c) of Definition 2.4 (under the consideration of Properties 1.4 and 1.5), we have that $s_0\big(Y(q,\dot{q}_d(t),\ddot{q}_d(t))\psi - s_P(K_P\bar{q})\big) \equiv Y(q,\dot{q}_d(t),\ddot{q}_d(t))\psi - s_P(K_P\bar{q})$ (see (3.75) and (3.57)), giving rise to an SPDhc+-like controller of the form

$$u = s_0\big(Y(q,\dot{q}_d(t),\ddot{q}_d(t))\psi - s_P(K_P\bar{q}) - K_D\dot{q}\big)$$

[13]Notice that the *internal* saturations, $\sigma_{Pi}(\cdot)$, in (3.75) are allowed to be any function satisfying Definition 2.4 and are consequently not tied to be linear saturations as originally formulated in [47].

Furthermore from items (a) of Definition 2.4 and 8a and 9 of Lemma 2.4 (under the satisfaction of inequalities (3.76) in the case SPDhc+-like controller obtained through (3.75)), $s_d(t, \bar{q}, \dot{\bar{q}}, \psi)$ in every one of the above cases in (3.71), (3.73), and (3.75) satisfies the expressions in (3.59) and (3.61). Further, notice that, through the satisfaction of (3.72), (3.74) (under the consideration of the strictly increasing character of the generalized saturation functions σ_{Pi} involved in the SPD+ case), and (3.76), every $s_d(t, \bar{q}, \dot{\bar{q}}, \psi)$ in expressions (3.71), (3.73), and (3.75) satisfies inequalities (3.62) too. Moreover, from points 3 and 4 of Lemma 2.4, one sees that $s_d(t, \bar{q}, \dot{\bar{q}}, \psi)$ in every one of the above cases in (3.71), (3.73), and (3.75) satisfies inequality (3.60) with

$$\kappa = \max_i \{\sigma'_{iM} k_{Di}\} \tag{3.77a}$$

where

$$\sigma'_{iM} = \begin{cases} \sigma'_{DiM} & \text{in the SP-SD+ case} \\ \sigma'_{PiM} & \text{in the SPD+ case} \\ \sigma'_{0iM} & \text{in the SPDhc+-like case} \end{cases} \tag{3.77b}$$

σ'_{DiM}, σ'_{PiM}, and σ'_{0iM} respectively being the positive bounds of $D^+\sigma_{Di}(\cdot)$, $\sigma'_{Pi}(\cdot)$, and $D^+\sigma_{0i}(\cdot)$, in accordance to item 2 of Lemma 2.4. ◁

3.3.2 Global adaptive tracking control

The result of the precedent section cannot be guaranteed as stated in Proposition 3.5 if the exact knowledge of the system parameters is not available. However, in such a situation, global tracking avoiding input saturation can still be accomplished through auxiliary dynamics in an adaptive control context. This is achieved by means of suitable strict bounds on the elements of ψ, as described next.

Let $M_a \triangleq \left(M_{a1}, \ldots, M_{a\rho}\right)^T$ and $\Psi_a \triangleq [-M_{a1}, M_{a1}] \times \cdots \times [-M_{a\rho}, M_{a\rho}]$, with M_{aj}, $j = 1, \ldots, \rho$, being positive constants such that

$$\psi_j < M_{aj} \tag{3.78a}$$

$\forall j \in \{1, \ldots, \rho\}$, and

$$B_{gi}^{M_a} < T_i \tag{3.78b}$$

$\forall i \in \{1, \ldots, n\}$, where, in accordance to Property 1.8a, $B_{gi}^{M_a}$ are positive constants such that $|g_i(w, z)| = |Y_{gi}(w)z| \leq B_{gi}^{M_a}$, $i = 1, \ldots, n$, $\forall (w, z) \in \mathbb{R}^n \times \Psi_a$, and consider a small enough desired-trajectory-related bound values B_{dv} and B_{da} (in accordance to Assumption 3.2) such that

$$|Y_i(q, \dot{q}_d(t), \ddot{q}_d(t))\vartheta| \leq B_{Di}^{Ma} < T_i \tag{3.78c}$$

$i = 1, \ldots, n$, $\forall q \in \mathbb{R}^n$, $\forall \vartheta \in \Psi_a$, $\forall t \geq 0$, where B_{Di}^{Ma}, $i = 1, \ldots, n$ are positive constants such that $|Y_i(w, x, y)z| \leq B_{Di}^{Ma}$, $i = 1, \ldots, n$, for all $(w, x, y, z) \in \mathbb{R}^n \times \mathcal{B}_{B_{dv}} \times \mathcal{B}_{B_{da}} \times \Psi_a$. Let us note that Assumption 3.1 ensures the existence of such positive values M_{aj}, $j = 1, \ldots, \rho$, satisfying inequalities (3.78a) and (3.78b) while, under Assumption 3.2, through the fulfillment of (3.78b), inequalities (3.78c) can always be

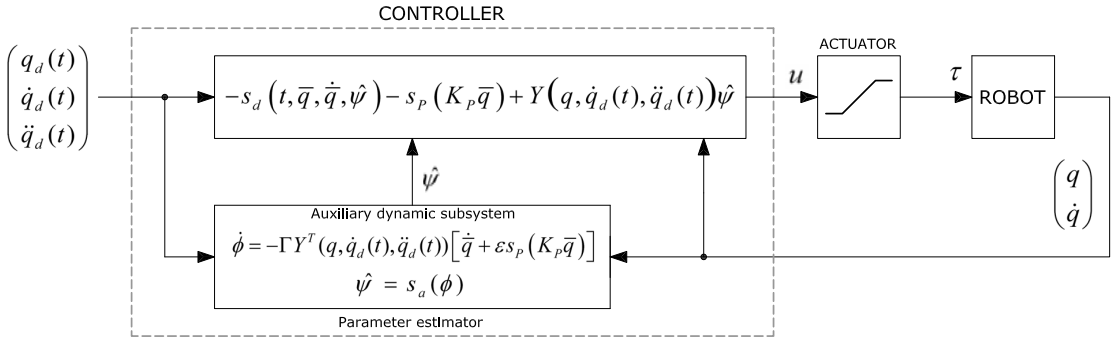

Figure 3.4: Block diagram of the proposed adaptive control scheme

satisfied through sufficiently small values of B_{dv} and B_{da} (see Remark 3.12). Notice further that inequalities (3.78b) are satisfied if $\sum_{j=1}^{p} B_{G_{ij}} M_{aj} < T_i$, $B_{G_i}\|M_a\| < T_i$, or $B_G\|M_a\| < T_i$, $i = 1, \ldots, n$ (see Property 1.8a.); actually, $\sum_{j=1}^{p} B_{G_{ij}} M_{aj}$, $B_{G_i}\|M_a\|$, or $B_G\|M_a\|$, may be taken as the value of $B_{gi}^{M_a}$ as long as inequality (3.78b) is satisfied. Similarly, inequalities (3.78c) are satisfied if $\sum_{j=i}^{p} B_{Y_{ij}} M_{aj} < T_i$, $B_{Y_i}\|M_a\| < T_i$, or $B_Y\|M_a\| < T_i$, $i = 1, \ldots, n$, where in accordance to Property 1.8b and Assumption 3.2, $B_{Y_{ij}}$, B_{Y_i}, and B_Y are positive constants such that $|Y_{ij}(w,x,y)| \leq B_{Y_{ij}}$, $\|Y_i(w,x,y)\| \leq B_Y$, respectively, for all $(w,x,y) \in \mathbb{R}^n \times \mathcal{B}_{B_{dv}} \times \mathcal{B}_{B_{da}}$; in fact, $B_{Y_{ij}} M_{aj}$, $B_{Y_i}\|M_a\|$, or $B_Y\|M_a\|$, may be taken as the value of $B_{D_i}^{Ma}$ as long as inequality (3.78c) is fulfilled.

Based on the generalized algorithm in Eq. (3.57), the proposed adaptive control scheme is defined as

$$u(t,q,\dot{q},\hat{\psi}) = -s_d(t,\bar{q},\dot{\bar{q}},\hat{\psi}) - s_P(K_P\bar{q}) + Y(q,\dot{q}_d(t),\ddot{q}_d(t))\hat{\psi} \tag{3.79}$$

with $s_P(\cdot)$, K_p, and $s_d(\cdot)$ as previously defined, $Y(q,\dot{q}_d(t),\ddot{q}_d(t))$ as defined in Section 3.3.1 (see Eq. (3.58)), and $\hat{\psi}$ (the vector of estimated parameters) being the output variable of an auxiliary dynamic subsystem defined as

$$\dot{\phi} = -\Gamma Y^T(q,\dot{q}_d(t),\ddot{q}_d(t))\left[\dot{\bar{q}} + \varepsilon s_P(K_P\bar{q})\right] \tag{3.80a}$$

$$\hat{\psi} = s_a(\phi) \tag{3.80b}$$

where ϕ is the (internal) state of the auxiliary dynamics in Eq. (3.80a);

$$\begin{aligned} s_a : \mathbb{R}^p &\to \mathbb{R}^p \\ x &\mapsto \Big(\sigma_{a1}(x_1)\ ,\ \ldots\ ,\ \sigma_{a\rho}(x_\rho)\Big)^T \end{aligned}$$

$\sigma_{aj}(\cdot)$, $j = 1, \ldots, \rho$, being **strictly increasing generalized saturation functions** with bounds M_{aj} as defined above, *i.e.* satisfying inequalities (3.78); $\Gamma \in \mathbb{R}^{\rho\times\rho}$ is a positive definite diagonal constant matrix, *i.e.* $\Gamma = \text{diag}[\gamma_1 \ldots, \gamma_\rho]$ with $\gamma_j > 0$ for all $j = 1, \ldots, \rho$; and ε is a positive constant satisfying inequality (3.65). A block diagram of the proposed adaptive control scheme is shown in Fig. 3.4.

Remark 3.13 Analogously to the adaptive regulation cases of Section 3.1 and 3.2, one can see from expressions (3.79)-(3.80), (3.65) that the proposed adaptive tracking

control scheme does not involve the exact values of the elements of ψ. Note further that by previous arguments, the satisfaction of the restriction of B_{dv} stated through Assumption 3.2 does not require the exact knowledge of the system parameters either. $\triangleleft$

Closed-loop analysis

Consider system (3.1)-(3.2) taking $u = u(t, q, \dot{q}, \hat{\psi})$ as defined through Eqs. (3.79)-(3.80). Observe that, under Assumption 3.1 and the consideration in (3.2), if the inequalities in (3.78) are satisfied, the fulfillment of (3.62) guarantees that

$$T_i > \big|u_i\big(t, q, \dot{q}, s_a(\phi)\big)\big| = |u_i| = |\tau_i| \quad i = 1, \ldots, n \quad \forall (t, q, \dot{\tilde{q}}, \phi) \in \mathbb{R}_+ \times \mathbb{R}^n \times \mathbb{R}^n \times \mathbb{R}^\rho \tag{3.81}$$

Thus, under the consideration of Property 1.5, the closed-loop system takes the form

$$\begin{aligned} H(q)\ddot{\tilde{q}} + \big[C(q, \dot{q}) + C(q, q_d(t))\big]\dot{\tilde{q}} + F\dot{\tilde{q}} \\ = -\, s_d\big(t, \bar{q}, \dot{\tilde{q}}, s_a(\phi)\big) - s_P(K_P\bar{q}) + Y(q, \dot{q}_d(t), \ddot{q}_d(t))\bar{s}_a(\bar{\phi}) \end{aligned} \tag{3.82a}$$

$$\dot{\bar{\phi}} = -\Gamma Y^T(q, \dot{q}_d, \ddot{q}_d)\big[\dot{\tilde{q}} + \varepsilon s_P(K_P\bar{q})\big] \tag{3.82b}$$

where $\bar{\phi} = \phi - \phi^*$ and

$$\bar{s}_a(\bar{\phi}) = s_a(\bar{\phi} + \phi^*) - s_a(\phi^*) \tag{3.83}$$

with $\phi^* = \big(\phi_1^*, \ldots, \phi_\rho^*\big)^T$ such that $s_a(\phi^*) = \psi$, or equivalently, $\phi_j^* = \sigma_{aj}^{-1}(\psi_j)$, $j = 1, \ldots, \rho$. Observe that, by item 8b of Lemma 2.4, the elements of $\bar{s}_a(\bar{\phi})$ in (3.83), *i.e.*

$$\bar{\sigma}_{aj}(\bar{\phi}_j) = \sigma_{aj}(\bar{\phi}_j + \phi_j^*) - \sigma_{aj}(\phi_j^*)$$

$j = 1, \ldots, \rho$, turn out to be strictly increasing generalized saturation functions.

Proposition 3.6 *Consider the closed-loop system in Eqs.* (3.82)*, under the satisfaction of Assumptions 3.1 and 3.2, and the conditions on the vector function s_d stated through expressions* (3.59)–(3.62)*. Thus, for any positive definite diagonal matrices K_P and Γ, and any ε satisfying* (3.65)*, the trivial solution $(\bar{q}, \bar{\phi})(t) \equiv (0_n, 0_\rho)$ is uniformly stable and, for any initial condition $\big(t_0, \bar{q}(t_0), \dot{\tilde{q}}(t_0), \bar{\phi}(t_0)\big) \in \mathbb{R}_+ \times \mathbb{R}^n \times \mathbb{R}^n \times \mathbb{R}^\rho$, the closed-loop system solution $(\bar{q}, \bar{\phi})(t)$ is bounded and such that $\bar{q}(t) \to 0_n$ as $t \to \infty$ with $|\tau_i(t)| = |u_i(t)| < T_i$, $i = 1, \ldots, n$, $\forall t \geq t_0$.* $\triangleleft$

Proof. By (3.81), we see that, along the system trajectories, $|\tau_i(t)| = |u_i(t)| < T_i$, $\forall t \geq 0$. This proves that, under the proposed adaptive scheme, input saturation is avoided. Now, in order to develop the stability/convergence analysis, let us define the scalar function

$$V_1(t, \bar{q}, \dot{\tilde{q}}, \bar{\phi}) = V_0(t, \bar{q}, \dot{\tilde{q}}) + \int_{0_p}^{\bar{\phi}} \bar{s}_a^T(r)\Gamma^{-1}dr \tag{3.84}$$

where $\int_{0_\rho}^{\bar{\phi}} \bar{s}_a^T(r)\Gamma^{-1}dr = \sum_{j=1}^{\rho} \int_0^{\bar{\phi}_j} \bar{s}_{aj}(r_j)\gamma_j^{-1}dr_j$, and $V_0(t, \bar{q}, \dot{\tilde{q}})$ is as defined in Eq. (3.64)[14]. Note that, from the positive definite and radially unbounded characters of

[14]The whole expression is given by $V_1(t, \bar{q}, \dot{\tilde{q}}, \bar{\phi}) = \frac{1}{2}\dot{\tilde{q}}^T H\big(\bar{q} + q_d(t)\big)\dot{\tilde{q}} + \varepsilon\dot{\tilde{q}}^T H\big(\bar{q} + q_d(t)\big)s_P(K_P\bar{q}) + \int_{0_n}^{\bar{q}} s_P^T(K_P r)dr + \int_{0_p}^{\bar{\phi}} \bar{s}_a^T(r)\Gamma^{-1}dr$

$V_0(t,\bar{q},\dot{\bar{q}})$ (shown in the proof of Proposition 3.5) and items 8b, 6, and 7 of Lemma 2.4 (through which the integral term in the right-hand side of Eq. (3.84) is concluded to be a radially unbounded positive definite decrescent function of $\bar{\phi}$), $V_1(t,\bar{q},\dot{\bar{q}},\bar{\phi})$ proves to be positive definite, radially unbounded, and decrescent. Its derivative along the system trajectories is given by

$$
\begin{aligned}
\dot{V}_1(t,\bar{q},\dot{\bar{q}},\bar{\phi}) = {} & \dot{\bar{q}}^T H\big(\bar{q}+q_d(t)\big)\ddot{\bar{q}} + \frac{1}{2}\dot{\bar{q}}^T \dot{H}\big(\bar{q}+q_d(t),\dot{\bar{q}}+\dot{q}_d(t)\big)\dot{\bar{q}} + \varepsilon s_P^T(K_P\bar{q}) H\big(\bar{q}+q_d(t)\big)\ddot{\bar{q}} \\
& + \varepsilon\dot{\bar{q}}^T \dot{H}\big(\bar{q}+q_d(t),\dot{\bar{q}}+\dot{q}_d(t)\big) s_P(K_P\bar{q}) + \varepsilon\dot{\bar{q}}^T H(q) s_P'(K_P\bar{q}) K_P\dot{\bar{q}} \\
& + s_P^T(K_P\bar{q})\dot{\bar{q}} + \bar{s}_a^T(\bar{\phi})\Gamma^{-1}\dot{\bar{\phi}} \\
= {} & \dot{\bar{q}}^T\Big[- C\big(\bar{q}+q_d(t),\dot{\bar{q}}+\dot{q}_d(t)\big)\dot{\bar{q}} - C\big(\bar{q}+q_d(t),\dot{q}_d(t)\big)\dot{\bar{q}} - F\dot{\bar{q}} \\
& \quad - s_d\big(\bar{q},\dot{\bar{q}},s_a(\phi)\big) - s_P(K_P\bar{q}) + Y\big(\bar{q}+q_d(t),\dot{q}_d(t),\ddot{q}_d(t)\big)\bar{s}_a(\bar{\phi})\Big] \\
& + \frac{1}{2}\dot{\bar{q}}^T \dot{H}\big(\bar{q}+q_d(t),\dot{\bar{q}}+\dot{q}_d(t)\big)\dot{\bar{q}} \\
& + \varepsilon s_P^T(K_P\bar{q})\Big[- C\big(\bar{q}+q_d(t),\dot{\bar{q}}+\dot{q}_d(t)\big)\dot{\bar{q}} - C\big(\bar{q}+q_d(t),\dot{q}_d(t)\big)\dot{\bar{q}} - F\dot{\bar{q}} \\
& \qquad - s_d\big(\bar{q},\dot{\bar{q}},s_a(\phi)\big) - s_P(K_P\bar{q}) + Y\big(\bar{q}+q_d(t),\dot{q}_d(t),\ddot{q}_d(t)\big)\bar{s}_a(\bar{\phi})\Big] \\
& + \varepsilon\dot{\bar{q}}^T \dot{H}\big(\bar{q}+q_d(t),\dot{\bar{q}}+\dot{q}_d(t)\big) s_P(K_P\bar{q}) + \varepsilon\dot{\bar{q}}^T H\big(\bar{q}+q_d(t)\big) s_P'(K_P\bar{q}) K_P\dot{\bar{q}} \\
& + s_P^T(K_P\bar{q})\dot{\bar{q}} - \bar{s}_a^T(\bar{\phi}) Y^T\big(\bar{q}+q_d(t),\dot{q}_d(t),\ddot{q}_d(t)\big)\big[\dot{\bar{q}} + \varepsilon s_P(K_P\bar{q})\big] \\
= {} & - \dot{\bar{q}}^T C\big(\bar{q}+q_d(t),\dot{q}_d(t)\big) - \dot{\bar{q}}^T F\dot{\bar{q}} - \dot{\bar{q}}^T s_d\big(t,\bar{q},\dot{\bar{q}},s_a(\phi)\big) \\
& - \varepsilon s_P^T(K_P\bar{q}) C\big(\bar{q}+q_d(t),\dot{q}_d(t)\big)\dot{\bar{q}} - \varepsilon s_P^T(K_P\bar{q}) F\dot{\bar{q}} \\
& - \varepsilon s_P^T(K_P\bar{q}) s_d\big(t,\bar{q},\dot{\bar{q}},s_a(\phi)\big) - \varepsilon s_P^T(K_P\bar{q}) s_P(K_P\bar{q}) \\
& + \varepsilon\dot{\bar{q}}^T\Big[C\big(\bar{q}+q_d(t),\dot{\bar{q}}\big) + C\big(\bar{q}+q_d(t),\dot{q}_d(t)\big)\Big] s_P(K_P\bar{q}) \\
& + \varepsilon\dot{\bar{q}}^T H\big(\bar{q}+q_d(t)\big) s_P'(K_P\bar{q}) K_P\dot{\bar{q}}
\end{aligned}
$$

where $H(q)\ddot{\bar{q}}$ have been replaced by their equivalent expression from the closed-loop manipulator dynamics in Eq. (3.82), Properties 1.2.1–1.2.3 have been used, and $s_P'(K_P\bar{q})$ was defined in (3.69). Observe that from Assumption 3.2, Properties 1.1–1.3, the satisfaction of (3.60) and (3.61), items (b) of Definition 2.4 and 2 of Lemma 2.4, and the positive definite character of K_P, we have that

$$\dot{V}_1(t,\bar{q},\dot{\bar{q}},\bar{\phi}) \leq -W_1(\bar{q},\dot{\bar{q}})$$

where $W_1(\bar{q},\dot{\bar{q}})$ was defined in (3.70) and shown to be a positive definite function in the proof of Proposition 3.5. Thus, we have that $\dot{V}_1(t,\bar{q},\dot{\bar{q}},\bar{\phi}) \leq 0$, $\forall (t,\bar{q},\dot{\bar{q}},\bar{\phi}) \in \mathbb{R}_+ \times \mathbb{R}^n \times \mathbb{R}^n \times \mathbb{R}^\rho$, with $\dot{V}_1(t,\bar{q},\dot{\bar{q}},\bar{\phi}) = 0 \iff (\bar{q},\dot{\bar{q}}) = (0_n,0_n)$. Therefore, by Lyapunov stability theory (applied to nonautonomous systems, refer to Section 2.3, Theorem 2.3) the trivial solution $(\bar{q},\bar{\phi})(t) \equiv (0_n,0_\rho)$ is concluded to be uniformly stable. Finally, by Theorem 2.3, we conclude that for an initial condition $\big(t_0,\bar{q}(t_0),\dot{\bar{q}}(t_0),\bar{\phi}(t_0)\big) \in \mathbb{R}_+ \times \mathbb{R}^n \times \mathbb{R}^n \times \mathbb{R}^\rho$, the closed-loop system solution $(\bar{q},\bar{\phi})(t)$ is bounded and such that $\bar{q}(t) \to 0_n$ as $t \to \infty$.

$\triangleleft$

Observe that even though the result stated through Proposition 3.6 does not permit to analytically conclude anything on the convergence of the parameter estimators $\hat{\psi}(t)$, it guarantees boundedness of the auxiliary states $\phi(t)$ (and actually of every closed-loop system variable). Recall further, from Section 1.4, that parameter estimator convergence is not part of the adaptive tracking goal. Further results in this direction could be contemplated through additional excitation persistency conditions [30], which is out of the scope of this work.

Remark 3.14 Adaptive versions of the SP-SD+ and SPD+ schemes of [47] and of the SPDhc+-like algorithm described in Remark 3.12 are obtained by considering in the proposed design method the expressions in (3.71), (3.73), and (3.75), respectively, with suitable adjustments on the saturation function parameter conditions. Thus, the adaptive SP-SD+ controller is obtained from (3.79) by taking

$$s_d(t, \bar{q}, \dot{\bar{q}}, \hat{\psi}) = s_D(K_D \dot{\bar{q}}) \tag{3.85}$$

with $s_D(\cdot)$ and K_D as defined in Remark 3.12, and the involved bound values, M_{Pi} and M_{Di}, satisfying

$$M_{Pi} + M_{Di} < T_i - B_{Di}^{Ma} \tag{3.86}$$

$i = 1, \ldots, n$, the adaptive SPD+ scheme is gotten by taking

$$s_d(t, \bar{q}, \dot{\bar{q}}, \hat{\psi}) = s_P(K_P \bar{q} + K_D \dot{\bar{q}}) - s_P(K_P \bar{q}) \tag{3.87}$$

with $s_P(\cdot)$ as defined for this case in Remark 3.12, and bound values satisfying

$$M_{Pi} \leq T_i - B_{Di}^{Ma} \tag{3.88}$$

$i = 1, \ldots, n$, and the adaptive SPDhc+-like algorithm is obtained by taking

$$s_d(t, \bar{q}, \dot{\bar{q}}, \hat{\psi}) = s_0\big(Y(q, \dot{q}_d(t), \ddot{q}_d(t))\hat{\psi} - s_P(K_P \bar{q})\big) - s_0\big(Y(q, \dot{q}_d(t), \ddot{q}_d(t))\hat{\psi} - s_P(K_P \bar{q}) - K_D \dot{\bar{q}}\big) \tag{3.89}$$

with $s_0(\cdot)$ as defined in Remark 3.12, and the involved saturation function parameters satisfying

$$B_{Di}^{M_a} + M_{Pi} < L_{0i} \leq M_{0i} < T_i \tag{3.90}$$

$i = 1, \ldots, n$. For these cases, κ in (3.65) remains as specified in Remark 3.12 (see Eqs. (3.77)). ◁

4

Simulation results

The effectiveness of the proposed schemes was corroborated through computer simulations considering the model of a 2-DOF manipulator corresponding to the experimental robotic arm used in [1, 47]. For this robot, the various terms characterizing the system dynamics in (3.1) are given by[1]

$$H(q) = \begin{pmatrix} 2.351 + 0.168\cos q_2 & 0.102 + 0.084\cos q_2 \\ 0.102 + 0.084\cos q_2 & 0.102 \end{pmatrix} \qquad [\mathrm{kg\,m^2}]$$

$$C(q,\dot{q}) = \begin{pmatrix} -0.084\dot{q}_2 \sin q_2 & -0.084(\dot{q}_1 + \dot{q}_2)\sin q_2 \\ 0.084\dot{q}_1 \sin q_2 & 0 \end{pmatrix} \qquad [\mathrm{kg\,m^2/s}]$$

$$F = \begin{pmatrix} 2.288 & 0 \\ 0 & 0.175 \end{pmatrix} \qquad [\mathrm{kg\,m^2/s}]$$

and

$$g(q) = \begin{pmatrix} 38.465\sin q_1 + 1.825\sin(q_1 + q_2) \\ 1.825\sin(q_1 + q_2) \end{pmatrix} \quad [\mathrm{Nm}]$$

Thus, Properties 1.1, 1.2.5, 1.3, and 1.4 are satisfied with $\mu_m = 0.088$ kg m^2, $\mu_M = 2.533$ kg m^2, $k_C = 0.1455$ kg m^2, $B_{g1} = 40.29$ Nm, $B_{g2} = 1.825$ Nm, $f_m = 0.175$

[1] A detailed procedure through which the generalized model of such a 2-DOF robotic arm is developed in Appendix A.

$\mathrm{kg\,m/s^2}$, $f_M = 2.288\ \mathrm{kg\,m/s^2}$, and

$$Y^T(q,\dot{q},\ddot{q}) = \begin{pmatrix} \ddot{q}_1 & 0 \\ (2\ddot{q}_1 + \ddot{q}_2)\cos(q_2) - \dot{q}_2(2\dot{q}_1 + \dot{q}_2)\sin(q_2) & \ddot{q}_1\cos(q_2) + \dot{q}_1^2\sin(q_2) \\ \ddot{q}_2 & \ddot{q}_1 + \ddot{q}_2 \\ \dot{q}_1 & 0 \\ 0 & \dot{q}_2 \\ \sin(q_1) & 0 \\ \sin(q_1+q_2) & \sin(q_1+q_2) \end{pmatrix}$$

$$\psi^T = \begin{pmatrix} 2.351 & 0.084 & 0.102 & 2.288 & 0.175 & 38.465 & 1.825 \end{pmatrix} \quad [\mathrm{Nm}]$$

In particular

$$Y_H(q,\ddot{q}) = \begin{pmatrix} \ddot{q}_1 & (2\ddot{q}_1 + \ddot{q}_2)\cos(q_2) & \ddot{q}_2 & 0 & 0 & 0 & 0 \\ 0 & \ddot{q}_1\cos(q_2) & q_1 + q_2 & 0 & 0 & 0 & 0 \end{pmatrix}$$

$$Y_C(q,\dot{q}) = \begin{pmatrix} 0 & 0 & -(2\dot{q}_1 + \dot{q}_2)\dot{q}_2\sin(q_2) & 0 & 0 & 0 & 0 \\ 0 & 0 & \dot{q}_1^2\sin(q_2) & 0 & 0 & 0 & 0 \end{pmatrix}$$

$$Y_F(\dot{q}) = \begin{pmatrix} 0 & 0 & 0 & \dot{q}_1 & 0 & 0 & 0 \\ 0 & 0 & 0 & 0 & \dot{q}_2 & 0 & 0 \end{pmatrix}$$

$$Y_g(q) = \begin{pmatrix} 0 & 0 & 0 & 0 & 0 & \sin(q_2) & \sin(q_1+q_2) \\ 0 & 0 & 0 & 0 & 0 & 0 & \sin(q_1+q_2) \end{pmatrix}$$

The maximum torques allowed (input saturation bounds) are $T_1 = 150$ Nm and $T_2 = 15$ Nm for the first and second links respectively. From these data one easily corroborates that Assumption 3.1 is fulfilled.

4.1 State feedback regulation

The proposed adaptive scheme in Eqs. (3.24)-(3.25a) was tested in its SP-SD, SPD, and SPDgc-like forms, under the respective consideration of expressions (3.34)-(3.35), (3.36)-(3.37), and (3.38)-(3.39). The involved saturation functions were defined as

$$\sigma_{Pi}(\varsigma) = M_{Pi}\,\mathrm{sat}(\varsigma/M_{Pi}) \quad \text{and} \quad \sigma_{Di}(\varsigma) = M_{Di}\,\mathrm{sat}(\varsigma/M_{Di})$$

$i = 1,\ldots,n$, in the SP-SD case;

$$\sigma_{Pi}(\varsigma) = \begin{cases} \varsigma & \forall|\varsigma| \le L_{Pi} \\ \mathrm{sign}(\varsigma)L_{Pi} + (M_{Pi} - L_{Pi})\tanh\left(\frac{\varsigma - \mathrm{sign}(\varsigma)L_{Pi}}{M_{Pi} - L_{Pi}}\right) & \forall|\varsigma| > L_{Pi} \end{cases}$$

$i = 1,\ldots,n$, with $0 < L_{Pi} < M_{Pi}$, in the SPD case;

$$\sigma_{Pi}(\varsigma) = M_{Pi}\,\mathrm{sat}(\varsigma/M_{P_i}) \quad \text{and} \quad \sigma_{0i}(\varsigma) = M_{0i}\,\mathrm{sat}(\varsigma/M_{0_i})$$

$i = 1, \ldots, n$, in the SPDgc-like case; and

$$\sigma_{aj}(\varsigma) = \begin{cases} \varsigma & \forall |\varsigma| \leq L_{aj} \\ \text{sign}(\varsigma) L_{aj} + (M_{aj} - L_{aj}) \tanh\left(\frac{\varsigma - \text{sign}(\varsigma) L_{aj}}{M_{aj} - L_{aj}}\right) & \forall |\varsigma| > L_{aj} \end{cases}$$

$j = 1, \ldots, p$, with $0 < L_{aj} < M_{aj}$, in all the three cases. Let us note that with these saturation functions we have $\sigma'_{PM} = \sigma'_{DM} = \sigma'_{0M} = 1$, and that in consequence, for the three controllers, inequality (3.5) is satisfied with $\kappa = \max_i\{k_{Di}\}$ (see Eqs. (3.22)).

The simulation implementations were run fixing the following saturation parameter values[2]: $M_{P1} = M_{D1} = 40$ and $M_{P2} = M_{D2} = 5$ in the SP-SD case; $M_{P1} = 80$, $M_{P2} = 10$, and $L_{Pi} = 0.9 M_{Pi}$, $i = 1, 2$, in the SPD case; $M_{P1} = 120$, $M_{01} = 50$, $M_{P2} = 12$, and $M_{02} = 7$ in the SPDgc-like case; and $M_{a1} = 50$, $M_{a2} = 3$, and $L_{aj} = 0.9 M_{aj}$, $j = 1, 2$, in all the three cases.

For comparison purposes, additional simulations were run considering the adaptive controller proposed by [50] —referred to as Z_e00—, *i.e.*

$$\begin{aligned} u &= G^T(q)\hat{\theta} - K_P T_h(\bar{q}) - K_D T_h(\dot{q}) \\ \dot{\hat{\theta}} &= P\big(Q(\bar{q}, \dot{q}), \hat{\theta}\big) \end{aligned}$$

where $T_h(x) = \big(\tanh(x_1), \ldots, \tanh(x_n)\big)^T$, $Q(\bar{q}, \dot{q}) = -\Gamma G^T(q)[\dot{q} + \varepsilon T_h(\bar{q})]$, the elements of P are defined as

$$P_j(Q, \hat{\theta}) = \begin{cases} Q_j & \text{if } \theta_{jm} < \hat{\theta}_j < \theta_{jM} \text{ or } \big(\hat{\theta}_j \leq \theta_{jm} \text{ and } Q_j \geq 0\big) \text{ or } \big(\hat{\theta}_j \geq \theta_{jM} \text{ and } Q_j \leq 0\big) \\ 0 & \text{if } \big(\hat{\theta}_j \leq \theta_{jm} \text{ and } Q_j < 0\big) \text{ or } \big(\hat{\theta}_j \geq \theta_{jM} \text{ and } Q_j > 0\big) \end{cases}$$

$j = 1, \ldots, p$, with θ_{jm} and θ_{jM} being known lower and upper bounds of θ_i respectively, and the initial auxiliary state values are taken such that $\hat{\theta}_j(0) \in [\theta_{jm}, \theta_{jM}]$, $j = 1, \ldots, p$. The parameter bounds were fixed at $\theta_{1m} = 10$, $\theta_{1M} = 50$, $\theta_{2m} = 0.5$, and $\theta_{2M} = 3$ [Nm].

Observe that —using Property 1.5— the gravity vector can be written as $g(q, \theta) = G(q)\theta$ with

$$G(q) = \begin{pmatrix} \sin q_1 & \sin(q_1 + q_2) \\ 0 & \sin(q_1 + q_2) \end{pmatrix} \quad \text{and} \quad \theta = \begin{pmatrix} 38.465 \\ 1.825 \end{pmatrix} \quad [\text{Nm}]$$

The results of two simulation tests (for every considered controller) are presented. The initial conditions and desired link positions in all the simulated cases were taken as $q_1(0) = q_2(0) = \dot{q}_1(0) = \dot{q}_2(0) = 0$; $\hat{\theta}_1(0) = 20$, $\hat{\theta}_2(0) = 1$ [Nm]; and $q_{d1} = q_{d2} = \pi/4$ [rad]. In the first implementation —referred to as Test 1.1—, a value of ε satisfying (3.10) was fixed for the SP-SD, SPD, and SPDgc-like algorithms; the control parameters (k_{Pi}, k_{Di}, $i = 1, 2$) and adaptation gains (γ_i, $i = 1, 2$) were determined from those giving rise to the best closed-loop response from numerous trail-and-error tests using the SPD control law, and the same fixed values were kept for the SP-SD and the SPDgc-like

[2] For the sake of simplicity, the units of the elements of the parameter vector θ, their estimation variables and related bounds and saturation function parameters, the auxiliary states, and the control and adaptation gains are omitted. The angles are expressed and measured in radians.

Table 4.1: Control parameter values for the state-feedback regulation scheme

	TEST 1.1		TEST 1.2	
Parameter	SP-SD SPD SPDgc-like	Z_e00	SP-SD SPD SPDgc-like	Z_e00
k_{P1}	100	75	100	100
k_{P2}	200	7	30	30
k_{D1}	50	4.5	50	1000
k_{D2}	3	3	3	250
γ_1	1000	1000	15	250
γ_2	750	750	0.35	20
ε	0.001	0.0001	0.1	0.1

algorithms. As for the Z_e00 controller, the selection of ε, control parameters, and adaptation gains was performed according to the tuning procedure of the algorithm as presented in [50], taking into account the pre-specified initial conditions and desired positions, and such that the greatest possible absolute value of the control signals at every link was ensured to be lower than the corresponding input saturation value (*i.e.* $\sum_{j=1}^{2} B_{G_{ij}}\theta_{jM} + k_{Pi} + k_{Di} < T_i$, $i = 1, 2$); under these considerations, the fixed parameters and gains were those giving rise to the best closed-loop performance after numerous trial-and-error tests. With the aim at improving the closed-loop performance obtained through Test 1.1, in the second implementation —referred to as Test 1.2—, a higher value of ε, disregarding inequality (3.10), was fixed for all the tested controllers (recall that the condition on ε, (3.10), is only sufficient, and that such a parameter is not involved in the condition stated to avoid input saturation, (3.7)). For the SP-SD, SPD, and SPDgc-like algorithms, the control parameters and adaptation gains were tuned as in the previously described case. As for the Z_e00 controller, the referred values were fixed such that the best closed-loop performance was obtained from numerous trial-and-error tests; the tuning conditions presented in [50] could not any longer be satisfied for the value of ε that was taken, and saturation avoidance was disregarded since control parameter tuning under such a consideration gave rise to extremely poor closed-loop performances. The resulting values for all the implemented controller at both tests are presented in Table 4.1.

Figures 4.1–4.3 show the position errors, control signals, and parameter estimators, for all the considered controllers at Test 1.1. Observe that in all the cases, the control objective is achieved avoiding input saturation. However, note that while around 100 sec is enough for the SP-SD, SPD, and SPDgc-like algorithms to achieve the desired stabilization, more than 10000 sec are needed by the Z_e00 controller. This can be better appreciated in the zoom of the responses presented at the right hand side of each figure. It can be also observed that the SPD algorithm converge faster than the others tested. As for the parameter estimator response, shown in figure 4.3, notice that even when the Z_e00 algorithm approaches faster to the real parameter value it never converges to it within the time the test was performed, *i.e.* 15000 sec, while the

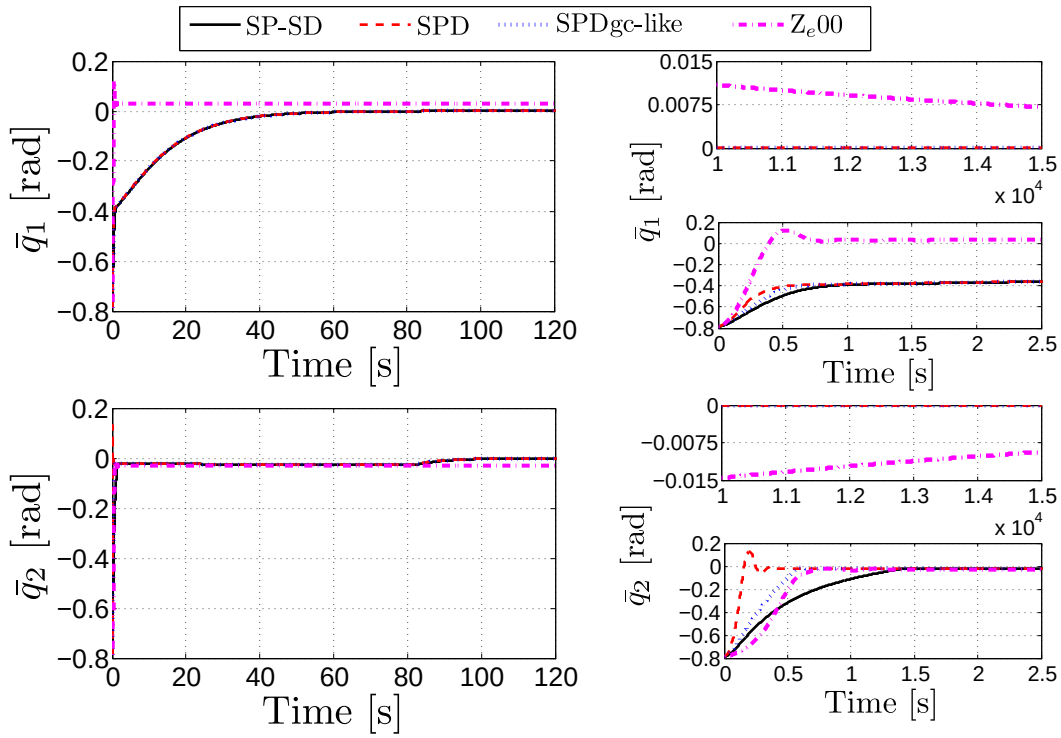

Figure 4.1: Test 1: position errors

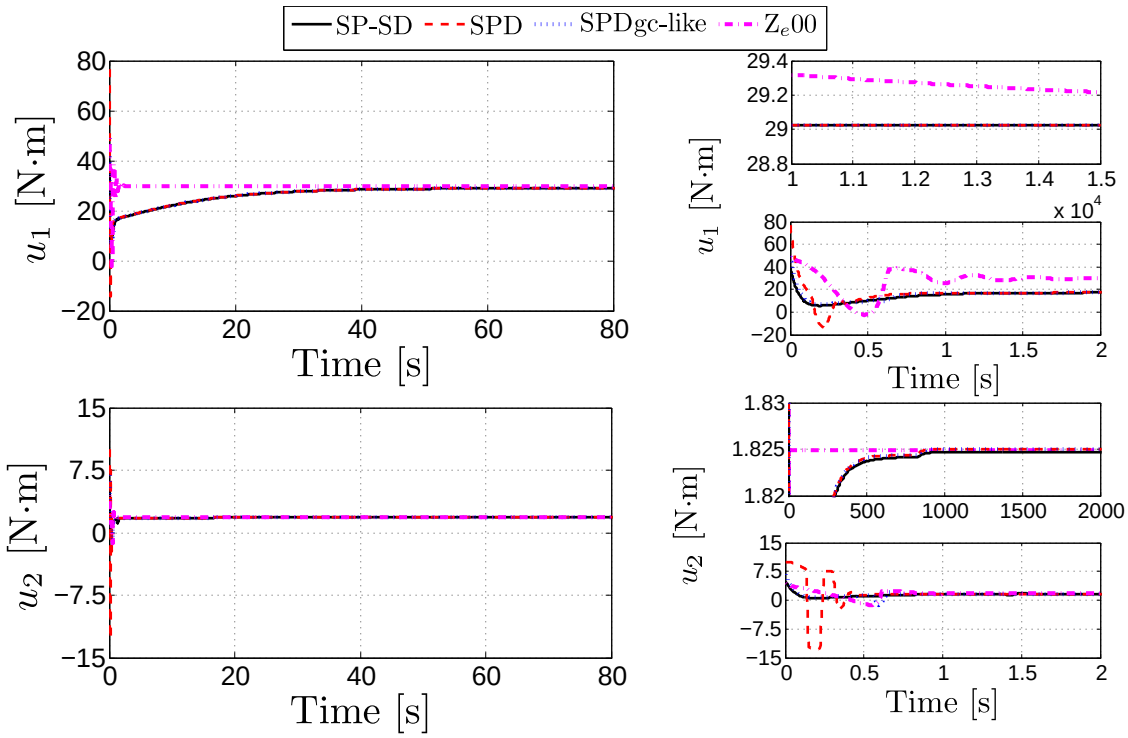

Figure 4.2: Test 1: control signals

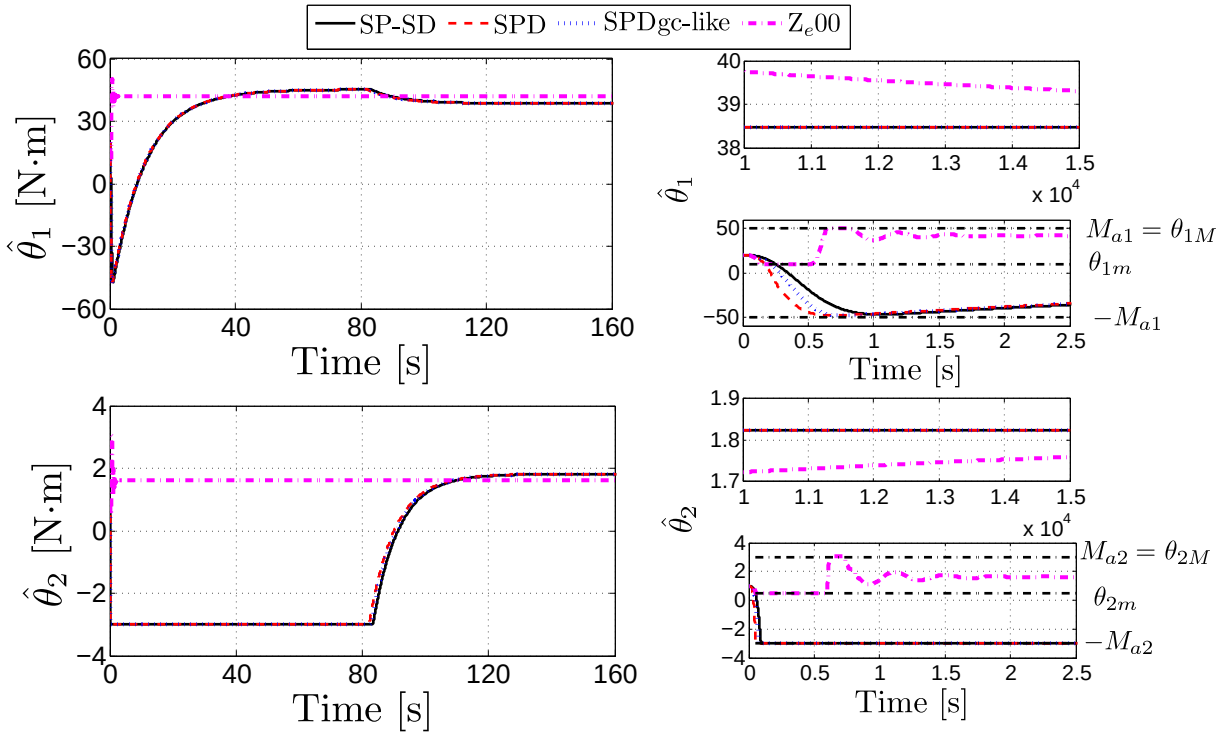

Figure 4.3: Test 1: parameter estimators

SP-SD, SPD and SPDgc-like controllers reach the real parameter value in about 120 sec.

Figures 4.4–4.6 show the results obtained through Test 1.2 for all the considered controllers. In all the simulated cases, the control objective is observed to be achieved avoiding input saturation, with a stabilization time considerably lower than in the previous test. Furthermore, the SP-SD, SPD, and SPDgc-like algorithms are still observed to achieve the desired convergence much faster than the Z$_e$00 controller. It can be seen in the right hand side zoom of the response in figure 4.4 that the algorithm Z$_e$00 achieves the control objective in about 60 sec. On the other hand, figure 4.6 shows the parameter estimation response for all tested control schemes, notice that the parametric convergence of the SP-SD, SPD, and SPD-gc like algorithms is faster than that of the Z$_e$00 controller.

Observe from Figures 4.3 and 4.6 that the parameter estimators converge to the real values θ_i, $i = 1, 2$. This is so in view of the selected desired configuration which gives rise to the satisfaction of the condition stated by Corollary 3.1.

4.2 Output feedback regulation

The saturation functions involved in the proposed scheme Eq. (3.40) —referred to as SP-SD$_c$-g$_a$ — were defined as

$$\sigma_{Pi}(\varsigma) = M_{Pi}\,\mathrm{sat}(\varsigma/M_{P_i}) \quad \text{and} \quad \sigma_{Di}(\varsigma) = M_{Di}\,\mathrm{sat}(\varsigma/M_{D_i})$$

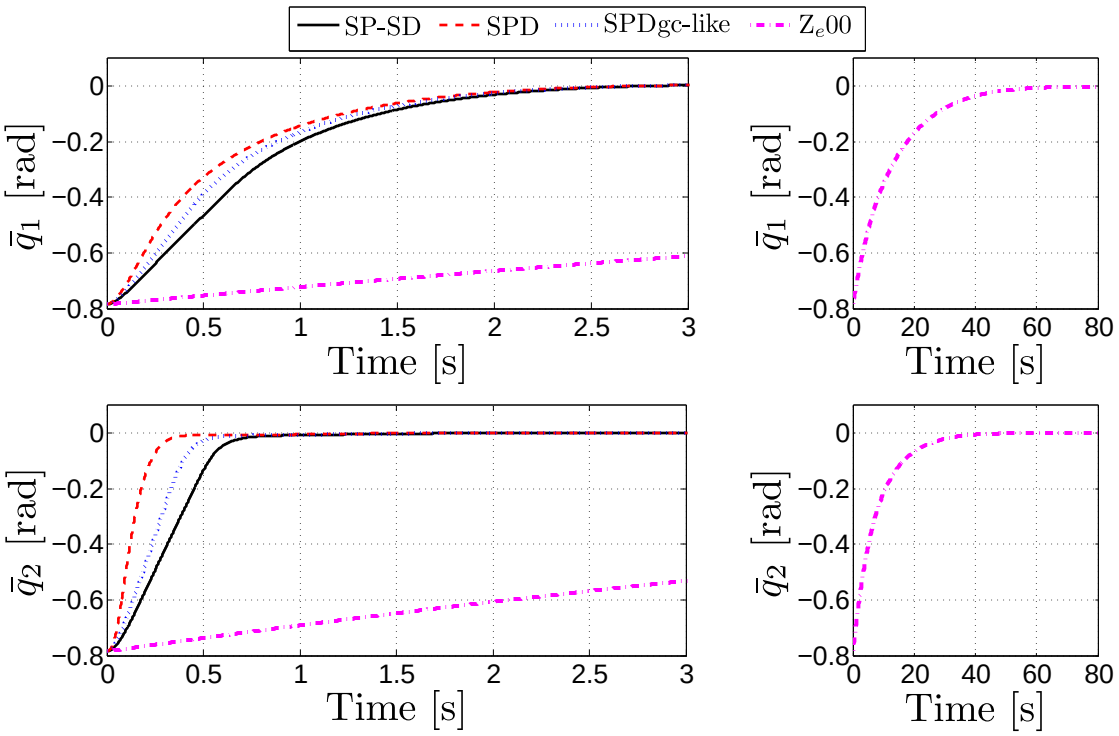

Figure 4.4: Test 1.2: position errors

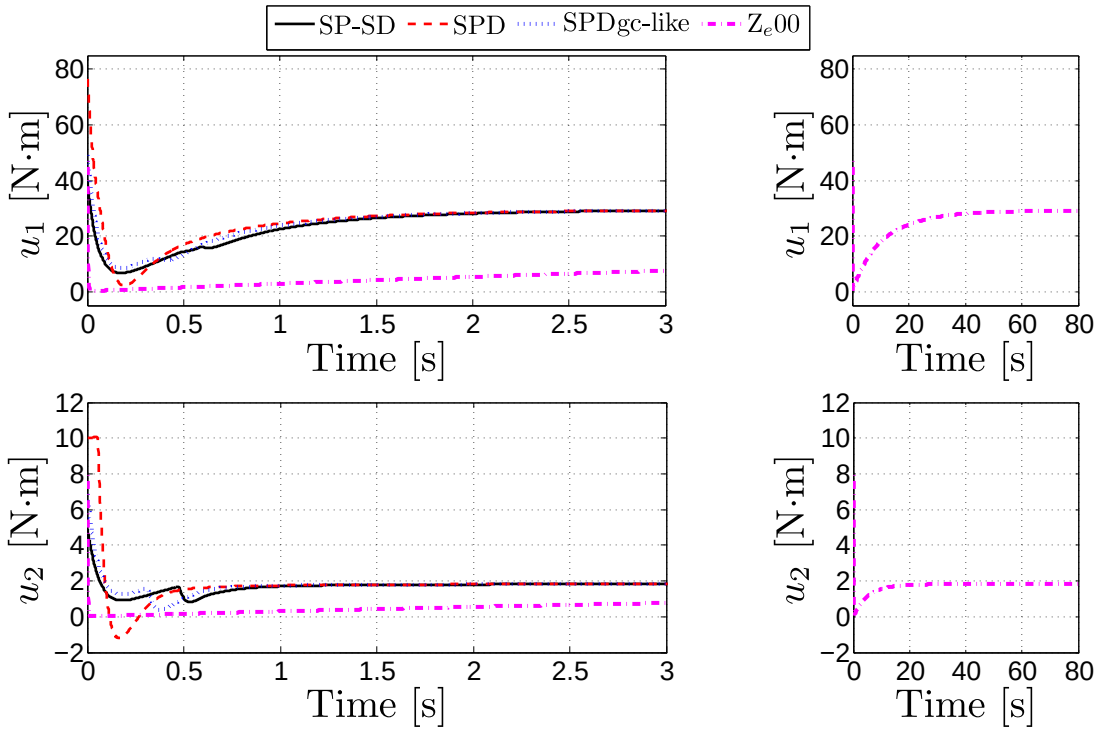

Figure 4.5: Test 1.2: control signals

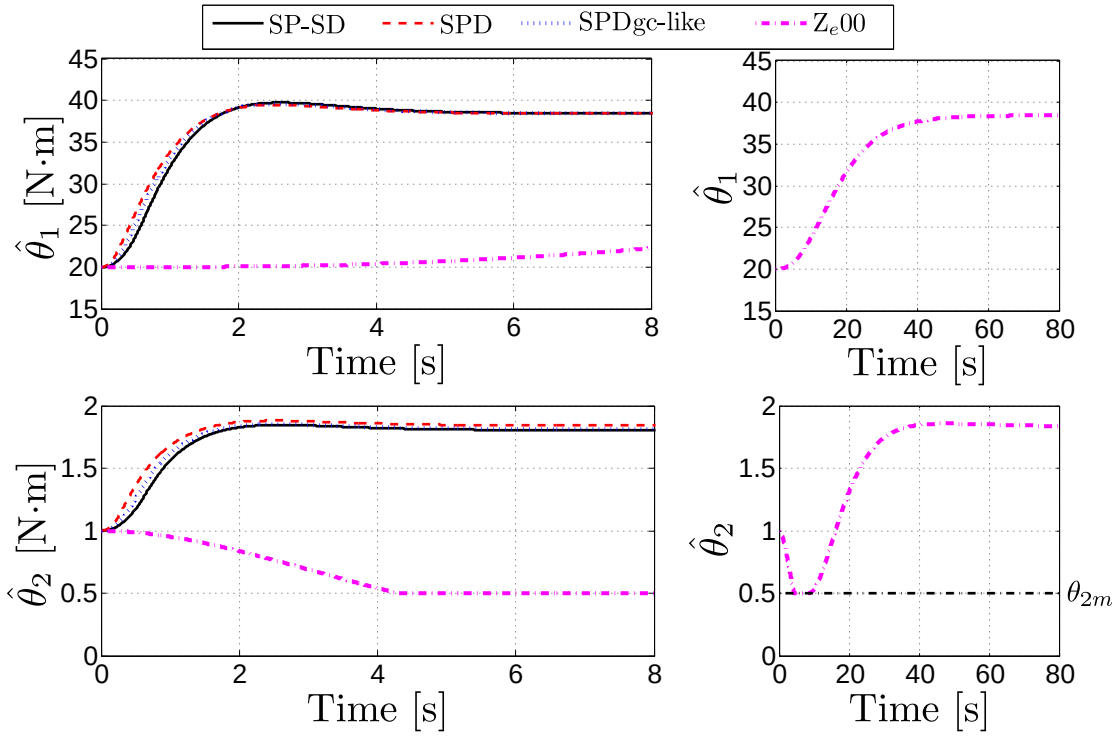

Figure 4.6: Test 1.2: parameter estimators

$i = 1, \ldots, n$, and

$$\sigma_{aj}(\varsigma) = \begin{cases} \varsigma & \forall |\varsigma| \leq L_{aj} \\ \text{sign}(\varsigma) L_{aj} + (M_{aj} - L_{aj}) \tanh\left(\frac{\varsigma - \text{sign}(\varsigma) L_{aj}}{M_{aj} - L_{aj}}\right) & \forall |\varsigma| > L_{aj} \end{cases}$$

$j = 1, \ldots, p$, with $0 < L_{aj} < M_{aj}$. Let us note that with these saturation functions we have $\sigma'_{PM} = \sigma'_{DM} = 1$. The simulation implementations were run fixing the following saturation parameter values (see footnote 2): $M_{P1} = M_{D1} = 40$ and $M_{P2} = M_{D2} = 5$; and $M_{a1} = 50$, $M_{a2} = 3$, and $L_{aj} = 0.9 M_{aj}$, $j = 1, 2$.

For comparison purposes, additional simulations were run considering the adaptive controller proposed by [25] —referred to as L00—, *i.e.*

$$\begin{aligned} u &= G^T(q_d)\hat{\theta} - K_P T_h(\lambda \bar{q}) - K_D T_h(\delta \vartheta) \\ \dot{\hat{\theta}} &= \beta G(q_d)^T \hat{\theta} \left[\dot{q} - \eta T_h(\delta \vartheta) + \mu T_h(\lambda \bar{q})\right] \\ \dot{\vartheta} &= \chi K \vartheta + K \dot{q} \end{aligned}$$

where $T_h(x) = \big(\tanh(x_1), \ldots, \tanh(x_n)\big)^T$, $K_D = \text{diag}[k_D]$, $K_P = \text{diag}[k_P]$, and $K = \text{diag}[k]$, with λ, δ, k_d, k_p, β, η, μ, k, and χ being positive constants.

The results of two simulation tests (for every considered controller) are presented. The initial conditions and desired link positions in all the simulated cases were taken as $q_1(0) = q_2(0) = \dot{q}_1(0) = \dot{q}_2(0) = 0$; $\hat{\phi}_1(0) = 20$, $\hat{\phi}_2(0) = 1$ [Nm]; $q_{d1} = \pi/4$, and $q_{d2} = \pi/2$ [rad]. In the first implementation —referred to as Test 1—, a value of ε

satisfying (3.44) was fixed for the SP-SD$_c$-g$_a$ algorithm; the control parameters (k_{Pi}, k_{Di}, $i = 1, 2$) and adaptation gains (γ_i, $i = 1, 2$) were determined from those giving rise to the best closed-loop response from numerous trail-and-error tests. As for the L00 controller the selection of control parameters as described in [25] could not be accomplished due to the impossibility of reconciling the inequalities proposed in their tuning procedure. In an effort to fulfill as many conditions as possible two different simulations were performed for the L00 controller, referred to as L00: Test A and L00: Test B (each of them disregarding one different inequality of the tuning criterion presented in [25]); under these considerations, the fixed parameters and gains were those giving rise to the best closed-loop performance after numerous trial-and-error tests.

With the aim at improving the closed-loop performance obtained through Test 1, in the second implementation —referred to as Test 2—, condition (3.44) was disregarded and hence a higher value of ε was fixed for the SP-SD$_c$-g$_a$ controller (recall that the condition on ε, (3.44), is only sufficient, and that such a parameter is not involved in the condition stated to avoid input saturation) while all conditions presented in the stability proof of [25] were disregarded for the L00 scheme. For the SP-SD$_c$-g$_a$ algorithm, the control parameters and adaptation gains were tuned as in the previously described case. As for the L00 controller, the referred values were fixed such that the best closed-loop performance was obtained from numerous trial-and-error tests; the conditions presented in [25] could not be satisfied any longer and saturation avoidance was disregarded since control parameter tuning under such a consideration gave rise to poor closed-loop performances. The resulting values for all the tested controller at both tests are presented in Table 4.2.

Figures 4.7–4.9 show the position errors, control signals, and parameter estimators, for both considered controllers at Test 1. The SP-SD$_c$-g$_a$ achieves the control objective without reaching the saturation bound. In the L00: Test A experiment the input saturation inequality considered in the tuning procedure and, as expected, the saturation bound is not reached but slow convergence time is observed; while in the L00: Test B trial convergence time is greatly improved but large oscillations and input saturation could not be avoided. The slow convergence of system parameters and states, observed in both tested controllers, is due to the small value of the selected control gains.

The responses obtained through Test 2 are shown in Figures 4.10–4.12, observe that faster convergence time is achieved through the selected control gains without oscillations notice however that a small overshoot is present and input saturation could not be avoided in the case of the L00 controller.

Observe from Figures 4.9 and 4.12 that the parameter estimators converge to the real values θ_i, $i = 1, 2$. This is so in view of the selected desired configuration which gives rise to the satisfaction of the condition stated by Corollary 3.2.

4.3 State feedback trajectory tracking

Considering the main characteristics of the proposed scheme —bounded adaptive— additional simulations were run for comparison purposes using an approach of analog

Table 4.2: Control parameter values for the output-feedback regulation scheme

	TEST 1			TEST 2	
Parameter	SP-SD$_c$-g$_a$	L00: Test A	L00: Test B	SP-SD$_c$-g$_a$	L00
k_{P1}	11	7	180	180	40
k_{P2}	11	7	180	150	40
k_{D1}	1	7	90	50	50
k_{D2}	3	7	90	6	50
γ_1	300			80	
γ_2	120			20	
ε	0.0035			0.035	
a_1	15			250	
a_2	15			200	
b_1	0.5			2.5	
b_2	0.025			17.5	
β		100	120		25
χ		10	10		5
η		0.05	0.05		1
μ		0.05	0.1		2
k		50	40		20
λ		1	3		10
δ		1	1		6

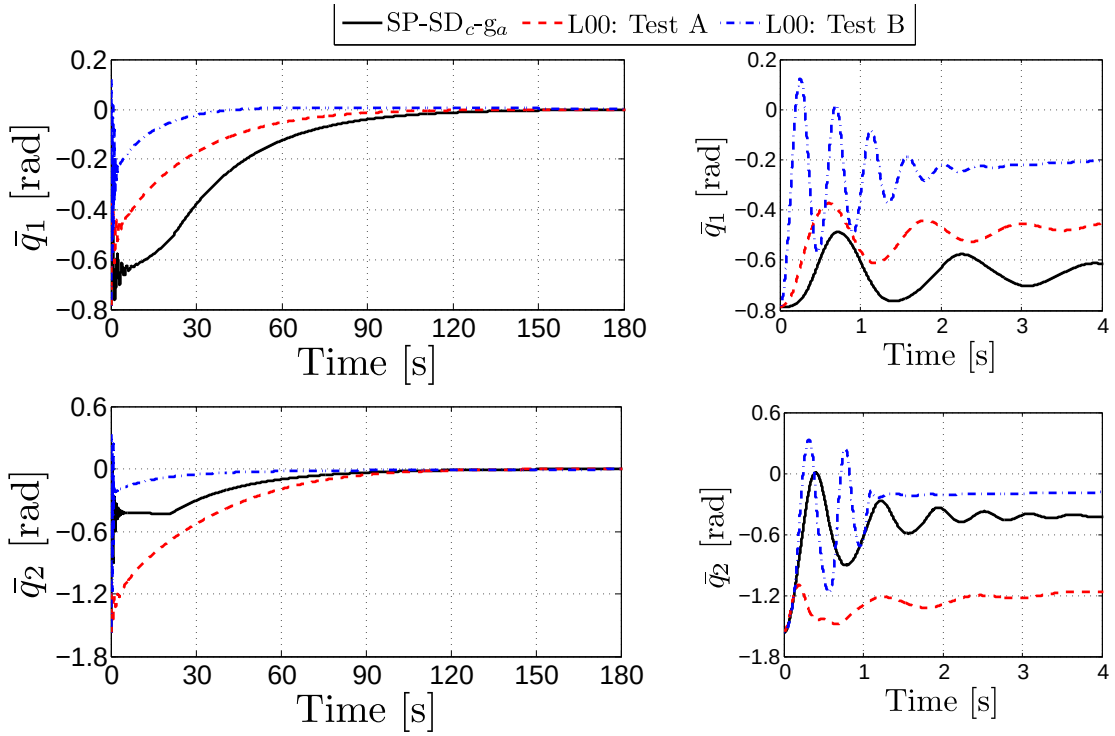

Figure 4.7: Test 1: position errors

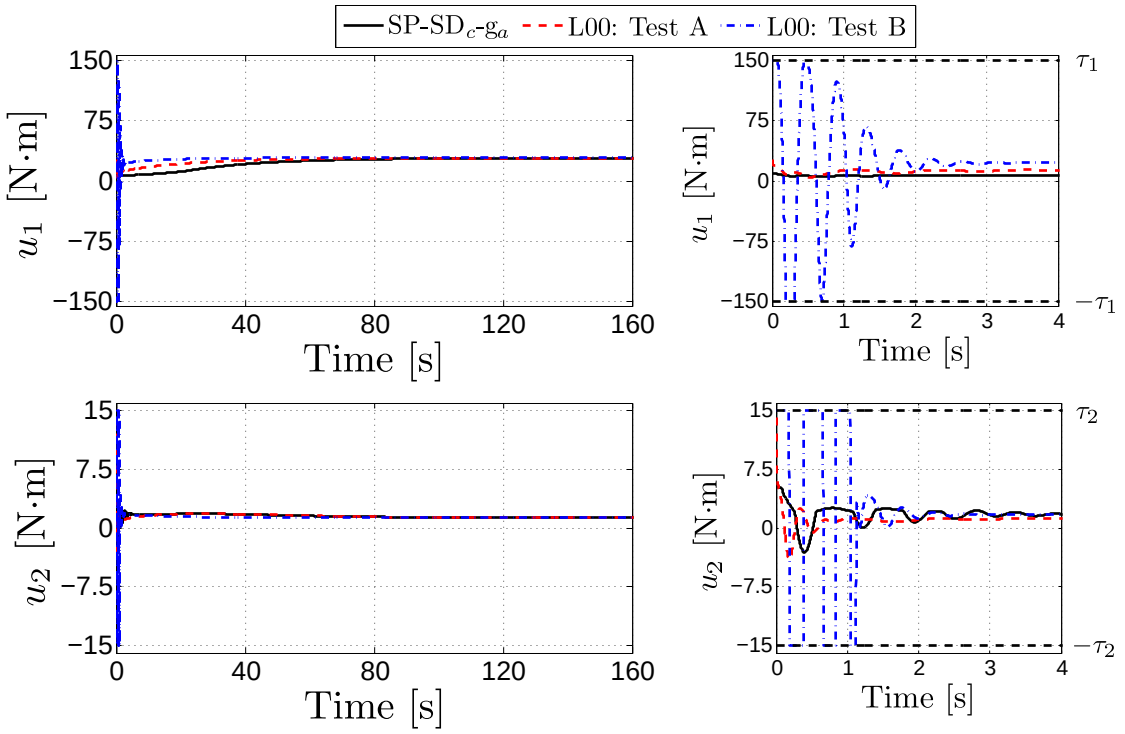

Figure 4.8: Test 1: control signals

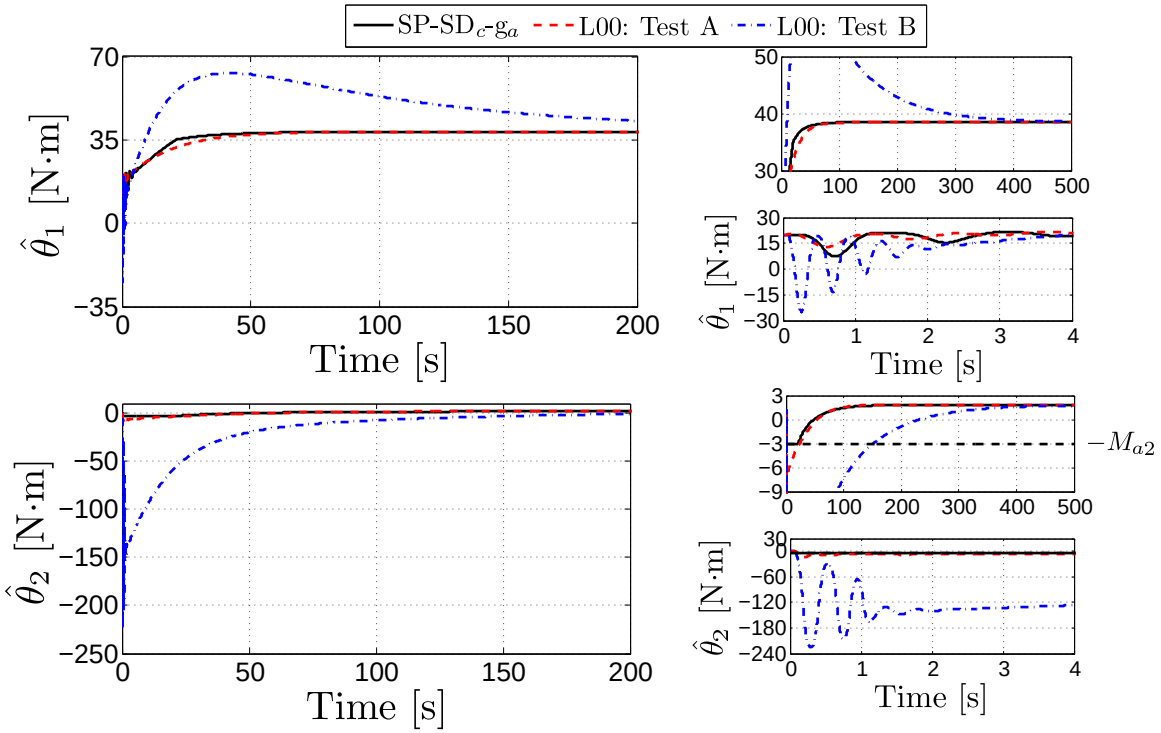

Figure 4.9: Test 1: parameter estimators

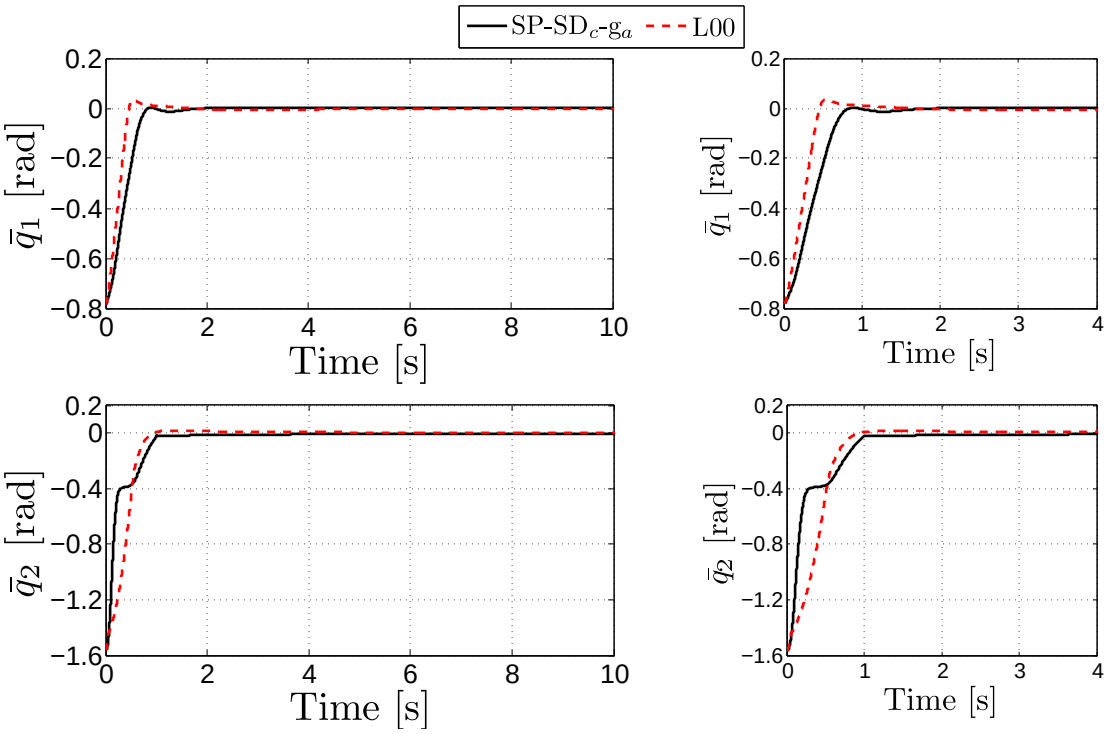

Figure 4.10: Test 2: position errors

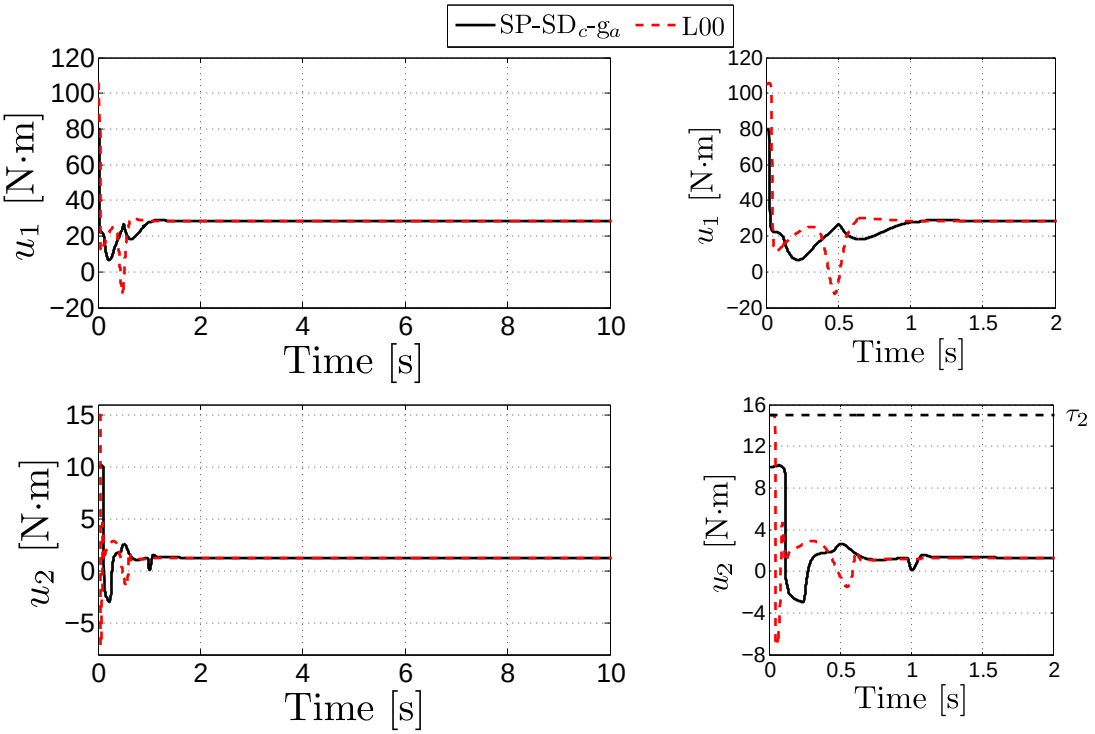

Figure 4.11: Test 2: control signals

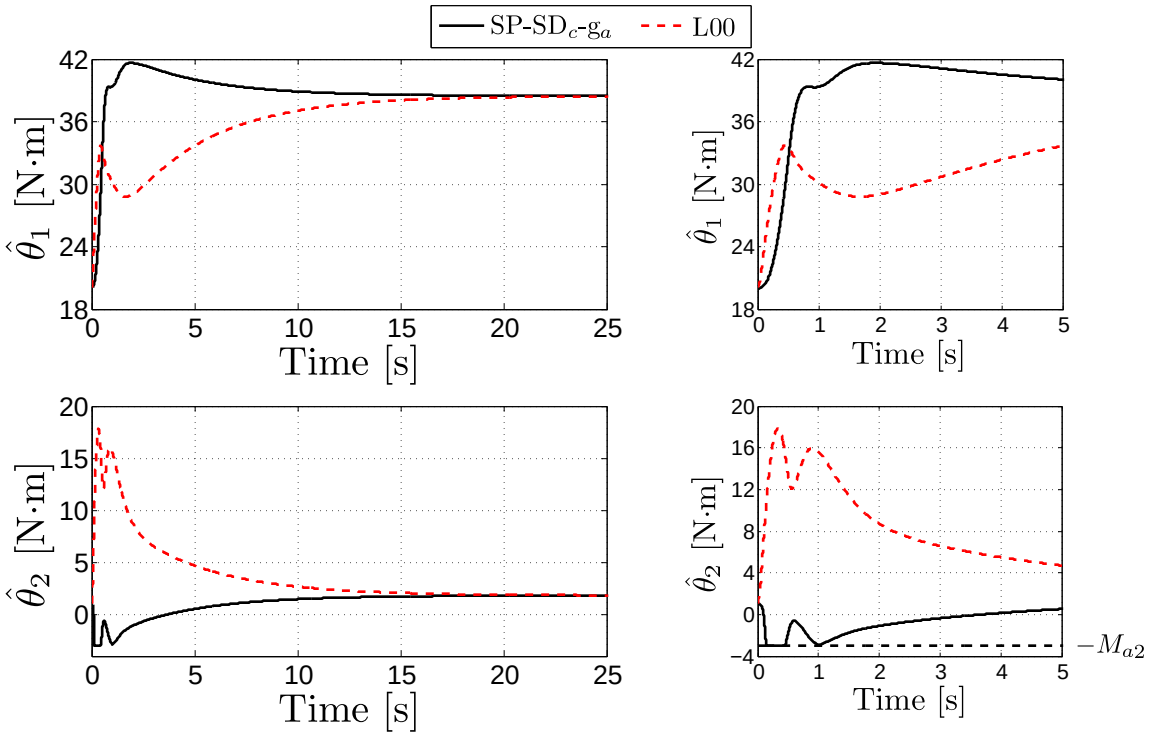

Figure 4.12: Test 2: parameter estimators

features. The chosen scheme, proposed by [12] —referred to as D$_e$99— is given by

$$u = Y_d(t)\hat{\psi} - K_P T_h(e) - K_D T_h(r)$$
$$\dot{\hat{\psi}} = P\big(Q(\bar{q}, \dot{\bar{q}}, \hat{\psi})\big)$$

where $Y_d(t) = Y_d(q_d, \dot{q}_d, \ddot{q}_d)$, $T_h(x) = \big(\tanh(x_1), \ldots, \tanh(x_n)\big)^T$; $e = q_d - q$; $r = \dot{e} + \alpha T_h(e)$; $Q(\bar{q}, \dot{q}, \hat{\psi}) = \Gamma Y_d^T(t)[\dot{\bar{q}} + \varepsilon T_h(\bar{q})]$; the elements of P are defined as

$$P_j(Q, \hat{\psi}) = \begin{cases} Q_j & \text{if } \psi_{jm} < \hat{\psi}_j < \psi_{jM} \text{ or } \big(\hat{\psi}_j \le \psi_{jm} \text{ and } Q_j \ge 0\big) \text{ or } \big(\hat{\psi}_j \ge \psi_{jM} \text{ and } Q_j \le 0\big) \\ 0 & \text{if } \big(\hat{\psi}_j \le \psi_{jm} \text{ and } Q_j < 0\big) \text{ or } \big(\hat{\psi}_j \ge \psi_{jM} \text{ and } Q_j > 0\big) \end{cases}$$

$j = 1, \ldots, \rho$, with ψ_{jm} and ψ_{jM} being known lower and upper bounds of ψ_j respectively; and the initial auxiliary state values are taken such that $\hat{\psi}_j(0) \in [\psi_{jm}, \psi_{jM}]$, $j = 1, \ldots, \rho$. The parameter bounds were fixed at $\big(\psi_{1m}\ \psi_{2m}\ \psi_{3m}\ \psi_{4m}\ \psi_{5m}\ \psi_{6m}\ \psi_{7m}\ \big) = \big(0.588\ \ 0.021\ \ 0.025\ \ 0.572\ \ 0.044\ \ 9.616\ \ 0.456\big)$ (see footnote 2), and $\psi_{jM} = M_{aj}$, $j = 1, \ldots, 7$, (these values are specified below).

The results of two experimental tests are presented. The initial link positions and velocities at all the executed simulations were $q_1(0) = q_2(0) = \dot{q}_1(0) = \dot{q}_2(0) = 0$, the auxiliary states were initiated at $\phi^T(0) = \big(2.88\ \ 0.103\ \ 0.125\ \ 2.803\ \ 0.214\ \ 47119\ \ 2.235\big)$; and the desired trajectory was defined as

$$q_{d1} = \frac{\pi}{2} + \sin(0.1t) \qquad \text{[rad/s]}$$
$$q_{d2} = \cos(0.1t) \qquad \text{[rad/s]}$$

Table 4.3: Control parameter values for the state-feedback tracking scheme: Test 1

Parameter	SP-SD+, SPD+, SPDhc+-like	D_e99
k_{P1}	50	200
k_{P2}	80	90
k_{D1}	3	70
k_{D2}	5	66
Γ	$\mathrm{diag}[50, 0.5, 0.1, 1.5, 0.1, 60, 2.5]$	$\mathrm{diag}[30, 0.05, 0.01, 1.5, 0.1, 20, 0.1]$
ε	0.00027	5

Le us note that with this desired trajectory Assumption 3.2 is satisfied with $B_{dv} = \omega < 1.2027 = f_m/k_C$ and $B_{da} = \omega^2$. The fixed saturation function parameters values for the SP-SD+, SPD+, and SPDhc+-like schemes were (see footnote 2) $M_{P1} = 40$, $M_{D1} = 40$, $M_{P2} = 4$, and $M_{D2} = 4$ for SP-SD+ scheme; $M_{P1} = 85$ and $M_{P2} = 8.5$ in the SPD+ case; $M_{01} = 130$, $M_{P1} = 45$, $M_{02} = 13$, and $M_{P2} = 4$ for the SPDhc+-like algorithm; and $L_{Pi} = 0.9M_{Pi}$, $i = 1, 2$, $M_a^T = \begin{pmatrix} 2.939 & 0.105 & 0.127 & 2.86 & 0.219 & 48.081 & 2.281 \end{pmatrix}$, $L_{aj} = 0.9M_{aj}$, $j = 1, \ldots, 7$, in all three cases. With these values inequalities (3.78), (3.86), (3.88), and (3.90) are satisfied with $\omega = 0.1$ rad/s, taking $B_{gi}^{Ma} = \sum_{j=1}^{7} B_{G_{ij}} M_{aj}$, $i = 1, 2$, *i.e.*

$$B_{g1}^{M_a} = M_{a6} + M_{a7} = 50.362 \quad \text{and} \quad B_{g2}^{M_a} = M_{a7} = 2.281$$

and $B_{Di}^{M_a} = \sum_{j=1}^{7} B_{Y_{ij}} M_{aj}$, $i = 1, 2$, *i.e.*

$$B_{D1}^{M_a} = \left(M_{a1} + \sqrt{10} M_{a2} + M_{a3}\right)\omega^2 + M_{a4}\omega + M_{a6} + M_{a7} = 58.6872$$

and

$$B_{D2}^{M_a} = \left(M_{a2} + \sqrt{2} M_{a3}\right)\omega^2 + M_{a5}\omega + M_{a7} = 2.9536$$

In the first implementation —referred to as Test 1— a sufficiently small value of ε was taken, for the SP-SD+, SPD+, and SPDhc+-like, guaranteeing satisfaction of inequalities (3.65). For the D_e99 algorithm, with the chosen auxiliary state variable initial condition, the inequality bounding the input torque stated in [12, Remark 3] could not be met while selecting proportional and derivative gains which fulfill the control objective, so it was disregarded. Under the stated considerations the tuning parameter combination giving rise to the best closed-loop performance —in terms mainly of stabilization time (as short as possible) and transient response (avoiding or lowering down overshoot and oscillations as much as possible)— was determined from numerous trial-and-error experiments for every implemented controller. The resulting values are presented in Table 4.3.

Figures 4.13–4.17 show the results of Test 1 for every implemented controller. Observe that even when $q(t)$ approaches $q_d(t)$ in short time for the D_e99 approach, the control inputs reach their respective saturation limits, u_2 remaining saturated all simulated time and in consequence giving rise to a small steady state error in $q_2(t)$. It can be observed that the parameter estimators convergence rate is slow due to the small value of ε, notice however that this fact does not prevent the tracking objective

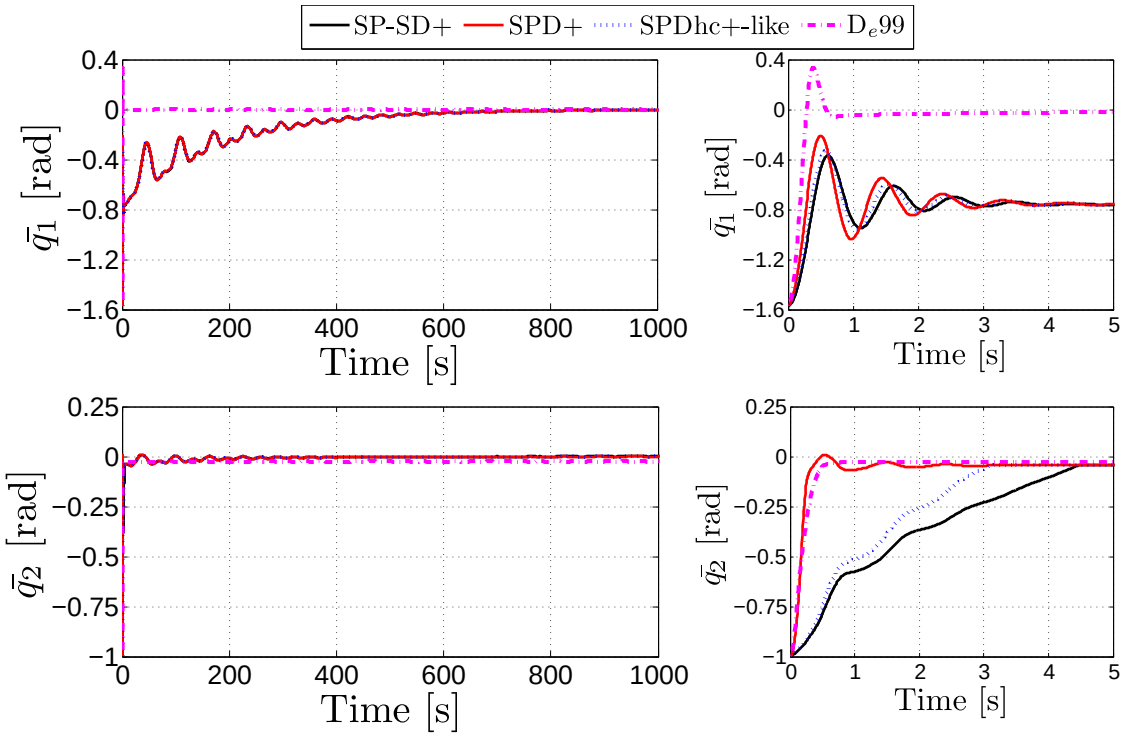

Figure 4.13: Test 1: position errors

Table 4.4: Control parameter values for the state-feedback tracking scheme: Test 2

Parameter	SP-SD+, SPD+, SPDhc+-like	D$_e$99
k_{P1}	100	80
k_{P2}	80	28
k_{D1}	30	25
k_{D2}	5	8
Γ	diag[60, 3, 0.5, 1.5, 10, 35, 10]	diag[30, 0.5, 0.1, 1.5, 0.1, 35, 6]
ε	0.02	2

to be reached. The SP-SD+, SPD+, and SPDhc+-like algorithms achieve the control objective without saturating the inputs but in a long period of time due to the small value of ε.

For the second implementation —referred to as Test 2—, in order to get faster responses for the SP-SD+, SPD+, and SPDhc+-like controller, a high value of ε was fixed (considerably higher than in the precedent tests) disregarding inequality (3.65) (recall that the condition stated by inequality (3.65) is only sufficient); and for the D$_e$99 the tuning procedure was disregarded only respecting the input torque bound so that an initial condition further away from the parameter real value could be chosen, the auxiliary state variable initial condition was taken as $\phi_j(0) = 0.5\psi_j$, for $j = 1, \ldots, 7$, for all controllers. The resulting values are presented in Table 4.4.

Figures 4.18–4.22 show the results of Test 2 for every implemented controller.

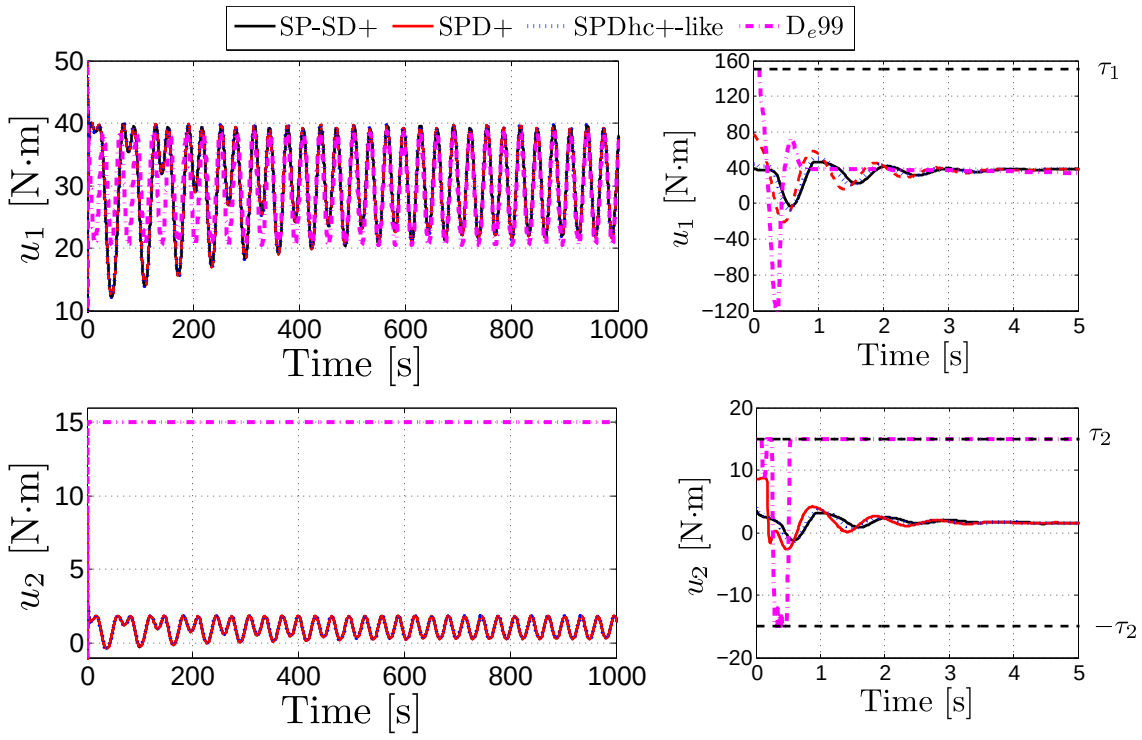

Figure 4.14: Test 1: control signals

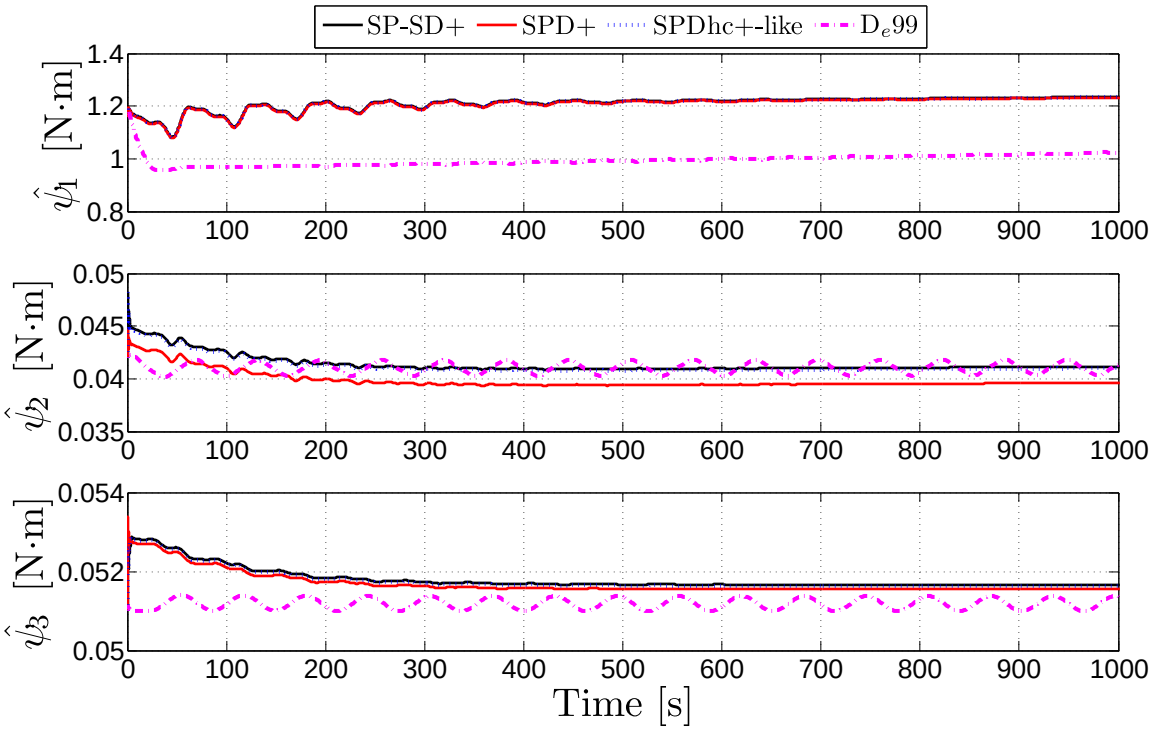

Figure 4.15: Test 1: parameter estimators

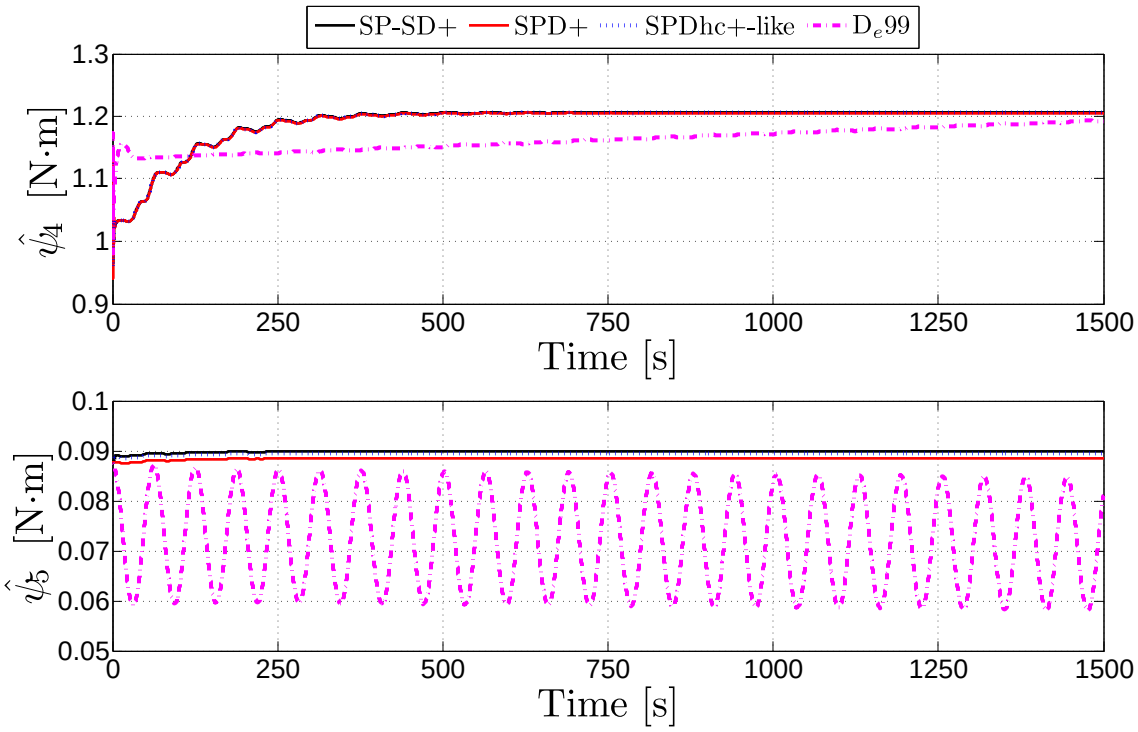

Figure 4.16: Test 1: parameter estimators

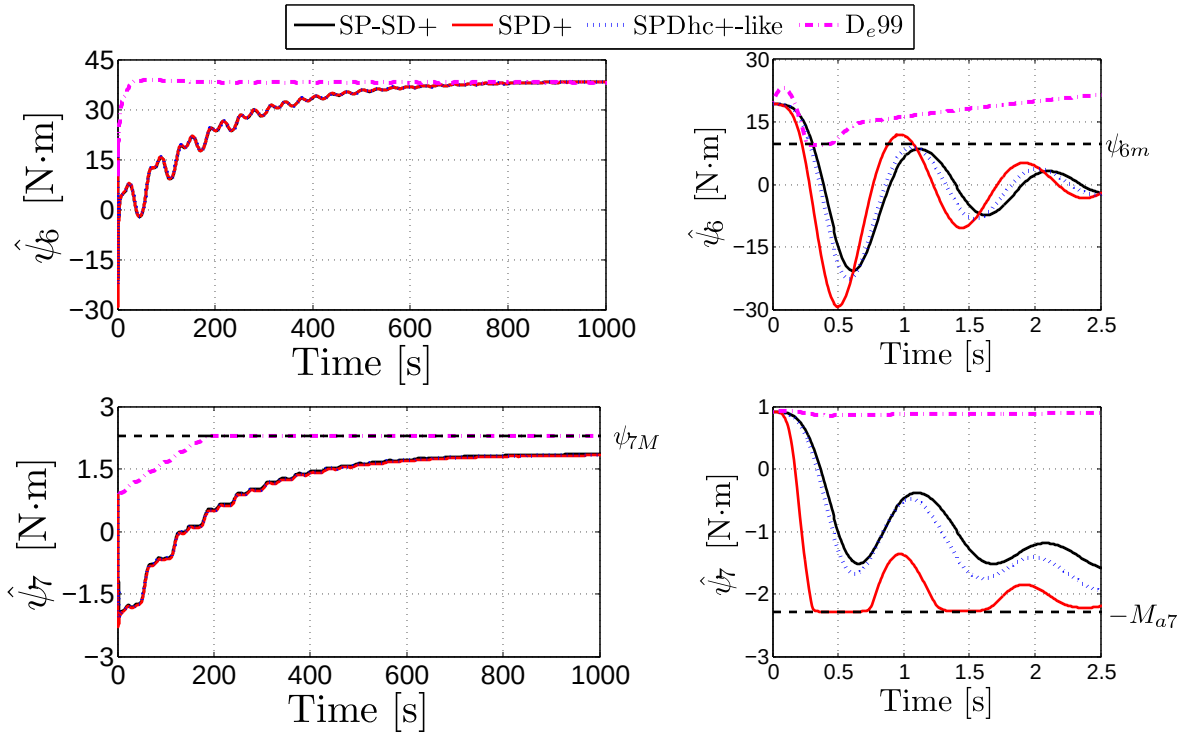

Figure 4.17: Test 1: parameter estimators

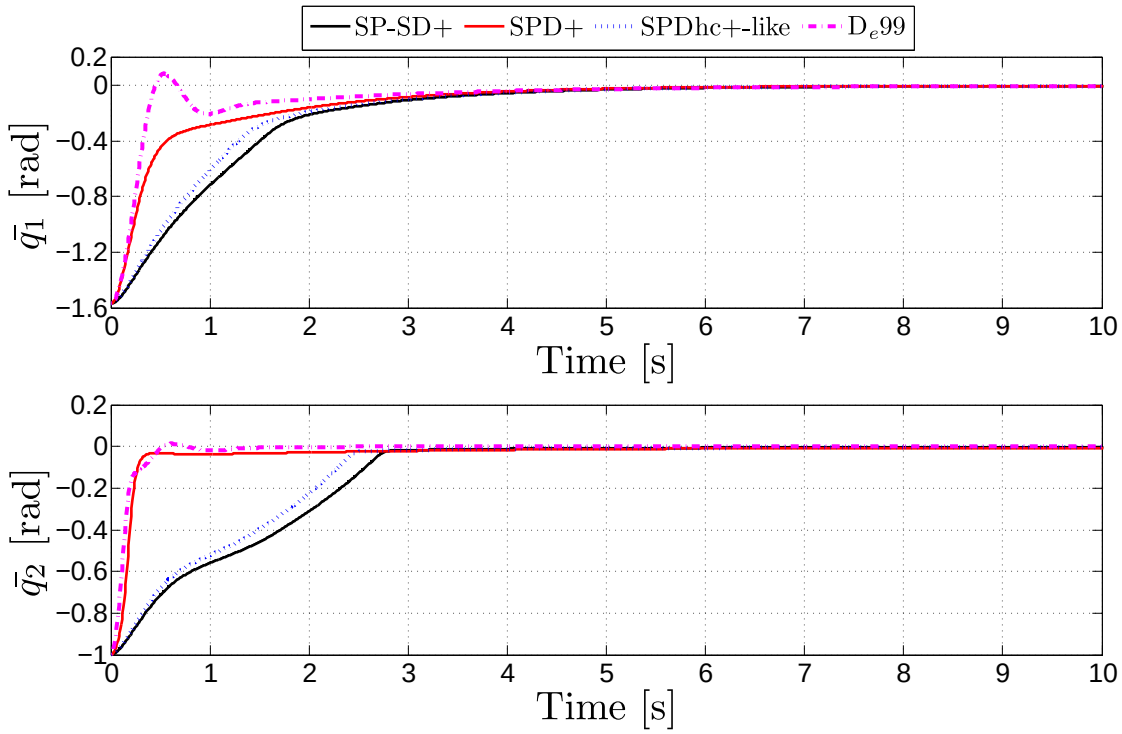

Figure 4.18: Test 2: position errors

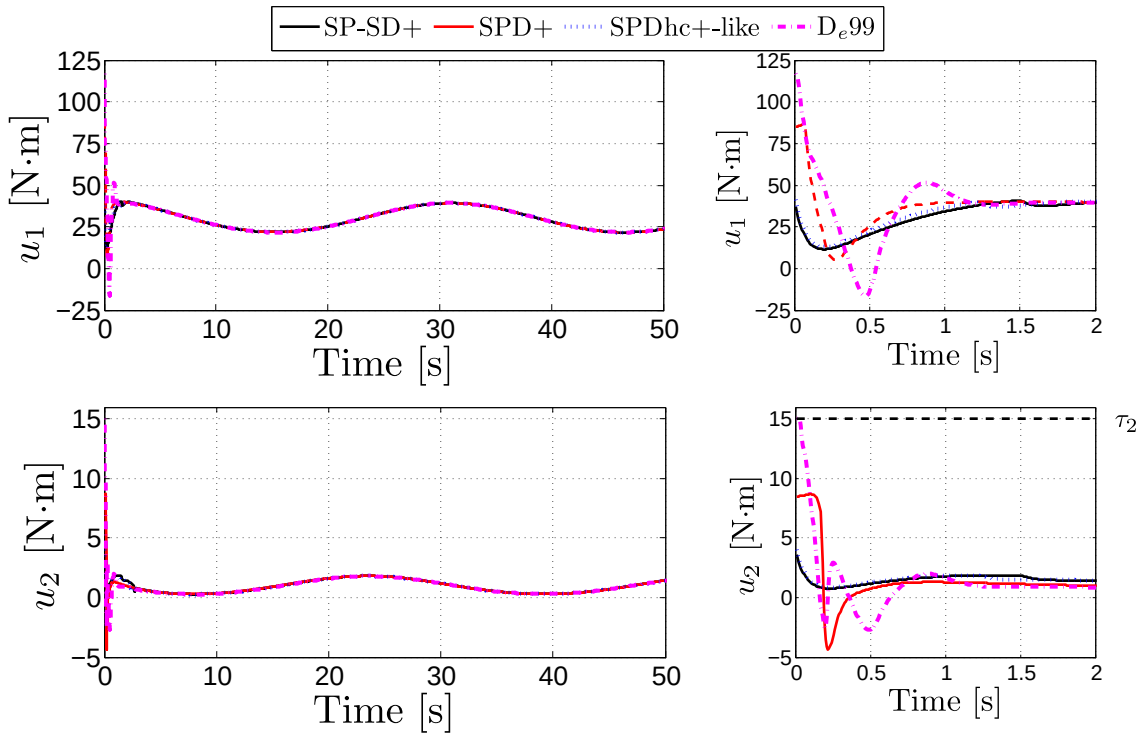

Figure 4.19: Test 2: control signals

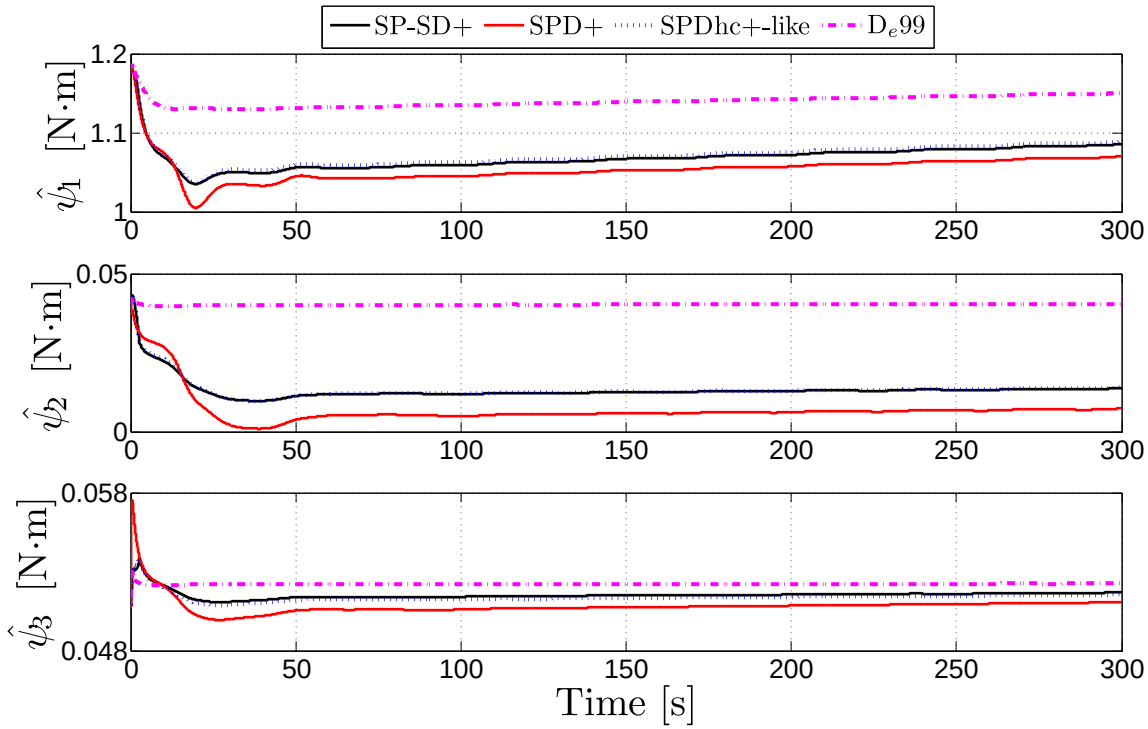

Figure 4.20: Test 2: parameter estimators

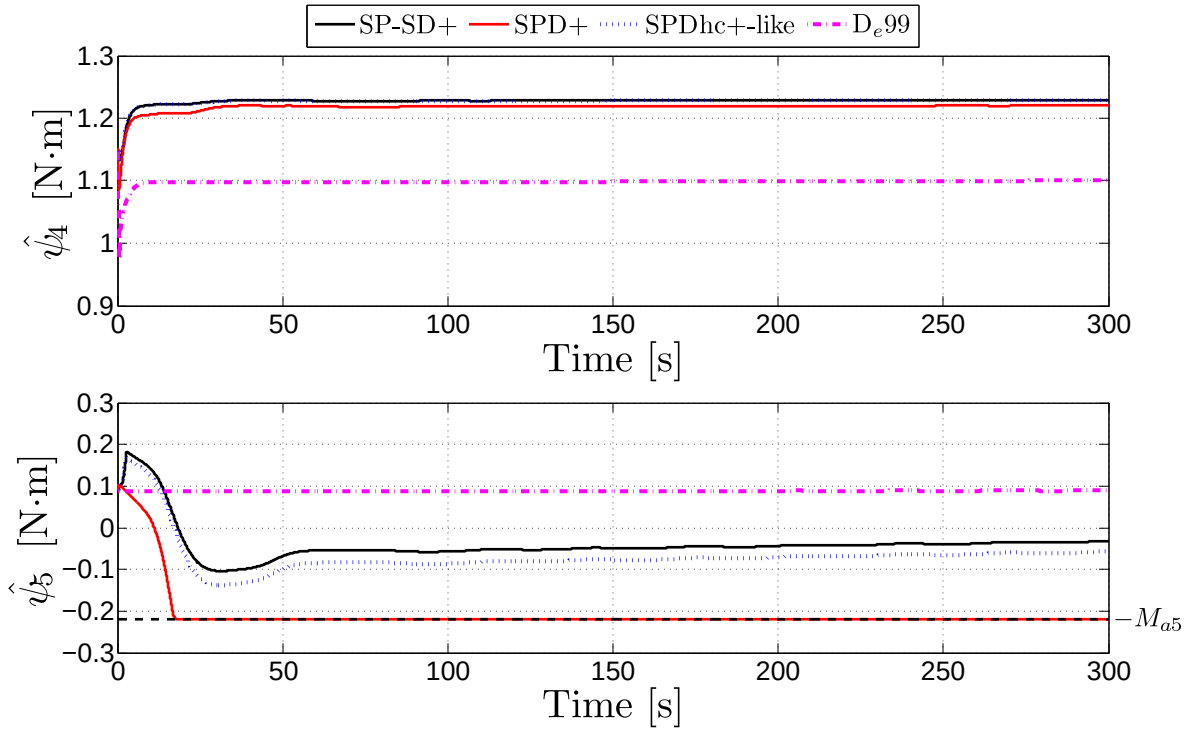

Figure 4.21: Test 2: parameter estimators

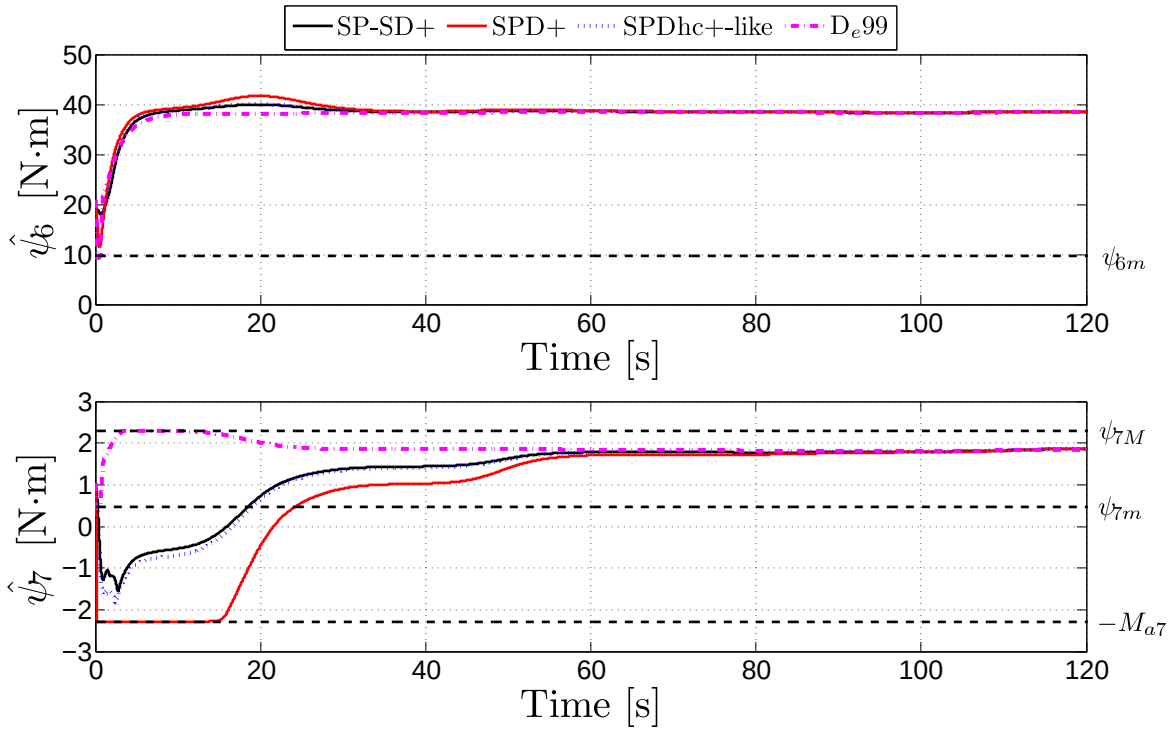

Figure 4.22: Test 2: parameter estimators

Observe that the SP-SD+, SPD+, and SPDhc+-like algorithms achieved the tracking objective —avoiding input saturation— considerably faster than in Test 1, and that the D$_e$99 controller failed to avoid input saturation. A suitable convergence of the parameter estimators could not be ensured in view of the high number of elements of ψ. This can be improved choosing desired trajectories satisfying persistency of excitation conditions.

5
Experimental results

Experimental implementations were carried out on two different manipulators: a 2-DOF device located at the IT de la Laguna and on a 3-DOF manipulator located at the BUAP. Experiments done in the 2-DOF robot were performed by Dr. Víctor Santibáñez while those obtained in the 3-DOF manipulator were carried out by the author of the dissertation with the support of Dr. Fernando Reyes.

State-feedback adaptive scheme experiment description

For all carried out experiments, the proposed adaptive schemes in Eqs. (3.24)-(3.25) was tested in its SP-SD, SPD, and SPDgc-like forms, under the respective consideration of expressions (3.34)-(3.35), (3.36)-(3.37), and (3.38)-(3.39). The involved saturation functions were defined as

$$\sigma_{Pi}(\varsigma) = M_{Pi}\,\mathrm{sat}(\varsigma/M_{P_i}) \quad \text{and} \quad \sigma_{Di}(\varsigma) = M_{Di}\,\mathrm{sat}(\varsigma/M_{D_i})$$

$i = 1, \ldots, n$ (in accordance to the number of links), in the SP-SD case;

$$\sigma_{Pi}(\varsigma) = \begin{cases} \varsigma & \forall |\varsigma| \leq L_{Pi} \\ \mathrm{sign}(\varsigma) L_{Pi} + (M_{Pi} - L_{Pi}) \tanh\left(\frac{\varsigma - \mathrm{sign}(\varsigma) L_{Pi}}{M_{Pi} - L_{Pi}}\right) & \forall |\varsigma| > L_{Pi} \end{cases}$$

with $0 < L_{Pi} < M_{Pi}$, $i = 1, \ldots, n$, in the SPD case;

$$\sigma_{Pi}(\varsigma) = M_{Pi}\,\mathrm{sat}(\varsigma/M_{P_i}) \quad \text{and} \quad \sigma_{0i}(\varsigma) = M_{0i}\,\mathrm{sat}(\varsigma/M_{0_i})$$

$i = 1, \ldots, n$, in the SPDgc-like case; and

$$\sigma_{aj}(\varsigma) = \begin{cases} \varsigma & \forall |\varsigma| \leq L_{aj} \\ \mathrm{sign}(\varsigma) L_{aj} + (M_{aj} - L_{aj}) \tanh\left(\frac{\varsigma - \mathrm{sign}(\varsigma) L_{aj}}{M_{aj} - L_{aj}}\right) & \forall |\varsigma| > L_{aj} \end{cases}$$

with $0 < L_{aj} < M_{aj}$, $j = 1, \ldots, p$ (according to the number of the system parameters involved in the gravity vector), in all the three cases. Let us note that with these saturation functions we have $\sigma'_{PiM} = \sigma'_{DiM} = \sigma'_{0iM} = 1$, $\forall i = 1, \ldots, n$, and that in consequence, for the three controllers, inequality (3.5) is satisfied with $\kappa = \max_i\{k_{Di}\}$ (see Eqs. (3.22)).

For comparison purposes, additional experiments were implemented considering the adaptive controller proposed in [50] —referred to as Z_e00—, shown in Eqs. (1.6), *i.e.*

$$u = G(q)\hat{\theta} - K_P T_h(\Lambda_P \bar{q}) - K_D T_h(\Lambda_D \dot{q})$$

$$\dot{\hat{\theta}} = P\big(Q(\bar{q}, \dot{q}, \hat{\theta}), \hat{\theta}\big)$$

with

$$P_j(Q, \hat{\theta}) = \begin{cases} Q_j & \text{if } \theta_{jm} < \hat{\theta}_j < \theta_{jM} \text{ or } \big(\hat{\theta}_j \leq \theta_{jm} \text{ and } Q_j \geq 0\big) \text{ or } \big(\hat{\theta}_j \geq \theta_{jM} \text{ and } Q_j \leq 0\big) \\ 0 & \text{if } \big(\hat{\theta}_j \leq \theta_{jm} \text{ and } Q_j < 0\big) \text{ or } \big(\hat{\theta}_j \geq \theta_{jM} \text{ and } Q_j > 0\big) \end{cases}$$

$j = 1, \ldots, p$.

For the Z_e00 scheme the parameter bounds were fixed at $\theta_{1m} = 10$, $\theta_{1M} = 50$, $\theta_{2m} = 0.5$, and $\theta_{2M} = 3$ [Nm].

Output-feedback adaptive scheme experiment description

As for the developed adaptive output feedback scheme in Eqs (3.40), (3.42)-(3.43), the saturation functions involved at the implementations were defined as

$$\sigma_{Pi}(\varsigma) = M_{Pi}\,\mathrm{sat}(\varsigma/M_{P_i}) \tag{5.2a}$$

$$\sigma_{Di}(\varsigma) = M_{Di}\,\mathrm{sat}(\varsigma/M_{D_i}) \tag{5.2b}$$

$i = 1, \ldots, n$, and

$$\sigma_{aj}(\varsigma) = \begin{cases} \varsigma & \forall |\varsigma| \leq L_{aj} \\ \mathrm{sign}(\varsigma) L_{aj} + (M_{aj} - L_{aj}) \tanh\left(\frac{\varsigma - \mathrm{sign}(\varsigma) L_{aj}}{M_{aj} - L_{aj}}\right) & \forall |\varsigma| > L_{aj} \end{cases}$$

$j = 1, \ldots, n$, with $0 < L_{aj} < M_{aj}$.

Let us note that with these saturations we have $\sigma'_{PiM} = \sigma'_{DiM} = 1$, $\forall i = 1, \ldots, n$. The saturation parameter values fixed at every implementation of the SP-SD_c-g_a were corroborated to satisfy inequalities (3.23) and (3.41), taking $B_{gi}^{M_a} = \sum_{j=1}^{2} B_{G_{ij}} M_{aj}$, $i = 1, \ldots, n$.

For comparison purposes, additional experiments were run implementing the output-feedback adaptive algorithm proposed in [25] —referred to as the L00 controller— (choice made in terms of the analog nature of the compared algorithms: output-feedback adaptive schemes developed in a bounded input context; comparison of controllers of different nature looses coherence) shown in Eq. (1.7), and briefly recalled here:

$$u = -K_P T_h(\lambda \bar{q}) - K_D T_h(\delta \vartheta) + G_d \hat{\theta}$$

$$\dot{q}_c = -\alpha K(q_c + K\bar{q})$$
$$\vartheta = q_c + K\bar{q}$$

$$\dot{\phi}_c = \beta G_d^T \left[\eta T_h(\delta\vartheta) - \mu T_h(\lambda\bar{q})\right]$$
$$\hat{\theta} = \phi_c - \beta G_d^T \bar{q}$$

At every implementation of the L00 algorithm, the P and D control gains, *i.e.* k_P and k_D, were fixed small enough to avoid input saturation (note that they fix the bounds of the SP and SD actions).

Trajectory tracking adaptive scheme experiment description

The proposed adaptive scheme in Eqs. (3.79)-(3.80) was tested in its SP-SD+, SPD+, and SPDhc+-like forms, under the respective consideration of expressions (3.85)-(3.86), (3.87)-(3.88), and (3.89)-(3.90). The involved saturation functions were defined as

$$\sigma_{Pi}(\varsigma) = \begin{cases} \varsigma & \forall|\varsigma| \leq L_{Pi} \\ \text{sign}(\varsigma)L_{Pi} + (M_{Pi} - L_{Pi})\tanh\left(\frac{\varsigma - \text{sign}(\varsigma)L_{Pi}}{M_{Pi} - L_{Pi}}\right) & \forall|\varsigma| > L_{Pi} \end{cases}$$

with $0 < L_{Pi} < M_{Pi}$, $1, \ldots, n$, in all the three cases;

$$\sigma_{Di}(\varsigma) = M_{Di}\,\text{sat}(\varsigma/M_{D_i})$$

$i = 1, \ldots, n$, in the SP-SD+ case;

$$\sigma_{0i}(\varsigma) = M_{0i}\,\text{sat}(\varsigma/M_{0_i})$$

$i = 1, \ldots, n$, in the SPDhc+-like case; and

$$\sigma_{aj}(\varsigma) = \begin{cases} \varsigma & \forall|\varsigma| \leq L_{aj} \\ \text{sign}(\varsigma)L_{aj} + (M_{aj} - L_{aj})\tanh\left(\frac{\varsigma - \text{sign}(\varsigma)L_{aj}}{M_{aj} - L_{aj}}\right) & \forall|\varsigma| > L_{aj} \end{cases}$$

with $0 < L_{aj} < M_{aj}$, $j = 1, \ldots, \rho$, in all the three cases. Let us note that with these saturation functions we have $\sigma'_{PiM} = \sigma'_{DiM} = \sigma'_{0iM} = 1$, $\forall i = 1, \ldots, n$, and that in consequence, for the three controllers, inequality (3.60) is satisfied with $\kappa = \max_i\{k_{Di}\}$ (see Eqs. (3.77)).

For comparison purposes, additional simulations were implemented considering the adaptive controller proposed by [12] —referred to as D_e99— (choice made in terms of the analog nature of the compared algorithms: bounded adaptive), *i.e.*

$$u = Y_d(t)\hat{\psi} - K_P T_h(\Lambda_P\bar{q}) - K_D T_h(\Lambda_D r)$$
$$\dot{\hat{\psi}} = P\big(Q(t,r), \hat{\theta}\big)$$

where $Y_d(t) = Y\big(q_d(t), \dot{q}_d(t), \ddot{q}_d(t)\big)$; $T_h(x) = \big(\tanh(x_1), \ldots, \tanh(x_n)\big)^T$; $\Lambda_P = \text{diag}[\lambda_{P1}, \ldots, \lambda_{Pn}]$ and $\Lambda_D = \text{diag}[\lambda_{D1}, \ldots, \lambda_{Dn}]$ with $\lambda_{Pi} = 1$ $[\text{rad}]^{-1}$ and $\lambda_{Di} = 1$ s/rad, for all $i \in \{1, \ldots, n\}$;

$$r = \dot{\bar{q}} + \varepsilon T_h(\bar{q})$$

Figure 5.1: Experimental setup

with ε being a positive constant;

$$Q(t,r) = -\Gamma Y_d^T(t) r$$

K_P, $K_D \in \mathbb{R}^{n\times n}$ and $\Gamma \in \mathbb{R}^{\rho\times\rho}$ are positive definite diagonal matrices; the elements of P are defined as

$$P_j(Q,\hat{\psi}) = \begin{cases} Q_j & \text{if } \psi_{jm} < \hat{\psi}_j < \psi_{jM} \text{ or } \big(\hat{\psi}_j \le \psi_{jm} \text{ and } Q_j \ge 0\big) \text{ or } \big(\hat{\psi}_j \ge \psi_{jM} \text{ and } Q_j \le 0\big) \\ 0 & \text{if } \big(\hat{\psi}_j \le \psi_{jm} \text{ and } Q_j < 0\big) \text{ or } \big(\hat{\psi}_j \ge \psi_{jM} \text{ and } Q_j > 0\big) \end{cases}$$

$j = 1, \ldots, p$, with ψ_{jm} and ψ_{jM} being known lower and upper bounds of ψ_j respectively.

5.1 Experiments on a 2-DOF manipulator

In order to experimentally corroborate the efficiency of the proposed controllers, real-time control implementations were carried out on a 2-DOF direct-drive manipulator. The experimental setup, shown in Fig. 5.1, is a prototype of the 2-revolute-joint robot arm used in [35] and [36], located at the *Instituto Tecnológico de la Laguna*. The actuators are direct-drive brushless motors operated in torque mode, so they act as torque source and accept an analog voltage as a reference of torque signal. The control algorithm is executed at a 2.5 ms sampling period in a control board (based on a DSP 32-bit floating point microprocessor) mounted on a PC-host computer. The manipulator software is in open architecture, whose platform is based in C language to run the control algorithm in real time.

For the considered experimental manipulator, Properties 1.4–1.5 are satisfied with (details on the dynamic model and parameter values are given in [35, 36]):

$$G(q) = \begin{pmatrix} \sin q_1 & \sin(q_1+q_2) \\ 0 & \sin(q_1+q_2) \end{pmatrix}, \ \theta = \begin{pmatrix} 38.465 \\ 1.825 \end{pmatrix} \text{ [Nm]} \tag{5.4}$$

$\mu_m = 0.088\ \mathrm{kg\,m^2}$, $\mu_M = 2.533\ \mathrm{kg\,m^2}$, $k_C = 0.1455\ \mathrm{kg\,m^2}$, $B_{g1} = 40.29$ Nm, $B_{g2} = 1.825$ Nm, $f_m = 0.175\ \mathrm{kg\,m^2/s}$, $f_M = 2.288\ \mathrm{kg\,m^2/s}$, and

$$\Upsilon(q) = \big(\cos q_1^* - \cos q_1 \ \ , \ \ \cos(q_1^* + q_2^*) - \cos(q_1+q_2)\big)$$

with $q^* = (q_1^*, q_2^*)^T$ being the reference configuration referred to in Property 1.5; in particular, for the two degree of freedom experimental implementations reported in this work, $q_1^* = \pi/2$ and $q_2^* = 0$ were taken. The maximum allowed torques (input saturation bounds) are $T_1 = 150$ Nm and $T_2 = 15$ Nm for the first and second links respectively. From these data, one easily corroborates that Assumption 3.1 is fulfilled.

5.1.1 State feedback regulation

The experimental implementations were run fixing the following saturation parameter values (recall footnote 2 of Chapter 4): $M_{P1} = 58$, $M_{D1} = 38$, $M_{P2} = 7$, and $M_{D2} = 4$ in the SP-SD case; $M_{P1} = 50$, $M_{P2} = 7$, and $L_{Pi} = 0.9M_{Pi}$, $i = 1, 2$, in the SPD case; $M_{01} = 120$, $M_{P1} = 50$, $M_{02} = 12$, and $M_{P2} = 7$ in the SPDgc-like case; and $M_{a1} = 50$, $M_{a2} = 3$, and $L_{aj} = 0.9M_{aj}$, $j = 1, 2$, in all the three cases. These saturation function parameter values were corroborated to satisfy inequalities (3.23), (3.35), (3.37), and (3.39), taking $B_{gi}^{M_a} = \sum_{j=1}^{2} B_{G_{ij}} M_{aj}$, $i = 1, 2$, *i.e.* $B_{g1}^{M_a} = 53$ and $B_{g2}^{M_a} = 3$.

The results of two experimental tests (for every implemented controller) are presented. The initial and desired link positions at all the executed experiments were $q_1(0) = q_2(0) = \dot{q}_1(0) = \dot{q}_2(0) = 0$ and $q_{d1} = q_{d2} = \pi/4$ [rad], while the auxiliary state variable initial values were taken as $\phi_1(0) = \phi_2(0) = 0$ for the SP-SD, SPD, and SPDgc-like algorithms, and $\phi_1(0) = 20$, $\phi_2(0) = 2$ [Nm] for the Z_e00 controller. Let us notice that through the selected desired configurations, the condition stated by Corollary 3.1 is satisfied.

With the aim at getting fast position responses, in the first implementation —referred to as Test 1—, high control gains were taken for the SP-SD, SPD, and SPDgc-like algorithms, and a consequent considerably small value of ε satisfying inequality (3.10) was fixed. As for the Z_e00 scheme, a relatively small value of ε was also taken (although several times higher than for the other algorithms) and reasonable values of the rest of the tuning parameters were fixed disregarding the tuning procedure stated in [50, Theorem 2] in order to prevent considerably slower responses, with control gains small enough to avoid input saturation (recall that they fix the bounds of the SP and SD actions). Under the stated considerations, the tuning parameter combination giving rise to the best closed-loop performance —in terms mainly of stabilization time (as short as possible) and transient response (avoiding or lowering down overshoot and oscillations as much as possible)— was determined from numerous trial-and-error experiments for every implemented controller. The resulting values are presented in Table 5.1.

Figures 5.2–5.4 show the results of Test 1 for every implemented controller. Observe that the SP-SD, SPD, and SPDgc-like algorithms achieve the position regulation objective —avoiding input saturation— in less than 2 seconds. On the other hand, the parameter estimators present important steady-state errors. These parametric convergence errors are mainly due to the unmodeled phenomena such as the static friction. It is worth pointing out that the small value of ε importantly reduces the ability of the adaptation auxiliary dynamics to decrease the parameter estimation steady state error. However, it is important to note that this does neither prevent the position regulation objective to be succeeded (avoiding input saturation), nor to achieve it in a consider-

Table 5.1: Control parameter values for the state-feedback regulation scheme: Test 1

Parameter	SP-SD	SPD	SPDgc-like	Z_e00
k_{P1}	2900	3500	3700	70
k_{P2}	225	250	250	9
k_{D1}	40	80	40	6.5
k_{D2}	3	6	3	2.5
γ_1	2.5	2.5	9	500
γ_2	0.05	0.05	0.15	2
ε	0.000021	0.000014	0.000017	0.0005

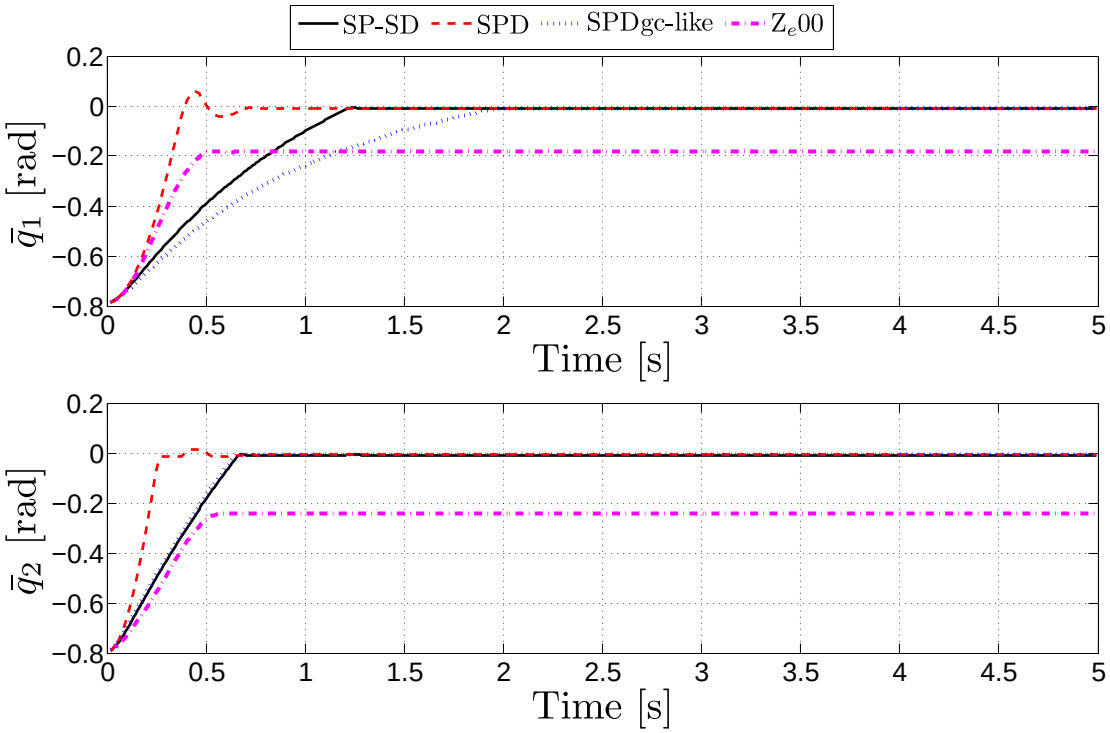

Figure 5.2: Test 1: position errors

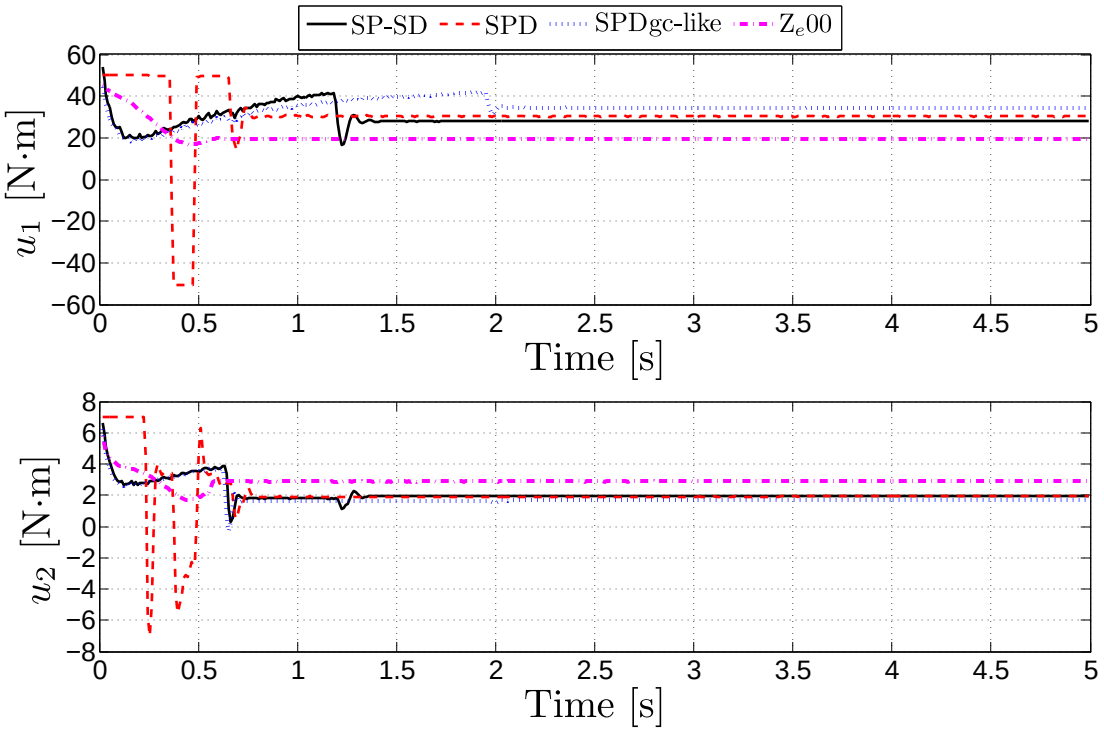

Figure 5.3: Test 1: control signals

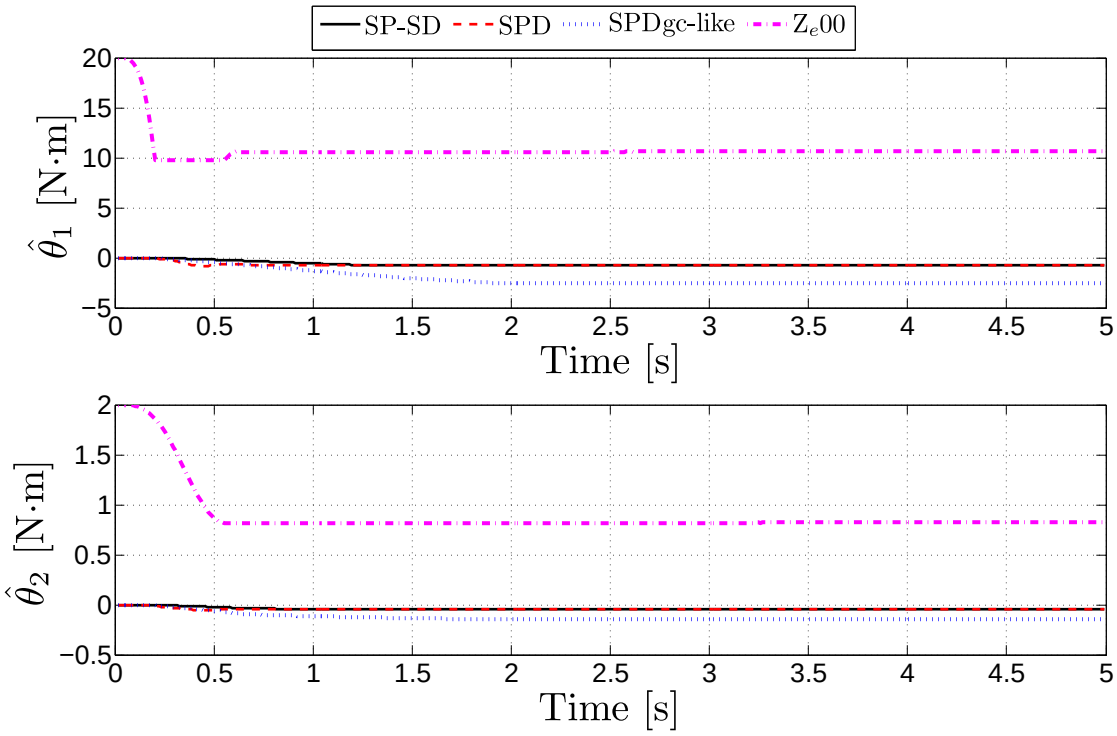

Figure 5.4: Test 1: parameter estimators

Table 5.2: Control parameter values for the state-feedback regulation scheme: Test 2

Parameter	SP-SD	SPD	SPDgc-like	Z_e00
k_{P1}	2100	1600	1850	75
k_{P2}	225	125	250	9
k_{D1}	40	80	40	6.5
k_{D2}	3	6	3	2.5
γ_1	0.5	0.5	9	375
γ_2	0.015	0.015	0.25	15
ε	3	2.5	0.31	0.1

ably short time. As for the additional implementation, notice that the Z_e00 controller generates lower bias in the parameter estimator steady-state values but the size of the errors is, however, observed to remain considerable and, more importantly, the position responses could not be stabilized at the desired value throughout the duration of the test.

In order to get an improved parameter estimation, in the second implementation —referred to as Test 2—, a higher value of ε was fixed for the SP-SD, SPD, and SPDgc-like algorithms (considerably higher than in the precedent tests) disregarding inequality (3.10) (recall that the condition stated by inequality (3.10) is only sufficient) keeping large control gains; in this context, for every one of the mentioned controllers, the tuning parameter combination giving rise to the best closed-loop performance was determined from numerous trial-and-error experiments. As for the Z_e00 scheme, an increased value of ε was also taken and adjustments in a control and the adaptation gains were done, keeping the rest of the control parameters with the same value taken in Test 1 but gains λ_{Pi}, $i = 1, 2$, (inside the hyperbolic tangent functions involved in the SP action) greater than unity were fixed; specifically: $\lambda_{P1} = 1.75$, $\lambda_{P1} = 3.5$ (rad^{-1}). The resulting values are presented in Table 5.2.

Figures 5.5–5.7 show the results of Test 2 for every implemented controller. Observe that, as in Test 1, the SP-SD, SPD, and SPDgc-like algorithms achieved the position regulation objective —avoiding input saturation— in less than 2 seconds. Moreover, an improved parameter estimation took place. In this direction, observe that, among the referred schemes, the algorithm with greatest parameter estimation bias is the one with the lowest value assigned to ε, corresponding to the SPDgc-like controller. As for the Z_e00 scheme, an improved parameter estimation, comparable to that obtained through the algorithms that took the highest value of ε *i.e.* the SP-SD and SPD controllers, is observed too. Nevertheless, position stabilization was not completely achieved throughout the duration of the test.

5.1.2 Output feedback regulation

The results of two experimental tests with $\alpha = 0$ are presented. The initial conditions and desired link positions at all the implementations were: $q_i(0) = \dot{q}_i(0) = q_{ci}(0) = \phi_{ci}(0) = 0$, $i = 1, 2$, and $q_{d1} = q_{d2} = \pi/4$ [rad]. Let us notice that, through these

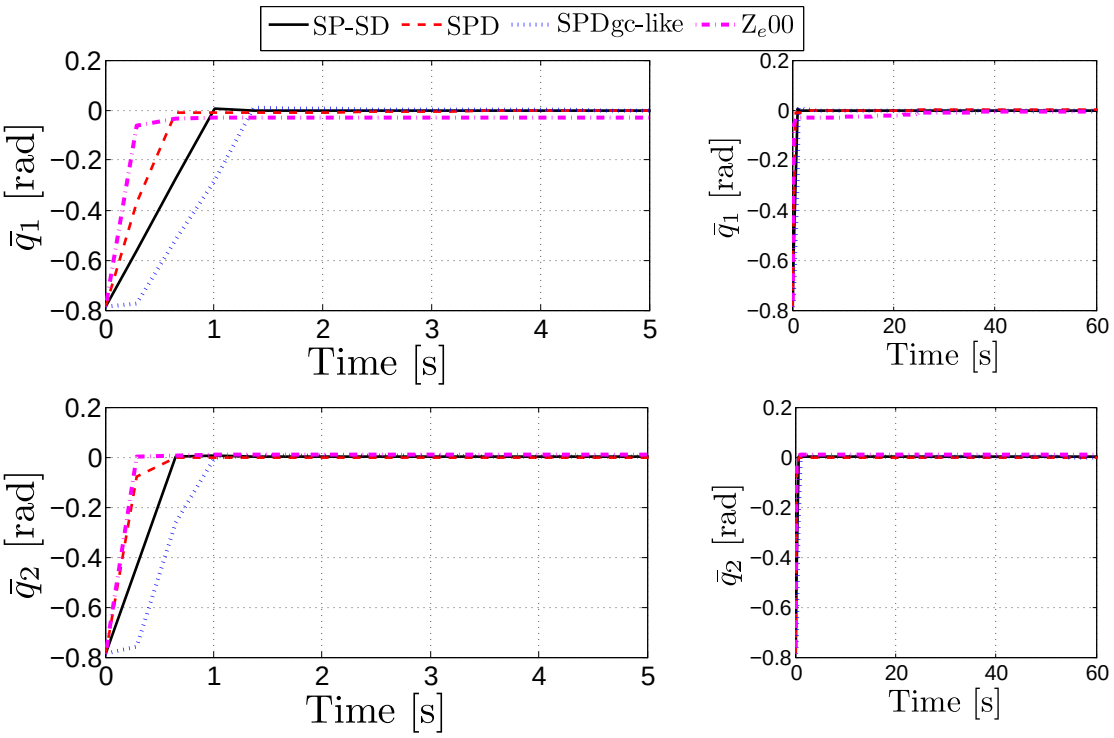

Figure 5.5: Test 2: position errors

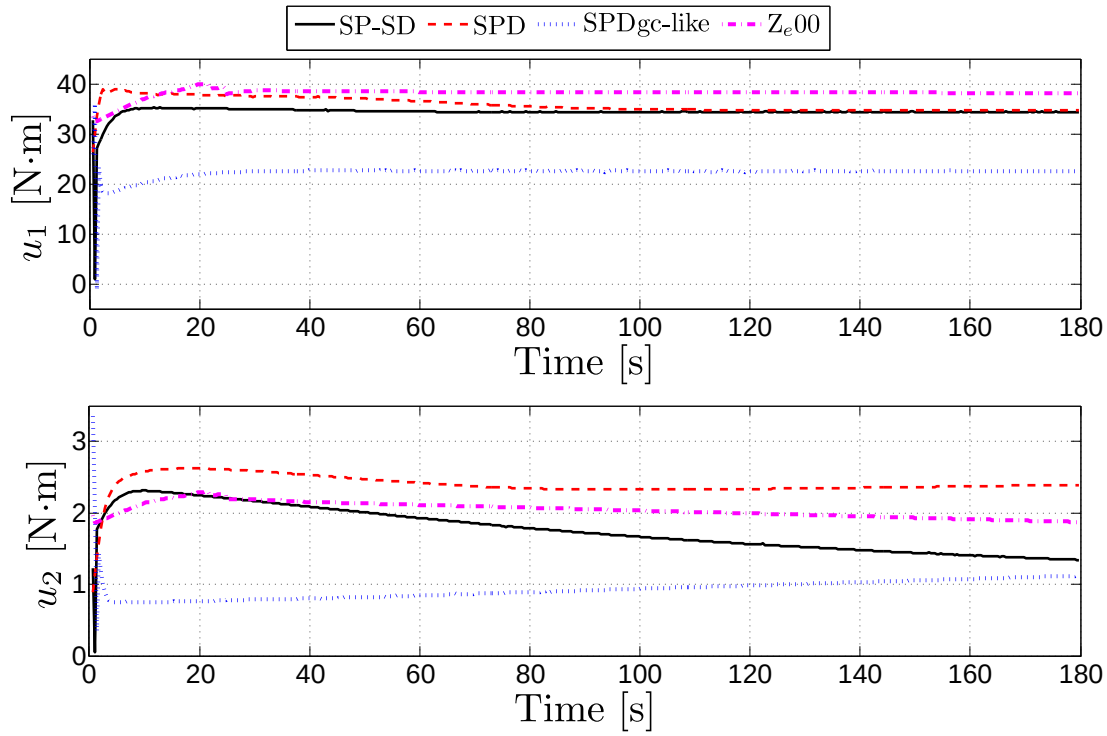

Figure 5.6: Test 2: control signals

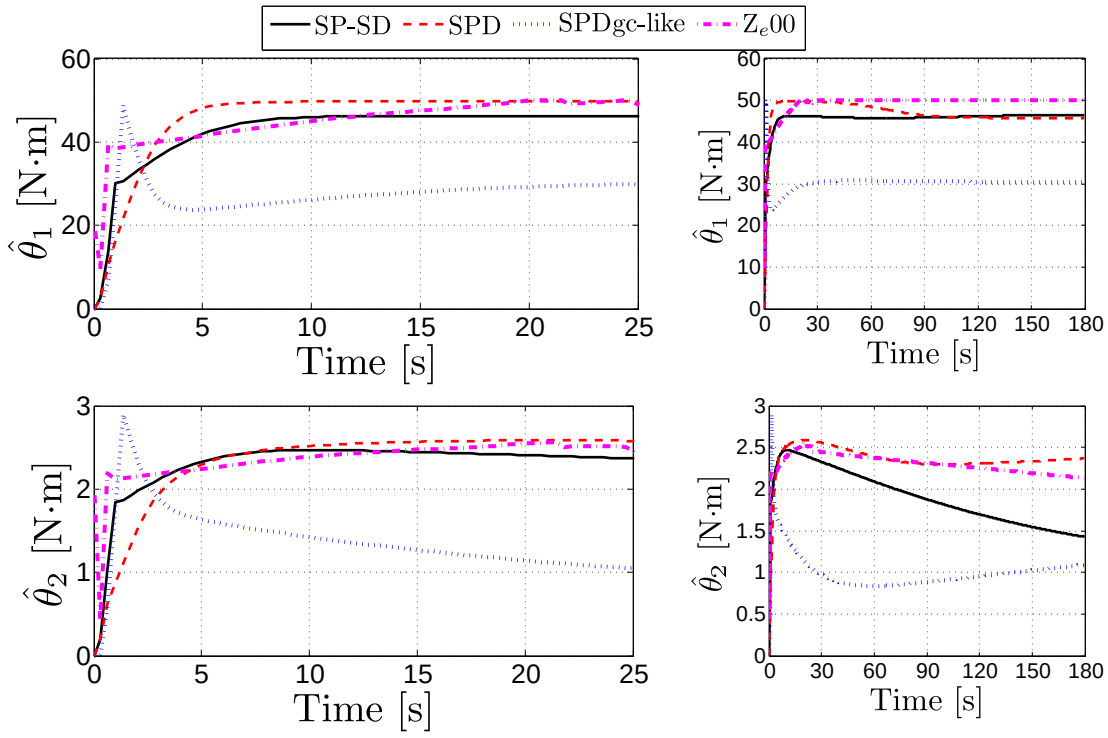

Figure 5.7: Test 2: parameter estimators

desired configurations, the condition stated by Corollary 3.2 is satisfied.

With the aim at getting fast position responses, in the first implementation —referred to as Test 1—, high control gains were taken for the SP-SD$_c$-g$_a$ scheme, and a consequent considerably small value of ε satisfying inequality (3.44) was fixed. As for the L00 algorithm, analogous small values of η and μ were considered, and reasonable values of the rest of the tuning parameters were fixed disregarding the tuning procedure stated in [25, Expressions (19)] in order to prevent extremely slow responses. Under the stated considerations, the tuning parameter combination giving rise to the best closed-loop performance —in terms mainly of stabilization time (as short as possible) and transient response (avoiding or lowering down overshoot and oscillations as much as possible)— was determined from numerous trial-and-error experiments for every implemented controller. For the SP-SD$_c$-g$_a$ scheme, the resulting values were: $K_P = \text{diag}[4000, 400]$ Nm/rad, $K_D = \text{diag}[50, 8]$ Nms/rad, $A = \text{diag}[80, 60]$ rad/s^2, $B = \text{diag}[20, 20]$ s^{-1}, $\Gamma = \text{diag}[40, 4]$ Nm, $\varepsilon = 1.36 \times 10^{-5}$ [Nms]$^{-1}$; and the saturation function bounds —all of them expressed in Nm— were: $M_{P1} = 29$, $M_{P2} = 3$, $M_{D1} = 50$, $M_{D1} = 6$, $M_{a1} = 50$, and $M_{a2} = 3$, with $L_{aj} = 0.9M_{aj}$, $j = 1, 2$. For the L00 controller, the resulting values were: $k_P = 9.2$ Nm, $k_D = 2.7$ Nm, $\lambda = 20$ [rad]$^{-1}$, $\delta = 10$ s/rad, $k = 20$ [s]$^{-1}$, $\alpha = 15$, $\beta = 25$ Nm/rad, $\eta = 0.015$ rad/s, and $\mu = 0.05$ rad/s.

Figures 5.8–5.10 show the results of Test 1 for both implemented controllers. Observe that the SP-SD$_c$-g$_a$ scheme achieved the regulation objective —avoiding input saturation— in less than 1 second. On the contrary, it took almost 80 seconds for the L00 algorithm to achieve the desired convergence and it also reached the input saturation limit. For the SP-SD$_c$-g$_a$ case, the parameter estimators present impor-

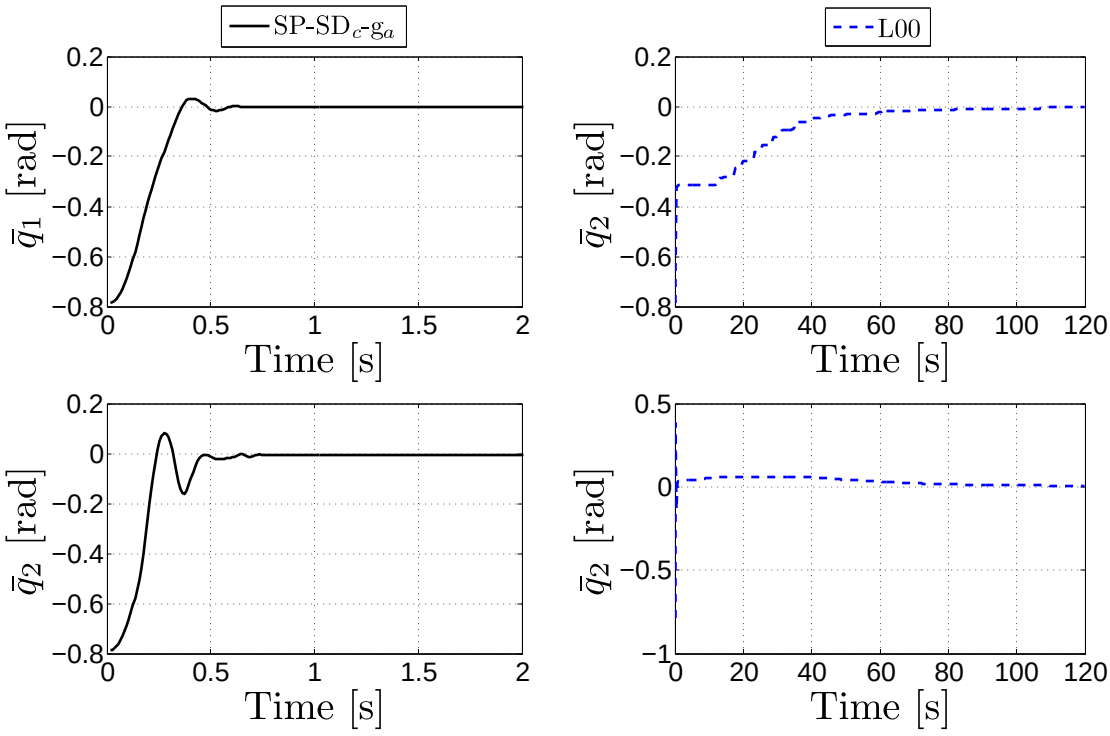

Figure 5.8: Test 1: position errors

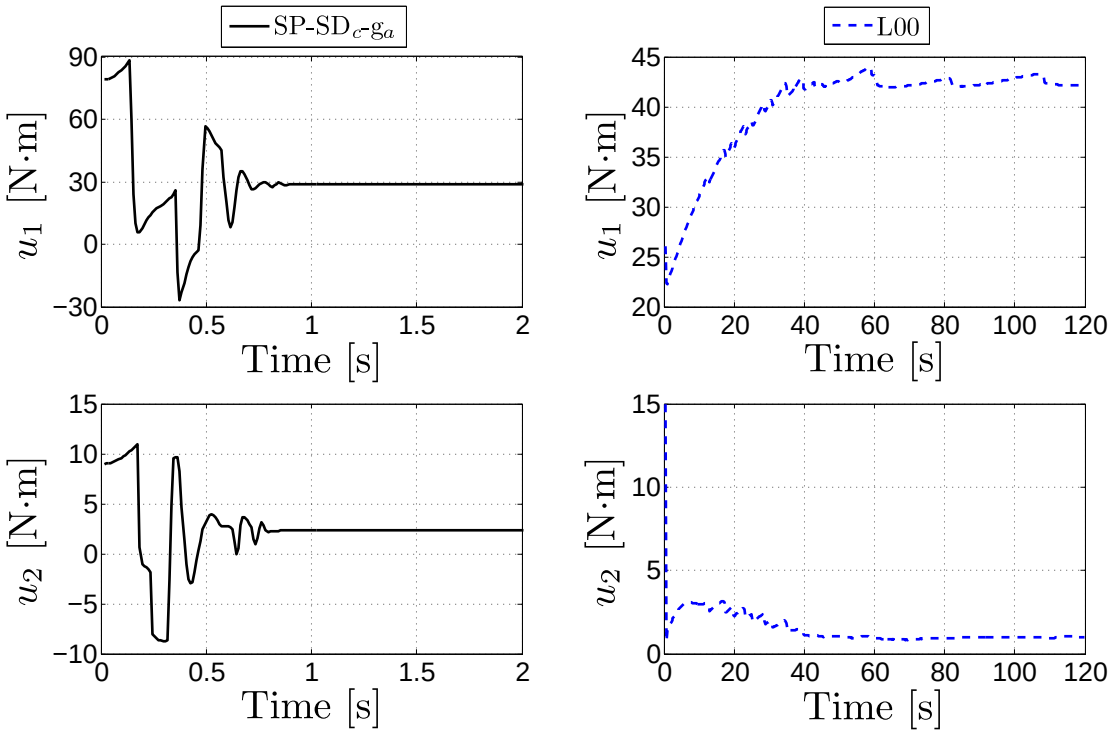

Figure 5.9: Test 1: control signals

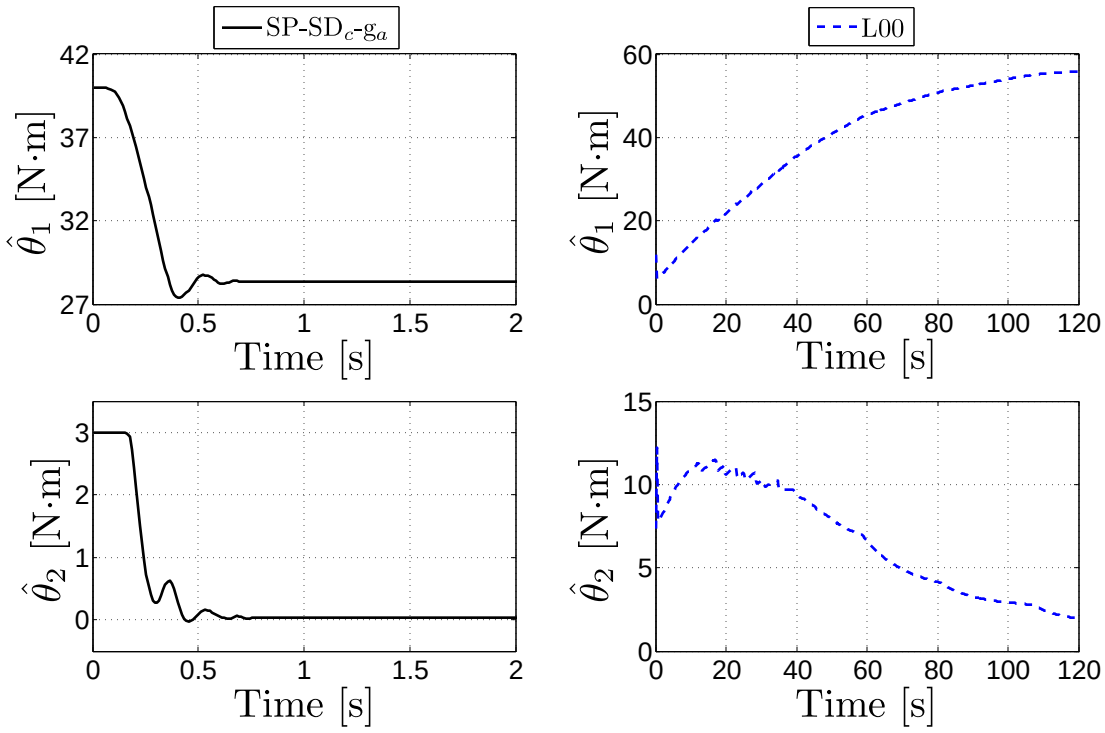

Figure 5.10: Test 1: parameter estimators

tant steady-state errors due to unmodeled phenomena and the adaptation dynamics decreased action —this is mainly because of the small value of ε and the fast time of response—. As for the L00 controller the parameter estimator were not observed to converge during the test. However, it is important to note that this does neither prevent the position regulation objective to be succeeded (avoiding input saturation), nor to achieve it in a considerably short time. By contrast, the L00 controller could not achieve a stabilization time shorter than 120 seconds, and the parameter estimation steady-state bias remained considerable. This is mainly due to the small control gains that the saturation avoidance inequality forces to take, particularly considering the common values that the algorithm proposed in [25] forces to use at every link (which prevents the possibility to take higher control gains at the links where $T_i - B_{gi}^{M_a}$ does not adopt its minimum value).

In the second implementation —referred to as Test 2—, large control gains and a high value of ε (considerably higher than in the precedent tests) disregarding inequality (3.44) (recall that the condition stated by inequality (3.44) is only sufficient) were fixed for the SP-SD$_c$-g$_a$ scheme. In this context, the tuning parameter combination giving rise to the best closed-loop performance was determined from numerous trial-and-error experiments. The resulting values were: $K_P = \text{diag}[2100, 225]$ Nm/rad, $K_D = \text{diag}[50, 8]$ Nms/rad, $A = \text{diag}[80, 60]$ rad/s^2, $B = \text{diag}[20, 20]$ s^{-1}, $\Gamma = \text{diag}[1, 0.1]$ Nm, $\varepsilon = 3$ [Nms]$^{-1}$; and the saturation function bounds —all of them expressed in Nm— were: $M_{P1} = 30$, $M_{P2} = 3$, $M_{D1} = 50$, $M_{D1} = 6$, $M_{a1} = 50$, and $M_{a2} = 3$, with $L_{aj} = 0.9M_{aj}$, $j = 1, 2$. As for the L00 scheme, considerably increased values of η and μ were also taken, and the rest of the tuning parameters were kept as in Test 1 except

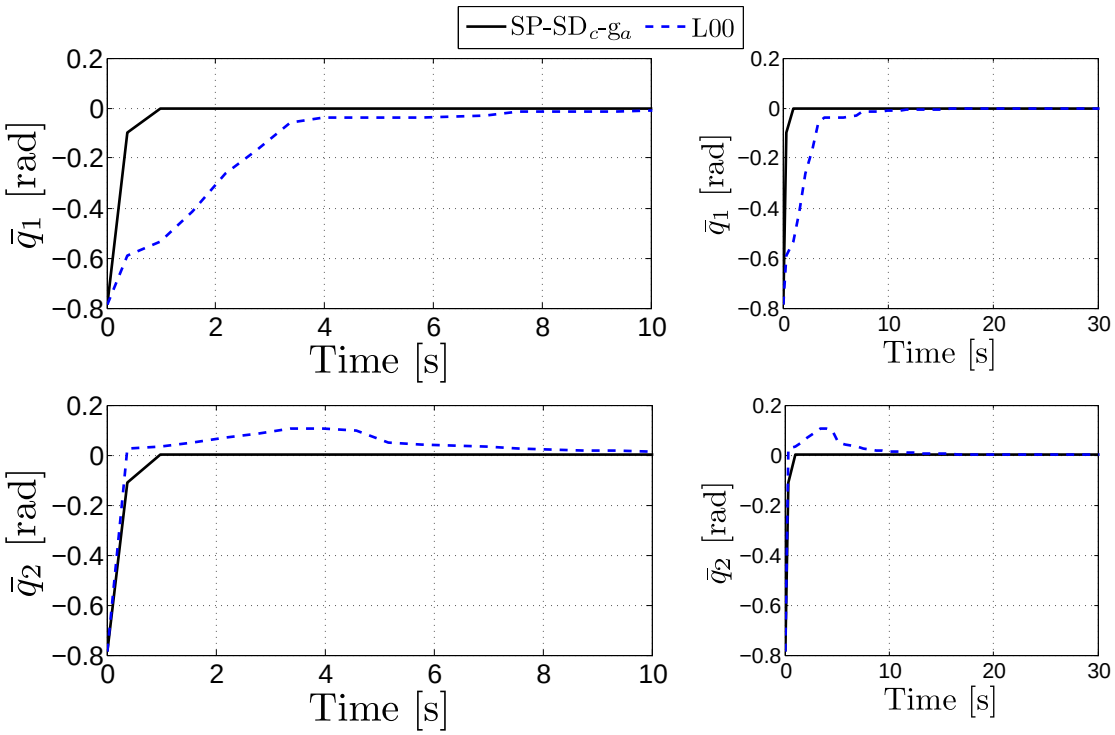

Figure 5.11: Test 2: position errors

for α and β which were adjusted adopting values that proved to be convenient during trial-and-error tests.

Figures 5.11–5.13 show the results of Test 2 for both implemented controllers. Observe that, similarly to Test 1, the SP-SD$_c$-g$_a$ scheme achieved the position regulation objective —avoiding input saturation— in around 1 second, and without the overshoot of the position error response in Test 1. Moreover, an improved parameter estimation took place; on the contrary, and similarly to that achieved in Test 1, longer position stabilization and parameter estimator convergence times are observed for the L00 controller.

5.1.3 State feedback trajectory tracking

At every experimental test, the initial link positions and velocities were taken as $q_i(0) = \dot{q}_i(0) = 0$, $i = 1, 2$. The auxiliary states were initiated at $\phi^T(0) = \begin{pmatrix} 2.88 & 0.103 & 0.125 & 2.803 & 0.214 & 47.119 & 2.235 \end{pmatrix}$ (see footnote 2) in the SP-SD+, SPD+, and SPDhc+-like cases and $\hat{\psi}^T(0) = \begin{pmatrix} 2.88 & 0.103 & 0.125 & 2.803 & 0.214 & 47.119 & 2.235 \end{pmatrix}$ in the case of the D$_e$99 algorithm. The desired trajectory for all the implemented controllers was defined as

$$q_d(t) = \begin{pmatrix} q_{d1}(t) \\ q_{d2}(t) \end{pmatrix} = \begin{pmatrix} \frac{\pi}{2} + \sin(\omega t) \\ \cos(\omega t) \end{pmatrix} \qquad \text{[rad]} \tag{5.5}$$

Let us note that with this desired trajectory, Assumption 2 is satisfied with $B_{dv} = \omega < 1.2027$ rad/s and $B_{da} = \omega^2$.

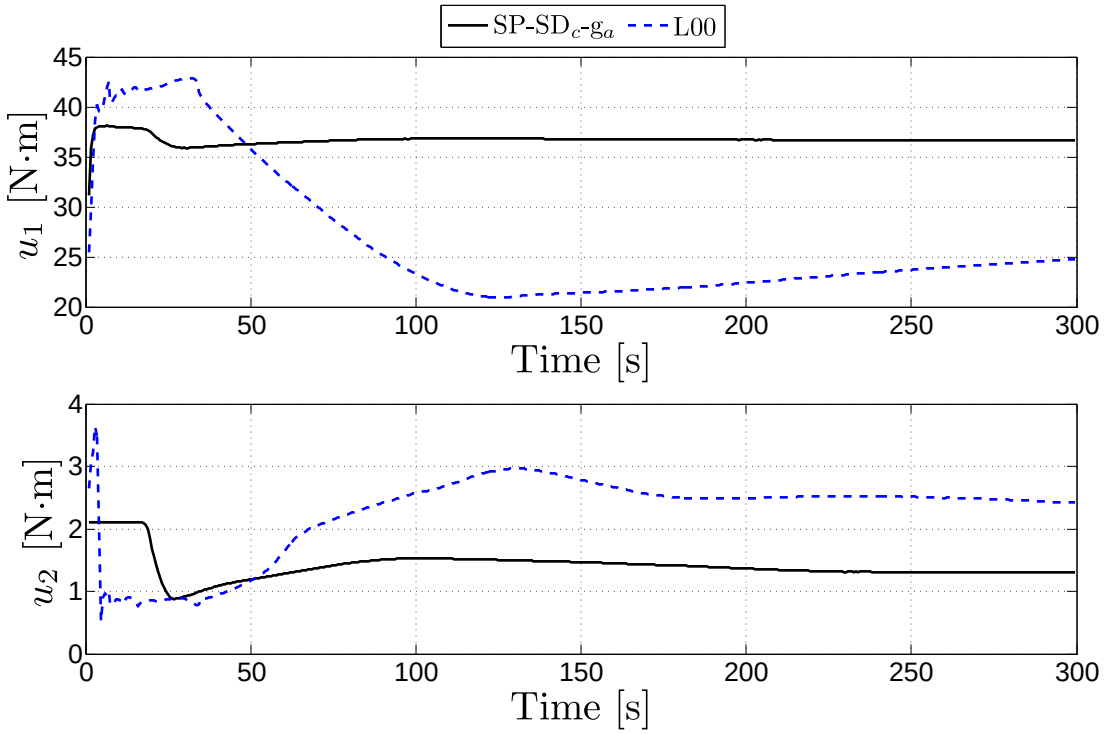

Figure 5.12: Test 2: control signals

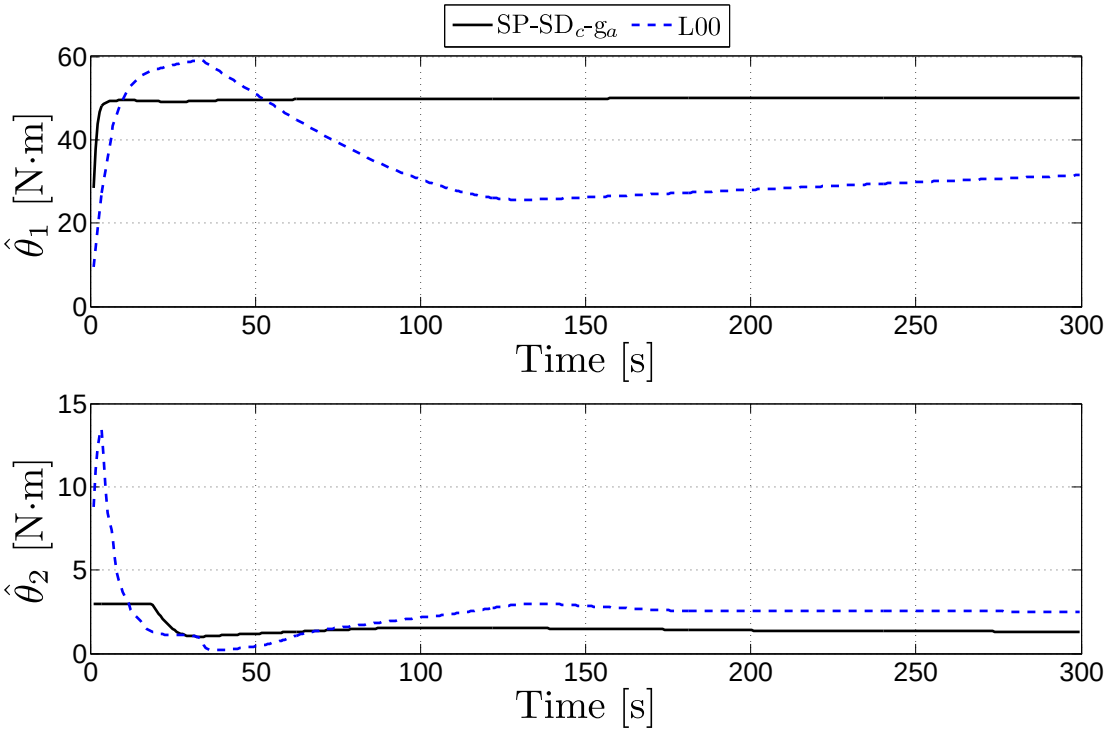

Figure 5.13: Test 2: parameter estimators

Table 5.3: Control parameter values for the state-feedback tracking scheme

Parameter	SP-SD+	SPD+	SPDhc+-like	D_e99
ε	1.0167×10^{-7}	1.0165×10^{-7}	4.15×10^{-8}	3
K_D	diag[20, 5]		diag[150, 20]	diag[10, 3.8]
K_P	diag[1500, 300]			diag[70, 7.9]
Γ	diag[20, 0.5, 0.1, 1.5, 0.1, 10, 0.25]			
Λ_P				diag[20, 10]
Λ_D				diag[3, 3]
RMS	0.0138	0.0106	0.0172	0.0314

For the adaptive SP-SD+, SPD+, and SPDhc+-like algorithms, a sufficiently small value of ε (satisfying inequality (3.65)) was taken and the saturation-function parameters as well as ω in (5.5) were fixed such that inequalities (3.72), (3.74), (3.76), and (3.78) were satisfied. Within the consequent limits, the saturation function bounds related to the SP and SD actions and the control and adaptation gains in K_P , K_D, and Γ were fixed after several trial-and-error simulation tests so as to have the best possible closed-loop performance —in terms mainly of stabilization time (as short as possible) and transient response (avoiding or lowering down overshoot and oscillations as much as possible)— and then refined experimentally. As for the D_e99 controller, a similar procedure was followed taking small enough control gains to avoid input saturation (recall that in this approach, the control gains in K_P and K_D respectively bound the P and D terms) but, with the aim to speed up the closed-loop responses, gains λ_{Pi} and λ_{Di}, $i = 1, 2$, (inside the hyperbolic tangent functions involved in the SP and SD actions) greater than unity were fixed. The resulting control parameter values for all the implemented schemes are presented in Table 5.3 As for the saturation function parameters involved in the SP-SD+, SPD+, and SPDhc+-like algorithms, the selected values were (refer to Chapter 4 footnote 2): $M_{P1} = 40$, $M_{D1} = 40$, $M_{P2} = 4$, and $M_{D2} = 4$ in the SP-SD+ case; $M_{P1} = 85$ and $M_{P2} = 8.5$ in the SPD+ case; $M_{01} = 130$, $M_{P1} = 45$, $M_{02} = 13$, and $M_{P2} = 4.5$ in the SPDhc+-like case; and $L_{Pi} = 0.9M_{Pi}$, $i = 1, 2$, $M_a^T = \begin{pmatrix}2.939 & 0.105 & 0.127 & 2.86 & 0.219 & 48.081 & 2.281\end{pmatrix}$, and $L_{aj} = 0.9M_{aj}$, $j = 1, \ldots, 7$, in all three cases. With these values, inequalities (3.72), (3.74), (3.76), (3.78), and Assumption 3.2 were corroborated to be satisfied with $B_{gi}^{M_a} = \sum_{j=1}^{7} B_{G_{ij}} M_{aj}$, $i = 1, 2$, *i.e.* $B_{g1}^{M_a} = M_{a6} + M_{a7} = 50.362$ Nm and $B_{g2}^{M_a} = M_{a7} = 2.281$ Nm, and $B_{Di}^{M_a} = \sum_{j=1}^{7} B_{Y_{ij}} M_{aj}$, $i = 1, 2$, *i.e.* $B_{D1}^{M_a} = \big(M_{a1} + \sqrt{10}M_{a1} + M_{a3}\big)\omega^2 + M_{a4}\omega + M_{a6} + M_{a7} = 58.6872$ Nm and $B_{D2}^{M_a} = \big(M_{a2} + \sqrt{2}M_{a3}\big)\omega^2 + M_{a5}\omega + M_{a7} = 2.9536$ Nm.

Figures 5.14–5.15 show the position error evolution and control signals obtained at every experimental test. Note that all the implemented controllers achieved the trajectory tracking objective —avoiding input saturation— in less that 2 seconds, with the SPD+ scheme being the one that gave rise to the fastest responses. This could be achieved preventing overshoot on the position error responses through the SPD+ and SPDhc+-like algorithms, while the SP-SD+ and D_e99 controllers could not avoid it. Let us further note that post-transient effects due to unmodelled phenomena, such as Coulomb friction, were present at all the closed-loop responses. They are observed

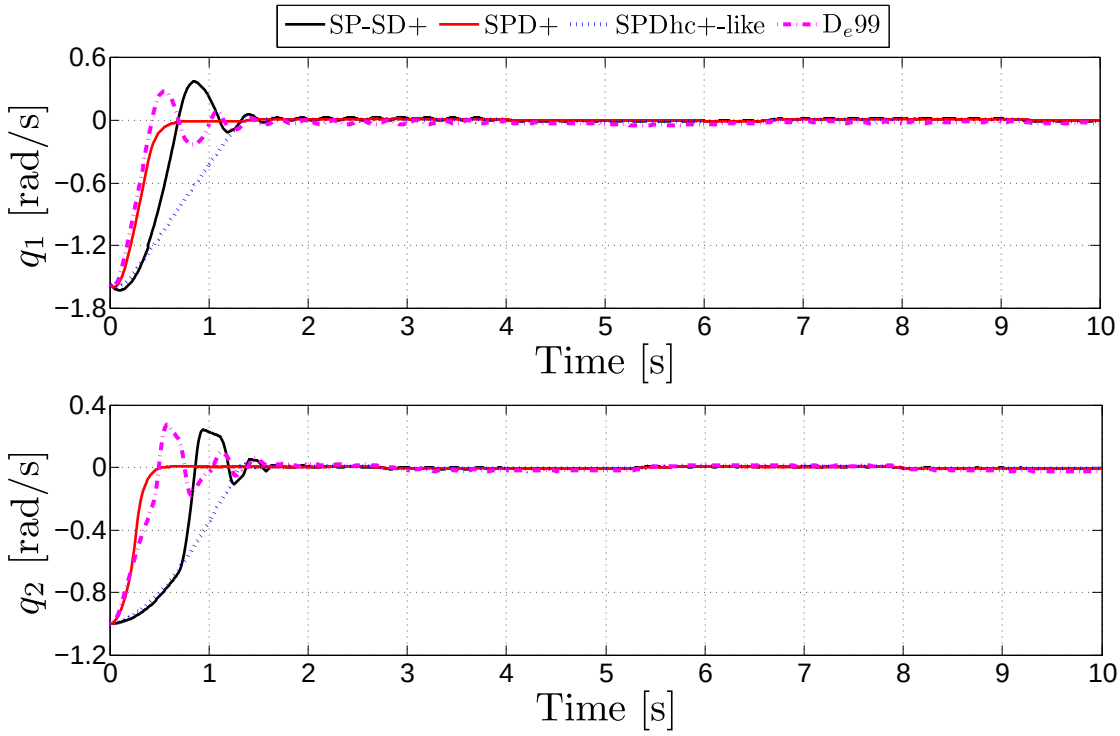

Figure 5.14: Test 2: position errors

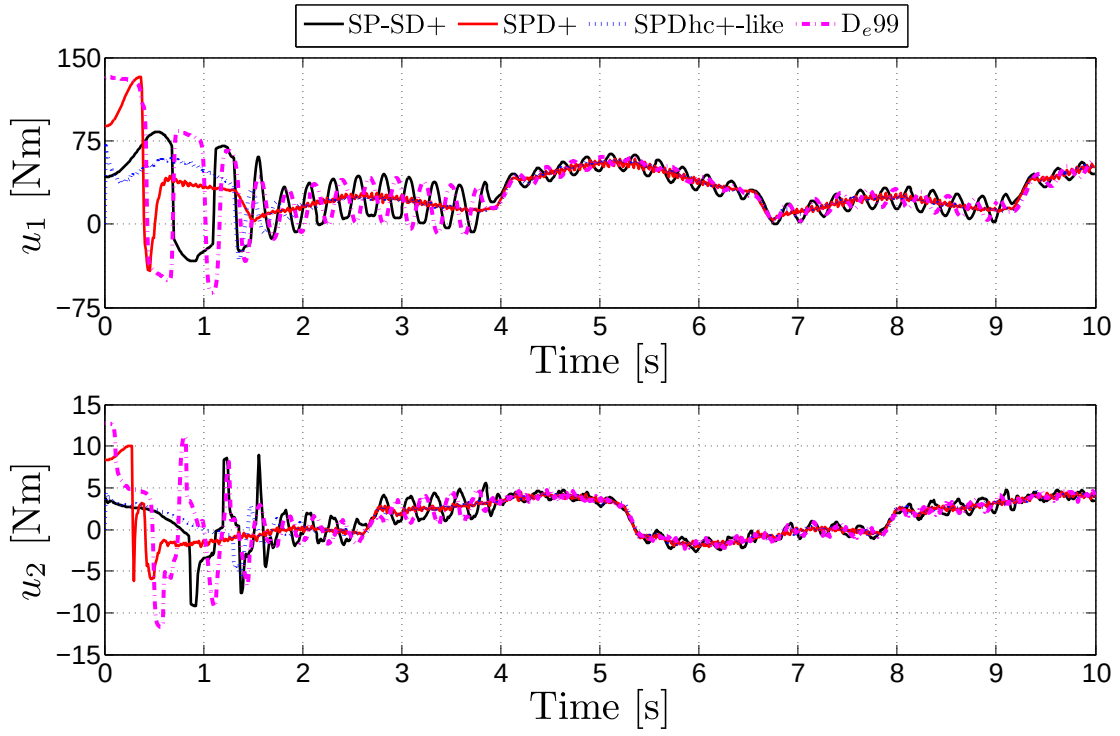

Figure 5.15: Test 2: control signals

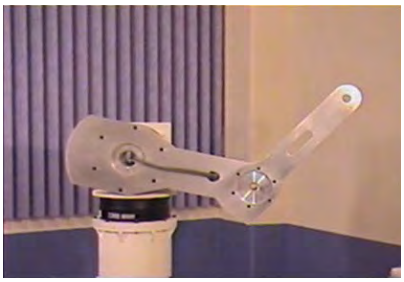

Figure 5.16: Experimental setup

in the position error graphs as small oscillations. In order to evaluate and compare the performance of the implemented controllers in relation to such a post-transient effect, the root mean square (RMS) of the position error, *i.e.* $\sqrt{\frac{1}{t_2-t_1}\int_{t_1}^{t_2}\|\bar{q}(t)\|^2 dt}$, was calculated from $t_1 = 2$ s to $t_2 = 10$ s. The values obtained from such a calculation are shown in Table I. Note that under such a criterion, the best performance was obtained through the SPDhc+-like algorithm, while the highest post-transient error was generated by the D_e99 controller. As for the parameter estimators, a considerably slow evolution was observed. This is due to the considerably small value of ε. Such a slow adaptation rate together with the high number of elements in θ and the unmodelled dynamics gave rise to parameter estimations with considerable bias. Improvements in this direction could be contemplated through different desired trajectories leading to the satisfaction of persistency of excitation conditions [30], which is out of the scope of this work. However, accuracy on the parameter estimation is not part of the motion control goal. Moreover, neither the slow evolution nor the biased convergence of the parameter estimators prevented the trajectory tracking objective to be accomplished —avoiding input saturation— or to be achieved in a considerably short time.

5.2 Experiments on a 3-DOF manipulator

The experimental setup used for the 3-DOF experiments, shown in Fig. 5.16, is a 3-revolute-joint anthropomorphic arm located at the *Benemerita Universidad Autonoma de Puebla*. The actuators are direct-drive brushless motors operated in torque mode, so they act as torque source and accept an analog voltage as a reference of torque signal. A more detailed technical description of this robot is given in [37].[1]

For the considered experimental manipulator, Properties 1.4 and 1.5 are satisfied with

$$G(q) = \begin{pmatrix} 0 & 0 \\ \sin q_2 & \sin(q_2+q_3) \\ 0 & \sin(q_2+q_3) \end{pmatrix} \ , \ \theta = \begin{pmatrix} 38.465 \\ 1.825 \end{pmatrix} \ \text{[Nm]} \tag{5.6}$$

$B_{g1} = 0$, $B_{g2} = 40.29$ Nm, and $B_{g3} = 1.825$ Nm, and

$$\Upsilon(q) = \begin{pmatrix} 1-\cos q_2 & 1-\cos(q_2+q_3) \end{pmatrix}$$

[1] A detailed procedure through which the generalized model of such a 3-DOF anthropomorphic manipulator is developed in Appendix A.

(with $q^* \in \mathcal{U}_0 \triangleq \{q \in \mathbb{R}^3 : q_2 = q_3 = 0\}$, *i.e.* such that $U(q^*, \theta) = 0$, $\forall q^* \in \mathcal{U}_0$; see Property 1.5). The maximum allowed torques (input saturation bounds) are $T_1 = 50$ Nm, $T_2 = 150$ Nm, and $T_3 = 15$ Nm for the first, second, and third links respectively. From these data, one easily corroborates that Assumption 3.1 is fulfilled.

5.2.1 State feedback regulation

For all performed experiments the desired configurations were chosen such that the condition stated by Corollaries 3.1 and 3.2 are satisfied. One can verify from $G(q)$ in (5.6) that, for the considered manipulator, the desired configurations are those $q_d \in \mathbb{R}^3$ such that $q_{d2} \neq m_1\pi$ and $q_{d2} + q_{d3} \neq m_2\pi$, for any $m_1, m_2 = 0, \pm 1, \pm 2, \ldots$.

The experimental implementation referred as Test 1 was run fixing the following saturation parameter values: $M_{P1} = M_{D1} = 20$, $M_{P2} = M_{D2} = 40$, and $M_{P3} = M_{D3} = 5$ in the SP-SD case; $M_{P1} = 40$, $M_{P2} = 80$, $M_{P3} = 10$, and $L_{Pi} = 0.9M_{Pi}$, $i = 1, 2, 3$, in the SPD case; $M_{01} = 40$, $M_{P1} = 35$ $M_{02} = 120$, $M_{P2} = 50$, $M_{03} = 12$, and $M_{P3} = 7$ in the SPDgc-like case; and $M_{a1} = 50$, $M_{a2} = 3$, and $L_{aj} = 0.9M_{aj}$, $j = 1, 2$, in all the three cases. For Test 2 saturation parameter values (in Nm) were set as: $M_{P1} = M_{D1} = 20$, $M_{P2} = M_{D2} = 35$, and $M_{P3} = M_{D3} = 4$ in the SP-SD case; $M_{P1} = 40$, $M_{P2} = 60$, $M_{P3} = 8$, and $L_{Pi} = 0.9M_{Pi}$, $i = 1, 2, 3$, in the SPD case; $M_{01} = 40$, $M_{P1} = 35$ $M_{02} = 130$, $M_{P2} = 40$, $M_{03} = 13$, and $M_{P3} = 6$ in the SPDgc-like case; and $M_{a1} = 70$, $M_{a2} = 5$, and $L_{aj} = 0.9M_{aj}$, $j = 1, 2, 3$, in all the three cases.

For comparison purposes, additional test were run considering the adaptive controller proposed by [50] —referred to as Z_e00—, described in Equations (1.6). The parameter bounds were fixed at $\theta_{1m} = 10$, $\theta_{1M} = 50$, $\theta_{2m} = 0.5$, and $\theta_{2M} = 3$ [Nm] for Test 1, and $\theta_{1m} = 10$, $\theta_{1M} = 70$, $\theta_{2m} = 0.5$, and $\theta_{2M} = 5$ [Nm] for Test 2.

The results of two experiments (for every implemented controller) are presented. The initial conditions and desired link positions in the first simulated case, Test 1, were taken as $q_1(0) = q_2(0) = q_3(0) = \dot{q}_1(0) = \dot{q}_2(0) = \dot{q}_3(0) = 0$; $\phi_1(0) = 20$, $\phi_2(0) = 1$ [Nm]; $q_{d1} = q_{d2} = \pi/4$ [rad], and $q_{d3} = \pi/2$ [rad]. For Test 2 initial conditions and desired link position were chosen as $q_1(0) = q_2(0) = q_3(0) = \dot{q}_1(0) = \dot{q}_2(0) = \dot{q}_3(0) = 0$; $\phi_1(0) = 20$, $\phi_2(0) = 1$ [Nm]; $q_{d1} = -\pi/3$ [rad], and $q_{d2} = q_{d3} = \pi/3$ [rad].

In the first implementation —referred to as Test 1—, a small value of ε satisfying (3.10) was fixed for the SP-SD, SPD, and SPDgc-like algorithms; the control parameters (k_{Pi}, k_{Di}, $i = 1, 2$) and adaptation gains (γ_i, $i = 1, 2$) were determined from those giving rise to the best closed-loop response from numerous trail-and-error tests using the SP-SD control law, and the same fixed values were kept for the SPD and the SPDgc-like algorithms. As for the Z_e00 controller, the selection of ε, control parameters, and adaptation gains was performed such that the greatest possible absolute value of the control signals at every link was ensured to be lower than the corresponding input saturation value (*i.e.* $\sum_{j=1}^{2} B_{G_{ij}}\theta_{jM} + k_{Pi} + k_{Di} < T_i$, $i = 1, 2$); under these considerations, the fixed parameters and gains were those giving rise to the best closed-loop performance after numerous trial-and-error tests.

With the aim at improving the closed-loop performance obtained through Test 1, in the second implementation —referred to as Test 2—, a higher value of ε was fixed for all the tested controllers (recall that the condition on ε, (3.10), is only sufficient, and

Table 5.4: Control parameter values for the state-feedback regulation scheme

	TEST 1		TEST 2	
Parameter	SP-SD SPD SPDgc-like	Z_e00	SP-SD SPD SPDgc-like	Z_e00
k_{P1}	200	800	500	800
k_{P2}	250	1800	350	1400
k_{P3}	120	180	180	150
k_{D1}	15	30	10	30
k_{D2}	15	100	30	140
k_{D3}	3	8	3	5
γ_1	150	150	5	20
γ_2	50	35	0.5	0.35
ε	0.0001	0.0001	1.5	1.5

that such a parameter is not involved in the condition stated to avoid input saturation, (3.7)). For the SP-SD, SPD, and SPDgc-like algorithms, the control parameters and adaptation gains were tuned as in the previously described case. As for the Z_e00 controller, the referred values were fixed such that the best closed-loop performance was obtained from numerous trial-and-error tests. Saturation avoidance was disregarded since control parameter tuning under such a consideration gave rise to extremely poor closed-loop performances. The resulting values for all the implemented controller at both tests are presented in Table 5.4.

Figures 5.17–5.19 show the position errors, control signals, and parameter estimators, for all the considered controllers at Test 1. Observe that in all the cases, the control objective is achieved avoiding input saturation. Note that, even when a small value of ε was used position error convergence is still achieved, however, this causes the performance of the parameter estimators to become slower which in addition to unmodeled phenomena results in biased estimations.

Figures 5.20–5.22 show the results obtained through Test 2 for all the considered controllers. In every tested algorithm, the control objective is observed to be achieved avoiding input saturation, with a stabilization time considerably lower than in the previous test. Nevertheless, the SP-SD, SPD, and SPDgc-like algorithms are still observed to achieve the desired convergence much faster than the Z_e00 controller.

Let us further note from Figures 5.19 and 5.22 that the parameter estimators converge to the real values θ_i, $i = 1, 2$. This is so in view of the selected desired configuration which gives rise to the satisfaction of the condition stated by Corollary 3.1.

5.2.2 Output feedback regulation

The results of two experimental tests $\alpha = -1$ are presented. The initial conditions at all the implementations were $q_i(0) = \dot{q}_i(0) = \vartheta_i(0) = 0$, $i = 1, 2, 3$, and $\phi_{c1}(0) = 20$, $\phi_{c2}(0) = 1$ [Nm]; the desired link positions were taken as $q_{d1} = q_{d2} = \pi/4$, $q_{d3} = \pi/2$ [rad] in the first experiment, and $q_{d1} = -\pi/3$, $q_{d2} = q_{d3} = \pi/3$ [rad] in the second

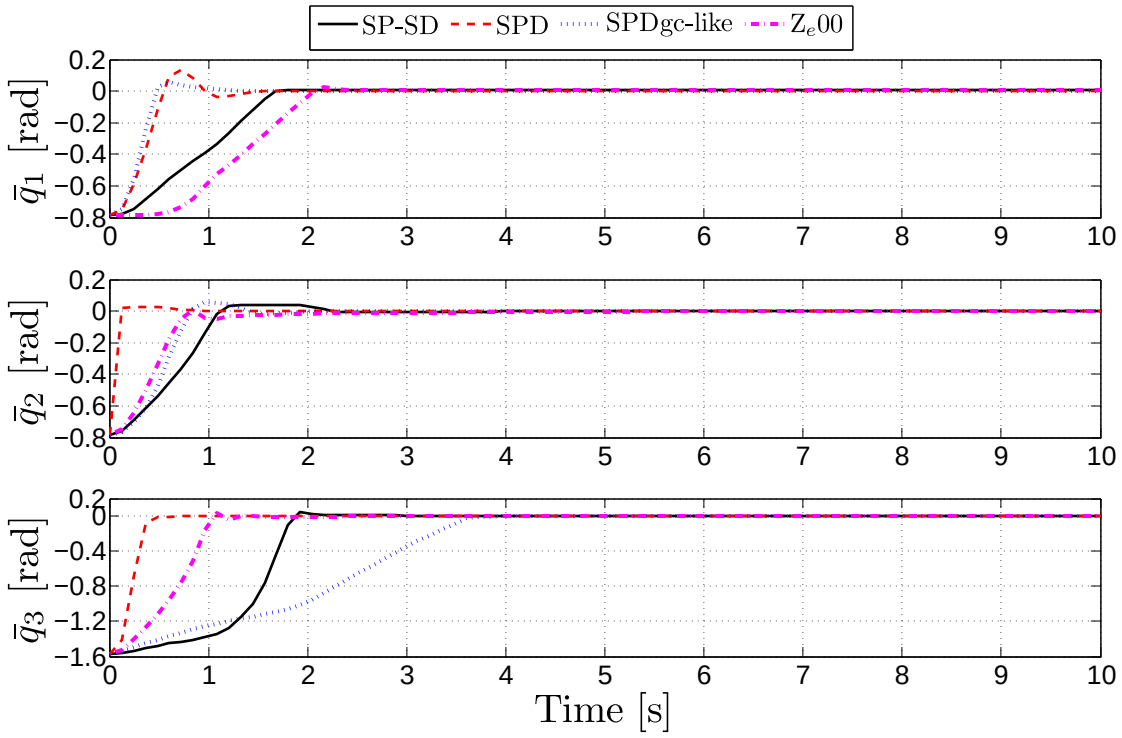

Figure 5.17: Test 1: position errors

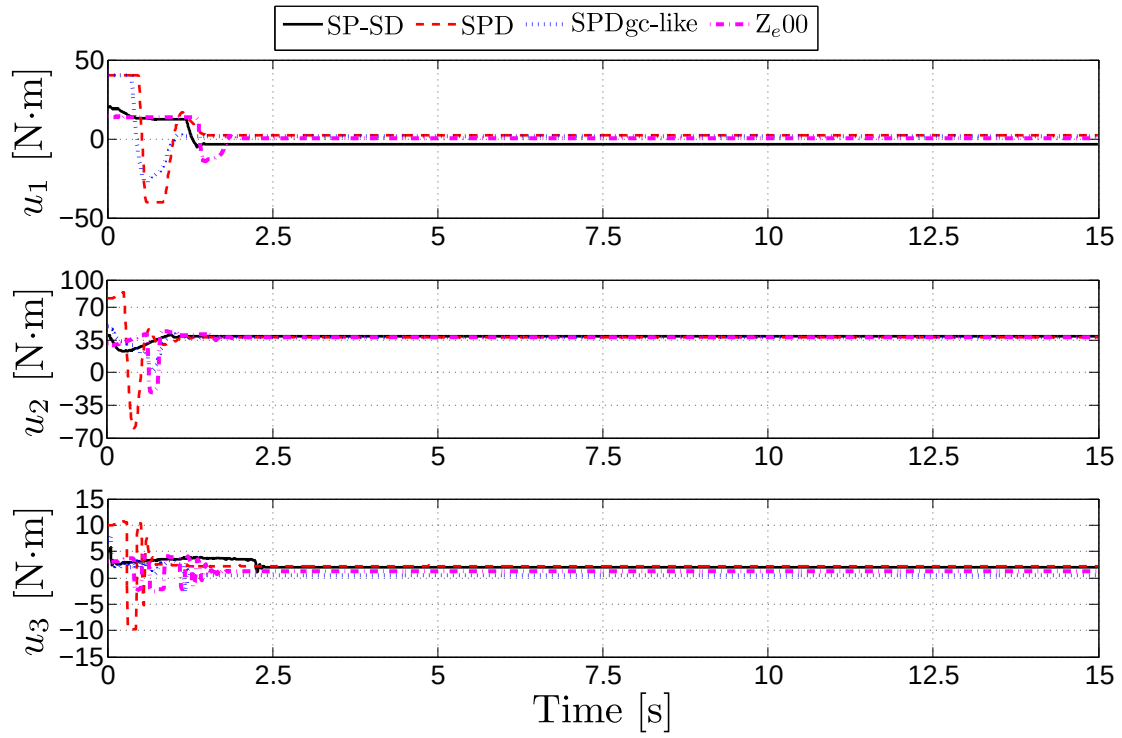

Figure 5.18: Test 1: control signals

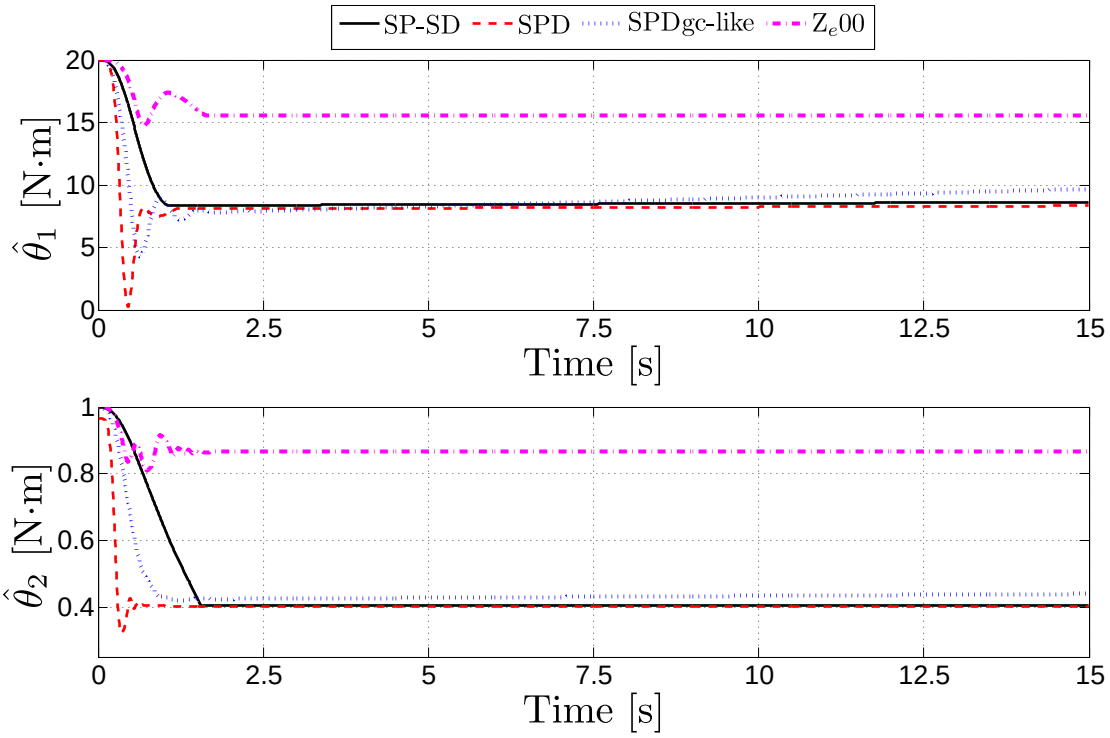

Figure 5.19: Test 1: parameter estimators

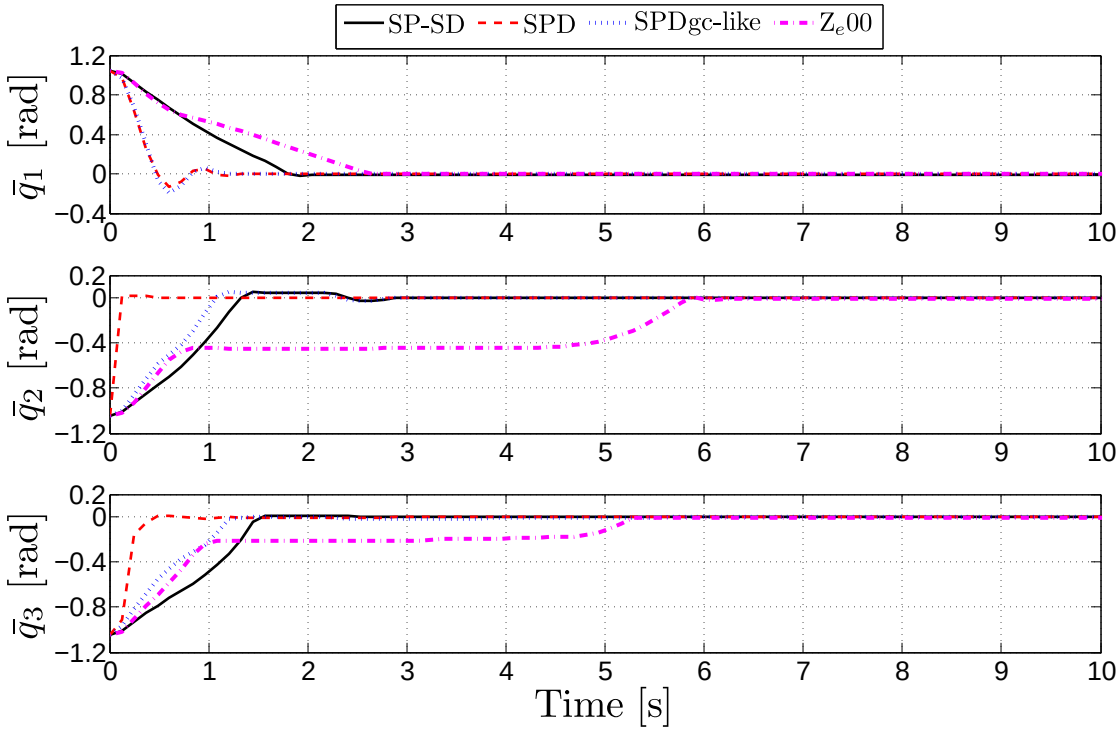

Figure 5.20: Test 2: position errors

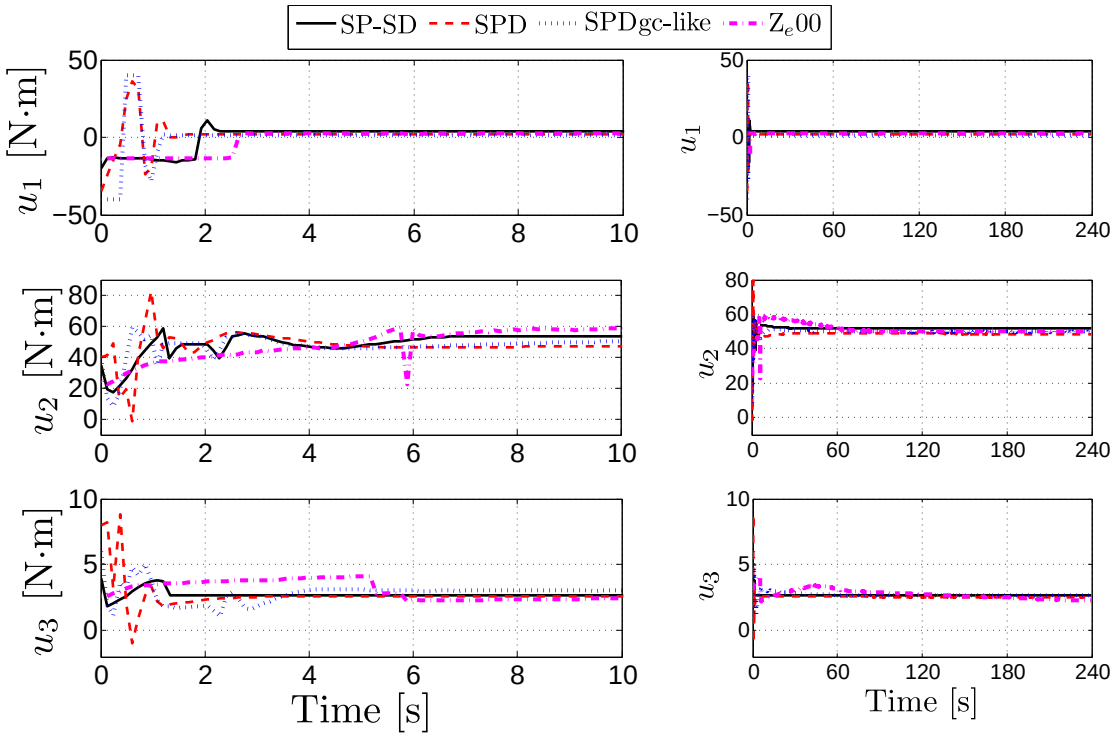

Figure 5.21: Test 2: control signals

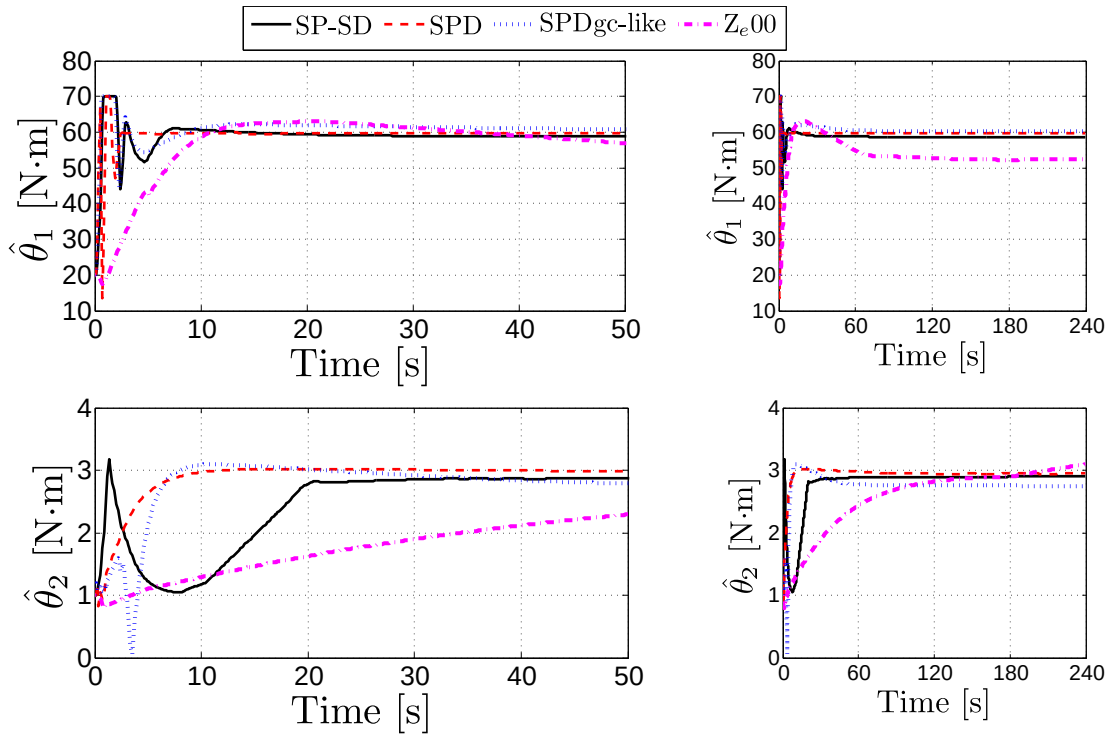

Figure 5.22: Test 2: parameter estimators

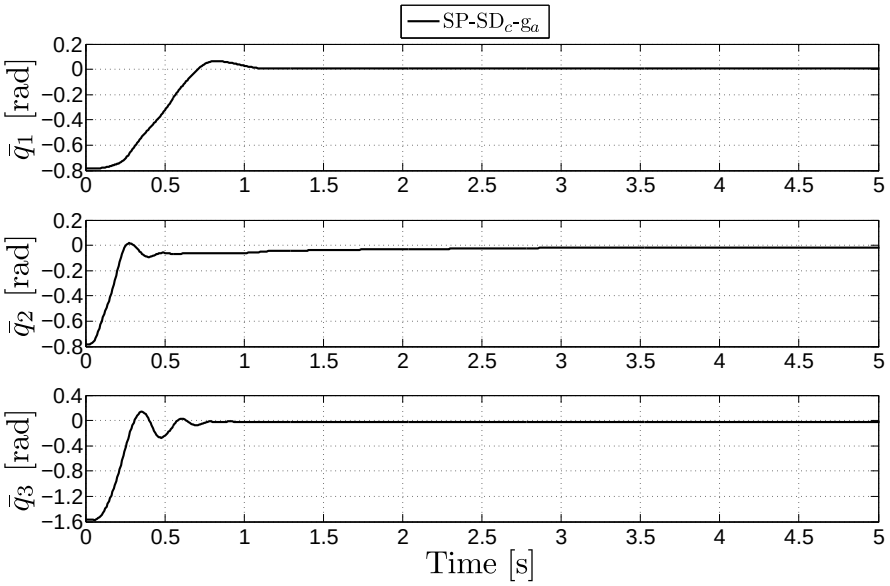

Figure 5.23: Test 1: position errors

one. Let us notice that, through these desired configurations, the condition stated by Corollary 3.2 is satisfied. [2]

In the first implementation —referred to as Test 1— a considerably small value of ε was fixed for the SP-SD$_c$-g$_a$ controller. With such a tiny value of ε, actually fixed at $\varepsilon = 0.0035$ $[\text{Nms}]^{-1}$, the tuning parameter combination giving rise to the best closed-loop performance —in terms mainly of stabilization time (as short as possible) and transient response (avoiding or lowering down overshoot and oscillations as much as possible)— was determined from numerous trial-and-error experiments. The resulting gains were: $K_P = \text{diag}[250, 350, 60]$ Nm/rad, $K_D = \text{diag}[25, 70, 15]$ Nms/rad, $A = \text{diag}[15, 50, 25]$ rad/s^2, $B = \text{diag}[5, 10, 25]$ s^{-1}, and $\Gamma = \text{diag}[150, 35]$ Nm; and the saturation function bounds were: $M_{P1} = M_{D1} = 20$, $M_{P2} = M_{D2} = 40$, $M_{P3} = M_{D3} = 5$, $M_{a1} = 50$, and $M_{a2} = 3$, with $L_{aj} = 0.9M_{aj}$, $j = 1, 2$; these saturation function parameter values were corroborated to satisfy inequalities (3.23) and (3.41), taking $B_{gi}^{M_a} = \sum_{j=1}^{2} B_{G_{ij}} M_{aj}$, $i = 1, 2, 3$, *i.e.* $B_{g1}^{M_a} = 0$, $B_{g1}^{M_a} = 53$, and $B_{g2}^{M_a} = 3$. As for the L00 controller, analogous small values of η and μ were considered. More importantly, in this test, control gains satisfying the saturation avoidance inequality, *i.e.* $k_P + k_D \leq \min_{i\in\{1,2,3\}} \left\{T_i - B_{gi}^{M_a}\right\}$ (as analogously or equivalently expressed in [25]), were taken. Unfortunately, this condition was so restrictive, that the closed-loop system could not even react. For this reason, corresponding results are not reported.

Figures 5.23–5.25 show the results of Test 1 for the SP-SD$_c$-g$_a$ controller. Observe that the regulation objective was achieved —avoiding input saturation— in less than 4 seconds. The parameter estimators took a considerably longer convergence time, though. Furthermore, a (small) steady-state error can be appreciated at such param-

[2] One can verify from $G(q)$ in (5.6) that, for the considered manipulator, the desired configurations that satisfy the condition stated by Corollary 3.2 are those $q_d \in \mathbb{R}^3$ such that $q_{d2} \neq m_1\pi$ and $q_{d2} + q_{d3} \neq m_2\pi$, for any $m_1, m_2 = 0, \pm 1, \pm 2, \ldots$

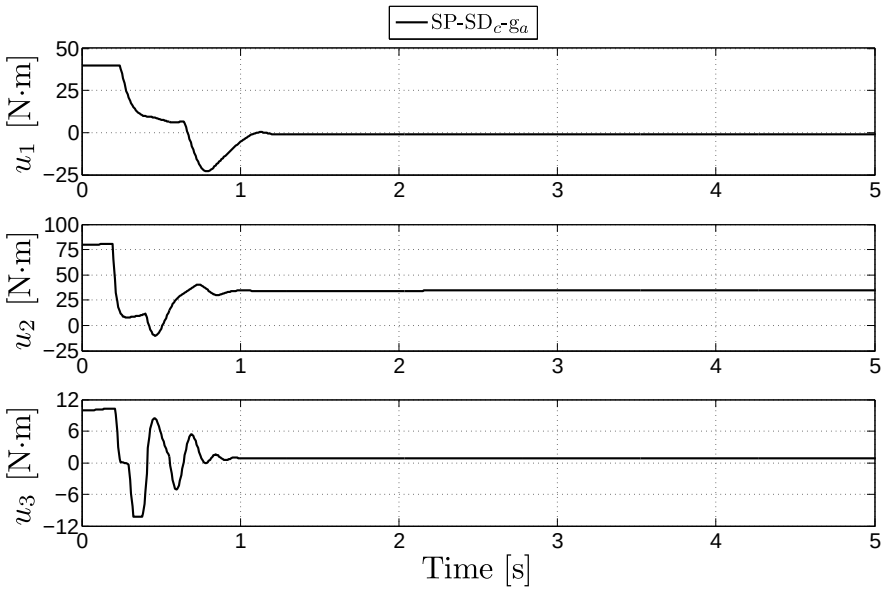

Figure 5.24: Test 1: control signals

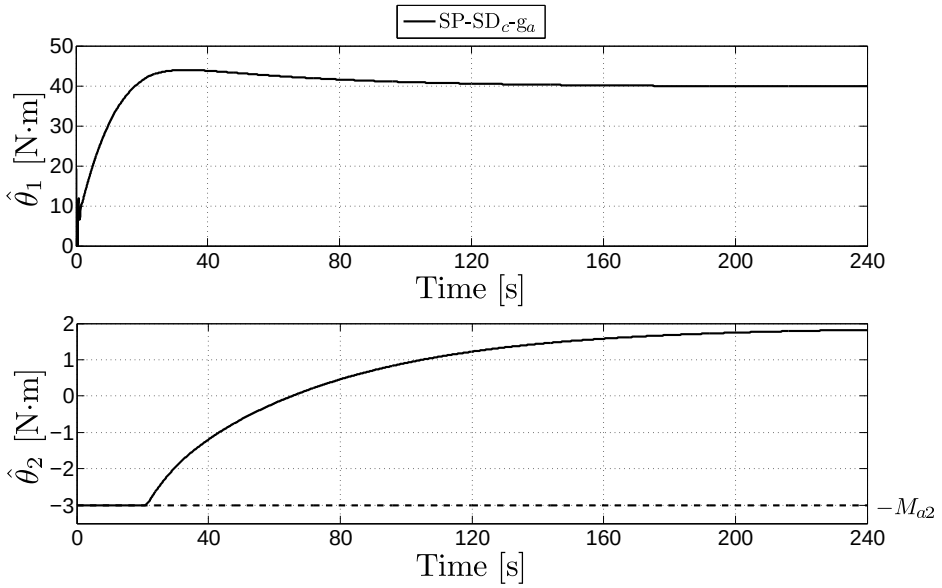

Figure 5.25: Test 1: parameter estimators

eter estimation variables. Such convergence errors are mainly due to the unmodeled phenomena such as the static friction.

With the aim at shortening the overall stabilization time (particularly considering the parameter estimator convergence time at this point), in the second implementation —referred to as Test 2—, a considerably higher value of ε was fixed for the SP-SD$_c$-g$_a$ controller (without any consideration on the possible satisfaction of inequality (3.44), as long as the closed-loop stability is not lost; recall that the condition stated by such inequality is only sufficient). With such a value of ε, actually fixed at $\varepsilon = 1.5$ [Nms]$^{-1}$, the tuning parameter combination giving rise to the best closed-loop performance was again determined from numerous trial-and-error experiments. The resulting gains were: $K_P = \text{diag}[350, 400, 75]$ Nm/rad, $K_D = \text{diag}[25, 50, 12]$ Nms/rad, $A = \text{diag}[15, 50, 35]$ rad/s^2, $B = \text{diag}[5, 10, 5]$ s^{-1}, and $\Gamma = \text{diag}[5, 0.5]$ Nm; and the saturation function bounds —expressed in Nm— were: $M_{P1} = M_{D1} = 20$, $M_{P2} = M_{D2} = 35$, $M_{P3} = M_{D3} = 4$, $M_{a1} = 70$, and $M_{a2} = 5$, with $L_{aj} = 0.9M_{aj}$, $j = 1, 2$; these saturation function parameter values were corroborated to satisfy inequalities (3.23) and (3.41), taking $B_{gi}^{M_a} = \sum_{j=1}^{2} B_{G_{ij}} M_{aj}$, $i = 1, 2, 3$, *i.e.* $B_{g1}^{M_a} = 0$, $B_{g1}^{M_a} = 75$, and $B_{g2}^{M_a} = 5$. As for the L00 controller, in order to avoid considerably slow responses, the tuning procedure presented in [25, Proposition 3] was not taken into account; not even the saturation avoidance inequality was regarded in view of the considerably poor closed-loop performance observed under its consideration. Moreover, in order to speed up the closed-loop responses, different P and D control gains were considered at every input control expression; in other words, K_P and K_D in (1.7) were taken in this test as $K_P = \text{diag}[k_{P1}, k_{P2}, k_{P3}]$ and $K_D = \text{diag}[k_{D1}, k_{D2}, k_{D3}]$ with gains k_{Pi} and k_{Di}, $i = 1, 2, 3$, that may have each of them its own different positive value. Under such considerations, the tuning parameter combination giving rise to the best closed-loop performance was determined, for this controller too, from numerous trial-and-error experiments. The resulting gains were: $K_P = \text{diag}[800, 1300, 200]$ Nm, $K_D = \text{diag}[5, 10, 10]$ Nm, $\lambda = 30$ [rad]$^{-1}$, $\delta = 5$ s/rad, $k = 50$ s^{-1}, $\omega = 5$, $\beta = 25$ Nm/rad, $\eta = 5$ rad/s, and $\mu = 10$ rad/s.

Figures 5.26–5.28 show the results of Test 2 for both implemented controllers. Observe that the regulation objective was this time achieved —avoiding input saturation— in less than 2 seconds. Moreover, the parameter estimators took a convergence time considerably shorter than in Test 1. The parametric estimation steady-state errors were however inevitable and could hardly be concluded to be smaller. Note on the other hand that the regulation objective is also achieved through the L00 controller, but that the position stabilization time was longer than 5 seconds. Moreover, a parameter estimator convergence time considerably longer than that obtained through the proposed scheme is further observed.

5.2.3 State feedback tracking control

At every experiment, the initial link positions and velocities were taken as $q_i(0) = \dot{q}_i(0) = 0$, $i = 1, 2, 3$. The auxiliary states were initiated at $\phi(0) = 0_{18}$ in the SP-SD+,

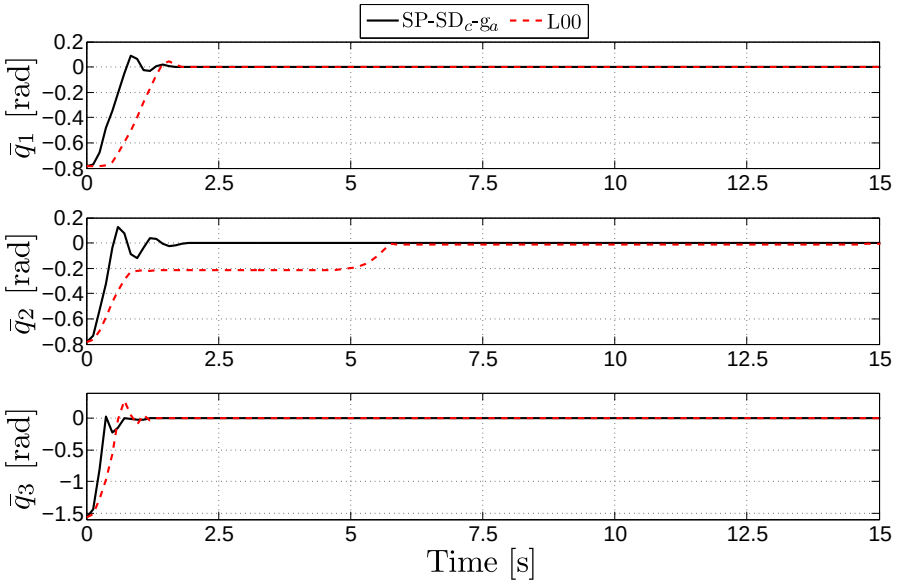

Figure 5.26: Test 2: position errors

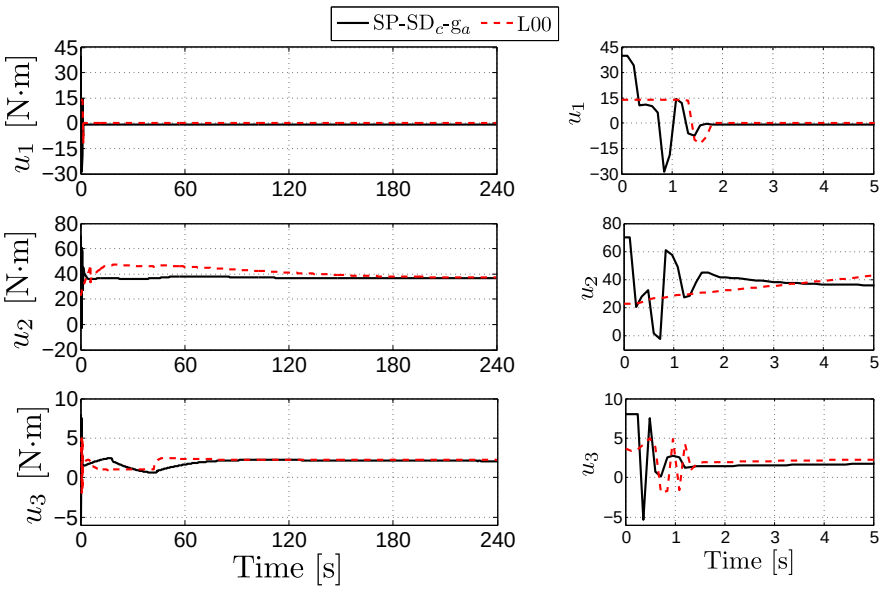

Figure 5.27: Test 2: control signals

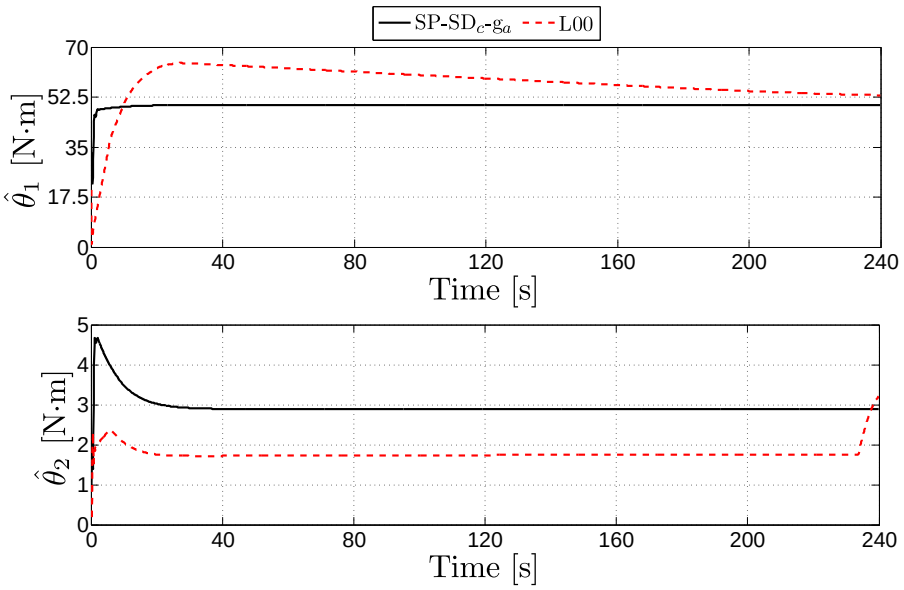

Figure 5.28: Test 2: parameter estimators

SPD+, and SPDhc+-like cases and $\hat{\psi}^T = 0_{18}$ in the case of the D$_e$99 algorithm[3]. The desired trajectory for all the implemented controllers was defined as

$$q_d(t) = \begin{pmatrix} q_{d1}(t) \\ q_{d2}(t) \\ q_{d3}(t) \end{pmatrix} = \begin{pmatrix} -\frac{\pi}{4} + \frac{\pi}{4}\cos(0.5t) \\ \frac{\pi}{6}\sin(0.5t) \\ \frac{\pi}{4} + \frac{\pi}{6}\sin(t) \end{pmatrix} \quad [\text{rad}]$$

Let us note that with this desired trajectory, Assumption 3.2 is satisfied with $B_{dv} = 1.255$ rad/s and $B_{da} = 0.574$ rad/s^2.

For the adaptive SP-SD+, SPD+, and SPDhc+-like algorithms, the saturation-function parameters were fixed such that inequalities (3.72), (3.74), (3.76), and (3.78) were satisfied. The control gains in K_P and K_D were fixed after several trial-and-error tests so as to have the best possible closed-loop performance. As for the D$_e$99 controller, a similar procedure was followed disregarding the input saturation avoidance inequality to achieve better closed-loop responses (recall that in this approach, the control gains in K_P and K_D respectively bound the P and D terms). The resulting control parameter values for all the implemented schemes are presented in Table 5.5. The elements of the diagonal of Γ are given by $\Gamma_j = 0.01$, $\forall j \in \{1, \ldots, 18\}/\{14, 15\}$, $\Gamma_{14} = 2.75$, and $\Gamma_{15} = 0.015$ N m/rad, for the SP-SD+, SPD+ and the SPDhc+-like controllers, while for D$_e$99 such values are given by $\Gamma_j = 0.01$, $\forall j \in \{1, \ldots, 18\}/\{14, 15\}$, $\Gamma_{14} = 20$, and $\Gamma_{15} = 5$ N m/rad.

As for the saturation function parameters involved in the SP-SD+, SPD+, and SPDhc+-like algorithms, the selected values were (refer to footnote 2): $M_{P1} = 11.5$, $M_{D1} = 11.5$, $M_{P2} = 27.5$, $M_{D2} = 27.5$, $M_{P3} = 4.25$, and $M_{D3} = 4.25$ in the SP-SD+

[3]Refer to Section A.2 of Appendix A for the description of the system parameters and consider the viscous friction coeficientes.

Table 5.5: Control parameter values for the state-feedback tracking scheme

Parameter	SP-SD+, SPD+, SPDhc+-like	D_e99
k_{P1}	380	150
k_{P2}	330	330
k_{P3}	180	30
k_{D1}	35	20
k_{D2}	13	30
k_{D3}	5	5
ε	1.5	1
Λ_P		diag[1, 1]
Λ_D		diag[1, 1]

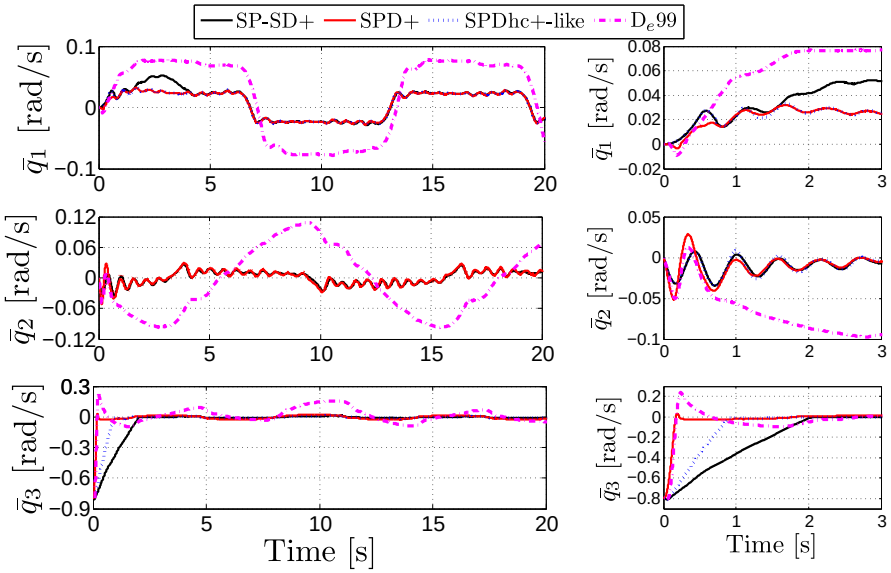

Figure 5.29: Position errors

case; $M_{P1} = 23$, $M_{P2} = 60$ and $M_{P3} = 8.5$ in the SPD+ case; $M_{01} = 45$, $M_{P1} = 18$, $M_{02} = 135$, and $M_{P2} = 41$, $M_{03} = 13.5$, and $M_{P3} = 7$ in the SPDhc+-like case; and $L_{Pi} = 0.9M_{Pi}$, $i = 1, 2, 3$, $M_a^T = \big(0.15 \quad 0.1 \quad 1.5 \quad 3 \quad 0.1 \quad 0.1 \quad 1.5 \quad 0.1 \quad 2 \quad 0.25 \quad 0.25 \quad 0.25 \quad 0.1 \quad 60 \quad 3 \quad 3.75 \quad 3 \quad 0.25\big)$ and $L_{aj} = 0.9M_{aj}$, $j = 1, \ldots, 18$, in all the three cases. With these values, inequalities (3.72), (3.74), (3.76), and (3.78) were corroborated to be satisfied.

Figures 5.29 and 5.30 show the position error evolution and control signals obtained through every implemented controller. Observe that the SP-SD+, SPD+, and SPDhc+-type schemes achieve the trajectory tracking objective —avoiding input saturation— in around 2 seconds with a post-transient oscillation of small amplitude, and even though the D_e99 controller attains the goal with the same stabilization time, the post-transient oscillation is wider. The evolution of the parameter estimators did not converge in all implemented controllers, but implemented simulations showed that only two estimators, those related to the parameters involved in the gravity force vec-

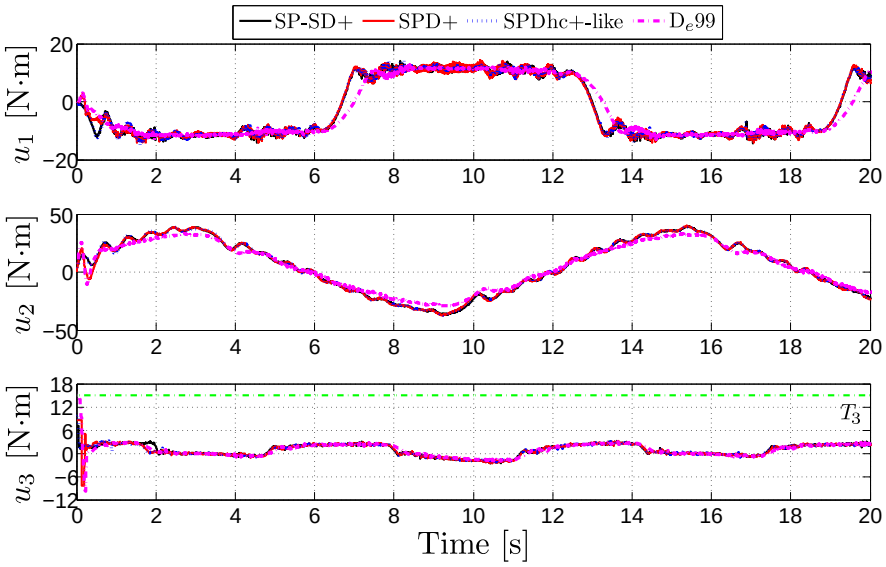

Figure 5.30: Control signals

Table 5.6: RMS steady-state error

	SP-SD+	SPD+	SPDhc+-like	D_e99	*units*
RMS	0.0276	0.0311	0.0269	0.1157	rad

tor, converged to the real values, and that the convergence rate depends on the value of ε, being faster for a higher value of ε. More estimators may be expected to converge to the real values through different desired trajectories leading to the satisfaction of *persistency of excitation* conditions [30] (this aspect is out of the scope of this work). Let us point out that these observations on the parameter estimator behavior did not prevent the trajectory tracking objective to either be accomplished —avoiding input saturation— or to achieve it in a considerably short time. The input control signal was observed to remain within the input saturation limits for the SP-SD+, SPD+, and SPDhc+-type algorithms, and for the D_e99 scheme the input saturation bound of the third link was reached.

To compare the performance of the implemented controllers the root mean square (RMS) of the position errors, *i.e.* $\sqrt{\frac{1}{t_2-t_1}\int_{t_1}^{t_2}\|\bar{q}(t)\|^2 dt}$, was calculated from $t_1 = 2$ s to $t_2 = 10$ s to avoid the transient response. The resulting values are shown in Table 5.6. The best performance was obtained through the SPDhc+-like algorithm, while the worst through the D_e99 scheme.

Figures 5.31 to 5.32 show the comparison results of the proposed controller in its SP-SD+, SPD+, and SPDhc+-like forms and their respective non-adaptive version using the nominal parameters, and tested with the same control gains (see Table 5.5) for both versions of each control scheme. Notice how the performance is considerably improved through the adaptive controller.

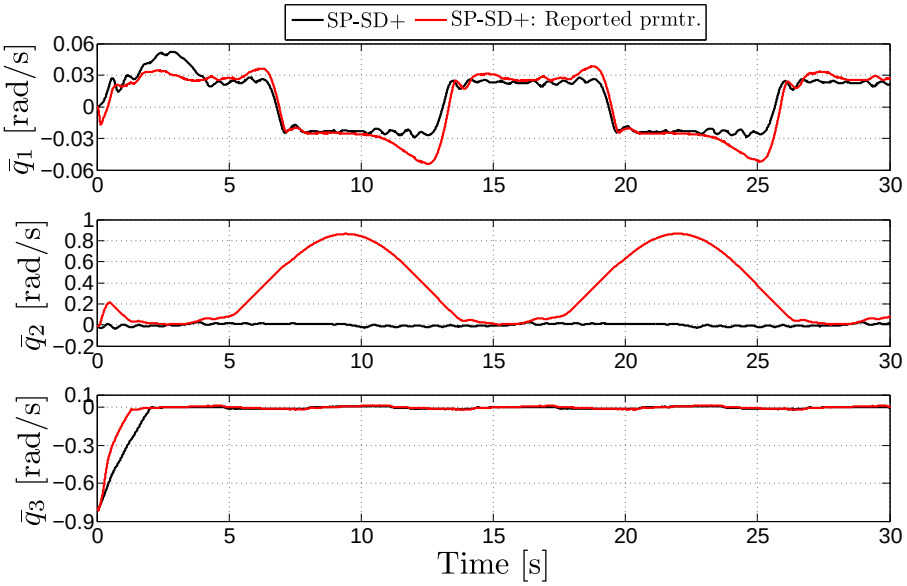

Figure 5.31: Test 2: Position errors of the SPSD+ scheme

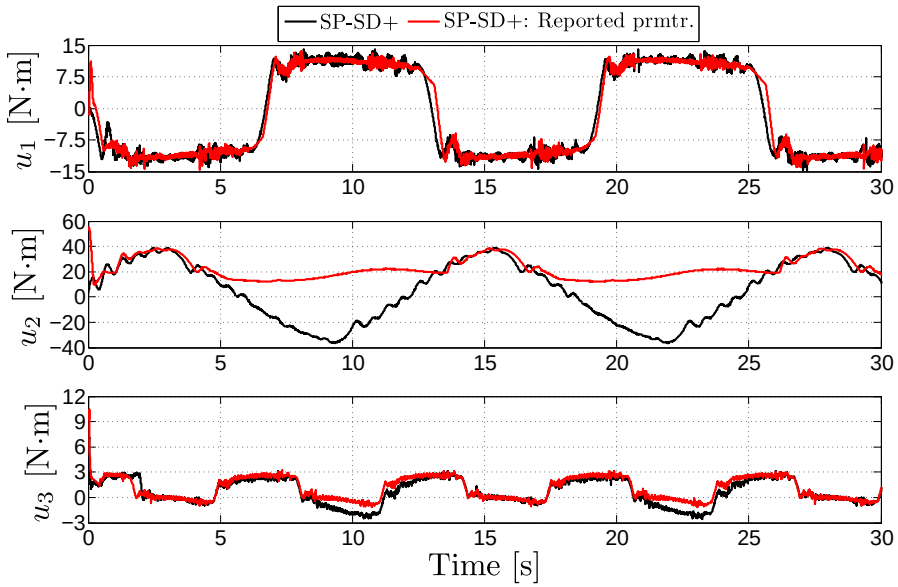

Figure 5.32: Test 2: Control signals of the SPSD+ scheme

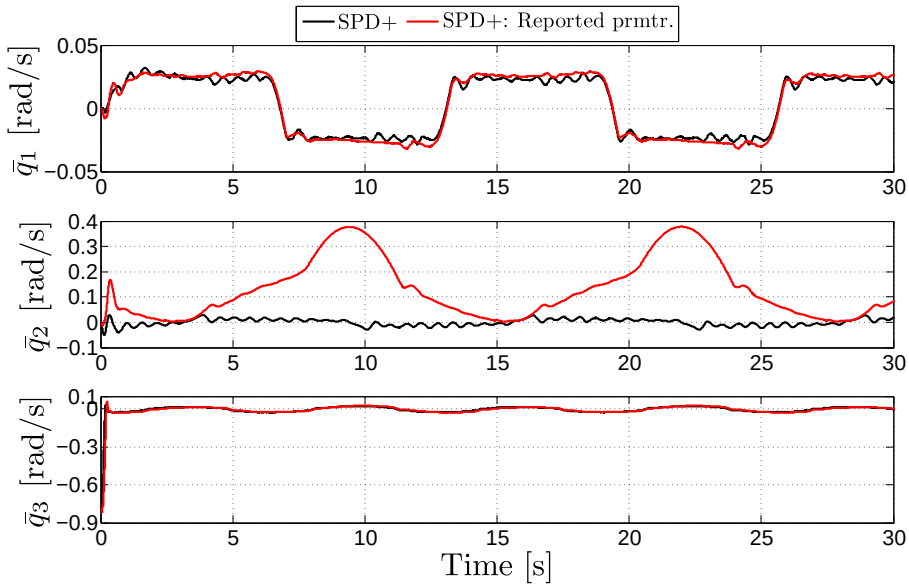

Figure 5.33: Test 2: Position errors of the SPD+ scheme

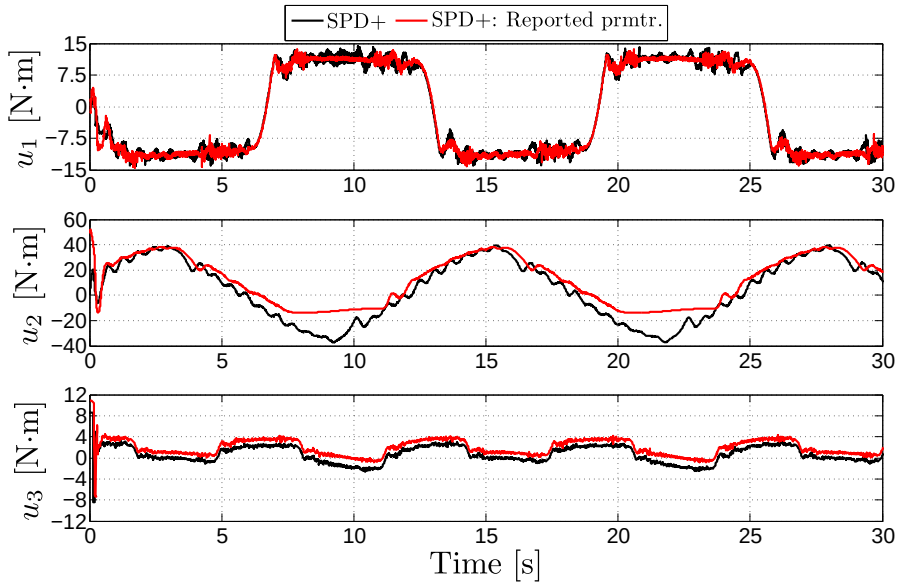

Figure 5.34: Test 2: Control signals of the SPD+ scheme

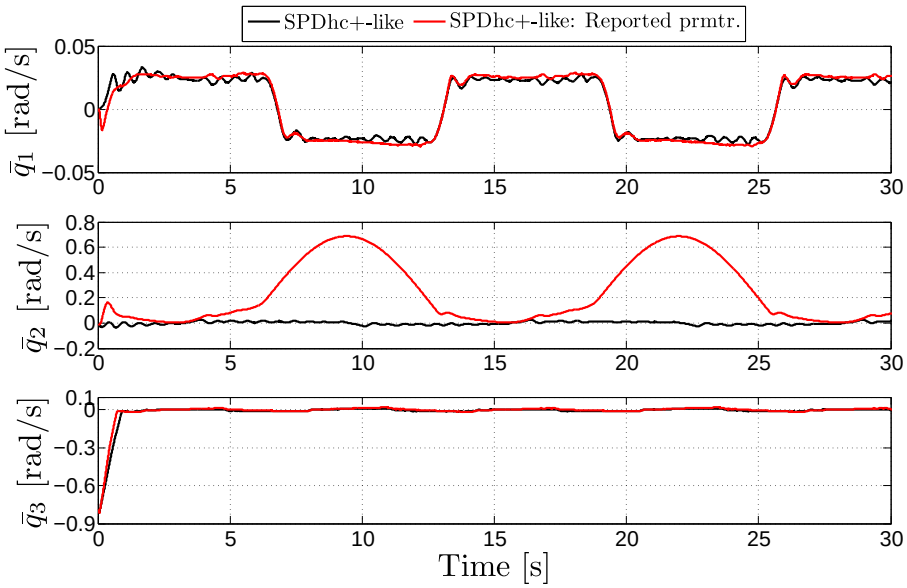

Figure 5.35: Test 2: Position errors of the SPDhc+-like scheme

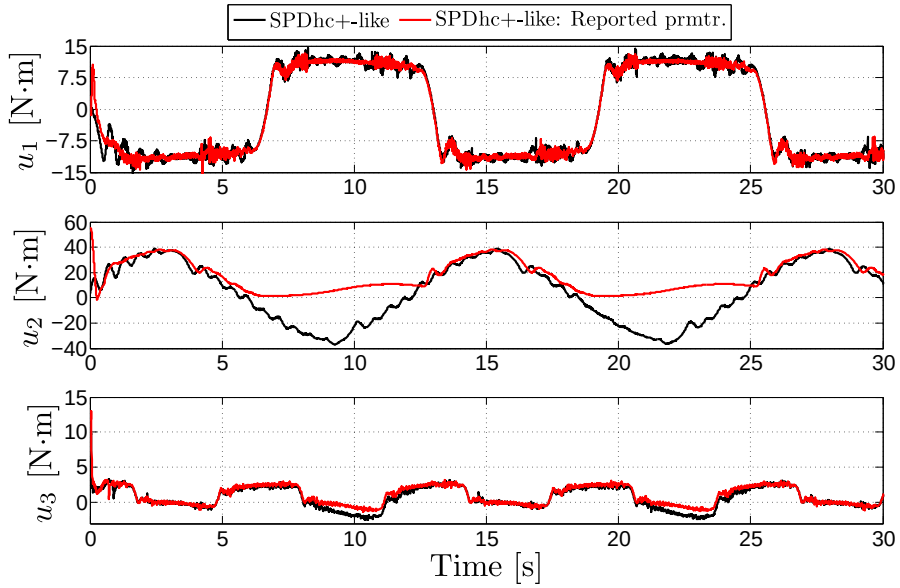

Figure 5.36: Test 2: Control signals of the SPDhc+-like scheme

6

Conclusions and perspectives

In this dissertation adaptive state feedback schemes for the global position and motion control of robot manipulators with bounded inputs were proposed. Both control strategies have a generalized structure that give rise to adaptive versions/extensions of several PD-type saturating controllers previously developed under the consideration of the exact knowledge of the system parameters. Furthermore, an output-feedback bounded adaptive algorithm that achieves global regulation —avoiding input saturation— in the absence of velocity measurements was also proposed. With respect to the previously developed approaches, the proposed algorithms guarantee the control objective: for any initial condition (global results), avoiding discontinuities throughout the scheme, preventing the inputs to reach their natural saturation limits, and imposing no *saturation-avoidance* restriction on the control gains. Moreover, the developed controllers are not restricted to the use of a specific saturation function to achieve the required boundedness, but may rather involve any one within a set of smooth and non-smooth (Lipschitz-continuous) bounded passive functions that include the hyperbolic tangent and the conventional saturation as particular cases. Their efficiency were corroborated through numerical simulations using a 2-DOF model, and through several experimental implementations using two different experimental devices. The results showed that it is always posible to reach the control objective —avoiding input saturation— quickly enough.

The adaptation dynamics of the output feedback scheme was first designed in its simplest form: involving only the position error vector. Then, an extended version additionally involving the estimation of the velocity vector was further designed for the sake of generality and since a previous approach included an analogous term. The first approach guarantees the control objective through a simpler implementation. The second one gives an additional degree of design flexibility that may be used for performance adjustment purposes.

It is important to remark that while through suitable desired target positions the

regulation designed schemes give rise to asymptotic approximations (happening to be exact under ideal conditions) of the parameters involved in the gravity vector, the tracking algorithm cannot ensure a similar convergence of the system dynamic parameter estimators. This is essentially due to the non-invariant asymptotic behavior that such estimators may have in the more general context of non-autonomous systems. The referred convergence could be guaranteed under additional *excitation-persistency* conditions. Nevertheless, the change rate and convergence properties of the parameter estimators do not prevent the regulation/tracking objective to be achieved or that such an achievement take place fast enough.

The adaptive tracking algorithm presented in this dissertation was designed assuming the availability of all system states. An output feedback version of such scheme proves to be convenient since not every manipulator is equipped with tachometers, and when velocity measurements are available they are usually noisy.

Through the adaptive regulation algorithms, global position control is now possible —avoiding input saturation— for manipulators with bounded inputs disregarding the exact value of system parameters and even in the absence of velocity measurements through the output-feedback version. However, the regressor matrix related to the gravity force vector is involved in the control expressions. Stabilization schemes that further avoid the system structure would prove to be a convenient future research work. Some algorithms of such a kind are already found in the literature but they are usually expressed though specific control expressions (for instance considering every term of the controller within a saturation function) and they generally give rise to complex tuning criteria. A generalized scheme that include multiple control structures with simplified tuning conditions is still missing in the literature.

A

Dynamics of two basic configurations

The intention of this appendix is to show a methodology to obtain the manipulator dynamics through the Jacobian. The dynamic models presented here were used for the experimental implementation of the adaptive tracking control scheme. The explicit form of the regression matrix —of each configuration— is shown after the development of the dynamics.

A.1 Dynamics of a 2-DOF robot manipulator

A two degree of freedom robot arm is shown in figure A.1. The intention of this section is to illustrate how to obtain the manipulator dynamics using the Euler-Lagrange equations of motion through the Jacobian using a well-known configuration in order to apply this methodology on a manipulator with different kinematic chain arrangements.

Let us begin with the development of the forward kinematics. The derivation of the dynamics by the Euler-Lagrange formulation requires the knowledge of the homogeneous matrices A_i, transforming the coordinates of some point from the reference frame $\{XYZ\}_i$ to the reference frame $\{XYZ\}_{i-1}$, for $i = 1, ..., n$, and whose product represents the kinematic model of the manipulator. These matrices can be obtained through the Denavit-Hartenberg (DH) convention. Consider the location of the inertial frame $\{XYZ\}_0$ and reference frames $\{XYZ\}_i$, for $i = 1, 2, 3$, attached to the manipulator joints as illustrated in Figure A.1. The resulting DH parameters are shown in Table A.1, where a_i is given by the distance between z_{i-1} and z_i axes measured along x_i axis; d_i is defined as the distance between the x_{i-1} and x_i axes measured along z_{i-1}; α_i represents the angle between z_{i-1} and z_i axes about the x_i axis; and θ_i is the angle between x_{i-1} and x_i axes about the z_i axis; α_i and θ_i. The homogeneous matrices ${}^{i-1}A_i$

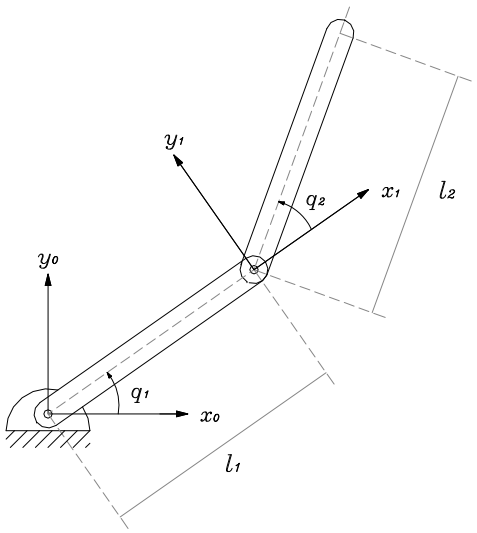

Figure A.1: 2 DOF Robot Manipulator

Table A.1: Denavit-Hartenberg parameters for the doble pendulum manipulator

i	a_i	d_i	α_i	θ_i
1	l_1	0	0	q_1
2	l_2	0	0	q_2

are obtained through four basic transformations,

$$
\begin{aligned}
{}^{i-1}A_i &= [\text{Rotation}(\theta_i, Z)][\text{Translation}(d_i, Z)][\text{Translation}(a_i, X)][\text{Rotation}(\alpha_i, X)] \\
&= \left[\begin{array}{cccc} c_{\theta_i} & -s_{\theta_i}c_{\alpha_i} & s_{\theta_i}s_{\alpha_i} & a_i c_{\theta_i} \\ s_{\theta_i} & c_{\theta_i}c_{\alpha_i} & -c_{\theta_i}s_{\alpha_i} & a_i s_{\theta_i} \\ 0 & s_{\alpha_i} & c_{\alpha_i} & d_i \\ \hline 0 & 0 & 0 & 1 \end{array}\right] = \left[\begin{array}{c|c} R_i & d_i \\ \hline 0_3 & 1 \end{array}\right]
\end{aligned}
\tag{A.1}
$$

For the considered manipulator, they are given by

$$
{}^{0}A_1 = \left[\begin{array}{ccc|c} \cos(q_1) & -\sin(q_1) & 0 & l_1\cos(q_1) \\ \sin(q_1) & \cos(q_1) & 0 & l_1\sin(q_1) \\ 0 & 0 & 1 & 0 \\ \hline 0 & 0 & 0 & 1 \end{array}\right] = \left[\begin{array}{c|c} R_1 & d_1 \\ \hline 0_3 & 1 \end{array}\right]
$$

$$
{}^{1}A_2 = \left[\begin{array}{ccc|c} \cos(q_2) & -\sin(q_2) & 0 & l_2\cos(q_2) \\ \sin(q_2) & \cos(q_2) & 0 & l_2\sin(q_2) \\ 0 & 0 & 1 & 0 \\ \hline 0 & 0 & 0 & 1 \end{array}\right] \left[\begin{array}{c|c} R_2 & d_2 \\ \hline 0_3 & 1 \end{array}\right]
$$

where $R_i \in \mathbb{R}^{3\times3}$ and $d_i \in \mathbb{R}^3$, $i = 1, 2$. The homogeneous transformation matrix

relating the origin of the inertial frame $\{XYZ\}_0$ to the tip of the last link is given by[1]

$$ {}^0T_n = \prod_{i=1}^{n} {}^{i-1}A_i = {}^0A_1 \dots {}^{n-1}A_n $$

where

$$ {}^0T_2 = {}^0A_1 {}^1A_2 = \begin{bmatrix} c_{12} & -s_{12} & 0 & l_1c_1 + l_2c_{12} \\ s_{12} & c_{12} & 0 & l_1s_1 + l_2s_{12} \\ 0 & 0 & 1 & 0 \\ 0 & 0 & 0 & 1 \end{bmatrix} $$

The latter developments are useful to compute the dynamics using the Euler-Lagrange equation (A.2)

$$ \tau = \frac{d}{dt}\left(\frac{\partial \mathcal{L}}{\partial \dot{q}}\right) - \frac{\partial \mathcal{L}}{\partial q} \tag{A.2} $$

where τ represents the force applied to the system and $\mathcal{L}(q, \dot{q})$ is the difference between the kinetic and potential energies, $\mathcal{L}(q, \dot{q}) = T(q, \dot{q}) - V(q)$, and it is called Lagrangian.

We first determine the kinetic energy by using the angular and linear velocities of each link. Defining the Jacobian as a map from joint velocity $\dot{q}$ to cartesian velocity, the jacobian matrix might be partitioned into a translational and an rotational part

$$ \begin{bmatrix} v \\ \omega \end{bmatrix} = J\dot{q} = \begin{bmatrix} J_v \\ J_\omega \end{bmatrix} \dot{q} $$

Using this definition the kinetic energy can be written as

$$ T(q, \dot{q}) = \frac{1}{2}\dot{q}^T \sum_{i=1}^{n} \left[m_i J_{vi}^T(q) J_{vi}(q) + J_{\omega i}^T(q) R_i(q) I_i R_i^T(q) J_{\omega i}(q) \right] \dot{q} \tag{A.3} $$

where

$$ I_i = \begin{bmatrix} I_{xi} & I_{xyi} & I_{xzi} \\ I_{xyi} & I_{yi} & I_{yzi} \\ I_{xzi} & I_{yzi} & I_{zi} \end{bmatrix} $$

is the inertia tensor and J_{vi} is the matrix formed from the first three rows of J_i and represents the translational velocity, $J_{\omega i}$ is the matrix formed with the last three rows of J_i and it represents the part of the Jacobian due to angular velocity, the matrix R_i represents a rotation to express the angular velocity in the frame attached to link i. The Jacobian of joint i is computed supposing that joints $i+1$ to n are not present —because they do not contribute to the velocity of joint i— and that the last reference frame is placed in the center of mass of the i-th link. With these, the Jacobian can be

[1] The following convention will be used $c_i \triangleq \cos(q_i)$, $s_i \triangleq \sin(q_i)$, $c_{ij} \triangleq \cos(q_i + q_j)$, and $s_{ij} \triangleq \sin(q_i + q_j)$ $\forall i, j \in \{1, 2, 3\}$.

written as

$$J_1 = \begin{bmatrix} J_{v_1} \\ J_{\omega_1} \end{bmatrix} = \begin{bmatrix} z_0 \times (d_1 - d_0) & 0_3 \\ z_0 & 0_3 \end{bmatrix} = \begin{bmatrix} -r_1 s_1 & 0 \\ -r_1 c_1 & 0 \\ 0 & 0 \\ 0 & 0 \\ 0 & 0 \\ 1 & 0 \end{bmatrix}$$

$$J_2 = \begin{bmatrix} J_{v_2} \\ J_{\omega_2} \end{bmatrix} = \begin{bmatrix} z_0 \times (d_2 - d_0) & z_1 \times (d_2 - d_1) \\ z_0 & z_1 \end{bmatrix} = \begin{bmatrix} -l_1 s_1 - r_2 s_{12} & -r_2 s_{12} \\ l_1 c_1 + r_2 c_{12} & r_2 c_{12} \\ 0 & 0 \\ 0 & 0 \\ 0 & 0 \\ 1 & 1 \end{bmatrix}$$

with J_{vi}, $J_{\omega i} \in \mathbb{R}^{3\times 2}$, $i = 1, 2$. The kinetic energy due to rotational velocity is given by

$$T_\omega(q, \dot{q}) = \frac{1}{2}\dot{q}^T \left[J_{\omega 1}^T(q) R_1(q) I_1 R_1^T(q) J_{\omega 1}(q) + J_{\omega 2}^T(q) R_2(q) I_2 R_2^T(q) J_{\omega 2}(q) \right] \dot{q}$$

where

$$\begin{aligned} J_{\omega 1}^T R_1 I_1 R_1^T J_{\omega 1} &= \left[\begin{smallmatrix} 0 & 0 & 1 \\ 0 & 0 & 0 \end{smallmatrix}\right] \left[\begin{smallmatrix} c_1 & -s_1 & 0 \\ s_1 & c_1 & 0 \\ 0 & 0 & 1 \end{smallmatrix}\right] I_1 \left[\begin{smallmatrix} c_1 & s_1 & 0 \\ -s_1 & c_1 & 0 \\ 0 & 0 & 1 \end{smallmatrix}\right] \left[\begin{smallmatrix} 0 & 0 \\ 0 & 0 \\ 1 & 0 \end{smallmatrix}\right] \\ &= \begin{bmatrix} I_{z1} & 0 \\ 0 & 0 \end{bmatrix} \\ J_{\omega 2}^T R_2 I_2 R_2^T J_{\omega 2} &= \left[\begin{smallmatrix} 0 & 0 & 1 \\ 0 & 0 & 1 \end{smallmatrix}\right] \left[\begin{smallmatrix} c_2 & -s_2 & 0 \\ s_2 & c_2 & 0 \\ 0 & 0 & 1 \end{smallmatrix}\right] I_2 \left[\begin{smallmatrix} c_2 & s_2 & 0 \\ -s_2 & c_2 & 0 \\ 0 & 0 & 1 \end{smallmatrix}\right] \left[\begin{smallmatrix} 0 & 0 \\ 0 & 0 \\ 1 & 1 \end{smallmatrix}\right] \\ &= \begin{bmatrix} I_{z2} & I_{z2} \\ I_{z2} & I_{z2} \end{bmatrix} \end{aligned}$$

The translational part of the kinetic energy is

$$T_v(q, \dot{q}) = \frac{1}{2}\dot{q}^T \left[m_1 J_{v1}^T(q) J_{v1}(q) + m_2 J_{v2}^T(q) J_{v2}(q) \right] \dot{q}$$

where

$$\begin{aligned} J_{v1}^T J_{v1} &= \begin{bmatrix} -r_1 s_1 & -r_1 c_1 & 0 \\ 0 & 0 & 0 \end{bmatrix} \begin{bmatrix} -r_1 s_1 & 0 \\ -r_1 c_1 & 0 \\ 0 & 0 \end{bmatrix} \\ &= \begin{bmatrix} r_1^2 & 0 \\ 0 & 0 \end{bmatrix} \\ J_{v2}^T J_{v2} &= \begin{bmatrix} -l_1 s_1 - r_2 s_{12} & l_1 c_1 + r_2 c_{12} & 0 \\ -r_2 s_{12} & r_2 c_{12} & 0 \end{bmatrix} \begin{bmatrix} -l_1 s_1 - r_2 s_{12} & -r_2 s_{12} \\ l_1 c_1 + r_2 c_{12} & r_2 c_{12} \\ 0 & 0 \end{bmatrix} \\ &= \begin{bmatrix} l_1^2 + r_2^2 + 2 l_1 r_2 c_2 & l_1 r_2 c_2 + r_2^2 \\ l_1 r_2 c_2 + r_2^2 & r_2^2 \end{bmatrix} \end{aligned}$$

Hence

$$T(q,\dot{q}) = \frac{1}{2}\dot{q}^T H(q)\dot{q}$$

where the inertia matrix $H(q)$ is given by

$$H(q) = \begin{bmatrix} m_1 r_1^2 + m_2(l_1^2 + r_2^2) + 2m_2 l_1 r_2 c_2 + I_{z1} + I_{z2} & m_2 l_1 r_2 c_2 + m_2 r_2^2 + I_{z2} \\ m_2 l_1 r_2 c_2 + m_2 r_2^2 + I_{z2} & m_2 r_2^2 + I_{z2} \end{bmatrix}$$

Supposing that the potential energy, V(q), is equal to zero when both links are resting downwards, it can be written as

$$V(q) = m_1 g r_1 (1 - c_1) + m_2 g\big[l_1(1 - c_1) + r_2(1 - c_{12})\big]$$

The Lagrangian is then

$$\mathcal{L}(q,\dot{q}) = T(q,\dot{q}) - V(q)$$

Applying the Euler-Lagrange equation and defining

$$C(q,\dot{q})\dot{q} \triangleq \dot{H}(q,\dot{q})\dot{q} + \frac{1}{2}\frac{\partial}{\partial q}(\dot{q}^T H(q)\dot{q})g(q) \triangleq \frac{\partial}{\partial q}\left(V^T(q)\right)$$

the dynamics are given by

$$\tau = H(q)\ddot{q} + C(q,\dot{q})\dot{q} + g(q)$$

The elements of the coriolis matrix $C(q,\dot{q})$ are known as Christoffel symbols of the first kind and are defined by

$$C_{ij}(q,\dot{q}) = \frac{1}{2}\sum_{k=1}^{n}\left(\frac{\partial H_{ij}}{\partial q_k} + \frac{\partial H_{ik}}{\partial q_j} - \frac{\partial H_{kj}}{\partial q_i}\right)\dot{q}_k \tag{A.4}$$

this representation is not unique and other definitions are posible. However, this particular choice has useful properties in control. The arrangement of the coriolis matrix $C(q,\dot{q})$, using Eq. (A.4) is given by

$$C(q,\dot{q}) = \begin{bmatrix} -m_2 l_1 r_2 s_2 \dot{q}_2 & -m_2 l_1 r_2 s_2(\dot{q}_1 + \dot{q}_2) \\ -m_2 l_1 r_2 s_2 \dot{q}_1 & 0 \end{bmatrix}$$

the gravity vector $g(q)$ is

$$g(q) = g\begin{bmatrix} m_1 r_1 s_1 + m_2(l_1 s_1 + r_2 s_{12}) \\ m_2 r_2 s_{12} \end{bmatrix}$$

Observe that $g(q)$ may be rewritten as $g(q) = G(q)\theta$ with

$$G(q) = \begin{pmatrix} s_1 & s_{12} \\ 0 & s_{12} \end{pmatrix} \quad \text{and} \quad \theta = \begin{pmatrix} g m_2 r_2 \\ g(m_1 r_1 + m_2 l_1) \end{pmatrix}$$

The dynamics satisfies the linear parametrization property $Y(q,\dot{q},\ddot{q})\psi = \tau$ with

$$Y(q,\dot{q},\ddot{q}) = \begin{bmatrix} \ddot{q}_1 & \ddot{q}_1 & (2\ddot{q}_1 + \ddot{q}_2)c_2 - \dot{q}_2 s_2(2\dot{q}_1 + \dot{q}_2) & s_{12} & s_1 \\ 0 & \ddot{q}_1 + \ddot{q}_2 & \ddot{q}_1 c_2 + \dot{q}_1^2 s_2 & s_{12} & 0 \end{bmatrix}$$

and

$$\psi_1 = m_1 r_1^2 + m_2 l_1^2 + I_{z1}$$
$$\psi_2 = m_2 r_2^2 + I_{z2}$$
$$\psi_3 = m_2 l_1 r_2$$
$$\psi_4 = g m_2 r_2$$
$$\psi_5 = g(m_1 r_1 + m_2 l_1)$$

A.2 Dynamics of a 3-DOF robot manipulator

Known as the anthropomorphic arm or articulated manipulator, its principal feature is that the revolution axis of the second joint is parallel to that of the third, being both perpendicular to the axis of revolution of the first joint. A common manipulator with this configuration is the PUMA 560 (see [20]).

Consider the location of the inertial frame $\{XYZ\}_0$ and reference frames $\{XYZ\}_i$, for $i = 1, 2, 3$, attached to the manipulator joints as illustrated in Figure A.2. Using the resulting DH parameters —shown in Table A.2—, the homogeneous matrices ${}^{i-1}A_i$ are obtained using Eq. (A.1). For the considered manipulator, they are given by Eqs. A.5.

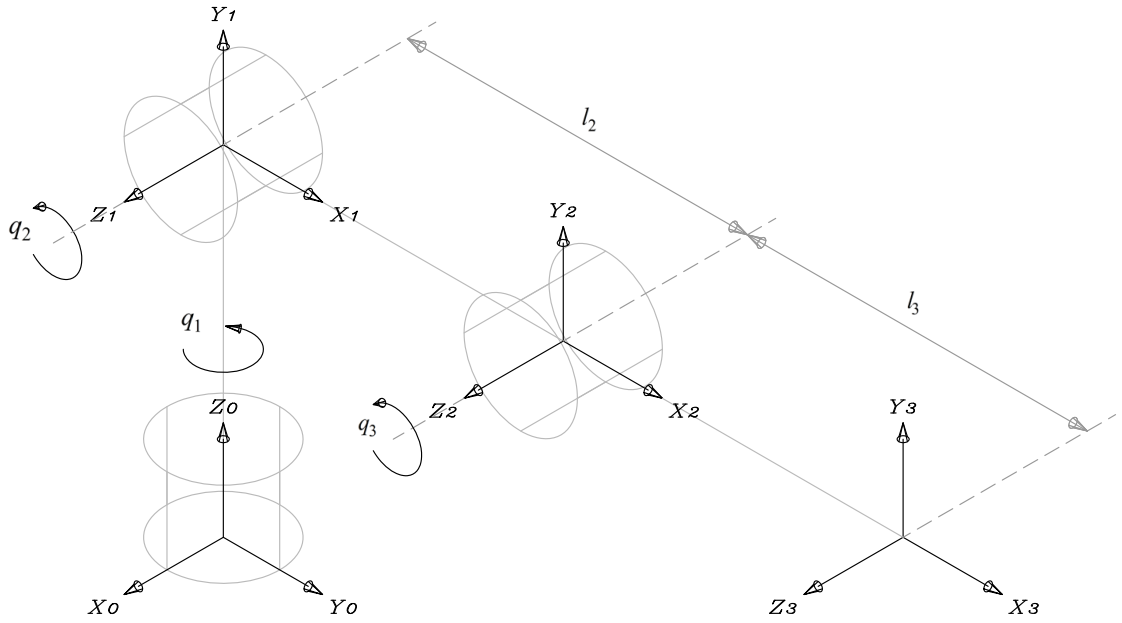

Figure A.2: Anthropomorphic manipulator

Table A.2: Denavit-Hartenberg parameter values

$i-$th link	a_i	d_i	α_i	θ_i
1	0	0	90^o	q_1
2	l_2	0	0	q_2
3	l_3	0	0	q_3

$$ {}^0A_1 = \left[\begin{array}{ccc:c} \cos q_1 & 0 & \sin q_1 & 0 \\ \sin q_1 & 0 & -\cos q_1 & 0 \\ 0 & 1 & 0 & 0 \\ \hdashline 0 & 0 & 0 & 1 \end{array}\right] = \left[\begin{array}{c:c} R_1 & d_1 \\ \hdashline 0_3 & 1 \end{array}\right] \tag{A.5a} $$

$$ {}^1A_2 = \left[\begin{array}{ccc:c} \cos q_2 & -\sin q_2 & 0 & l_2\cos q_2 \\ \sin q_2 & \cos q_2 & 0 & l_2\sin q_2 \\ 0 & 0 & 1 & 0 \\ \hdashline 0 & 0 & 0 & 1 \end{array}\right] = \left[\begin{array}{c:c} R_2 & d_2 \\ \hdashline 0_3 & 1 \end{array}\right] \tag{A.5b} $$

$$ {}^2A_3 = \left[\begin{array}{ccc:c} \cos q_3 & -\sin q_3 & 0 & l_3\cos q_3 \\ \sin q_3 & \cos q_3 & 0 & l_3\sin q_3 \\ 0 & 0 & 1 & 0 \\ \hdashline 0 & 0 & 0 & 1 \end{array}\right] = \left[\begin{array}{c:c} R_3 & d_3 \\ \hdashline 0_3 & 1 \end{array}\right] \tag{A.5c} $$

The forward kinematics are described by

$$ {}^0T_3 = \prod_{i=1}^{3} {}^{i-1}A_i = {}^0A_1\,{}^1A_2\,{}^2A_3 $$

where

$$ T_2^0 = T_1^0T_2^1 = \begin{bmatrix} c_1c_2 & -c_1s_2 & s_1 & l_2c_1c_2 \\ s_1c_2 & -s_1s_2 & -c_1 & l_2s_1c_2 \\ s_2 & c_2 & 0 & l_2s_2 \\ 0 & 0 & 0 & 1 \end{bmatrix} $$

$$ T_3^0 = T_2^0T_3^2 = \begin{bmatrix} c_1c_{23} & -c_1s_{23} & s_1 & l_3c_1c_{23} + l_2c_1c_2 \\ s_1c_{23} & -s_1s_{23} & -c_1 & l_3s_1c_{23} + l_2s_1c_2 \\ s_{23} & c_{23} & 0 & l_3s_{23} + l_2s_2 \\ 0 & 0 & 0 & 1 \end{bmatrix} $$

As described in the preceding section, these are used to compute the Jacobian of each joint, and using the translational and rotational part of the Jacobian matrices the kinetic energy can be expressed as in (A.6).

$$ T(q,\dot{q}) = \frac{1}{2}\dot{q}^T \sum_{i=1}^{3} \left[m_i J_{vi}^T(q) J_{vi}(q) + J_{\omega i}^T(q) R_i(q) I_i R_i^T(q) J_{\omega i}(q)\right]\dot{q} \tag{A.6} $$

Using the frame location shown in figures A.3 to compute the Jacobian matrices of

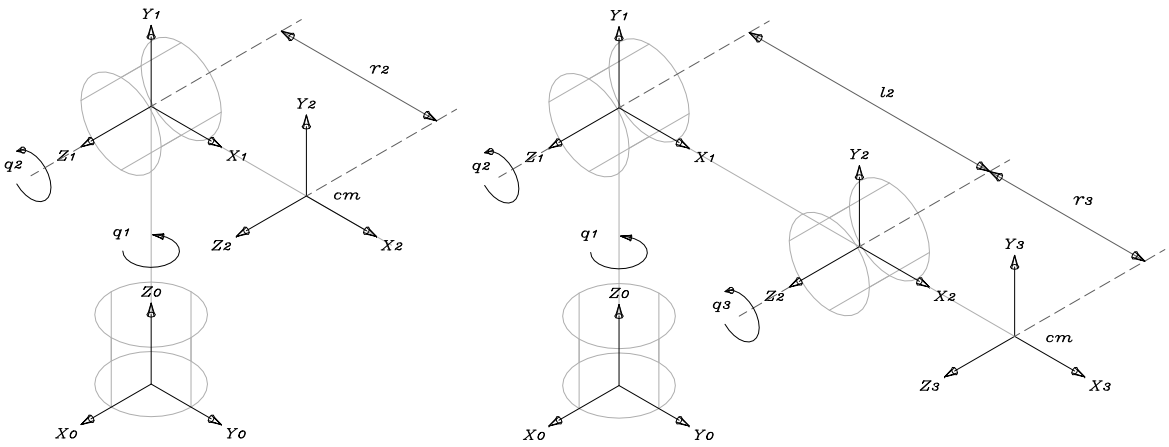

(a) Second joint (b) Third joint

Figure A.3: Frame placement to compute the Jacobian of each joint

joint i, we get

$$J_1 = \begin{bmatrix} J_{v1} \\ J_{\omega 1} \end{bmatrix} = \begin{bmatrix} z_0 \times (d_1 - d_0) & 0_3 & 0_3 \\ z_0 & 0_3 & 0_3 \end{bmatrix} = \begin{bmatrix} 0_3^T & 0_3^T & 0_3^T \\ 0 & 0 & 0 \\ 0 & 0 & 0 \\ 1 & 0 & 0 \end{bmatrix}$$

$$J_2 = \begin{bmatrix} J_{v2} \\ J_{\omega 2} \end{bmatrix} = \begin{bmatrix} z_0 \times (d_2 - d_0) & z_1 \times (d_2 - d_1) & 0_3 \\ z_0 & z_1 & 0_3 \end{bmatrix}$$

$$= \begin{bmatrix} -r_2 s_1 c_2 & -r_2 c_1 s_2 & 0 \\ r_2 c_1 c_2 & -r_2 s_1 s_2 & 0 \\ 0 & r_2 c_2 & 0 \\ 0 & s_1 & 0 \\ 0 & -c_1 & 0 \\ 1 & 0 & 0 \end{bmatrix}$$

$$J_3 = \begin{bmatrix} J_{v3} \\ J_{\omega 3} \end{bmatrix} = \begin{bmatrix} z_0 \times (d_3 - d_0) & z_1 \times (d_3 - d_1) & z_2 \times (d_3 - d_2) \\ z_0 & z_1 & z_2 \end{bmatrix}$$

$$= \begin{bmatrix} -s_1(r_3 c_{23} + l_2 c_2) & -c_1(r_3 s_{23} + l_2 s_2) & -r_3 c_1 s_{23} \\ c_1(r_3 c_{23} + l_2 c_2) & -s_1(r_3 s_{23} + l_2 s_2) & -r_3 s_1 s_{23} \\ 0 & r_3 c_{23} + l_2 c_2 & r_3 c_{23} \\ 0 & s_1 & s_1 \\ 0 & -c_1 & -c_1 \\ 1 & 0 & 0 \end{bmatrix}$$

where $J_{vi},\ J_{\omega i} \in \mathbb{R}^{3\times 3}$, $i = 1, 2, 3$. With these, the products appearing in equation (A.6) are

$$J_{\omega 1}^T R_1 I_1 R_1^T J_{\omega 1} = \begin{bmatrix} 0 & 0 & 1 \\ 0 & 0 & 0 \\ 0 & 0 & 0 \end{bmatrix} \begin{bmatrix} c_1 & 0 & s_1 \\ s_1 & 0 & -c_1 \\ 0 & 1 & 0 \end{bmatrix} I_1 \begin{bmatrix} c_1 & s_1 & 0 \\ 0 & 0 & 1 \\ s_1 & -c_1 & 0 \end{bmatrix} \begin{bmatrix} 0 & 0 & 0 \\ 0 & 0 & 0 \\ 1 & 0 & 0 \end{bmatrix}$$

$$= \begin{bmatrix} I_{y1} & 0 & 0 \\ 0 & 0 & 0 \\ 0 & 0 & 0 \end{bmatrix}$$

$$J_{\omega 2}^T R_2 I_2 R_2^T J_{\omega 2} = \begin{bmatrix} 0 & 0 & 1 \\ s_1 & -c_1 & 0 \\ 0 & 0 & 0 \end{bmatrix} \begin{bmatrix} c_1c_2 & -c_1s_2 & s_1 \\ s_1c_2 & -s_1s_2 & -c_1 \\ s_2 & c_2 & 0 \end{bmatrix} I_2 \begin{bmatrix} c_1c_2 & s_1c_2 & s_2 \\ -c_1s_2 & -s_1s_2 & c_2 \\ s_1 & -c_1 & 0 \end{bmatrix} \begin{bmatrix} 0 & s_1 & 0 \\ 0 & -c_1 & 0 \\ 1 & 0 & 0 \end{bmatrix}$$

$$= \begin{bmatrix} I_{x2}s_2^2 + 2I_{xy2}s_2c_2 + I_{y2}c_2^2 & I_{xz2}s_2 + I_{yz2}c_2 & 0 \\ I_{xz2}s_2 + I_{yz2}c_2 & I_{z2} & 0 \\ 0 & 0 & 0 \end{bmatrix}$$

$$J_{\omega 3}^T R_3 I_3 R_3^T J_{\omega 3} = \begin{bmatrix} 0 & 0 & 1 \\ s_1 & -c_1 & 0 \\ s_1 & -c_1 & 0 \end{bmatrix} \begin{bmatrix} c_1c_{23} & -c_1s_{23} & s_1 \\ s_1c_{23} & -s_1s_{23} & -c_1 \\ s_{23} & c_{23} & 0 \end{bmatrix} I_3 \begin{bmatrix} c_1c_{23} & s_1c_{23} & s_{23} \\ -c_1s_{23} & -s_1s_{23} & c_{23} \\ s_1 & -c_1 & 0 \end{bmatrix} \begin{bmatrix} 0 & s_1 & s_1 \\ 0 & -c_1 & -c_1 \\ 1 & 0 & 0 \end{bmatrix}$$

$$= \begin{bmatrix} I_{x3}s_{23}^2 + 2I_{xy3}s_{23}c_{23} + I_{y3}c_{23}^2 & I_{xz3}s_{23} + I_{yz3}c_{23} & I_{xz3}s_{23} + I_{yz3}c_{23} \\ I_{xz3}s_{23} + I_{yz3}c_{23} & I_{z3} & I_{z3} \\ I_{xz3}s_{23} + I_{yz3}c_{23} & I_{z3} & I_{z3} \end{bmatrix}$$

$$J_{v1}^T J_{v1} = \begin{bmatrix} 0 & 0 & 0 \\ 0 & 0 & 0 \\ 0 & 0 & 0 \end{bmatrix}$$

$$J_{v2}^T J_{v2} = \begin{bmatrix} -r_2s_1c_2 & r_2c_1c_2 & 0 \\ -r_2c_1s_2 & -r_2s_1s_2 & r_2c_2 \\ 0 & 0 & 0 \end{bmatrix} \begin{bmatrix} -r_2s_1c_2 & -r_2c_1s_2 & 0 \\ r_2c_1c_2 & -r_2s_1s_2 & 0 \\ 0 & r_2c_2 & 0 \end{bmatrix}$$

$$= \begin{bmatrix} r_2^2c_2^2 & 0 & 0 \\ 0 & r_2^2 & 0 \\ 0 & 0 & 0 \end{bmatrix}$$

$$J_{v3}^T J_{v3} = \begin{bmatrix} -s_1(r_3c_{23}+l_2c_2) & c_1(r_3c_{23}+l_2c_2) & 0 \\ -c_1(r_3s_{23}+l_2s_2) & -s_1(r_3s_{23}+l_2s_2) & r_3c_{23}+l_2c_2 \\ -r_3c_1s_{23} & -r_3s_1s_{23} & r_3c_{23} \end{bmatrix} \begin{bmatrix} -s_1(r_3c_{23}+l_2c_2) & -c_1(r_3s_{23}+l_2s_2) & -r_3c_1s_{23} \\ c_1(r_3c_{23}+l_2c_2) & -s_1(r_3s_{23}+l_2s_2) & -r_3s_1s_{23} \\ 0 & r_3c_{23}+l_2c_2 & r_3c_{23} \end{bmatrix}$$

$$= \begin{bmatrix} (r_3c_{23} + l_2c_2)^2 & 0 & 0 \\ 0 & r_3^2 + l_2^2 + 2r_3l_2c_3 & r_3^2 + r_3l_2c_3 \\ 0 & r_3^2 + r_3l_2c_3 & r_3^2 \end{bmatrix}$$

the kinetic energy is finally given by

$$T(q, \dot{q}) = \frac{1}{2}\dot{q}^T H(q)\dot{q}$$

where $H(q) \in \mathbb{R}^{3\times3}$ is the inertia matrix and its elements $H_{ij} \in \mathbb{R}$ are given by

$$\begin{aligned}
H_{11} =\ & I_{y1} + I_{x2}s_2^2 + 2I_{xy2}s_2c_2 + I_{y2}c_2^2 + I_{x3}s_{23}^2 + 2I_{xy3}s_{23}c_{23} + I_{y3}c_{23}^2 + m_2r_2^2c_2^2 \\
& + m_3(r_3c_{23} + l_2c_2)^2 \\
H_{12} =\ & I_{xz2}s_2 + I_{yz2}c_2 + I_{xz3}s_{23} + I_{yz3}c_{23} \\
H_{13} =\ & I_{xz3}s_{23} + I_{yz3}c_{23} \\
H_{21} =\ & I_{xz2}s_2 + I_{yz2}c_2 + I_{xz3}s_{23} + I_{yz3}c_{23} \\
H_{22} =\ & I_{z2} + I_{z3} + m_2r_2^2 + m_3(r_3^2 + l_2^2 + 2r_3l_2c_3) \\
H_{23} =\ & I_{z3} + m_3(r_3^2 + r_3l_2c_3) \\
H_{31} =\ & I_{xz3}s_{23} + I_{yz3}c_{23} \\
H_{32} =\ & I_{z3} + m_3(r_3^2 + r_3l_2c_3) \\
H_{33} =\ & I_{z3} + m_3r_3^2
\end{aligned}$$

Assuming that $V(q) = 0$ with the second and third links resting downwards, the potential energy is given by

$$V(q) = m_2gr_2(1 - c_2) + m_3g\big[l_2(1 - c_2) + r_3(1 - c_{23})\big]$$

Using the Euler-Lagrange equation, the dynamics is obtained as

$$\tau = H(q)\ddot{q} + \dot{H}(q,\dot{q})\dot{q} + \frac{1}{2}\frac{\partial}{\partial q}(\dot{q}^TH(q)\dot{q}) + \frac{\partial}{\partial q}\left(V(q)\right)$$

With the vectors $C(q,\dot{q})\dot{q} \triangleq \dot{H}(q,\dot{q})\dot{q} + \frac{1}{2}\frac{\partial}{\partial q}(\dot{q}^TH(q)\dot{q})$ and $g(q) \triangleq \frac{\partial}{\partial q}\left(V^T(q)\right)$, the dynamics can be written as

$$\tau = H(q)\ddot{q} + C(q,\dot{q})\dot{q} + g(q)$$

The vector due to gravitational forces is given by

$$g(q) = g\begin{bmatrix} 0 \\ m_2r_2s_2 + m_3(l_2s_2 + r_3s_{23}) \\ m_3r_3s_{23} \end{bmatrix}$$

The elements of the $C(q,\dot{q})$, obtained through equation (A.4), are given by

$$
\begin{aligned}
C_{11} = & -\big[(m_2r_2^2 + I_{y2} - I_{x2})s_2c_2 + m_3(r_3c_{23} + l_2c_2)(r_3s_{23} + l_2s_2) + (I_{y3} - I_{x3})s_{23}c_{23} \\
& + I_{xy2}(s_2^2 - c_2^2)\big]\dot{q}_2 - \big[(m_3r_3^2 + I_{y3} - I_{x3})s_{23}c_{23} + m_3r_3l_2c_2s_{23}\big]\,\dot{q}_3 \\
& - I_{xy3}(s_{23}^2 - c_{23}^2)(\dot{q}_2 + \dot{q}_3) \\
C_{12} = & -\big[(m_2r_2^2 + I_{y2} - I_{x2})s_2c_2 + m_3(r_3c_{23} + l_2c_2)(r_3s_{23} + l_2s_2) + (I_{y3} - I_{x3})s_{23}c_{23} \\
& + I_{xy2}(s_2^2 - c_2^2)\big]\dot{q}_1 + [I_{xz2}c_2 - I_{yz2}s_2]\,\dot{q}_2 + (I_{xz3}c_{23} - I_{yz3}s_{23})(\dot{q}_2 + \dot{q}_3) \\
& + (I_{xz3}c_{23} - I_{yz3}s_{23})(\dot{q}_2 + \dot{q}_3) \\
C_{13} = & -\big[(m_3r_3^2 + I_{y3} - I_{x3})s_{23}c_{23} + m_3r_3l_2c_2s_{23}\big]\,\dot{q}_1 + (I_{xz3}c_{23} - I_{yz3}s_{23})(\dot{q}_2 + \dot{q}_3) \\
C_{21} = & \big[(m_2r_2^2 + I_{y2} - I_{x2})s_2c_2 + m_3(r_3c_{23} + l_2c_2)(r_3s_{23} + l_2s_2) + (I_{y3} - I_{x3})s_{23}c_{23} \\
& + I_{xy2}(s_2^2 - c_2^2)\big]\dot{q}_1 \\
C_{22} = & -m_3r_3l_2s_3\dot{q}_3 \\
C_{23} = & -m_3r_3l_2s_3(\dot{q}_2 + \dot{q}_3) \\
C_{31} = & \big[(m_3r_3^2 + I_{y3} - I_{x3})s_{23}c_{23} + m_3r_3l_2c_2s_{23}\big]\,\dot{q}_1 \\
C_{32} = & \, m_3r_3l_2s_3\dot{q}_2 \\
C_{33} = & \, 0
\end{aligned}
$$

Notice that the location of the inertial frame does not play an important role in the dynamics. For the developed dynamic model, the gravity vector satisfies the linear parametrization property with

$$
g(q) = G(q)\psi = \begin{bmatrix} 0 & 0 \\ s_2 & s_{23} \\ 0 & s_{23} \end{bmatrix} \begin{bmatrix} g(m_2r_2 + m_3l_2) \\ gm_3r_3 \end{bmatrix}
$$

Even more, the dynamic model can be expressed as the product of a matrix $Y(q,\dot{q},\ddot{q}) \in \mathbb{R}^{3\times 15}$ containing only states an a vector $\psi \in \mathbb{R}^{15}$ containing the system parameters. Observe that this parametrization is not unique since the parameter grouping can be arranged in many other ways, from all investigated parameterizations the presented one was found to have the minimum size for vector ψ. The componentes of vector ψ are as follows

$$
\begin{aligned}
&\psi_1 = I_{z3} && \psi_2 = m_3r_3^2 && \psi_3 = m_3r_3l_2 \\
&\psi_4 = m_3l_2^2 + m_2r_2^2 + I_{z2} && \psi_5 = I_{xz3} && \psi_6 = I_{yz3} \\
&\psi_7 = I_{y2} - I_{x2} + m_3l_2^2 + m_2r_2^2 && \psi_8 = I_{y3} - I_{x3} + m_3r_3^2 && \psi_9 = I_{y1} + I_{x2} + I_{x3} \\
&\psi_{10} = I_{xy2} && \psi_{11} = I_{xz2} && \psi_{12} = I_{yz2} \\
&\psi_{13} = I_{xy3} && \psi_{14} = g(m_2r_2 + m_3l_2) && \psi_{15} = gm_3r_3
\end{aligned}
$$

and the entries of $Y(q,\dot{q},\ddot{q})$ are

The first row elements are given by

$$Y_{1\,1} = 0 \qquad Y_{1\,2} = 0$$
$$Y_{1\,3} = 2\ddot{q}_1 c_2 c_{23} - 2\dot{q}_1\dot{q}_2 s(2q_2 + q_3) - 2\dot{q}_1\dot{q}_3 c_2 s_{23} \qquad Y_{1\,4} = 0$$
$$Y_{1\,5} = (\ddot{q}_2 + \ddot{q}_3)s_{23} + (\dot{q}_2 + \dot{q}_3)^2 c_{23} \qquad Y_{1\,6} = (\ddot{q}_2 + \ddot{q}_3)c_{23} - (\dot{q}_2 + \dot{q}_3)^2 s_{23}$$
$$Y_{1\,7} = \ddot{q}_1 c_2^2 - 2\dot{q}_1\dot{q}_2 s_2 c_2 \qquad Y_{1\,8} = \ddot{q}_1 c_{23}^2 - 2\dot{q}_1(\dot{q}_2 + \dot{q}_3)s_{23}c_{23}$$
$$Y_{1\,9} = \ddot{q}_1 \qquad Y_{1\,10} = 2\ddot{q}_1 s_2 c_2 - 2\dot{q}_1\dot{q}_2(s_2^2 - c_2^2)$$
$$Y_{1\,11} = \ddot{q}_2 s_2 + \dot{q}_2^2 c_2 \qquad Y_{1\,12} = \ddot{q}_2 c_2 + \dot{q}_2^2 s_2$$
$$Y_{1\,13} = 2\ddot{q}_1 s_{23} c_{23} - \dot{q}_1(\dot{q}_2 + \dot{q}_3)(s_{23}^2 - c_{23}^2) \qquad Y_{1\,14} = 0$$
$$Y_{1\,15} = 0$$

The second row elements are

$$Y_{2\,1} = \ddot{q}_2 + \ddot{q}_3 \qquad Y_{2\,2} = \ddot{q}_2 + \ddot{q}_3 \qquad Y_{2\,3} = 2\ddot{q}_2 c_3 + \ddot{q}_3 c_3 + \dot{q}_1^2 s(2q_2 + q_3) - \dot{q}_2\dot{q}_3 s_{23} - \dot{q}_3(\dot{q}_2 + \dot{q}_3)s_3$$
$$Y_{2\,4} = \ddot{q}_2 \qquad Y_{2\,5} = \ddot{q}_1 s_{23} \qquad Y_{2\,6} = \ddot{q}_1 c_{23}$$
$$Y_{2\,7} = \dot{q}_1^2 s_2 c_2 \qquad Y_{2\,8} = \dot{q}_1^2 s_{23} c_{23} \qquad Y_{2\,9} = 0$$
$$Y_{2\,10} = \dot{q}_1^2(s_2^2 - c_2^2) \qquad Y_{2\,11} = \ddot{q}_1 s_2 \qquad Y_{2\,12} = \ddot{q}_1 c_2$$
$$Y_{2\,13} = 0 \qquad Y_{2\,14} = s_2 \qquad Y_{2\,15} = s_{23}$$

And the third row elements are

$$Y_{3\,1} = \ddot{q}_2 + \ddot{q}_3 \qquad Y_{3\,2} = \ddot{q}_2 + \ddot{q}_3 \qquad Y_{3\,3} = \ddot{q}_2 c_3 + \dot{q}_1^2 s_{23} c_2 + \dot{q}_2^2 s_3$$
$$Y_{3\,4} = 0 \qquad Y_{3\,5} = \ddot{q}_1 s_{23} \qquad Y_{3\,6} = \ddot{q}_1 c_{23}$$
$$Y_{3\,7} = 0 \qquad Y_{3\,8} = \dot{q}_1^2 s_{23} c_{23} \qquad Y_{3\,9} = 0$$
$$Y_{3\,10} = 0 \qquad Y_{3\,11} = 0 \qquad Y_{3\,12} = 0$$
$$Y_{3\,13} = 0 \qquad Y_{3\,14} = 0 \qquad Y_{3\,15} = s_{23}$$

Bibliography

[1] E. Aguiñaga-Ruiz, A. Zavala-Río, V. Santibáñez, and F. Reyes, "Gobal trajectory tracking through static feedback for robot manipulators with bounded inputs," *IEEE Transactions on Control Systems Technology*, **17**(4):934–944, 2009.

[2] S. Arimoto, "Fundamental problems of robot control: Part I, Innovations in the realm of robot servo-loops," *Robotica*, **13**(1):19–27, 1995.

[3] S. Arimoto, "Fundamental problems of robot control: Part II, A nonlinear circut theory towards the understanding of dexterous motions," *Robotica*, **13**(2):111–122, 1995.

[4] S. Arimoto, *Control Theory of Non-Linear Mechanical Systems: A Passivity-Based and Circuit-Theoretic Approach*, Oxford University Press, Oxford, 1996.

[5] B. Armstrong-Hélouvry, *Control of Machines with Friction*, Kluwer Academic Publishers, Boston, 1991.

[6] H. Berghuis and H. Nijmeijer, "A passivity approach to controller-observer design for robots," *IEEE Transactions on Robotics and Automation*, **9**(6):740–754, 1993.

[7] D.S. Bernstein and A.N. Michel, "A choronological bibliography on saturating actuators," *International Journal of Robust and Nonlinear Control*, **5**(5):375–380, 1995.

[8] I.V. Burkov, "Stabilization of mechanical systems *via* bounded control and without velocity measurements," *Proc. 2nd Russian-Swedish Control Conference*, St. Petersburg, Russia, pp. 37–41, 1995.

[9] I.V. Burkov and L.B. Freidovich, "Stabilization of the position of a Lagrangian system with elastic elements and bounded control with and without measurement of velocities," *J. Appl. Maths. Mechs.*, **61**(3):433–441, 1997.

[10] B.S. Chen and S.S. Wang, "The stability of feedback control with nonlinear saturating actuator: time domain approach," *IEEE Transactions on Automatic Control*, **33**(5):483–487, 1988.

[11] R. Colbaugh, E. Barany, and K. Glass, "Global regulation of uncertain manipulators using bounded controls," *Proc. 1997 IEEE International Conference on Robotics and Automation*, Albuquerque, NM, pp. 1148–1155, 1997.

[12] W.E. Dixon, M.S. de Queiroz, F. Zhang, D.M. Dawson, "Tracking control of robot manipulators with bounded torque inputs," *Robotica*, **17**(2):121–129, 1999.

[13] W.E. Dixon, "Adaptive regulation of amplitud limited robot manipulators with uncertain kinematics and dynamics," *IEEE Transactions on Automatic Control*, **52**(3):448–493, 2007.

[14] M. Gautier and W. Khalil, "On the identification of the inertial parameters of robots," *Proc. 27th Conference on Decision and Control*, Austin, TX, pp. 2264–2269, 1988.

[15] H. Goldstain, *Classical Mechanics*, 2nd edition, Addison-Wesley Longman, Inc., 1980.

[16] W. Hahn, *Stability of Motion*, Springer-Verlag, Berlin, 1967.

[17] C. Hu, B. Yao, Z. Chen, and Q. Wang, "Adaptive robust repetitive control of an industrial biaxial precision gantry for contouring tasks," *IEEE Transactions on Control Systems Technology*, **19**(6):1559–1568, 2011.

[18] P. Kapasouris and M. Athans, "Control systems with rate and magnitude saturation for neutrally stable open loop systems," *Proc. 29th IEEE Conference on Decision and Control*, Honolulu, HI , pp. 3404–3409, 1990.

[19] R. Kelly, V. Santibáñez, and H. Berghuis, "Point-to-point robot control under actuator constraints," *Control Engineering Practice*, **5**(11):1555–1562, 1997.

[20] R. Kelly, V. Santibáñez, and A. Loría, *Control of Robot Manipulators in Joint Space*, Springer, London, 2005.

[21] H.K. Khalil, *Nonlinear Systems*, 2nd edition, Prentice-Hall, Upper Saddle River, NJ, 1996.

[22] H.K. Khalil, *Nonlinear Systems*, 3rd edition, Prentice-Hall, Upper Saddle River, NJ: Prentice-Hall, 2002.

[23] R.L. Kosut, "Design of linear systems with saturating linear control and bounded states," *IEEE Transactions on Automatic Control*, **28**(1):121–124, 1983.

[24] N.J. Krikelis and S.K. Barkas, "Design of tracking systems subject to actuator saturation and integrator wind-up," *International Journal of Control*, **39**(4):667–682, 1984.

[25] A. Laib, "Adaptive output regulation of robot manipulators under actuator constraints," *IEEE Transactions on Robotics and Automation*, **16**(1):29–35, 2000.

[26] F.L. Lewis, D.M. Dawson, and C.T. Abdallah, *Robot Manipulator Control: Theory and Practice*, Marcel Dekker, Inc., New York, 2004.

[27] S. Liuzzo and P. Tomei, "Global adaptive learning control of robotic manipulators by output error feedback," *Int. J. of Adaptive Control and Signal Processing*, **23**(1):97–109, 2009.

[28] D.J. López-Araujo, A. Zavala-Río, V. Santibáñez, and F. Reyes, "Global adaptive regulation of robot manipulators with bounded inputs," *Proc. 10th International IFAC Symposium on Robot Control*, Dubrovnik, Croatia, pp. 806–813, 2012.

[29] A. Loría, R. Kelly, R. Ortega, and V. Santibáñez, "On global output feedback regulation of Euler-Lagrange systems with bounded inputs," *IEEE Transactions on Automatic Control*, **42**(8):1138–1143, 1997.

[30] A. Loría, R. Kelly, A.R. Teel, "Uniform parametric convergence in the adaptive control of mechanical systems," *European Journal of Control*, **11**(2):87–111, 2005.

[31] L. Meirovitch, *Methods of analitycal dynamics*, McGraw-Hill Book Company, New York , 1970.

[32] A.N. Michel, L. Hou, and D. Liu, *Stability of Dynamical Systems*, Birkhäuser, Boston, 2008.

[33] R. Ortega, A. Loría, R. Kelly, and L. Praly, "On passivity-based output feedback global stabilization of Euler-Lagrange systems," *Proc. 33th IEEE Conference on Decision and Control*, Lake Buena Vista, FL, pp. 381–386, 1994.

[34] B.S. Park, J.Y. Lee, J.B. Park, and Y.H. Choi, "Adaptive control for input-constrained linear systems," *International Journal of Control, Automation, and Systems*, **10**(5):890–896, 2012.

[35] F. Reyes and R. Kelly, "Experimental evaluation of identification schemes on a direct drive robot," *Robotica*, **15**(5):563–571, 1997.

[36] F. Reyes and R. Kelly, "Experimental evaluation of model-based controllers on a direct-drive robot arm," *Mechatronics*, **11**(3):267–282, 2001.

[37] F. Reyes and A. Rosado, "Polinomyal family of PD-type controllers for robot manipulators," *Control Engineering Practice*, **13**(4):441–450, 2005.

[38] N. Rouche, P. Habets, and M. Laloy, *Stability Theory by Lyapunov's Direct Method*, Springer-Verlag, New York, 1977.

[39] V. Santibáñez and R. Kelly, "Global regulation for robot manipulators under SP-SD feedback," *Proc. 1996 IEEE Int. Conference on Robotics and Automation*, Minneapolis, MN, pp. 927–932, 1996.

[40] V. Santibáñez and R. Kelly, "On global regulation of robot manipulators: Saturated linear state feedback and saturated linear output feedback," *European Journal of Control*, **3**(2):104–113, 1997.

[41] V. Santibáñez, R. Kelly, and F. Reyes, "A new set-point controller with bounded torques for robot manipulators," *IEEE Transactions on Industrial Electronics*, **45**(1):126–133, 1998.

[42] L. Sciavicco and B. Siciliano, *Modelling and Control of Robot Manipulators*, Springer, London, 2000.

[43] R. Sepulchre, M. Janković, and P. Kokotovic, *Constructive Nonlinear Control*, Springer-Verlag, London, 1997.

[44] M. Takegaki and S. Arimoto, "A new feedback method for dynamic control of manipulators," *Journal of Dynamic Systems, Measurement, and Control*, **102**(2):119–125, June 1981.

[45] A.R. Teel, "Global stabilization and restricted tracking for multiple integrators with bounded controls," *Systems and Control Letters*, **18**(1):165–171, 1992.

[46] P. Tomei, "Adaptive PD controller for robot manipulator," *IEEE Transactions of Robotics and Automation*, **7**(4):565–570, 1991.

[47] A. Zavala-Río and V. Santibáñez, "Simple extensions of the PD-With-Gravity-Compensation control law for robot manipulators with bounded inputs," *IEEE Trans. on Control Systems Technology*, **14**(5):958–965, 2006.

[48] A. Zavala-Río and V. Santibáñez, "A natural saturating extension of the PD-with-desired-gravity-compensation control law for robot manipulators with bounded inputs," *IEEE Transactions on Robotics*, **23**(2):386–391, 2007.

[49] A. Zavala-Río, E. Aguiñaga-Ruiz, and V. Santibáñez, "Gobal trajectory tracking through output feedback for robot manipulators with bounded inputs," *Asian Journal of Control*, **13**(3):430–438, 2011.

[50] E. Zergeroglu, W. Dixon, A. Behal, and D. Dawson, "Adaptive set-point control of robotic manipulators with amplitud-limited control inputs," *Robotica*, **18**(2):171–181, 2000.